Biological Consequences of Specific and Promiscuous A-to-I RNA Editing Revealed Through Precise Genetic Engineering.

Yiannis A. Savva

M.A., Central Connecticut State University, 2004

B.S., Central Connecticut State University, 2003

A Dissertation Submitted in Partial Fulfillment of the Requirements for the Degree of Doctor of Philosophy in the Department of Molecular Biology, Cell Biology, and Biochemistry at Brown University

Providence, Rhode Island

May 2011

This dissertation by Yiannis A. Savva is accepted in its present form by the Department of Molecular Biology, Cell Biology, and Biochemistry as satisfying the dissertation requirement for the degree of Doctor of Philosophy.

Date_____ _____
Robert A. Reenan, Ph.D., Advisor

Recommended to the Graduate Council

Date_____ _____
Michael McKeown, Ph.D., Reader

Date_____ _____
Mark Johnson, Ph.D., Reader

Date_____ _____
Judith Bender, Ph.D., Reader

Date_____ _____
Gordon G. Carmichael, Ph.D., Reader

Approved by the Graduate Council

Date_____ _____
Peter Weber, Ph.D., Dean of the Graduate School

Yiannis A. Savva

Brown University
Department Molecular Biology, Cell Biology, Biochemistry
Box G
Providence, RI 02912
Yiannis_Savva@brown.edu

83 Medway Street
Providence, RI 02912
(401) 952-0180

Birthplace: Nicosia, Cyprus

EDUCATION

Ph.D. Brown University, Providence, RI 2006-Present
Molecular Biology, Cell Biology, and Biochemistry
Expected Graduation Date: May 2011
Title: "Biological Consequences of Specific and Promiscuous A-to-I RNA Editing Revealed Through Precise Genetic Engineering".
Advisor: Robert A. Reenan, Ph.D

University of Connecticut Health Center, Farmington, CT 2004-2006
Ph.D. Program in Biomedical Science
Concentration in Genetics and Developmental Biology
Advisor: Robert A. Reenan, Ph.D

M.A. Central Connecticut State University, New Britain, CT 2003-2004
Major: Molecular Biology

B.S. Central Connecticut State University, New Britain, CT 2000-2003
Cum Laude, Departmental Honors
Major: Cellular and Molecular Biology
Minor: Chemistry

RESEARCH EXPERIENCE

Doctoral Dissertation
Brown University, 2006-Present

- Conducted experiments in *Drosophila melanogaster* to investigate the role of A-to-I RNA editing in modulating complex behavior.
- Genetically engineered the endogenous *dAdar* locus by homologous recombination to generate: $dAdar^{HA}$, $dAdar^{Hyp}$, $dAdar^{WTLoxP}$, $dAdar^{S}$, and $dAdar^{S\text{-}HA}$ alleles.
- Evaluated the global status of mRNA re-coding events in $dAdar^{Hyp}$, $dAdar^{WTLoxP}$, $dAdar^{S}$, and $dAdar^{G}$ alleles through sequencing of RT-PCR products form various

male and female tissues.
- Evaluated behavioral phenotypes of *dAdar*^{Hyp}, *dAdar*^{WTLoxP}, *dAdar*^{S}, and *dAdar*^{G} alleles, including locomotor activity, sleep, and mating behavior.
- Examined the localization of dADAR using HA-tagged transgene versions of various alleles in whole salivary glands and in polytene chromosomes.
- Used homologous recombination to create *in vivo* deletion mutations of tandemly repeated copies of the transposable element *Hoppel* to investigate the role of A-to-I RNA editing in heterochromatic gene silencing.

Undergraduate research
Central Connecticut State University, Department of Biology; 2003
Laboratory of Michael A. Davis, PhD

- Conducted experiments in various soil bacteria to identify novel antibacterial compounds as potentially new antibiotics.
- Examined the effects of various bacterial strains on growth media and identified *Bacillus polymyxa* as a potential bacterial strain that secrets a potent antibacterial compound.
- Used several purification methods and spectroscopic techniques to determine molecular structures of different antibacterial compounds.

Central Connecticut State University, Department of Chemistry; 2002
Laboratory of Neil M. Glagovich, PhD

- Conducted experiments to resolve racemic mixtures of aldehydes and ketones using chiral diols.

TEACHING EXPERIENCE

Biology Department, Brown University, Spring 2007
Teaching Assistant, Microbiology

- Undergraduate course in microbiology.
- Attended lectures, prepare laboratory material, held office hours for student questions and tutoring.
- Graded homework assignments, quizzes, and exams.
- Maintained grading spreadsheets and student information for faculty lecturers.

Chemistry Department, Central Connecticut State University, Fall 2004
Teaching Assistant, Organic chemistry

- Prepared laboratories for organic chemistry experiments, once a week for 10 sessions.

- Graded homework assignments, quizzes, and exams.
- Maintained grading spreadsheets and student information for faculty lecturers.

Biology Department, Central Connecticut State University, Summer 2003
Tutor, Chemistry for undergraduate pre-med majors.

- Held a six-week chemistry course for pre-med students requiring additional instruction in general and organic chemistry.
- Designed practice questions and topic-specific lecture and supplementary materials.
- Conducted review lectures based on student-initiated topics of interest.

Biology Department, Central Connecticut State University, Spring 2003
Teaching Assistant, Laboratory Tutorial for area middle-school students.

- Assisted faculty and students in a laboratory practicum designed to expose middle school students to forensic science and DNA technology.
- Helped students with fingerprint analysis, blood-typing, and genotype analysis through PCR and electrophoresis of DNA products.
- 4-5 sessions held over the course of the spring semester.

PUBLICATIONS

Yiannis A. Savva, James E.C Jepson, Asli Sahin, Arthur U. Sudgen, Ryan Bell, Lauren Alpert, Charles Lawrence, and Robert A. Reenan. Fine-tuning of mRNA re-coding and complex behavior by auto-regulatory RNA editing. *Submitted*.

James E.C Jepson, Kyle A. Jay, **Yiannis A. Savva**, and Robert A. Reenan. Visualizing inter-individual variation in adenosine-to-inosine RNA editing. *Submitted*.

Balpreet Bhogal, James E.C Jepson, **Yiannis A. Savva**, Robert A. Reenan, Anita Pepper and Thomas A. Jongens. Modulation of dADAR-dependent RNA editing by the Drosophila fragile X mental retardation protein. *Submitted*.

Jepson, J.E., **Savva, Y.A**., Yokose, C., Sugden, A.U., Sahin, A., and Reenan, R.A. (2011) Engineered alterations in RNA editing modulate complex behavior in Drosophila: regulatory diversity of adenosine deaminase acting on RNA (ADAR) targets. The Journal of biological chemistry, *286 (10)*, 8325-8337.

St Laurent, G., 3rd, **Savva, Y.A**., and Reenan, R. (2009). Enhancing non-coding RNA information content with ADAR editing. Neuroscience letters *466*, 89-98.

Olson, S., Blanchette, M., Park, J., **Savva, Y**., Yeo, G.W., Yeakley, J.M., Rio, D.C., and Graveley, B.R. (2007). A regulator of Dscam mutually exclusive splicing fidelity. Nature structural & molecular biology *14*, 1134-1140.

CONFERENCE ABSTRACTS

Yiannis A. Savva, James E.C Jepson, and Robert A. Reenan. (2009). Examining the importance of ADAR auto-editing in *Drosophila*. Poster Session 50th Annual Drosophila research conference. March 4th, 2009. Chicago, Illinois.

Yiannis A. Savva and Michael A. Davis. (2004). Antibacterial Conpounds Isolated From the Soil Bacterium *Bacillus Polymyxa*. Presentation session 58th Annual Eastern Colleges Science Conference, April 2, 2004. Manhattan College, Riverdale, NY.

Kelly Bristol, Arlene Swierczynski, Jennifer Tassy, **Yiannis A. Savva**, Nicole Dlugokinski, Elena Gelzinis, Melissa Mendonez, Lorry Straughn, Priscilla Paiva, and Michael A. Davis. (2004). Characterization of antibacterial compounds produced by soil bacteria. Poster session 58th Annual Eastern Colleges Science Conference, April 2, 2004. Manhattan College, Riverdale, NY.

Yiannis A. Savva and Neil M. Glagovich (2003). Utilizing chiral diols to resolve racemic mixtures of aldehydes and ketones. Poster session 57th Annual Eastern Colleges Science Conference, April 12, 2003. Ithaca college, Ithaca, NY.

AWARDS

David DeRuccio Award for Graduate Student Achievement. Central Connecticut State University, Department of Biological Sciences, May 12, 2004.

Diane Wowk Award for Outstanding Service to the Department of Biological Sciences. Central Connecticut State University, Department of Biological Sciences, May 12, 2004.

Best Poster Award, Eastern Colleges Science Conference. "Utilizing chiral diols to resolve racemic mixtures of aldehydes and ketones." 57th Annual Eastern Colleges Science Conference, April 12, 2003. Ithaca college, Ithaca, NY.

Dedication

I dedicate this thesis to my wonderful parents, Andrea Savva and Maria Savva. You have always been there for me through every step in my life's journey. I could not have achieved all that I have without your endless love and support. I also want to dedicate this thesis to my lovely sisters, Valentina Savva and Christiana Savva. I love you both with all my heart. Thank you for your love and support. Lastly, I want to dedicate this thesis to my brother, Alexis Savva. Thank you for your support and understanding all these years.

Acknowledgements

I would like to thank my graduate thesis advisor, Dr. Robert Reenan, for convincing me to pursue my graduate studies in RNA editing. You have been an incredible mentor and a great friend. Thank you for the opportunity to learn and work in your lab. Thank you for being an inspiration and a force in my graduate studies. Most importantly, thank you for teaching me what it takes to become a successful and independent researcher.

I would also like to thank Cindi Staber, my "mimi". Thank you for your patience and support all these years. Every molecular technique I know is a result of your vast wealth of knowledge. Thank you for being there in the good and the bad times of science. Thank you for your comments on manuscripts and your ideas about experiments. Thank you for being there for me, always. I love you mimi.

I would like to thank my thesis committee members: Dr. Michael McKeown, Dr. Mark Johnson, Dr. Judith Bender, and Dr. Gordon G. Carmichael. Thank you all for accepting to be members of my thesis committee. Thank you for your participation in meetings as well as my thesis defense. Thank you for your comments and advice. Your feedback on my thesis project helped me tremendously.

I would also like to thank Elaine Butler and Rosemarie Antoni for all their hard work in keeping up with my administrative paper work. Thank you very much for your help and assistance. I also want to thank you for your hard work in making my transition here at Brown University as simple as possible.

Last, I would like to thank Dr Steve Helfand for his support and encouragement throughout the years.

Table of Contents

Table of Figures

List of Tables

CHAPTER 1: INTRODUCTION

Expansion of the eukaryotic proteome by post-transcriptional gene regulation

Genetic information within each cell of every living organism is stored in DNA molecules. An extensive network of cellular machines decodes the genetic information through transcription of DNA into RNA and translation of RNA with high fidelity to generate protein products, which are used by cells to carry out their basic biological functions such as metabolism, molecular transport, and division. The unidirectional flow of information from DNA to RNA leading to the generation of proteins is known as the central dogma of molecular biology (Crick, 1958). Coupling of all cellular functions in an orchestrated manner bestows organismal complexity, including a vast behavioral repertoire of learning, memory, and adaptation in response to environmental stimuli.

It was originally believed that differences in complexity between eukaryotes arose from variations in genomic coding potential. After the sequencing of several eukaryotic genomes it became apparent that the number of genes does not correlate with morphological or behavioral complexity (Baltimore, 2001). Mammals appear to be immensely more complex than other eukaryotes, but their gene number (~20,000) (Clamp et al., 2007) does not vary enormously when compared to a fly's (~14,000) (Adams et al., 2000), or a nematode's (~20,000) (*C. elegans* Sequencing Consortium, 1998). It is now clear that organismal complexity develops through the expansion of the information potential encoded by a genome through post-transcriptional modifications such as alternative splicing and RNA editing (Nilsen and Graveley, 2010; Nishikura, 2010).

Transcription of genes results in the generation of nuclear precursor messenger RNAs (pre-mRNAs) that contain the information for protein synthesis in a discontinuous form. The pre-mRNA contains coding (exons) and non-coding sequences (introns), and further processing by the splicing machinery, the spliceosome, ensures the removal of introns. Splicing generates mature messenger RNAs (mRNAs), which are translated by ribosomes in the cytoplasm into protein products. The discovery that diverse immunoglobulin proteins are encoded by the same gene (Alt et al., 1980) provided evidence that one gene does not necessarily encode for only one protein. Soon after, it was revealed that differential inclusion or exclusion of exons by alternative RNA splicing mediates the production of distinct immunoglobulin mRNAs (Early et al., 1980). Recent studies indicate that up to 95% of human pre-mRNAs are alternatively spliced, yielding diverse collections of exons in mRNAs (Pan et al., 2008; Wang et al., 2008). The *Drosophila* gene *Down syndrome cell adhesion molecule (Dscam)* has the potential to generate ~38,000 different mRNAs through alternative splicing (Schmucker et al., 2000), a number much greater than the total number of genes present in the whole genome of the organism. Thus, alternative splicing expands the eukaryotic proteome by selective inclusion or exclusion of existing genomic information to generate a myriad of related protein isoforms.

In contrast, RNA editing of select genes generates subtly different protein products by altering single nucleotides. Adenosine to inosine (A-to-I) RNA editing selectively converts specific adenosines in pre-mRNAs to inosines. Upon translation, the ribosomal machinery interprets inosines as guanosines (Basillo et al., 1962), causing A $\rightarrow$ G changes in the coding sequence. This may result in amino acid substitutions that

generate protein products not specified by the literal genomic information. If the protein diversification that can be generated by RNA editing is considered together with the enormous potential diversity created by alternative splicing, the number of distinct protein isoforms that may be encoded by a genome is astonishing. For example, the *Drosophila paralytic* gene has the potential to encode for more than two million protein isoforms as a result of combinatorial processing via alternative splicing and RNA editing (Hanrahan et al., 2000; Loughney et al., 1989; Reenan et al., 2000; Thackeray and Ganetzky, 1994). Thus, RNA editing has the capability to increase eukaryotic proteomic diversity by generating novel genetic information, a fascinating phenomenon that does not comply with the canonical rules of the central dogma.

A-to-I RNA editing is mediated by adenosine deaminase acting on RNA (ADAR) enzymes

A-to-I RNA editing is mediated by adenosine deaminases acting on RNA (ADARs), which hydrolytically deaminate adenosines to inosines in double stranded RNA (dsRNA) substrates (Bass, 2002; Nishikura, 2010) (Fig 1.1A). ADARs were first identified using antisense RNAs in *Xenopus laevis* eggs, a study designed to determine novel functions of maternal mRNAs during development (Bass and Weintraub, 1987). These studies revealed that stable RNA hybrids between endogenous sense and injected antisense RNAs are infrequent due to a novel unwinding activity (Bass and Weintraub, 1987; Rebagliati and Melton, 1987). After closer examination of the final products from the unwinding reaction, it became clear that specific adenosine residues were converted to inosines, resulting in the destabilization of the RNA duplex (Bass and Weintraub,

1988; Wagner et al., 1989). Subsequently, various enzymes were cloned and characterized as adenosine deaminases that recognize dsRNA (Kim et al., 1994a; Kim et al., 1994b; Melcher et al., 1996b; O'Connell and Keller, 1994; O'Connell et al., 1995).

ADARs are highly conserved in metazoans (Bass, 2002). Mammalian genomes encode three ADAR enzymes; ADAR1, ADAR2, and ADAR3 (Nishikura, 2010), the *C. elegans* genome encodes two, *Ce*ADR1 and *Ce*ADR2 (Tonkin et al., 2002), while only a single *adar* locus is present in the *Drosophila* genome (Palladino et al., 2000b). Furthermore, ADAR enzymes are also present in the invertebrate genomes of both sea urchin and sea anemone, suggesting an early origin of RNA editing enzymes in metazoan evolution (Jin et al., 2009). In contrast, ADAR genes do not appear to be present in fungal, plant and yeast genomes.

Interestingly, although prokaryotic genomes do not contain ADARs, they do encode a transfer RNA (tRNA) adenosine deaminase (TadA), which modifies specific tRNAs (Wolf et al., 2002). Orthologs of this RNA editing enzyme, adenosine deaminases acting on tRNAs (ADATs), are also highly conserved in metazoa and catalyze the deamination of specific adenosines to inosines adjacent to or at the anticodon position of tRNAs (Gerber and Keller, 2001). Sequence homology between the catalytic domains of ADARs and ADATs suggests a model in which tRNA modifying enzymes are the evolutionary ancestors of ADARs. In this model, an ADAT acquired one or more dsRNA binding domains that allowed recognition and binding of dsRNAs. This evolutionary novelty is thought to have conferred selective advantage due to repair of lethal DNA mutations by A-to-I modifications on mRNAs (Bass, 2002).

Transcriptional and posttranscriptional regulation of *Drosophila* ADAR

In contrast to the mammalian and *C. elegans* genomes, *Drosophila* possesses just a single *adar* locus, located on the X chromosome (Palladino et al., 2000b). However, posttranscriptional modifications such as alternative splicing and RNA editing can generate multiple ADAR isoforms (Palladino et al., 2000b) (Fig. 1.2). For example, inclusion of an alternatively spliced exon (3a) occurs by splicing to an alternative 5' splice donor site resulting in the incorporation of 37 extra amino acids between the two dsRBDs (Palladino et al., 2000b). The inclusion or exclusion of this alternative exon alters the linear distance between the two double-stranded RNA binding domains (dsRBDs), potentially regulating substrate specificity through binding. The *in vivo* significance of this alternative splicing event is still unclear, but *in vitro* editing assays suggest that inclusion of the 3a exon decreases editing levels of at least one target transcript (Keegan et al., 2005).

The *adar* transcript is also subject to an auto-editing event that results in a serine to glycine coding change at a highly conserved residue in the deaminase domain (Palladino et al., 2000b). Similar to ADAR expression, this auto-editing event was found to be developmentally regulated and is only detectable at the pupal (~5%) and adult stages (~40%) (Palladino et al., 2000b). *In vitro*, *adar* auto-editing decreases enzymatic activity on two target adenosines, suggesting a negative auto-regulatory feedback mechanism for ADAR activity (Keegan et al., 2005).

Additionally, the *Drosophila adar* locus is transcriptionally regulated by two alternative promoters, -4a and -4b, similar to mammalian ADAR1. The two promoters

are differentially regulated in a temporal manner during development. Transcripts driven by the -4a promoter are detected throughout development, while -4b transcripts are only detected at the adult stage (Palladino et al., 2000b). ADAR expression and auto-editing appear to be predominantly adult-specific, suggesting that expansion of the proteome via RNA editing is primarily required at later stages of development.

ADAR enzyme domain structure and function during A-to-I RNA editing

All ADAR enzymes share a common domain structure consisting of one to three dsRNA binding domains (dsRBD) and a catalytic deaminase domain found at the N and C termini of the protein, respectively (Bass, 2002). Human ADARs possess two or three dsRBDs, while the *C. elegans* enzymes contain one or two. The single *Drosophila* ADAR contains two dsRBDs similar to the mammalian ADAR2 (Nishikura, 2010) (Fig. 1.3). The crystal structure of the human ADAR2 deaminase domain suggests that the formation of a catalytic center and the presence of a cofactor are requirements for the deamination reaction to occur. In the active site, a glutamic acid residue (E396) hydrogen bonds to a water molecule, while a histidine (H394), and two cysteine residues (C451 and C516) coordinate a zinc ion that activates the water molecule for nucleophilic attack (Macbeth et al., 2005). Buried in the catalytic core, an inositol hexakisphosphate (IP_6) molecule stabilizes multiple arginine and lysine residues and is required for catalytic activity (Macbeth et al., 2005). IP_6 is an abundant metabolic product implicated in various cellular processes, including transcription (York et al., 1999), DNA repair

(Hanakahi and West, 2002) and chromatin remodeling (Shen et al., 2003), suggesting an unexpected association between RNA editing and diverse cellular pathways.

ADAR binding requires direct contact between the dsRBDs and dsRNA substrates (Valente and Nishikura, 2007). Nuclear magnetic resonance and X-ray crystallography studies have revealed that the binding of double stranded RNA binding proteins (dsRBPs) to dsRNA is not sequence specific (Bycroft et al., 1995; Nanduri et al., 1998; Ryter and Schultz, 1998). This is a consequence of the structure adopted by most RNA molecules. Usually an RNA adopts a double-helical structure, known as an A-form helix, which contains a deep and narrow major groove, prohibiting both accessibility and recognition at the single nucleotide level.

Consistent with the binding properties of other dsRBPs, ADARs can bind to any dsRNA without sequence preference (Nishikura et al., 1991). For example, ADARs can bind to dsRNAs that form short duplexes (~20-50bp) with mismatches, bulges and loops (imperfect dsRNAs) as well as perfectly base-paired long dsRNAs (~100-1000bp). The structural diversity of RNA substrates results in a wide range of ADAR specificities (Bass, 2002; Nishikura, 2006). In short imperfect RNA duplexes, ADARs deaminate select adenosines (specific RNA editing). In contrast, promiscuous editing of multiple adenosines, also known as hyper-editing, usually occurs in long, perfectly paired RNA duplexes (Fig. 1.4).

ADARs modify specific adenosines to inosines in imperfectly duplex RNAs of select transcripts (Nishikura, 2010). ADAR substrates can be generated from exonic sequences that fold back on each other to form simple hairpins (Bhalla et al., 2004; Hanrahan et al., 2000; Keegan et al., 2005; Ohlson et al., 2007). In addition, intronic

noncoding sequences with extensive complementarity to upstream or downstream exons containing the adenosine destined to be edited can form structurally diverse RNA duplexes. These intronic elements, also known as editing site complementary sequences (ECS), can form simple exon-intron hairpin structures (Burns et al., 1997; Hanrahan et al., 2000; Higuchi et al., 1993; Lomeli et al., 1994; Wang et al., 2000) or more complex RNA secondary structures such as pseudoknots (Reenan, 2005) (Fig. 1.5).

The majority of ECS-mediated dsRNA structures usually contain mismatches, bulges, and loops. It is thought that the presence of such structural imperfections directs the binding of ADARs to specific locations on the RNA duplex without any sequence recognition. However, upon binding, ADARs exhibit sequence preferences for modifying select adenosines over others. *In vitro* studies using synthetic editing substrates revealed that ADAR enzymes preferentially target adenosines with a uridine as a 5' neighbor (Lehmann and Bass, 2000; Polson and Bass, 1994). In addition, adenosines found in mismatches with cytosines are edited more efficiently when compared to other adenosines (Wong et al., 2001).

The mechanism of A-to-I RNA editing

The involvement of RNA editing in creating an alternative 3′ splice site, which regulates ADAR2 expression and editing activity *in vivo* (Rueter et al., 1999), suggests that RNA editing must precede splicing. In addition, intronic sequences form dsRNAs with coding regions to serve as ADAR substrates, indicating that editing and splicing must be synchronized. Thus, in circumstances in which editing must take place before

splicing, a regulatory mechanism must exist to ensure an accurate coordination of RNA processing events. It should be noted that in RNA duplexes generated exclusively by exonic sequences, such as the *para Fsp* site (Hanrahan et al., 2000), RNA editing could occur after splicing.

Considerable evidence suggests that RNA processing, including capping, splicing, and polyadenylation, occurs cotranscriptionally, implying that RNA editing must also be cotranscriptional. During transcription, the C-terminal domain (CTD) of RNA polymerase II coordinates RNA processing events with high fidelity (Kornblihtt et al., 2004; Maniatis and Reed, 2002; Zorio and Bentley, 2004). The CTD is also required for coordination of cotranscriptional editing and splicing of the GluR-B pre-mRNA, an ADAR substrate. During processing of this pre-mRNA, the CTD decreases the splicing rate substantially to ensure that RNA editing proceeds before splicing. A non-functional CTD results in premature splicing, consequently abolishing editing (Ryman et al., 2007).

After the RNA editing reaction, the dsRNA must be resolved for further processing of the pre-mRNA. Usually during ADAR substrate RNA duplex formation, splicing signals are base-paired with complementary sequences, thus preventing their interpretation by the splicing machinery. Therefore, dsRNA helicases may be involved in the resolution of these duplexes. *Drosophila* Maleless (Mle), a dsRNA helicase, is thought to be required for the resolution of an exon-intron dsRNA that directs editing of the *paralytic* pre-mRNA. The mle^{napts} mutant background contains significantly fewer full-length Na^+ channel transcripts because of aberrant splicing that occurs at the edited region (Reenan et al., 2000). It has been proposed that if the dsRNA remains unresolved, the 5’ splice donor site of the edited exon becomes inaccessible to the spliceosome,

leading to exon skipping and nonfunctional Na^+ channels (Reenan et al., 2000). This model suggests that resolution of dsRNA complementary structures that direct RNA editing is required for further appropriate processing of pre-mRNAs. Whether the Mle helicase is involved in the resolution of structures that direct RNA editing in other pre-mRNAs remains to be established.

The catalytic domain of ADAR is highly homologous to the catalytic domain of cytidine deaminase (CDA) family of editing enzymes (Gerber and Keller, 1999). APOBEC-1 is a cytidine deaminase that edits cytidine to uridine (C-to-U) in *apolipoprotein B* mRNAs (Lau et al., 1994; MacGinnitie et al., 1995; Navaratnam et al., 1998). Homodimerization of cytidine deaminases is required for catalytic activity (MacGinnitie et al., 1995; Navaratnam et al., 1998). Since the key residues that coordinate the zinc ion within the catalytic domain of both ADAR and CDAs are highly conserved, ADARs may also function as dimers (Gerber and Keller, 1999). *In vitro*, both fly and mammalian ADARs require homodimerization for enzymatic activity (Cho et al., 2003; Gallo et al., 2003). Furthermore, fluorescence resonance energy transfer (FRET) experiments revealed that both ADAR1 and ADAR2 homodimerize in human cells independent of RNA binding (Chilibeck et al., 2006). ADAR enzymes can also form heterodimers, perhaps altering enzymatic activity, suggesting that differential ADAR isoform combinations could increase the repertoire of recoding output (Gallo et al., 2003).

The observations that RNA editing must precede splicing, that an RNA helicase may be required for the resolution of RNA duplexes, and that dimerization may be a requirement for ADAR enzymatic activity, suggest a model for the mechanism of A-to-I

RNA editing of pre-mRNAs (Fig. 1.6). In this model, RNA polymerase transcribes the exon destined to be edited by ADAR. Concurrently, the CTD domain slows splicing rates until the downstream intronic elements are transcribed. These elements fold back on the exon, leading to the generation of an RNA duplex that serves as an ADAR substrate. One ADAR monomer binds to the duplex followed by the recruitment and binding of an additional monomer. The dimerization of the ADAR enzyme positions a specific adenosine into the catalytic domain, possibly due to conformational changes upon RNA binding, leading to deamination. While the RNA polymerase continues to transcribe the rest of the pre-mRNA, an RNA helicase resolves the dsRNA before splicing occurs. After RNA processing is completed, the mature mRNA is exported to the cytoplasm for translation.

Tissue and cellular distribution of ADARs

Mammalian ADAR1 and ADAR2 are expressed in many tissues, whereas ADAR3 is only present in the brain (Chen et al., 2000; Melcher et al., 1996a; Melcher et al., 1996b). Alternative promoter usage generates a full length (ADAR1p150) and a N-terminally truncated (ADAR1p110) ADAR1 isoform in mammalian cells (Patterson and Samuel, 1995). While both the long and short isoforms contain three dsRNA-binding domains and a deaminase domain, their cellular distribution is different. ADAR1p110 exclusively localizes to the nucleus (Desterro et al., 2003; Sansam et al., 2003), while the ADAR1p150 isoform shuttles in and out of the nucleus, though it predominantly accumulates in the cytoplasm (Patterson and Samuel, 1995; Poulsen et al., 2001). The

cytoplasmic localization of ADAR1p150 suggests that a select class of dsRNAs could be targeted outside the nucleus. However, cytoplasmic localization of RNA editing enzymes is unusual.

Within a cell, ADARs are strongly localized to the nucleus. More specifically, ADAR1p110 and ADAR2 are present in the nucleolus and this localization is dependent on functional dsRBDs (Desterro et al., 2003; Sansam et al., 2003). ADAR nucleolar localization may be mediated by dsRNAs generated from ribosomal RNAs (rRNAs) and small nucleolar RNAs (snoRNAs), both known to be concentrated in the nucleolus. To date there is no evidence that ADARs can modify rRNAs or snoRNAs, thus the significance of this nucleolar localization remains enigmatic. However, translocation of ADAR2 from the nucleolus to the nucleoplasm results in higher editing levels in pre-mRNA substrates (Sansam et al., 2003). Therefore, the nucleolar localization of ADARs may represent a cellular mechanism for regulating editing of pre-mRNAs through ADAR sequestration.

In *Drosophila*, d*Adar* transcripts are predominately restricted in the nervous system. More specifically transcripts were shown to accumulate in both the embryonic ventral nerve cord and the brain (Palladino et al., 2000b). During adulthood, d*Adar* transcripts accumulate in cortical regions of the central brain as well as in neurons of the lamina (Ma et al., 2001). However, the complete expression pattern and cellular distribution of ADAR in adult flies remains unknown. The localization of both mammalian and fly ADARs to the brain, suggests an important role for RNA editing in the functioning of the nervous system.

Identification of ADAR pre-mRNA targets

Because inosine appears after reverse transcription as guanosine, electropherograms derived from edited cDNAs include mixed A/G peaks (Fig. 1.8). Such discrepancies in electropherograms are considered to be the signature of RNA editing. The comparison of cDNA to genomic DNA sequences led to the accidental discovery of RNA editing sites in various organisms (Bass, 2002; Nishikura, 2010). To further understand the biological significance of RNA editing, contemporary studies use novel approaches including comparative genomics and deep sequencing technologies to identify new RNA editing sites (Wulff et al., 2010).

Comparative genomics approaches have uncovered an intriguing phylogenetic signature of A-to-I RNA editing in *Drosophila* (Hoopengardner et al., 2003). Comparison of 18 different *Drosophila* species revealed intronic cis-elements necessary for RNA duplex formation that are highly conserved (Hoopengardner et al., 2003). Furthermore, sequence conservation is higher in exonic sequences near editing sites compared to adjacent exons that are not modified by ADAR (Hoopengardner et al., 2003). Using this pattern of conservation as a possible signature of RNA editing, comparisons between species of *Drosophila* led to the identification of approximately 50 new editing sites found in 16 different genes. These genes encode proteins that are involved in electrical and chemical neurotransmission, including pre-synaptic enzymes, voltage- and ligand-gated ion channels (Hoopengardner et al., 2003). Most of the ADAR modifications in these nervous system specific targets result in non-synonymous codon changes in functionally important residues (Fig. 1.9), suggesting a crucial role of RNA editing in

protein function. A more recent study in *Drosophila* using deep sequencing technology led to the identification of 972 new editing sites in 561 genes involved, not only in neurotransmission, but in a wide range of other functions suggesting that RNA editing events are more widespread than previously anticipated (Graveley et al., 2010).

Furthermore, ~207 human pre-mRNAs are subject to A-to-I specific RNA editing as identified by deep sequencing (Li et al., 2009). Most of the identified human mRNAs editing sites reside in ion channels and G-protein-coupled receptors, supporting previous reports that RNA editing targets in mammals are also involved in the functioning of the nervous system (Bhalla et al., 2004; Burns et al., 1997; Higuchi et al., 1993; Ohlson et al., 2007).

Consequences of RNA editing on protein function

According to canonical Watson-Crick bonding, adenosine base pairs with uridine. Inosine shares the base pairing properties of guanosine, and thus base pairs with cytosine (Fig. 1.1B). Therefore, the translation machinery interprets inosine as if it were guanosine, altering the triplet codon and possibly leading to amino acid substitutions in protein products. Over half the triplet codons in the genetic code may be reassigned through RNA editing (Fig. 1.7). Due to the degeneracy of the genetic code, RNA editing can cause both synonymous and non-synonymous amino acid substitutions. However, RNA editing predominantly results in non-synonymous changes, and thus the diversification of protein products. While the functional consequences of most specific recoding events are currently unknown, various studies in different genetic model

organisms indicate that RNA editing of mRNAs can result in profound changes in protein properties.

Mammalian, glutamate receptor channels (GluRs) are involved in fast neurotransmission at synapses in the brain (Dingledine et al., 1999), and are specifically recoded via RNA editing at multiple sites (Higuchi et al., 1993; Seeburg and Hartner, 2003). At one of these sites, A-to-I modification results in an amino acid substitution of arginine for glutamine (Q/R site) in the pore-loop domain of the GluR-B subunit (Higuchi et al., 1993). This amino acid substitution leads to reduced channel conductance and permeability to Ca^{2+} ions (Dingledine et al., 1999; Seeburg et al., 2001). In addition, the presence of the arginine residue in the pore-loop acts as an endoplasmic reticulum retention signal (Greger et al., 2002). This retention mechanism inhibits homodimerization of edited channel subunits allowing only channels that consist of both edited and unedited subunit forms to exit, thus regulating synaptic signals through the diversification of channel subunit assembly (Greger et al., 2002).

Within the mammalian brain, serotonin signaling is promoted through a diverse family of G protein-coupled receptors (GPCRs) (Hoyer et al., 2002). One of these receptors undergoes A-to-I modification at five adenosines, resulting in codon changes within the second intracellular loop (Burns et al., 1997). RNA editing at these select adenosines leads to amino acid substitutions, causing an increase of the oligomerization potential of GPCRs and altering the ligand binding affinity of these receptors (Burns et al., 1997; Niswender et al., 1999; Wang et al., 2000).

Potassium ion (K^+) channels are highly conserved, integral membrane proteins that form aqueous pores for K^+ flow across cellular membranes (Miller, 2000). These

channels are involved in the regulation of various neuronal properties, including firing rates, resting potential, and recovery following an action potential (Pongs, 1999). Metazoan potassium channel pre-mRNAs undergo A-to-I RNA editing (Hoopengardner et al., 2003; Patton et al., 1997; Rosenthal and Bezanilla, 2002). While recoding events occur in different positions in the mammalian, fly, and squid K^+ channels, the functional consequences resulting from RNA editing are highly conserved. Amino acid substitutions that result from editing predominantly regulate the rate of inactivation of K^+ channels (Bhalla et al., 2004; Ingleby et al., 2009; Rosenthal and Bezanilla, 2002). These results suggest the importance of RNA editing in regulating potassium channel function throughout the animal kingdom.

These functional studies in GluR, GPCRs, and K^+ channels demonstrate that RNA editing has profound and specific consequences on the functionality of the protein products of its mRNA targets. However, much remains unknown about the effect of RNA editing on a multitude of other mRNA targets, providing great opportunities for further study.

ADARs are required for appropriate nervous system function

RNA editing deficiencies generated in various model genetic organisms, including mammals, worms, and flies, result in profound physiological consequences. Mice homozygous for ADAR1 null mutations die during early embryonic development. Isolation and examination of ADAR1$^{-/-}$ embryos before death revealed widespread apoptosis in multiple tissues as the major cause of embryonic lethality (Wang et al.,

2004). These results suggest that A-to-I editing of a currently unknown dsRNA target(s) is required for embryonic development of mice. Furthermore, ADAR2$^{-/-}$ mice appear morphologically normal but suffer from repeated seizure episodes and die soon after birth due to lack of editing at the GluR-B Q/R site (Higuchi et al., 2000). A GluR-B allele that contains an arginine (R) codon at the Q/R site (GluR-B^{R}) rescues the ADAR2$^{-/-}$ phenotypes and mice appear normal throughout development (Higuchi et al., 2000). Thus, the GluR-B transcript is the most physiologically critical ADAR2 substrate in mice.

Homozygous deletions in *C. elegans* of both ADR1 and ADR2 result in defects in chemotaxis (Tonkin et al., 2002). ADAR's role in the chemosensation pathway and the targets involved in this behavioral response are currently unknown. However, when ADAR deficient worms are crossed to strains that are incapable of eliciting an RNA interference (RNAi) response, the chemotaxis defect is moderately rescued (Tonkin and Bass, 2003). These results suggest that in the absence of ADAR, dsRNAs that were otherwise protected by editing can enter the RNAi pathway leading to their degradation.

In *Drosophila*, deletion of the single *adar* locus results in severe neurological defects, including extreme uncoordination, seizures, temperature-sensitive paralysis, lack of courtship display in males, and neurodegeneration (Palladino et al., 2000a). While all neurological phenotypes increase in severity with age, ADAR$^{-/-}$ flies morphology and lifespan appears to be normal. Contrary to *C. elegans*, double mutants in both editing activity and RNAi response fail to rescue the neurological phenotypes (Jepson and Reenan, 2009). These results suggest that the neurological defects in ADAR null flies are

due to the lack of editing of nervous system mRNAs rather from the spurious entry of dsRNAs in the RNAi pathway.

Nevertheless, ADAR deficiencies in the above model genetic systems point out crucial roles for RNA editing in the appropriate functioning of the nervous system and the regulation of adult-stage behaviors.

Consequences of specific A-to-I RNA editing in non-coding sequences

RNA editing affects splicing

During formation of a dsRNA ADAR substrate, intronic cis-acting sequences can form RNA duplexes with splicing sites. ADARs can then modify select adenosines in splicing signals, resulting in the creation or elimination of splicing sites. The spliceosome recognizes inosine as guanosine in similar fashion to the translational machinery. A canonical 5' splice site (GU) and 3' acceptor site (AG) can be created via the deamination of AU to IU = GU and AA to AI = AG, respectively (Valente and Nishikura, 2005). Correspondingly, a canonical 3' splice site (AG) can be destroyed by RNA editing of AG to IG = GG (Valente and Nishikura, 2005). Mammalian ADAR2 edits its own transcript (auto-editing) leading to the generation of a novel 3' splice site, which results in the inclusion of 47 nucleotides (Rueter et al., 1999). The inclusion causes a decrease in ADAR2 protein expression due to a frameshift and translation from an internal but inefficient initiation site (Rueter et al., 1999). The regulation of *adar*2 transcript splicing via RNA editing represents a negative regulatory feedback mechanism to modulate

ADAR2 protein levels since inhibition of auto-editing *in vivo* increases ADAR2 expression and editing at many target adenosines in the transcriptome (Feng et al., 2006).

Specific A-to-I RNA editing of *Alu* elements

In primates, A-to-I editing predominantly occurs in *Alu* sequences (Athanasiadis et al., 2004; Kim et al., 2004) resulting in the diversification of the transcriptome (Paz-Yaacov et al. 2010). *Alu* transposable elements are mobile, short DNA sequences that constitute 10% of the human genome (Lander et al., 2001). Editing in these widespread genomic elements results in the posttranscriptional creation of splicing signals that leads to exonization (Athanasiadis et al., 2004). A-to-I editing in the human nuclear prelamin A recognition factor (NARF), generates a novel 3' splice site and alters the splicing enhancer signals (Lev-Maor et al., 2007). These post-transcriptional modifications are necessary for the inclusion of *Alu* elements in coding sequences in a tissue-specific manner (Lev-Maor et al., 2007). Furthermore, ADAR1 small RNA-mediated knockdown results in the aberrant exonization of *Alu* elements in a seryl-tRNA synthetase gene (SARS), suggesting that RNA editing could globally regulate *Alu* exonization events within the transcriptome (Sakurai et al. 2010). Thus, RNA editing in *Alu* elements may represent an evolutionary mechanism for generating novel functional proteins through the exaptation of transposed elements into protein domains (Moller-Krull et al., 2008).

Regulation of miRNA biogenesis and function through RNA editing

Select deamination of adenosines found in non-coding regions can influence the biogenesis and target recognition of small interfering RNAs (siRNAs) involved in RNA interference (RNAi) (Nishikura, 2006). Micro RNAs (miRNAs) are highly conserved ~18-20nt non-coding RNAs that mediate gene silencing and regulate diverse cellular processes including development, differentiation, and apoptosis (Bartel, 2004; Meister et al., 2004). Encoded within non-coding regions, hairpin miRNA structures (pri-miRNAs) are post-transcriptionally processed by Drosha, an RNAse III enzyme, in the nucleus to yield ~70nt double stranded miRNA precursors (pre-miRNAs) (Kim, 2005). Export of these precursors to the cytoplasm leads to further processing by Dicer to generate short RNA duplexes. Once loaded into a silencing complex, miRNAs guide degradation or translational repression of target mRNAs in a sequence specific manner (Bartel, 2004; Kim, 2005).

pri-miRNAs are fold-back dsRNA molecules which could serve as ADAR subtrates. Indeed, several miRNA precursors undergo A-to-I RNA editing at select adenosines (Blow et al., 2006; Luciano et al., 2004). ADAR2 null mice exhibit significantly higher levels of miR-142 compared to wild-type control mice (Yang et al., 2006). Editing of pri-miR-142 near the base of the hairpin inhibits Drosha cleavage, *in vitro* (Yang et al., 2006) (Fig. 1.10B). Furthermore, specific RNA editing of pre-miR-151 near the hairpin loop allows Drosha cleavage and nuclear export but inhibits Dicer cleavage, resulting in the accumulation of pre-miR-151 in the cytoplasm (Kawahara et

al., 2007a) (Fig. 1.10C). Editing of an adenosine within the miR-376 seed region is also sufficient to redirect silencing to a new target (Kawahara et al., 2007b) (Fig. 1.10D).

Consequences of promiscuous A-to-I RNA editing

Non-coding transcripts, sense-antisense RNA interactions, and exogenous RNAs can form long perfectly base-paired RNA duplexes that can serve as ADAR substrates (Bass, 2002; Nishikura, 2006). In these molecules, ADAR acts promiscuously resulting in up to 50% adenosine to inosine conversions (Nishikura et al., 1991; Polson and Bass, 1994). Promiscuous editing causes structural distortions that affect the stability of the dsRNA, given that I·U wobble base pairs are much less stable than Watson-Crick A-U base pairs (Serra et al., 2004). Inosine-rich dsRNAs (I-RNAs) have at least two fates; retention in the nucleus or cytoplasmic degradation.

Nuclear retention

Select nuclear dsRNA molecules undergo hyperediting, resulting in nuclear retention (Kumar and Carmichael, 1997). Synthetic I-RNAs are recognized and bound to $p54^{nrb}$, an inosine-specific dsRNA binding protein, initiating the formation of a protein complex with matrin-3, a nuclear matrix protein (Zhang and Carmichael, 2001). This complex may anchor I-RNAs to the nuclear matrix, regulating their export to the cytoplasm (Zhang and Carmichael, 2001). Analysis of *Alu* repeats in the 3'UTR of a reporter system revealed higher levels of A-to-I modifications in RNAs isolated from the

nucleus compared to those from the cytoplasm. In addition, nuclear-retained RNAs showed almost complete colocalization with $p54^{nrb}$ (Chen et al., 2008). These results suggest that hyperedited RNAs are retained in the nucleus due to their association with the $p54^{nrb}$ complex, thus inhibiting their translation.

The mouse cationic amino acid transporter 2 (CAT2) RNA is trapped within nuclear speckles and is only exported to the cytoplasm during stress (Prasanth et al., 2005). Interestingly, the 3'UTR of this RNA, which is required for nuclear retention, is edited at multiple adenosine residues. Whether editing affects the export of this RNA from the nucleus to the cytoplasm is still unclear.

Cellular defense

The cellular presence of long dsRNAs is commonly indicative of invading nucleic acid parasites such as viruses and can elicit a variety of cellular responses. One such response is the adenosine deamination mediated by ADARs. Hyperediting has been detected in different viral RNAs, including polyoma (Kumar and Carmichael, 1997), measles (Bass et al., 1989), human parainfluenza (Murphy et al., 1991), and hepatitis C (Taylor et al., 2005). In addition, an ADAR1 isoform present in the cytoplasm can be induced by interferon response (Patterson and Samuel, 1995), a feature of antiviral defense mechanisms. These observations led to the proposal that hyperediting may act as an antiviral defense mechanism. Indeed, editing of hepatitis C RNAs limits viral replication (Taylor et al., 2005). In addition, I-RNAs are recognized and degraded rapidly by Tudor staphylococcal nuclease (Tudor-SN) *in vitro* (Scadden, 2005). Thus,

hyperediting could represent an efficient cellular defense mechanism, for marking viral RNAs for degradation (Fig. 1.11B).

Regulation of RNA interference by ADARs

Viral infection, injection of dsRNA, and endogenous sources of dsRNAs all lead to the production of siRNAs that direct a sequence-specific silencing mechanism (Hannon, 2002). This phenomenon, also known as RNA interference, is evolutionarily conserved and regulates both gene expression and transposable element surveillance (Ghildiyal and Zamore, 2009). The biogenesis of siRNAs requires processing of long dsRNA structures by a class of RNase III-like ribonuclease enzymes, called Dicer (Bernstein et al., 2001). The siRNA duplexes generated by Dicer are unwound for the incorporation of a single-stranded RNA (guide RNA) into the RNA-induced silencing complex (RISC). Ultimately, the targeting of RISC by the small guide RNA initiates transcriptional and post-transcriptional sequence-specific silencing (Hannon, 2002).

C. elegans possess a potent RNAi response in most tissues. However, in neurons this silencing mechanism is much less efficient (Timmons et al., 2001). These observations suggest that neuronal cells possess a mechanism that inhibits RNAi. Both RNA editing and RNAi pathways involve dsRNAs, and ADAR modification of dsRNAs in neurons may antagonize the RNAi pathway at two levels. First, ADAR modification could alter the structure of dsRNA substrates leading to poor Dicer processing and thus decreased siRNA production. Second, RNA editing of siRNAs may prevent base pairing with mRNA targets, inhibiting the RISC cleavage step of RNAi (Nishikura, 2006).

siRNA biogenesis is progressively inhibited with increased RNA editing *in vitro* (Scadden and Smith, 2001a, b) (Fig 1.11B). In addition to I-RNAs being poor Dicer substrates, a single A-to-I modification in the mature siRNA may result in reduced RNAi efficacy (Scadden and Smith, 2001a, b). The *in vivo* functional consequences of ADAR's antagonistic effects on RNAi are still unclear.

ADAR1 and ADAR2 are catalytically active on dsRNAs *in vitro* (Gerber et al., 1997; Lai et al., 1997; Melcher et al., 1996b). However, ADAR3 is not capable of deaminating adenosine residues at previously known RNA editing sites or adenosine residues present in synthetic long RNA duplexes (Chen et al., 2000). These results suggest that the binding of ADAR enzymes to dsRNA molecules could have a wide range of biological functions, independent of enzymatic activity.

In vitro studies of synthetic 21-nt siRNA duplexes in electrophoretic mobility shift assays revealed that ADAR1p150 binds to siRNAs with high affinity independent of catalytic activity (Yang et al., 2005) (Fig 1.12). Sequestration of siRNA duplexes by ADAR results in a less potent RNAi response, and ADAR1 null cells exhibit more effective gene silencing by siRNAs when compared to wild-type cells (Yang et al., 2005). ADAR1 expression increases in mice injected with high doses of nonspecific siRNAs, suggesting that this is a feedback loop mechanism that regulates the cellular concentration of siRNAs through sequestration by ADAR (Hong et al., 2005). This feedback mechanism may represent a cellular immune response against the invasion of viral dsRNAs.

ADAR binding can also influence the fate of nuclear dsRNAs. Catalytically inactive ADAR2 inhibited Drosha cleavage of pri-miRNAs, resulting in a significant

reduction in mature miRNAs (Heale et al., 2009). These results suggest that ADAR binding can influence the RNAi pathway independent of catalytic activity.

Recent evidence suggests that ADAR interacts with the endogenous RNAi pathway in *Drosophila* (Kawamura et al., 2008). It was originally believed that endogenous small interfering RNAs (esiRNAs) were only present in organisms that possess RNA-dependent RNA polymerases (RDRPs). In plants,*C. elegans*, and fission yeast, RDRPs transcribe single-stranded RNA (ssRNA), generating dsRNA molecules that can be processed by Dicer for the biogenesis of esiRNAs (Okamura and Lai, 2008). However, genomic sources that encode for RNA duplexes can trigger the production of esiRNAs. In flies and mammals, both intramolecular and intermolecular dsRNAs can generate esiRNAs in somatic cells (Ghildiyal et al., 2008). These duplexes can be generated through transcription of transposons present in inverted orientation, convergent or bidirectional transcription, and trans-interactions between complementary RNAs (Ghildiyal and Zamore, 2009) (Fig 1.13). Purification and characterization of esiRNAs from *Drosophila* S2 cells revealed that the majority of esiRNAs are generated from transposable elements (TEs), suggesting that esiRNAs direct a somatic defense mechanism to repress TE activity (Kawamura et al., 2008). Indeed, mutations in or depletion of Dicer-2, the ribonuclease necessary for the biogenesis of esiRNAs, results in elevated levels of TE transcripts (Chung et al., 2008; Czech et al., 2008; Ghildiyal et al., 2008; Kawamura et al., 2008). In addition, a large number of esiRNAs possess adenosine to guanosine single nucleotide substitutions, suggesting that the endogenous dsRNA molecules that generate esiRNAs can serve as ADAR substrates (Kawamura et al., 2008). Although, the functional consequences of the interaction of RNA editing and esiRNA

silencing pathways are currently unknown, additional evidence suggests that ADARs could be involved in the regulation of heterochromatic gene silencing (Fagegaltier et al., 2009).

ADARs may regulate heterochromatic silencing

Drosophila pericentromeric regions are highly heterochromatic and interact with histone H3 methylation on lysine 9 (H3K9). This association recruits Heterochromatin Protein 1 (HP1) that initiates a silencing-spreading mechanism to neighboring genes (Ebert et al., 2006). Mutations of several proteins involved in the *Drosophila* Piwi RNAi pathway, which is involved in the suppression of TEs in the gonads, result in profound alterations in HP1 distribution on polytene chromosomes (Pal-Bhadra et al., 2004). In *S. pombe*, esiRNAs are involved in transcriptional gene silencing by directing the formation of heterochromatin (Martienssen et al., 2008), suggesting that the esiRNAs in *Drosophila* could serve similar roles. Over-expression of both the B2 and P19 proteins, viral suppressors of RNAi, result in the suppression of esiRNA biogenesis and activity in *Drosophila*. This leads to less potent heterochromatic silencing through alterations in the chromosomal distribution of both the histone methyl transferase Su(var)3-9 and HP1 (Fagegaltier et al., 2009). Therefore, esiRNAs may regulate heterochromatin formation in somatic tissues. The finding that ADAR targets esiRNA precursors indicates that the RNA editing pathway could regulate heterochromatic gene silencing by antagonizing both the biogenesis and activity of esiRNAs.

Further implicating the involvement of RNA editing in heterochromatic gene silencing, the dodeca-satellite binding protein 1 (DDP1) recognizes and binds I-RNAs in *Drosophila*. DDP1 associates with HP1 almost exclusively on polytene chromosomes in highly heterochromatic genomic regions, including telomeres and the chromocenter (Cortes et al., 1999). Elimination of DDP1 by RNAi in S2 cells results in several defects, including alterations in the structure of the chromocenter and mislocalization of HP1 (Wang et al., 2005). Furthermore, the mammalian homolog of DDP1, Vigulin, also binds to hyper-edited RNAs and forms a complex containing ADAR1, RNA helicase A (RHA), histone variant H2AX, and HP1 (Wang et al., 2005). Binding of Vigulin to hyperedited RNAs may direct this complex to select genomic loci, initiating heterochromatin formation (Zhou et al., 2008).

RNAi-dependent heterochromatin formation mediated by *1360* elements

Studies in *Drosophila* over the past two decades have accumulated a vast array of data characterizing the initiation and maintenance of heterochromatin. *Drosophila* chromosome 4, also known as the dot chromosome, has been the focus of such studies because it is highly heterochromatic (Riddle et al., 2009). Heterochromatin is considered to contain both high levels of transposable elements and low gene density, resulting in a compact DNA organization compared to euchromatin (Grewal and Elgin, 2007). These differences in chromatin organization are usually probed using position effect variegation (PEV), a phenomenon in which a euchromatic gene juxtaposed near a heterochromatic region is silenced (Locke et al., 1988). In *Drosophila*, PEV is monitored using

expression of a *white*$^{+}$ mini-gene reporter in eye ommatidia (Grewal and Elgin, 2007). A *white*$^{+}$ reporter that is fully expressed results in a red eye while the same reporter exhibits a variegating eye phenotype when stochastically silenced via heterochromatization (Fig. 1.14).

An investigation of the heterochromatic domains using PEV revealed that the dot chromosome is largely heterochromatic, but euchromatic domains also exist (Riddle et al., 2008). More importantly, a specific transposable element, the *1360*, was implicated in heterochromatin formation (Sun et al., 2004). A single copy of the *1360* element is capable of both initiating and spreading silencing at a neighboring promoter (Haynes et al., 2006), and reporters placed within 10 kb of a *1360* element can be silenced (Riddle et al., 2008). Interestingly, short RNA species that correspond to sense and antisense strands of *1360* elements are detected in KC cells, suggesting processing by the RNAi machinery (Haynes et al., 2006). Curiously, reporters are also silenced without having a *1360* element nearby, implicating additional transposable elements in the formation of heterochromatin. Given that transposable elements in the genome must be silenced because of their powerful mutagenic potential, any TE sequence could serve as a target for initiating heterochromatin formation.

Various heterochromatic proteins associate with the dot chromosome. Both proteins HP1 and H3K9 associate within heterochromatic regions in polytene chromosomes, including the telomeres, the chromocenter, and the dot chromosome (Cowell et al., 2002; Jacobs et al., 2001; James et al., 1989). The mechanisms for targeting these proteins to heterochromatic regions are still not well understood. Recent studies of RNAi and its role in transposon control suggest an attractive model of how

heterochromatin associated proteins can target repetitive DNA sequences to initiate heterochromatin formation. In particular, the germline-specific piRNA pathway is involved in the silencing of transposable elements (Aravin et al., 2007a; Aravin et al., 2007b). In *Drosophila*, Piwi-interacting small interfering RNAs (piRNAs) are thought to be generated from long single-stranded RNA transcripts derived from transposon-rich loci (Brennecke et al., 2007). The piRNAs could serve in the targeting of the heterochromatic machinery to specific loci and transposable elements within the genome. Indeed, *piwi* mutants are sterile due to deregulation of transposable elements, suggesting the importance of the piRNA pathway in the silencing of these elements in the germ line (Aravin et al., 2007a). Furthermore, mutations in *piwi* act as suppressors of variegation, suggesting a role for this pathway in heterochromatin formation (Haynes et al., 2006; Pal-Bhadra et al., 2004). Thus, an inefficient RNAi response could lead to deregulation of hererochromatic domains, resulting in the activation of TEs.

In somatic cells esiRNAs silence transposable elements in a similar fashion to piRNAs in the germ line. Mutations in genes involved in the biogenesis or activity of the esiRNAi pathway act as suppressors of PEV, suggesting that this pathway also directs the formation of heterochromatin (Fagegaltier et al., 2009). One major difference between these two RNAi pathways is that esiRNAs arise from dsRNA molecules, whereas piRNAs arise from single-stranded transcripts. ADARs may target these dsRNA molecules in the nervous system, thus antagonizing the RNAi response. The observation that edited esiRNAs are occupying active RISC complexes (Kawamura et al., 2008) suggests that ADARs may potentially affect transposon silencing by regulating heterochromatin formation.

Open questions and current motivations for this study

Diverse RNA editing systems are functionally active throughout metazoan transcriptomes (Bass, 2001). Intriguingly, the adenosine to inosine (A-to-I) RNA editing system, which is catalyzed by ADARs, is particularly active in the brain of higher eukaryotes (Nishikura, 2010). In previous sections of this work I emphasize the progress thus far achieved in ADAR biology including the identification of coding and non-coding RNA editing targets, the crystallization of the catalytic domain, the identification of their mechanistic preferences and specificities for site selective editing, and the consequences of specific and promiscuous editing in RNA transcripts. Furthermore, generation of ADAR deficiencies in various genetic model systems highlights an important role for these enzymes in the functioning of the nervous system (Higuchi et al., 2000; Palladino et al., 2000a; Tonkin et al., 2002).

Although much progress has been made in the A-to-I RNA editing field over the last two decades, significant questions remain in our mechanistic understanding of how ADAR activity in the nervous system regulates both behavioral outputs and organismal fitness. *Drosophila* provides an ideal genetic system to study A-to-I RNA editing due to the presence of a single *adar* locus (Palladino et al., 2000b) In addition, an abundance of known target adenosines are present in a host of mRNAs encoding ion channels and pre-synaptic release proteins (Hoopengardner et al., 2003). Furthermore, recent advances in the use of genetic techniques, such as ends-out homologous recombination, allow precise *in vivo* engineering of the *Drosophila* genome.

dADAR transcripts are detected predominately in the brain of both *Drosophila* embryos and adults (Ma et al., 2002; Palladino et al., 2000b). However, the complete ADAR expression and cellular distribution pattern in the adult nervous system is still unknown. The lack of a commercially available antibody has hindered our understanding on this subject. Furthermore, although previous studies using two substrates suggest that dADAR auto-editing acts to reduce its own catalytic activity *in vitro* (Keegan et al., 2005), it's *in vivo* consequences regarding the global regulation of the fly inosinome and adult-stage behaviors are still unknown. Lastly, several lines of evidence indicate that ADARs can antagonize RNAi-mediated gene silencing (Nishikura, 2006). Editing of endogenous small interfering RNAs in flies (Kawamura et al., 2008) suggests that ADARs interact with the endogenous RNAi pathway. The consequences, however, of such interactions and their effect on both gene expression and transposable element regulation in neuronal transcriptomes remain enigmatic.

In this study I will use ends-out homologous recombination to address these issues, including defining the detailed expression profile of dADAR in the adult fly nervous system, the *in vivo* consequences of dADAR auto-editing on mRNA recoding and organismal behavior, and the regulation of heterochromatin formation by dADAR. The following chapters of this thesis substantially augment our understanding of the mechanisms regulating dADAR activity and how these processes contribute to *Drosophila* physiology and behavior. Lastly, I will provide evidence that ADARs interact with transposable element transcripts and demonstrate that this interaction can regulate heterochromatin formation *in vivo*. The research here highlights a more global function

for RNA editing regarding neuronal transcriptomic regulation and emphasizes its pivotal role in organismal fitness.

REFERENCES

Adams, M.D., Celniker, S.E., Holt, R.A., Evans, C.A., Gocayne, J.D., Amanatides, P.G., Scherer, S.E., Li, P.W., Hoskins, R.A., Galle, R.F., *et al.* (2000). The genome sequence of Drosophila melanogaster. Science (New York, NY *287*, 2185-2195.

Alt, F.W., Bothwell, A.L., Knapp, M., Siden, E., Mather, E., Koshland, M., and Baltimore, D. (1980). Synthesis of secreted and membrane-bound immunoglobulin mu heavy chains is directed by mRNAs that differ at their 3' ends. Cell *20*, 293-301.

Aravin, A.A., Hannon, G.J., and Brennecke, J. (2007a). The Piwi-piRNA pathway provides an adaptive defense in the transposon arms race. Science (New York, NY *318*, 761-764.

Aravin, A.A., Sachidanandam, R., Girard, A., Fejes-Toth, K., and Hannon, G.J. (2007b). Developmentally regulated piRNA clusters implicate MILI in transposon control. Science (New York, NY *316*, 744-747.

Athanasiadis, A., Rich, A., and Maas, S. (2004). Widespread A-to-I RNA editing of Alu-containing mRNAs in the human transcriptome. PLoS biology *2*, e391.

Baltimore, D. (2001). Our genome unveiled. Nature *409*, 814-816.

Bartel, D.P. (2004). MicroRNAs: genomics, biogenesis, mechanism, and function. Cell *116*, 281-297.

Basillo, C., Wahba, A., Lengyel, P., Speyer, J., and Ochoa, S. (1962). Synthetic polynucleotides and the amino acid code. V. Proceedings of the National Academy of Sciences of the United States of America *48*, 613-616.

Bass, B.L. (2001). RNA Editing. Oxford University Press, 94-95.

Bass, B.L. (2002). RNA editing by adenosine deaminases that act on RNA. Annual review of biochemistry *71*, 817-846.

Bass, B.L., and Weintraub, H. (1987). A developmentally regulated activity that unwinds RNA duplexes. Cell *48*, 607-613.

Bass, B.L., and Weintraub, H. (1988). An unwinding activity that covalently modifies its double-stranded RNA substrate. Cell *55*, 1089-1098.

Bass, B.L., Weintraub, H., Cattaneo, R., and Billeter, M.A. (1989). Biased hypermutation of viral RNA genomes could be due to unwinding/modification of double-stranded RNA. Cell *56*, 331.

Bernstein, E., Caudy, A.A., Hammond, S.M., and Hannon, G.J. (2001). Role for a bidentate ribonuclease in the initiation step of RNA interference. Nature *409*, 363-366.

Bhalla, T., Rosenthal, J.J., Holmgren, M., and Reenan, R. (2004). Control of human potassium channel inactivation by editing of a small mRNA hairpin. Nature structural & molecular biology *11*, 950-956.

Blow, M.J., Grocock, R.J., van Dongen, S., Enright, A.J., Dicks, E., Futreal, P.A., Wooster, R., and Stratton, M.R. (2006). RNA editing of human microRNAs. Genome biology *7*, R27.

Brennecke, J., Aravin, A.A., Stark, A., Dus, M., Kellis, M., Sachidanandam, R., and Hannon, G.J. (2007). Discrete small RNA-generating loci as master regulators of transposon activity in Drosophila. Cell *128*, 1089-1103.

Burns, C.M., Chu, H., Rueter, S.M., Hutchinson, L.K., Canton, H., Sanders-Bush, E., and Emeson, R.B. (1997). Regulation of serotonin-2C receptor G-protein coupling by RNA editing. Nature *387*, 303-308.

Bycroft, M., Grunert, S., Murzin, A.G., Proctor, M., and St Johnston, D. (1995). NMR solution structure of a dsRNA binding domain from Drosophila staufen protein reveals homology to the N-terminal domain of ribosomal protein S5. The EMBO journal *14*, 3563-3571.

C. elegans Sequencing Consortium (1998). Genome sequence of the nematode C. elegans: a platform for investigating biology. Science (New York, NY *282*, 2012-2018.

Chen, C.X., Cho, D.S., Wang, Q., Lai, F., Carter, K.C., and Nishikura, K. (2000). A third member of the RNA-specific adenosine deaminase gene family, ADAR3, contains both single- and double-stranded RNA binding domains. RNA (New York, NY *6*, 755-767.

Chen, L.L., DeCerbo, J.N., and Carmichael, G.G. (2008). Alu element-mediated gene silencing. The EMBO journal *27*, 1694-1705.

Chilibeck, K.A., Wu, T., Liang, C., Schellenberg, M.J., Gesner, E.M., Lynch, J.M., and MacMillan, A.M. (2006). FRET analysis of in vivo dimerization by RNA-editing enzymes. The Journal of biological chemistry *281*, 16530-16535.

Cho, D.S., Yang, W., Lee, J.T., Shiekhattar, R., Murray, J.M., and Nishikura, K. (2003). Requirement of dimerization for RNA editing activity of adenosine deaminases acting on RNA. The Journal of biological chemistry *278*, 17093-17102.

Chung, W.J., Okamura, K., Martin, R., and Lai, E.C. (2008). Endogenous RNA interference provides a somatic defense against Drosophila transposons. Curr Biol *18*, 795-802.

Clamp, M., Fry, B., Kamal, M., Xie, X., Cuff, J., Lin, M.F., Kellis, M., Lindblad-Toh, K., and Lander, E.S. (2007). Distinguishing protein-coding and noncoding genes in the human genome. Proceedings of the National Academy of Sciences of the United States of America *104*, 19428-19433.

Cortes, A., Huertas, D., Fanti, L., Pimpinelli, S., Marsellach, F.X., Pina, B., and Azorin, F. (1999). DDP1, a single-stranded nucleic acid-binding protein of Drosophila, associates with pericentric heterochromatin and is functionally homologous to the yeast Scp160p, which is involved in the control of cell ploidy. The EMBO journal *18*, 3820-3833.

Cowell, I.G., Aucott, R., Mahadevaiah, S.K., Burgoyne, P.S., Huskisson, N., Bongiorni, S., Prantera, G., Fanti, L., Pimpinelli, S., Wu, R., *et al.* (2002). Heterochromatin, HP1 and methylation at lysine 9 of histone H3 in animals. Chromosoma *111*, 22-36.

Crick, F.H. (1958). On protein synthesis. Symposia of the Society for Experimental Biology *12*, 138-163.

Czech, B., Malone, C.D., Zhou, R., Stark, A., Schlingeheyde, C., Dus, M., Perrimon, N., Kellis, M., Wohlschlegel, J.A., Sachidanandam, R., *et al.* (2008). An endogenous small interfering RNA pathway in Drosophila. Nature *453*, 798-802.

Desterro, J.M., Keegan, L.P., Lafarga, M., Berciano, M.T., O'Connell, M., and Carmo-Fonseca, M. (2003). Dynamic association of RNA-editing enzymes with the nucleolus. Journal of cell science *116*, 1805-1818.

Dingledine, R., Borges, K., Bowie, D., and Traynelis, S.F. (1999). The glutamate receptor ion channels. Pharmacological reviews *51*, 7-61.

Early, P., Rogers, J., Davis, M., Calame, K., Bond, M., Wall, R., and Hood, L. (1980). Two mRNAs can be produced from a single immunoglobulin mu gene by alternative RNA processing pathways. Cell *20*, 313-319.

Ebert, A., Lein, S., Schotta, G., and Reuter, G. (2006). Histone modification and the control of heterochromatic gene silencing in Drosophila. Chromosome Res *14*, 377-392.

Fagegaltier, D., Bouge, A.L., Berry, B., Poisot, E., Sismeiro, O., Coppee, J.Y., Theodore, L., Voinnet, O., and Antoniewski, C. (2009). The endogenous siRNA pathway is involved in heterochromatin formation in Drosophila. Proceedings of the National Academy of Sciences of the United States of America *106*, 21258-21263.

Feng, Y., Sansam, C.L., Singh, M., and Emeson, R.B. (2006). Altered RNA editing in mice lacking ADAR2 autoregulation. Molecular and cellular biology *26*, 480-488.

Gallo, A., Keegan, L.P., Ring, G.M., and O'Connell, M.A. (2003). An ADAR that edits transcripts encoding ion channel subunits functions as a dimer. The EMBO journal *22*, 3421-3430.

Gerber, A., O'Connell, M.A., and Keller, W. (1997). Two forms of human double-stranded RNA-specific editase 1 (hRED1) generated by the insertion of an Alu cassette. RNA (New York, NY *3*, 453-463.

Gerber, A.P., and Keller, W. (1999). An adenosine deaminase that generates inosine at the wobble position of tRNAs. Science (New York, NY *286*, 1146-1149.

Gerber, A.P., and Keller, W. (2001). RNA editing by base deamination: more enzymes, more targets, new mysteries. Trends in biochemical sciences *26*, 376-384.

Ghildiyal, M., Seitz, H., Horwich, M.D., Li, C., Du, T., Lee, S., Xu, J., Kittler, E.L., Zapp, M.L., Weng, Z., *et al.* (2008). Endogenous siRNAs derived from transposons and mRNAs in Drosophila somatic cells. Science (New York, NY *320*, 1077-1081.

Ghildiyal, M., and Zamore, P.D. (2009). Small silencing RNAs: an expanding universe. Nat Rev Genet *10*, 94-108.

Graveley, B.R., Brooks, A.N., Carlson, J.W., Duff, M.O., Landolin, J.M., Yang, L., Artieri, C.G., van Baren, M.J., Boley, N., Booth, B.W., *et al.* (2010). The developmental transcriptome of Drosophila melanogaster. Nature.

Greger, I.H., Khatri, L., and Ziff, E.B. (2002). RNA editing at arg607 controls AMPA receptor exit from the endoplasmic reticulum. Neuron *34*, 759-772.

Grewal, S.I., and Elgin, S.C. (2007). Transcription and RNA interference in the formation of heterochromatin. Nature *447*, 399-406.

Hanakahi, L.A., and West, S.C. (2002). Specific interaction of IP6 with human Ku70/80, the DNA-binding subunit of DNA-PK. The EMBO journal *21*, 2038-2044.

Hannon, G.J. (2002). RNA interference. Nature *418*, 244-251.

Hanrahan, C.J., Palladino, M.J., Ganetzky, B., and Reenan, R.A. (2000). RNA editing of the Drosophila para Na(+) channel transcript. Evolutionary conservation and developmental regulation. Genetics *155*, 1149-1160.

Haynes, K.A., Caudy, A.A., Collins, L., and Elgin, S.C. (2006). Element 1360 and RNAi components contribute to HP1-dependent silencing of a pericentric reporter. Curr Biol *16*, 2222-2227.

Heale, B.S., Keegan, L.P., McGurk, L., Michlewski, G., Brindle, J., Stanton, C.M., Caceres, J.F., and O'Connell, M.A. (2009). Editing independent effects of ADARs on the miRNA/siRNA pathways. The EMBO journal *28*, 3145-3156.

Higuchi, M., Maas, S., Single, F.N., Hartner, J., Rozov, A., Burnashev, N., Feldmeyer, D., Sprengel, R., and Seeburg, P.H. (2000). Point mutation in an AMPA receptor gene

rescues lethality in mice deficient in the RNA-editing enzyme ADAR2. Nature *406*, 78-81.

Higuchi, M., Single, F.N., Kohler, M., Sommer, B., Sprengel, R., and Seeburg, P.H. (1993). RNA editing of AMPA receptor subunit GluR-B: a base-paired intron-exon structure determines position and efficiency. Cell *75*, 1361-1370.

Hong, J., Qian, Z., Shen, S., Min, T., Tan, C., Xu, J., Zhao, Y., and Huang, W. (2005). High doses of siRNAs induce eri-1 and adar-1 gene expression and reduce the efficiency of RNA interference in the mouse. The Biochemical journal *390*, 675-679.

Hoopengardner, B., Bhalla, T., Staber, C., and Reenan, R. (2003). Nervous system targets of RNA editing identified by comparative genomics. Science (New York, NY *301*, 832-836.

Hoyer, D., Hannon, J.P., and Martin, G.R. (2002). Molecular, pharmacological and functional diversity of 5-HT receptors. Pharmacology, biochemistry, and behavior *71*, 533-554.

Ingleby, L., Maloney, R., Jepson, J., Horn, R., and Reenan, R. (2009). Regulated RNA editing and functional epistasis in Shaker potassium channels. The Journal of general physiology *133*, 17-27.

Jacobs, S.A., Taverna, S.D., Zhang, Y., Briggs, S.D., Li, J., Eissenberg, J.C., Allis, C.D., and Khorasanizadeh, S. (2001). Specificity of the HP1 chromo domain for the methylated N-terminus of histone H3. The EMBO journal *20*, 5232-5241.

James, T.C., Eissenberg, J.C., Craig, C., Dietrich, V., Hobson, A., and Elgin, S.C. (1989). Distribution patterns of HP1, a heterochromatin-associated nonhistone chromosomal protein of Drosophila. European journal of cell biology *50*, 170-180.

Jepson, J.E., and Reenan, R.A. (2009). Adenosine-to-inosine genetic recoding is required in the adult stage nervous system for coordinated behavior in Drosophila. The Journal of biological chemistry *284*, 31391-31400.

Jin, Y., Zhang, W., and Li, Q. (2009). Origins and evolution of ADAR-mediated RNA editing. IUBMB life *61*, 572-578.

Kawahara, Y., Zinshteyn, B., Chendrimada, T.P., Shiekhattar, R., and Nishikura, K. (2007a). RNA editing of the microRNA-151 precursor blocks cleavage by the Dicer-TRBP complex. EMBO reports *8*, 763-769.

Kawahara, Y., Zinshteyn, B., Sethupathy, P., Iizasa, H., Hatzigeorgiou, A.G., and Nishikura, K. (2007b). Redirection of silencing targets by adenosine-to-inosine editing of miRNAs. Science (New York, NY *315*, 1137-1140.

Kawamura, Y., Saito, K., Kin, T., Ono, Y., Asai, K., Sunohara, T., Okada, T.N., Siomi, M.C., and Siomi, H. (2008). Drosophila endogenous small RNAs bind to Argonaute 2 in somatic cells. Nature *453*, 793-797.

Keegan, L.P., Brindle, J., Gallo, A., Leroy, A., Reenan, R.A., and O'Connell, M.A. (2005). Tuning of RNA editing by ADAR is required in Drosophila. The EMBO journal *24*, 2183-2193.

Kim, D.D., Kim, T.T., Walsh, T., Kobayashi, Y., Matise, T.C., Buyske, S., and Gabriel, A. (2004). Widespread RNA editing of embedded alu elements in the human transcriptome. Genome research *14*, 1719-1725.

Kim, U., Garner, T.L., Sanford, T., Speicher, D., Murray, J.M., and Nishikura, K. (1994a). Purification and characterization of double-stranded RNA adenosine deaminase from bovine nuclear extracts. The Journal of biological chemistry *269*, 13480-13489.

Kim, U., Wang, Y., Sanford, T., Zeng, Y., and Nishikura, K. (1994b). Molecular cloning of cDNA for double-stranded RNA adenosine deaminase, a candidate enzyme for nuclear RNA editing. Proceedings of the National Academy of Sciences of the United States of America *91*, 11457-11461.

Kim, V.N. (2005). MicroRNA biogenesis: coordinated cropping and dicing. Nature reviews *6*, 376-385.

Kornblihtt, A.R., de la Mata, M., Fededa, J.P., Munoz, M.J., and Nogues, G. (2004). Multiple links between transcription and splicing. RNA (New York, NY *10*, 1489-1498.

Kumar, M., and Carmichael, G.G. (1997). Nuclear antisense RNA induces extensive adenosine modifications and nuclear retention of target transcripts. Proceedings of the National Academy of Sciences of the United States of America *94*, 3542-3547.

Lai, F., Chen, C.X., Carter, K.C., and Nishikura, K. (1997). Editing of glutamate receptor B subunit ion channel RNAs by four alternatively spliced DRADA2 double-stranded RNA adenosine deaminases. Molecular and cellular biology *17*, 2413-2424.

Lander, E.S., Linton, L.M., Birren, B., Nusbaum, C., Zody, M.C., Baldwin, J., Devon, K., Dewar, K., Doyle, M., FitzHugh, W., *et al.* (2001). Initial sequencing and analysis of the human genome. Nature *409*, 860-921.

Lau, P.P., Zhu, H.J., Baldini, A., Charnsangavej, C., and Chan, L. (1994). Dimeric structure of a human apolipoprotein B mRNA editing protein and cloning and chromosomal localization of its gene. Proceedings of the National Academy of Sciences of the United States of America *91*, 8522-8526.

Lehmann, K.A., and Bass, B.L. (2000). Double-stranded RNA adenosine deaminases ADAR1 and ADAR2 have overlapping specificities. Biochemistry *39*, 12875-12884.

Lev-Maor, G., Sorek, R., Levanon, E.Y., Paz, N., Eisenberg, E., and Ast, G. (2007). RNA-editing-mediated exon evolution. Genome biology *8*, R29.

Li, J.B., Levanon, E.Y., Yoon, J.K., Aach, J., Xie, B., Leproust, E., Zhang, K., Gao, Y., and Church, G.M. (2009). Genome-wide identification of human RNA editing sites by parallel DNA capturing and sequencing. Science (New York, NY *324*, 1210-1213.

Locke, J., Kotarski, M.A., and Tartof, K.D. (1988). Dosage-dependent modifiers of position effect variegation in Drosophila and a mass action model that explains their effect. Genetics *120*, 181-198.

Lomeli, H., Mosbacher, J., Melcher, T., Hoger, T., Geiger, J.R., Kuner, T., Monyer, H., Higuchi, M., Bach, A., and Seeburg, P.H. (1994). Control of kinetic properties of AMPA receptor channels by nuclear RNA editing. Science (New York, NY *266*, 1709-1713.

Loughney, K., Kreber, R., and Ganetzky, B. (1989). Molecular analysis of the para locus, a sodium channel gene in Drosophila. Cell *58*, 1143-1154.

Luciano, D.J., Mirsky, H., Vendetti, N.J., and Maas, S. (2004). RNA editing of a miRNA precursor. RNA (New York, NY *10*, 1174-1177.

Ma, E., Gu, X.Q., Wu, X., Xu, T., and Haddad, G.G. (2001). Mutation in pre-mRNA adenosine deaminase markedly attenuates neuronal tolerance to O2 deprivation in Drosophila melanogaster. The Journal of clinical investigation *107*, 685-693.

Ma, E., Tucker, M.C., Chen, Q., and Haddad, G.G. (2002). Developmental expression and enzymatic activity of pre-mRNA deaminase in Drosophila melanogaster. Brain research *102*, 100-104.

Macbeth, M.R., Schubert, H.L., Vandemark, A.P., Lingam, A.T., Hill, C.P., and Bass, B.L. (2005). Inositol hexakisphosphate is bound in the ADAR2 core and required for RNA editing. Science (New York, NY *309*, 1534-1539.

MacGinnitie, A.J., Anant, S., and Davidson, N.O. (1995). Mutagenesis of apobec-1, the catalytic subunit of the mammalian apolipoprotein B mRNA editing enzyme, reveals distinct domains that mediate cytosine nucleoside deaminase, RNA binding, and RNA editing activity. The Journal of biological chemistry *270*, 14768-14775.

Maniatis, T., and Reed, R. (2002). An extensive network of coupling among gene expression machines. Nature *416*, 499-506.

Martienssen, R.A., Kloc, A., Slotkin, R.K., and Tanurdzic, M. (2008). Epigenetic inheritance and reprogramming in plants and fission yeast. Cold Spring Harbor symposia on quantitative biology *73*, 265-271.

Meister, G., Landthaler, M., Dorsett, Y., and Tuschl, T. (2004). Sequence-specific inhibition of microRNA- and siRNA-induced RNA silencing. RNA (New York, NY *10*, 544-550.

Melcher, T., Maas, S., Herb, A., Sprengel, R., Higuchi, M., and Seeburg, P.H. (1996a). RED2, a brain-specific member of the RNA-specific adenosine deaminase family. The Journal of biological chemistry *271*, 31795-31798.

Melcher, T., Maas, S., Herb, A., Sprengel, R., Seeburg, P.H., and Higuchi, M. (1996b). A mammalian RNA editing enzyme. Nature *379*, 460-464.

Miller, C. (2000). An overview of the potassium channel family. Genome biology *1*, REVIEWS0004.

Moller-Krull, M., Zemann, A., Roos, C., Brosius, J., and Schmitz, J. (2008). Beyond DNA: RNA editing and steps toward Alu exonization in primates. Journal of molecular biology *382*, 601-609.

Murphy, D.G., Dimock, K., and Kang, C.Y. (1991). Numerous transitions in human parainfluenza virus 3 RNA recovered from persistently infected cells. Virology *181*, 760-763.

Nanduri, S., Carpick, B.W., Yang, Y., Williams, B.R., and Qin, J. (1998). Structure of the double-stranded RNA-binding domain of the protein kinase PKR reveals the molecular basis of its dsRNA-mediated activation. The EMBO journal *17*, 5458-5465.

Navaratnam, N., Fujino, T., Bayliss, J., Jarmuz, A., How, A., Richardson, N., Somasekaram, A., Bhattacharya, S., Carter, C., and Scott, J. (1998). Escherichia coli cytidine deaminase provides a molecular model for ApoB RNA editing and a mechanism for RNA substrate recognition. Journal of molecular biology *275*, 695-714.

Nilsen, T.W., and Graveley, B.R. (2010). Expansion of the eukaryotic proteome by alternative splicing. Nature *463*, 457-463.

Nishikura, K. (2010). Functions and regulation of RNA editing by ADAR deaminases. Annual review of biochemistry *79*, 321-349.

Nishikura, K. (2006). Editor meets silencer: crosstalk between RNA editing and RNA interference. Nature reviews *7*, 919-931.

Nishikura, K., Yoo, C., Kim, U., Murray, J.M., Estes, P.A., Cash, F.E., and Liebhaber, S.A. (1991). Substrate specificity of the dsRNA unwinding/modifying activity. The EMBO journal *10*, 3523-3532.

Niswender, C.M., Copeland, S.C., Herrick-Davis, K., Emeson, R.B., and Sanders-Bush, E. (1999). RNA editing of the human serotonin 5-hydroxytryptamine 2C receptor silences constitutive activity. The Journal of biological chemistry *274*, 9472-9478.

O'Connell, M.A., and Keller, W. (1994). Purification and properties of double-stranded RNA-specific adenosine deaminase from calf thymus. Proceedings of the National Academy of Sciences of the United States of America *91*, 10596-10600.

O'Connell, M.A., Krause, S., Higuchi, M., Hsuan, J.J., Totty, N.F., Jenny, A., and Keller, W. (1995). Cloning of cDNAs encoding mammalian double-stranded RNA-specific adenosine deaminase. Molecular and cellular biology *15*, 1389-1397.

Ohlson, J., Pedersen, J.S., Haussler, D., and Ohman, M. (2007). Editing modifies the GABA(A) receptor subunit alpha3. RNA (New York, NY *13*, 698-703.

Okamura, K., and Lai, E.C. (2008). Endogenous small interfering RNAs in animals. Nature reviews *9*, 673-678.

Pal-Bhadra, M., Leibovitch, B.A., Gandhi, S.G., Rao, M., Bhadra, U., Birchler, J.A., and Elgin, S.C. (2004). Heterochromatic silencing and HP1 localization in Drosophila are dependent on the RNAi machinery. Science (New York, NY *303*, 669-672.

Palladino, M.J., Keegan, L.P., O'Connell, M.A., and Reenan, R.A. (2000a). A-to-I pre-mRNA editing in Drosophila is primarily involved in adult nervous system function and integrity. Cell *102*, 437-449.

Palladino, M.J., Keegan, L.P., O'Connell, M.A., and Reenan, R.A. (2000b). dADAR, a Drosophila double-stranded RNA-specific adenosine deaminase is highly developmentally regulated and is itself a target for RNA editing. RNA (New York, NY *6*, 1004-1018.

Pan, Q., Shai, O., Lee, L.J., Frey, B.J., and Blencowe, B.J. (2008). Deep surveying of alternative splicing complexity in the human transcriptome by high-throughput sequencing. Nature genetics *40*, 1413-1415.

Patterson, J.B., and Samuel, C.E. (1995). Expression and regulation by interferon of a double-stranded-RNA-specific adenosine deaminase from human cells: evidence for two forms of the deaminase. Molecular and cellular biology *15*, 5376-5388.

Patton, D.E., Silva, T., and Bezanilla, F. (1997). RNA editing generates a diverse array of transcripts encoding squid Kv2 K+ channels with altered functional properties. Neuron *19*, 711-722.

Paz-Yaacov, N., Levanon, E.Y., Nevo, E., Kinar, Y., Harmelin, A., Jacob-Hirsch, J., Amariglio, N., Eisenberg, E., and Rechavi, G. (2010). Adenosine-to-inosine RNA editing

shapes transcriptome diversity in primates. Proceedings of the National Academy of Sciences of the United States of America *107*, 12174-12179.

Polson, A.G., and Bass, B.L. (1994). Preferential selection of adenosines for modification by double-stranded RNA adenosine deaminase. The EMBO journal *13*, 5701-5711.

Pongs, O. (1999). Voltage-gated potassium channels: from hyperexcitability to excitement. FEBS letters *452*, 31-35.

Poulsen, H., Nilsson, J., Damgaard, C.K., Egebjerg, J., and Kjems, J. (2001). CRM1 mediates the export of ADAR1 through a nuclear export signal within the Z-DNA binding domain. Molecular and cellular biology *21*, 7862-7871.

Prasanth, K.V., Prasanth, S.G., Xuan, Z., Hearn, S., Freier, S.M., Bennett, C.F., Zhang, M.Q., and Spector, D.L. (2005). Regulating gene expression through RNA nuclear retention. Cell *123*, 249-263.

Rebagliati, M.R., and Melton, D.A. (1987). Antisense RNA injections in fertilized frog eggs reveal an RNA duplex unwinding activity. Cell *48*, 599-605.

Reenan, R.A. (2005). Molecular determinants and guided evolution of species-specific RNA editing. Nature *434*, 409-413.

Reenan, R.A., Hanrahan, C.J., and Ganetzky, B. (2000). The mle(napts) RNA helicase mutation in drosophila results in a splicing catastrophe of the para Na+ channel transcript in a region of RNA editing. Neuron *25*, 139-149.

Riddle, N.C., Leung, W., Haynes, K.A., Granok, H., Wuller, J., and Elgin, S.C. (2008). An investigation of heterochromatin domains on the fourth chromosome of Drosophila melanogaster. Genetics *178*, 1177-1191.

Riddle, N.C., Shaffer, C.D., and Elgin, S.C. (2009). A lot about a little dot - lessons learned from Drosophila melanogaster chromosome 4. Biochemistry and cell biology = Biochimie et biologie cellulaire *87*, 229-241.

Rosenthal, J.J., and Bezanilla, F. (2002). Extensive editing of mRNAs for the squid delayed rectifier K+ channel regulates subunit tetramerization. Neuron *34*, 743-757.

Rueter, S.M., Dawson, T.R., and Emeson, R.B. (1999). Regulation of alternative splicing by RNA editing. Nature *399*, 75-80.

Ryman, K., Fong, N., Bratt, E., Bentley, D.L., and Ohman, M. (2007). The C-terminal domain of RNA Pol II helps ensure that editing precedes splicing of the GluR-B transcript. RNA (New York, NY *13*, 1071-1078.

Ryter, J.M., and Schultz, S.C. (1998). Molecular basis of double-stranded RNA-protein interactions: structure of a dsRNA-binding domain complexed with dsRNA. The EMBO journal *17*, 7505-7513.

Sakurai, M., Yano, T., Kawabata, H., Ueda, H., and Suzuki, T. (2010). Inosine cyanoethylation identifies A-to-I RNA editing sites in the human transcriptome. Nature chemical biology *6*, 733-740.

Sansam, C.L., Wells, K.S., and Emeson, R.B. (2003). Modulation of RNA editing by functional nucleolar sequestration of ADAR2. Proceedings of the National Academy of Sciences of the United States of America *100*, 14018-14023.

Scadden, A.D. (2005). The RISC subunit Tudor-SN binds to hyper-edited double-stranded RNA and promotes its cleavage. Nature structural & molecular biology *12*, 489-496.

Scadden, A.D., and Smith, C.W. (2001a). RNAi is antagonized by A-->I hyper-editing. EMBO reports *2*, 1107-1111.

Scadden, A.D., and Smith, C.W. (2001b). Specific cleavage of hyper-edited dsRNAs. The EMBO journal *20*, 4243-4252.

Schmucker, D., Clemens, J.C., Shu, H., Worby, C.A., Xiao, J., Muda, M., Dixon, J.E., and Zipursky, S.L. (2000). Drosophila Dscam is an axon guidance receptor exhibiting extraordinary molecular diversity. Cell *101*, 671-684.

Seeburg, P.H., and Hartner, J. (2003). Regulation of ion channel/neurotransmitter receptor function by RNA editing. Current opinion in neurobiology *13*, 279-283.

Seeburg, P.H., Single, F., Kuner, T., Higuchi, M., and Sprengel, R. (2001). Genetic manipulation of key determinants of ion flow in glutamate receptor channels in the mouse. Brain research *907*, 233-243.

Serra, M.J., Smolter, P.E., and Westhof, E. (2004). Pronounced instability of tandem IU base pairs in RNA. Nucleic acids research *32*, 1824-1828.

Shen, X., Xiao, H., Ranallo, R., Wu, W.H., and Wu, C. (2003). Modulation of ATP-dependent chromatin-remodeling complexes by inositol polyphosphates. Science (New York, NY *299*, 112-114.

Sun, F.L., Haynes, K., Simpson, C.L., Lee, S.D., Collins, L., Wuller, J., Eissenberg, J.C., and Elgin, S.C. (2004). cis-Acting determinants of heterochromatin formation on Drosophila melanogaster chromosome four. Molecular and cellular biology *24*, 8210-8220.

Taylor, D.R., Puig, M., Darnell, M.E., Mihalik, K., and Feinstone, S.M. (2005). New antiviral pathway that mediates hepatitis C virus replicon interferon sensitivity through ADAR1. Journal of virology *79*, 6291-6298.

Thackeray, J.R., and Ganetzky, B. (1994). Developmentally regulated alternative splicing generates a complex array of Drosophila para sodium channel isoforms. J Neurosci *14*, 2569-2578.

Timmons, L., Court, D.L., and Fire, A. (2001). Ingestion of bacterially expressed dsRNAs can produce specific and potent genetic interference in Caenorhabditis elegans. Gene *263*, 103-112.

Tonkin, L.A., and Bass, B.L. (2003). Mutations in RNAi rescue aberrant chemotaxis of ADAR mutants. Science (New York, NY *302*, 1725.

Tonkin, L.A., Saccomanno, L., Morse, D.P., Brodigan, T., Krause, M., and Bass, B.L. (2002). RNA editing by ADARs is important for normal behavior in Caenorhabditis elegans. The EMBO journal *21*, 6025-6035.

Valente, L., and Nishikura, K. (2005). ADAR gene family and A-to-I RNA editing: diverse roles in posttranscriptional gene regulation. Progress in nucleic acid research and molecular biology *79*, 299-338.

Valente, L., and Nishikura, K. (2007). RNA binding-independent dimerization of adenosine deaminases acting on RNA and dominant negative effects of nonfunctional subunits on dimer functions. The Journal of biological chemistry *282*, 16054-16061.

Wagner, R.W., Smith, J.E., Cooperman, B.S., and Nishikura, K. (1989). A double-stranded RNA unwinding activity introduces structural alterations by means of adenosine to inosine conversions in mammalian cells and Xenopus eggs. Proceedings of the National Academy of Sciences of the United States of America *86*, 2647-2651.

Wang, E.T., Sandberg, R., Luo, S., Khrebtukova, I., Zhang, L., Mayr, C., Kingsmore, S.F., Schroth, G.P., and Burge, C.B. (2008). Alternative isoform regulation in human tissue transcriptomes. Nature *456*, 470-476.

Wang, Q., Miyakoda, M., Yang, W., Khillan, J., Stachura, D.L., Weiss, M.J., and Nishikura, K. (2004). Stress-induced apoptosis associated with null mutation of ADAR1 RNA editing deaminase gene. The Journal of biological chemistry *279*, 4952-4961.

Wang, Q., O'Brien, P.J., Chen, C.X., Cho, D.S., Murray, J.M., and Nishikura, K. (2000). Altered G protein-coupling functions of RNA editing isoform and splicing variant serotonin2C receptors. Journal of neurochemistry *74*, 1290-1300.

Wang, Q., Zhang, Z., Blackwell, K., and Carmichael, G.G. (2005). Vigilins bind to promiscuously A-to-I-edited RNAs and are involved in the formation of heterochromatin. Curr Biol *15*, 384-391.

Wolf, J., Gerber, A.P., and Keller, W. (2002). tadA, an essential tRNA-specific adenosine deaminase from Escherichia coli. The EMBO journal *21*, 3841-3851.

Wong, S.K., Sato, S., and Lazinski, D.W. (2001). Substrate recognition by ADAR1 and ADAR2. RNA (New York, NY *7*, 846-858.

Wulff, B.E., Sakurai, M., and Nishikura, K. (2010). Elucidating the inosinome: global approaches to adenosine-to-inosine RNA editing. Nat Rev Genet *12*, 81-85.

Yang, W., Chendrimada, T.P., Wang, Q., Higuchi, M., Seeburg, P.H., Shiekhattar, R., and Nishikura, K. (2006). Modulation of microRNA processing and expression through RNA editing by ADAR deaminases. Nature structural & molecular biology *13*, 13-21.

Yang, W., Wang, Q., Howell, K.L., Lee, J.T., Cho, D.S., Murray, J.M., and Nishikura, K. (2005). ADAR1 RNA deaminase limits short interfering RNA efficacy in mammalian cells. The Journal of biological chemistry *280*, 3946-3953.

York, J.D., Odom, A.R., Murphy, R., Ives, E.B., and Wente, S.R. (1999). A phospholipase C-dependent inositol polyphosphate kinase pathway required for efficient messenger RNA export. Science (New York, NY *285*, 96-100.

Zhang, Z., and Carmichael, G.G. (2001). The fate of dsRNA in the nucleus: a p54(nrb)-containing complex mediates the nuclear retention of promiscuously A-to-I edited RNAs. Cell *106*, 465-475.

Zhou, J., Wang, Q., Chen, L.L., and Carmichael, G.G. (2008). On the mechanism of induction of heterochromatin by the RNA-binding protein vigilin. RNA (New York, NY *14*, 1773-1781.

Zorio, D.A., and Bentley, D.L. (2004). The link between mRNA processing and transcription: communication works both ways. Experimental cell research *296*, 91-97.

A.

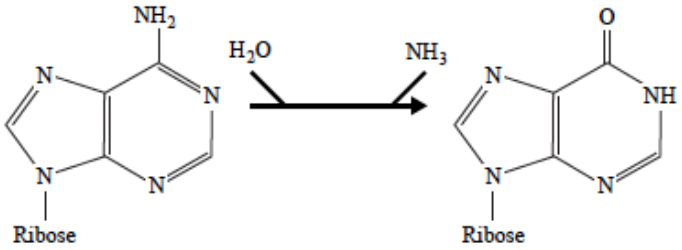

Adenosine Inosine

B.

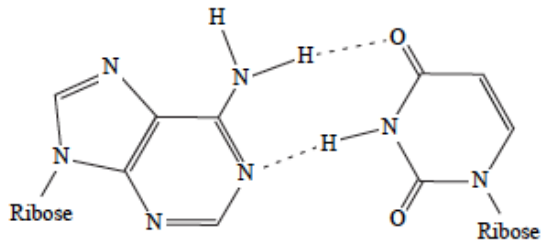

Adenosine Uridine

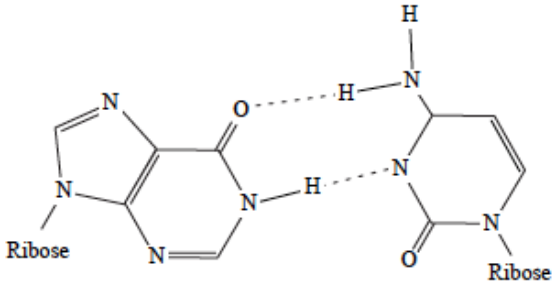

Inosine Cytidine

FIGURE 1.1. Hydrolytic deamination of adenosine to inosine by ADAR. (A) An adenosine is converted to inosine via the hydrolytic deamination of the adenine base. (B) Adenosine base pairs with uridine according to the Watson-Crick bonding configurations. In contrast, inosine shares the binding properties of guanosine and therefore base pairs with cytosine.

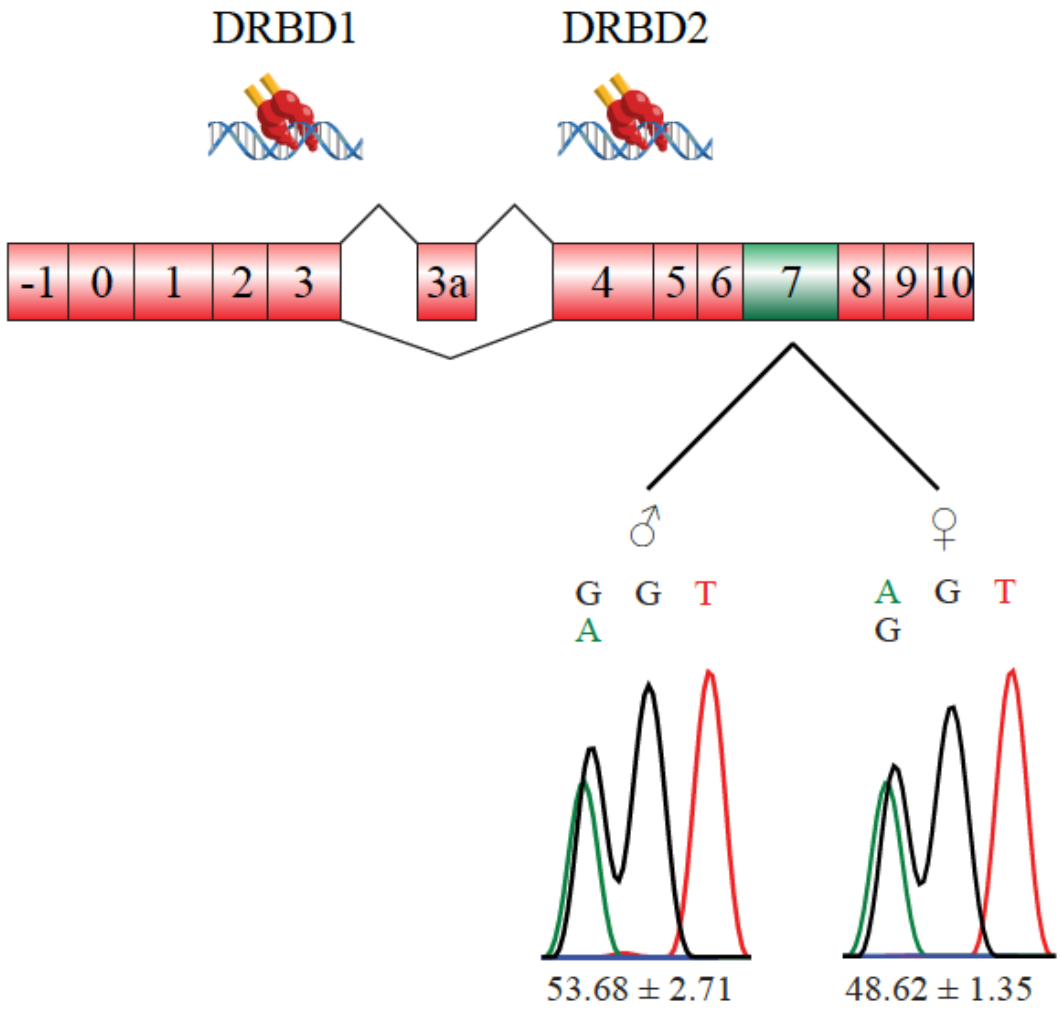

FIGURE 1.2. Posttranscriptional regulation of *Drosophila* ADAR. Inclusion or exclusion of an alternatively spliced exon, termed 3a, alters the linear distance between the double-stranded RNA binding domains (dsRBDs). Furthermore, an auto-editing event in exon 7 results in a serine to glycine (S → G) amino acid substitution in the deaminase domain. Example electropherograms showing the auto-editing levels from adult male (~54%) and female heads (~49%).

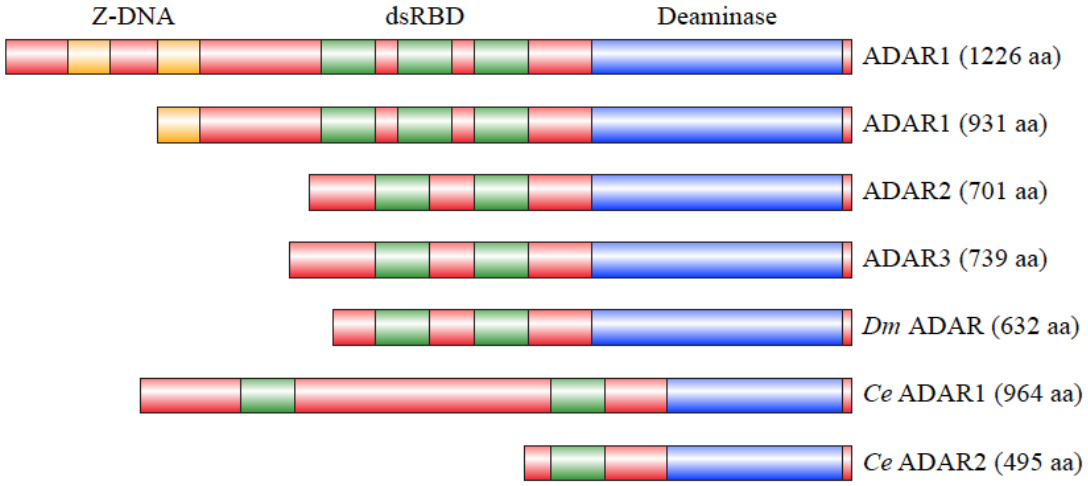

FIGURE 1.3. Domain structure of ADAR enzymes. Three human adenosine deaminase acting on RNA family members (ADAR1-3), *D. melanogaster* (*Dm*) ADAR, and two *C. elegans* (*Ce*) proteins, ADAR1-2, share common structural domains, including a deaminase catalytic domain and one to three double-stranded RNA binding domains (dsRBDs). Certain domain features, such as Z-DNA binding, are unique to human ADAR family members. Two human ADAR1 products are produced due to alternative promoter usage during transcription (Redrawn from information contained in Nishikura, 2006).

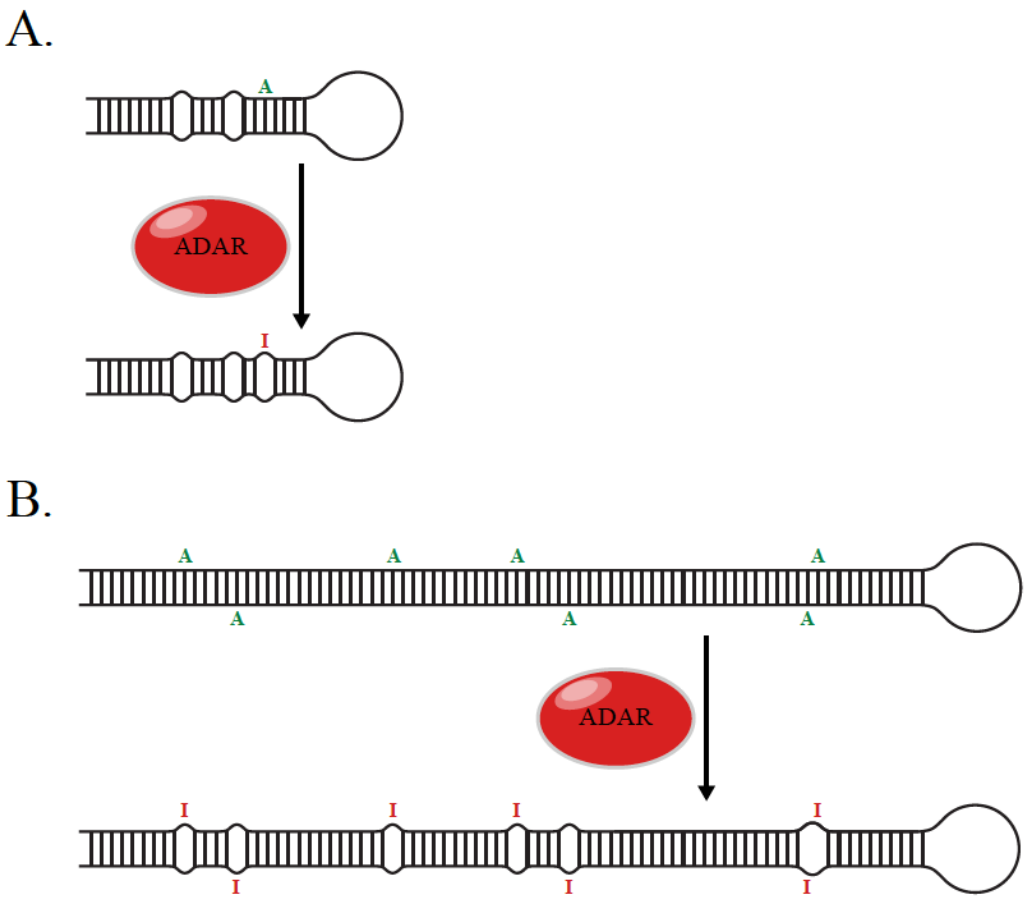

FIGURE 1.4. Editing-site selectivity of ADAR enzymes. A-to-I RNA editing of dsRNAs can be specific or promiscuous leading to deamination of select or random adenosines, respectively. (A) ADARs deaminate specific adenosines in short imperfect RNA duplexes (~20-50bp). (B) In contrast, promiscuous editing of multiple adenosines occurs in long, perfectly paired dsRNAs (~100-1000bp).

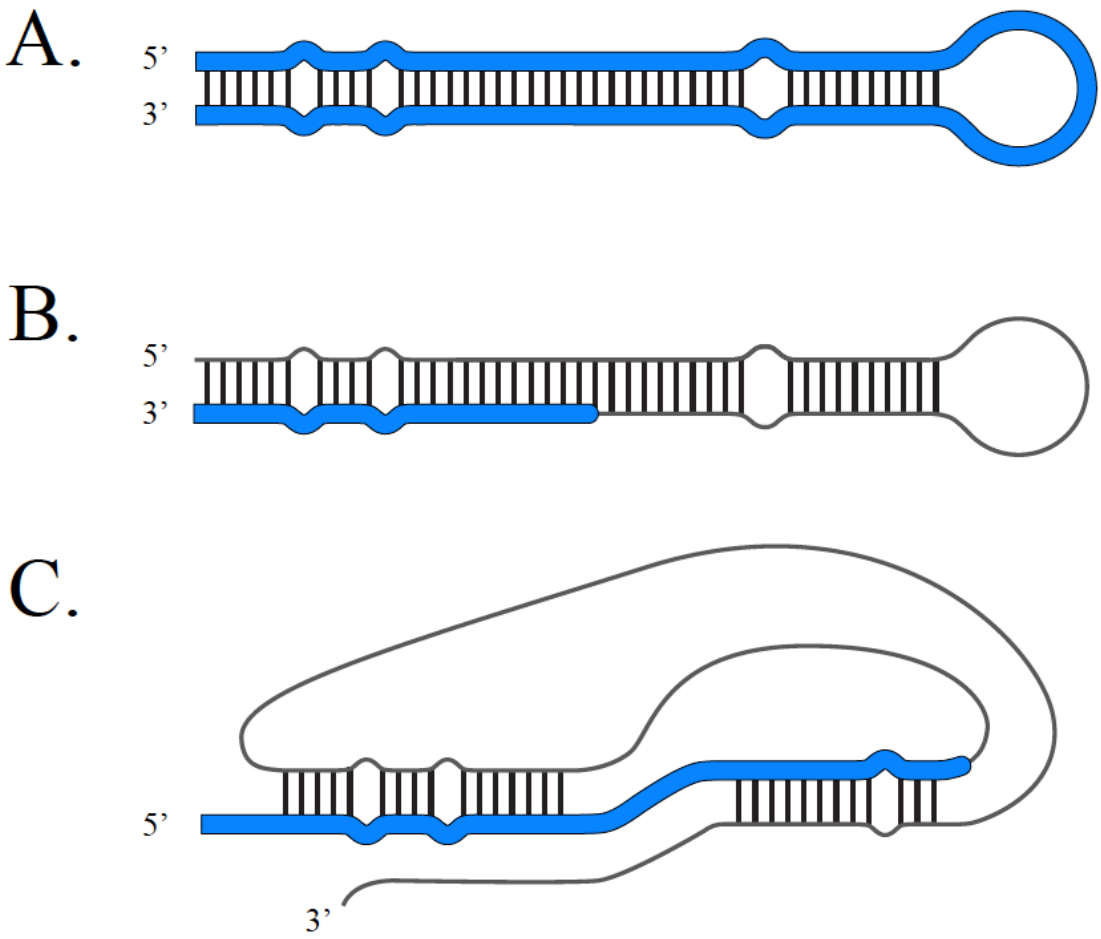

FIGURE 1.5. Schematic diagrams illustrating structurally diverse dsRNAs that serve as ADAR substrates. (A) Exonic sequences fold-back on each other to generate a simple hairpin. (B) Intronic sequences with extensive complementarity to the exon destined to be edited can generate an exon-intron hairpin structure. (C) Intronic sequences can also generate complex dsRNA structures when base-pairing with exonic sequences, such as a pseudoknot. Exonic sequences are shown as blue while intronic sequences are shown as grey.

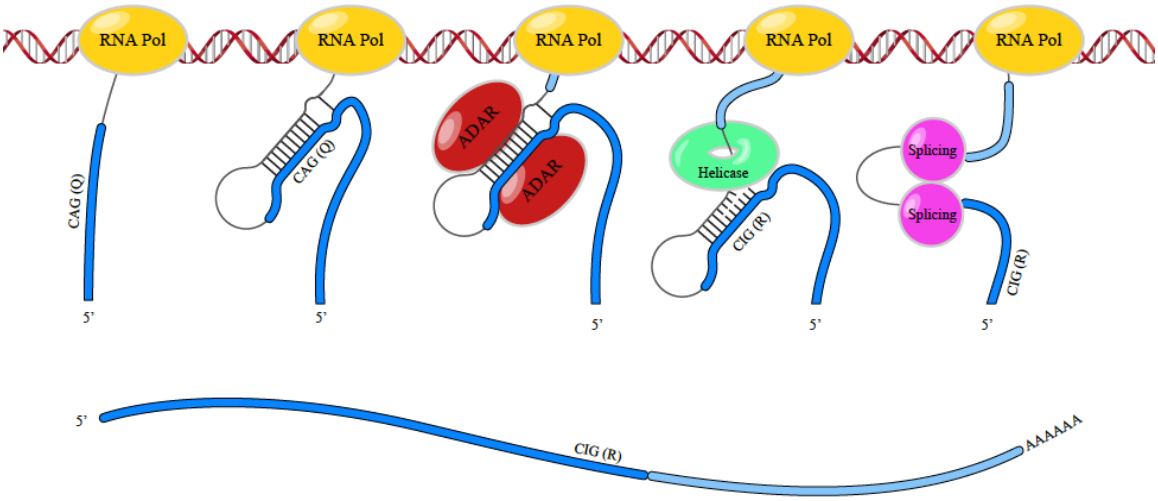

FIGURE 1.6. The proposed A-to-I RNA editing mechanism for pre-mRNAs. RNA polymerase transcribes the exon destined to be edited and the editing complementary intronic sequences. An imperfect short dsRNA is generated that serves as an ADAR substrate. Two ADAR monomers are required for the deamination reaction to occur. While the RNA polymerase continues to transcribe the rest of the pre-mRNA, a dsRNA helicase resolves the RNA duplex before RNA splicing is initiated. After completion of RNA processing, the mature mRNA is exported to the cytoplasm for translation.

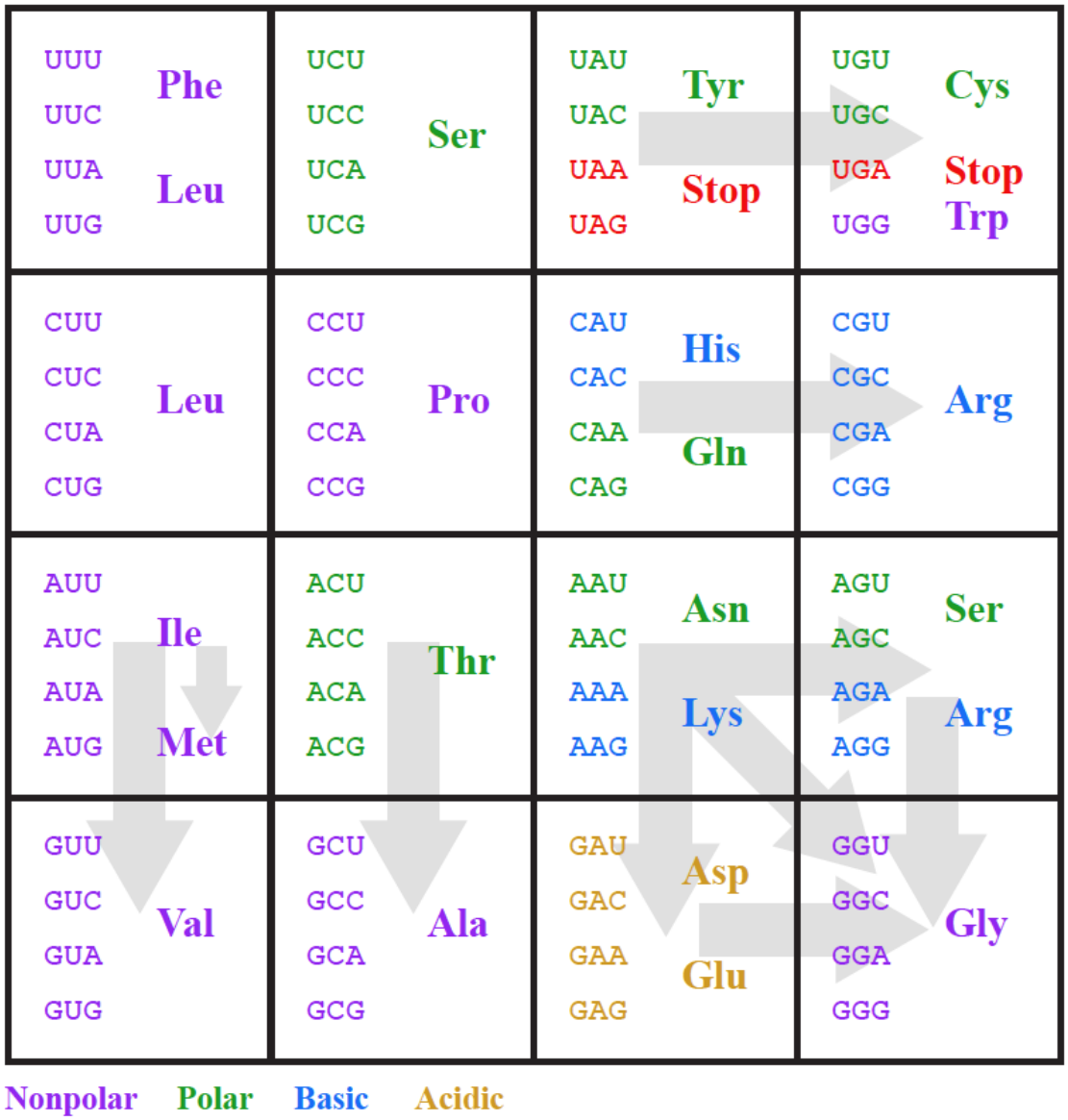

FIGURE 1.7. Amino acid recoding via RNA editing. More than half of the codons of the genetic code can be reassigned. Grey arrows indicate non-synonymous amino acid substitutions possible due to A-to-I RNA editing.

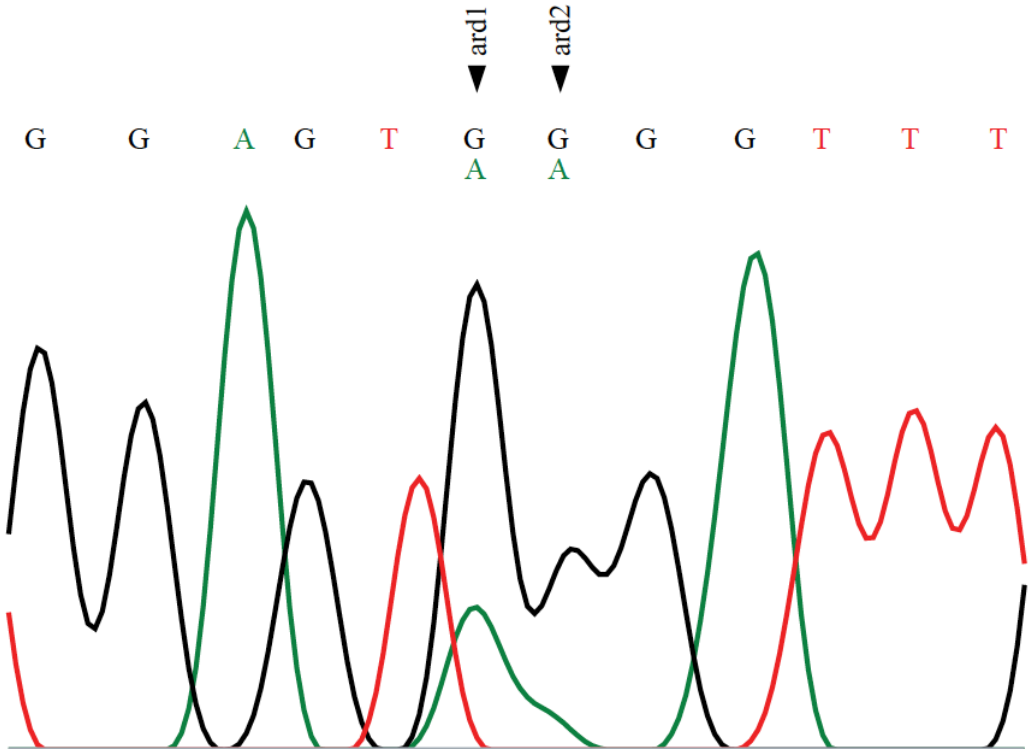

FIGURE 1.8. The signature of A-to-I RNA editing. An example electropherogram of the *ard* ligand-gated ion channel cDNA, showing mixed A/G peaks. Black arrows indicate the edited adenosines.

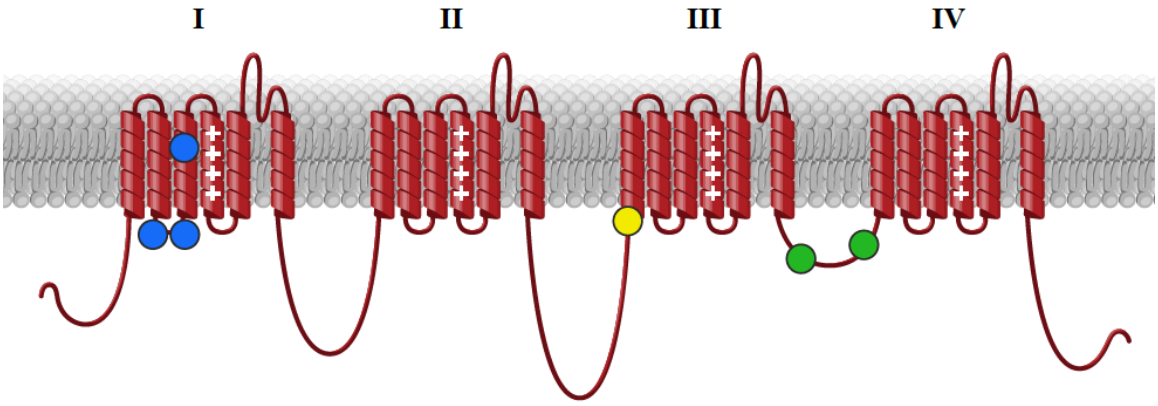

FIGURE 1.9. ADAR recoding occurs in functionally important amino acid residues. A schematic diagram illustrating four homologous domains of Na^+ and Ca^{2+}channels. Each subunit consists of six transmembrane-spanning helices (red). The + symbol indicates the voltage sensors. Blue spheres indicate RNA editing sites in L-type Ca^{2+} channels. The yellow sphere indicates an editing site found in the Caα1T T-type Ca^{2+} channel, while the green spheres represent editing sites in DSCI Na^+ channel (Redrawn from information contained in Hoopengardner et al., 2003).

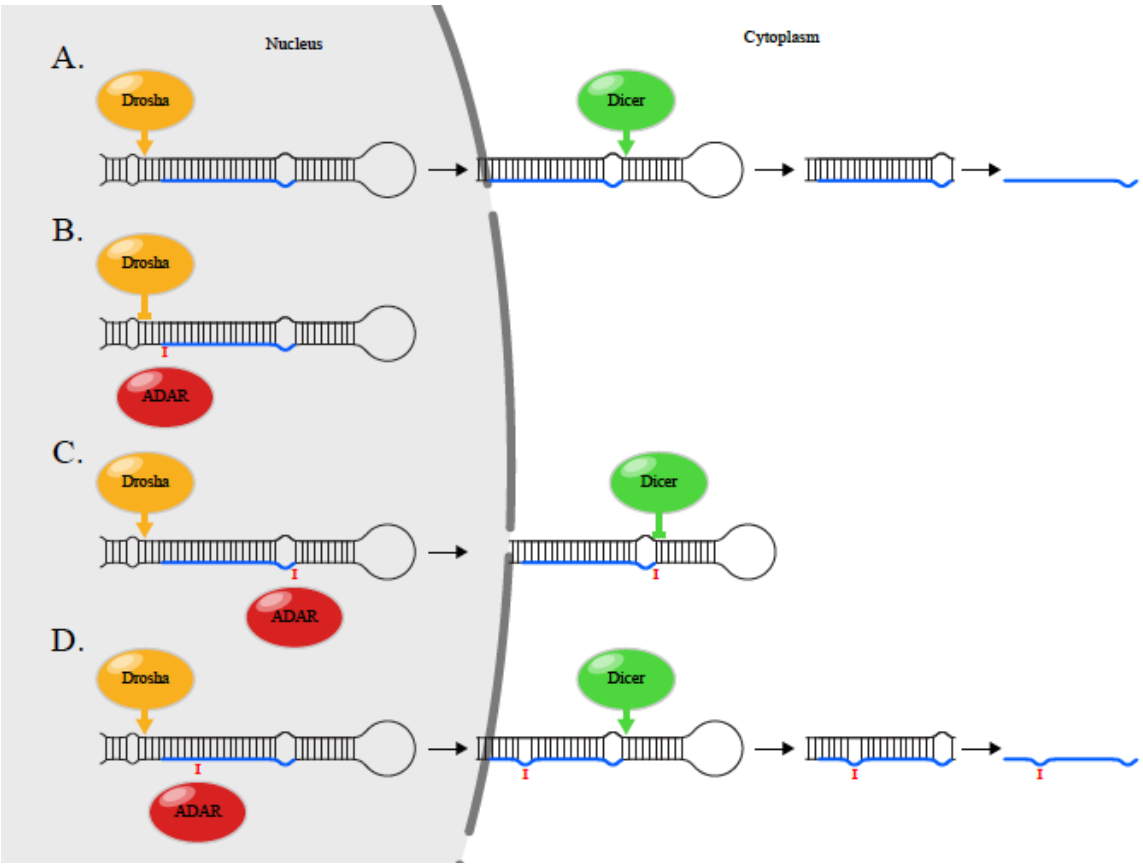

FIGURE 1.10. Regulation of the miRNA pathway via RNA editing. (A) Within the nucleus, hairpin miRNA structures (pri-miRNAs) are post-transcriptionally cleaved by Drosha to yield miRNA precursors (pre-miRNAs). In the cytoplasm, Dicer processing of pre-miRNAs generates short RNA duplexes that encode the mature miRNA (blue). (B) Specific A-to-I RNA editing near the base of the pri-miRNA results in the inhibition of Drosha cleavage preventing the biogenesis of mature miRNAs. (C) Specific editing near the loop of the pri-miRNA inhibits Dicer processing in the cytoplasm. (D) Editing of an adenosine within the seed region of the mature miRNA results to its redirection to a new target (Redrawn from information contained in Nishikura, 2010).

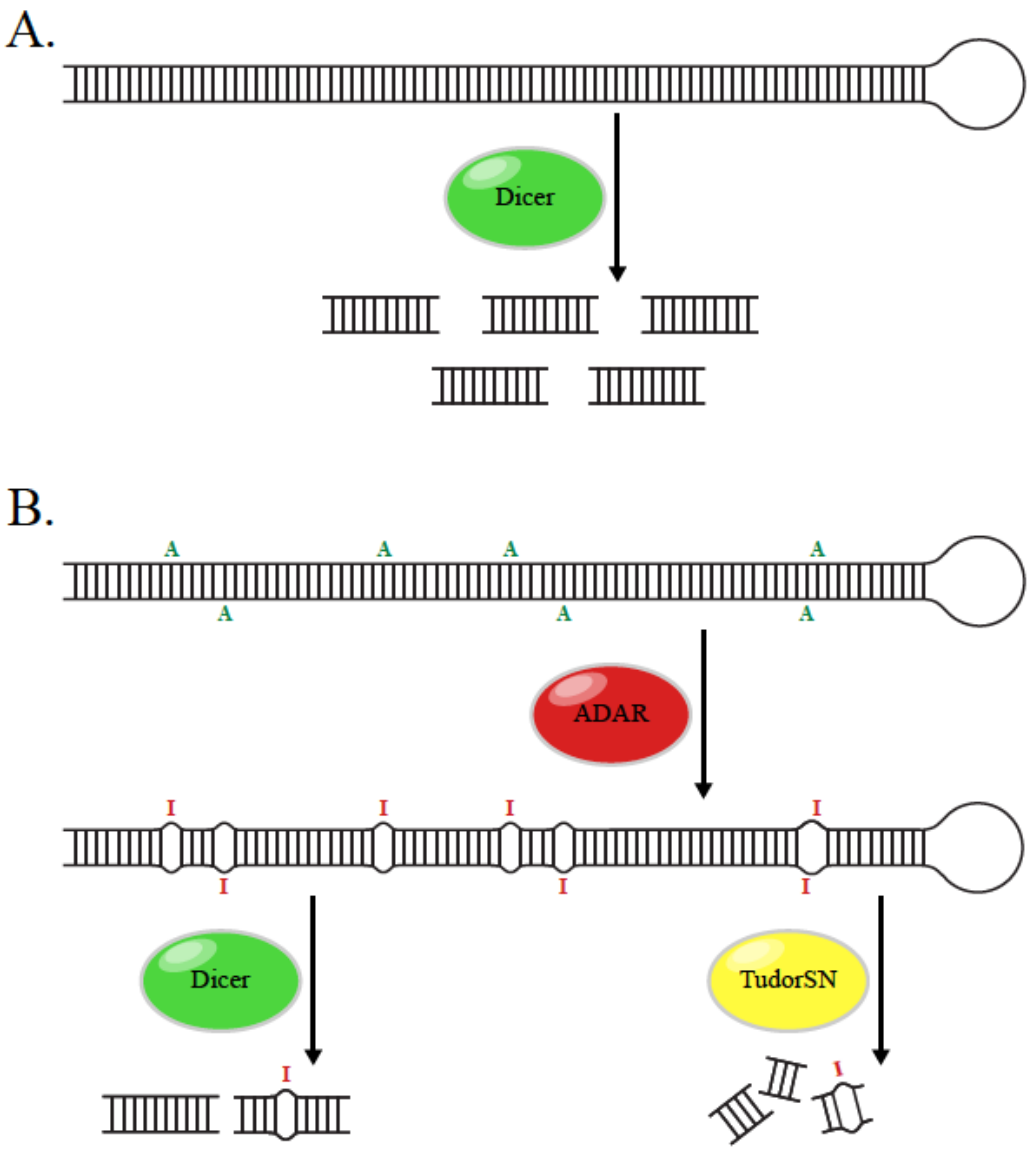

FIGURE 1.11. Regulation of RNA interference by ADARs. (A) Dicer processing of long perfect dsRNAs leads to the generation of small interfering RNAs (siRNAs) that direct sequence-specific silencing. (B) Promiscuous RNA editing of dsRNAs results in poor Dicer processing, leading to the generation of fewer siRNAs. In addition, inosine-rich dsRNAs can be degraded by Tudor-SN (Redrawn from information contained in Nishikura, 2010).

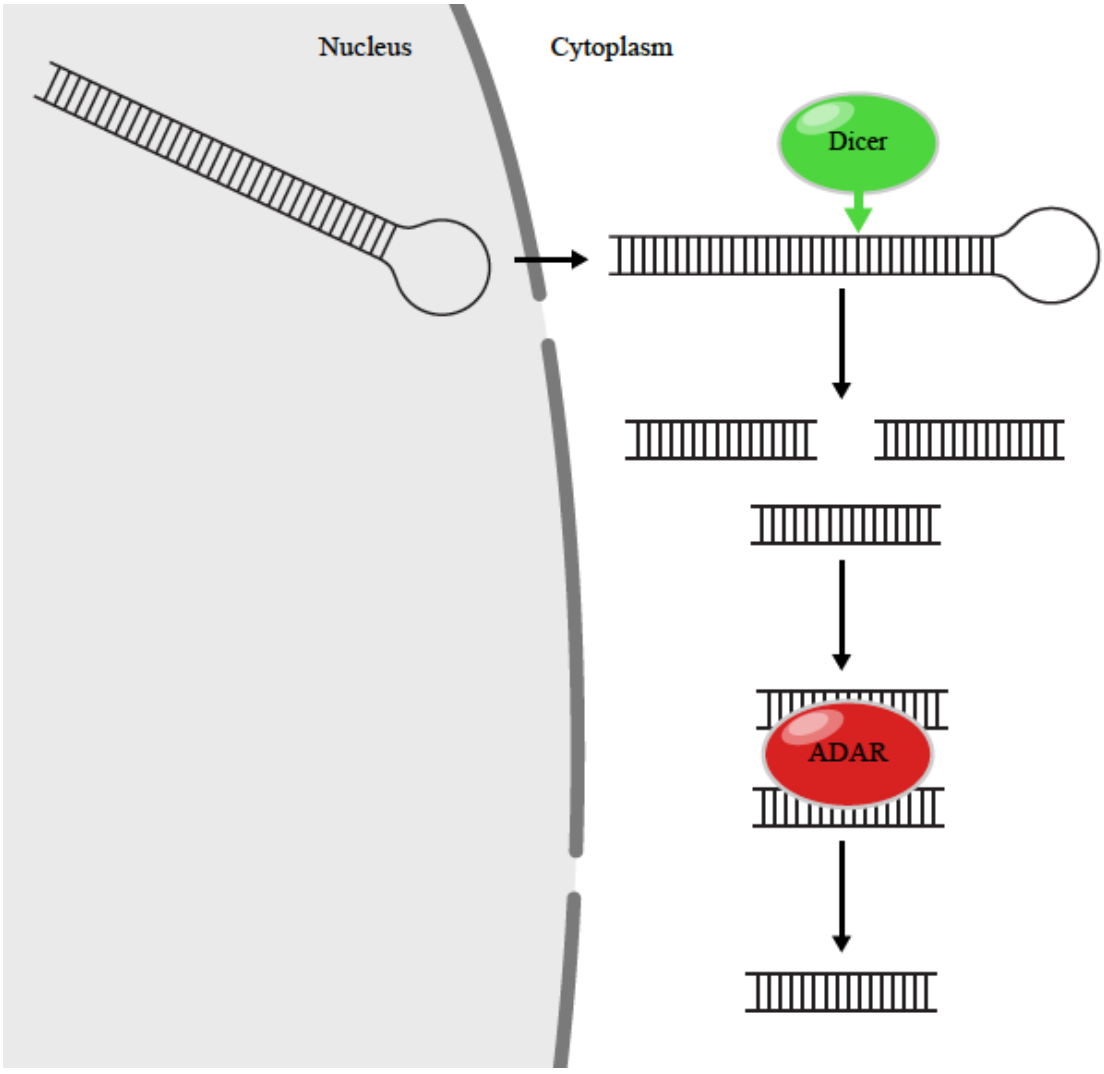

FIGURE 1.12. Sequestration of siRNA duplexes through ADAR binding. ADAR in the cytoplasm can bind to siRNA duplexes with high affinity, resulting in a less potent RNAi response. Thus, ADARs can antagonize the RNAi pathway through RNA binding, independent of catalytic activity.

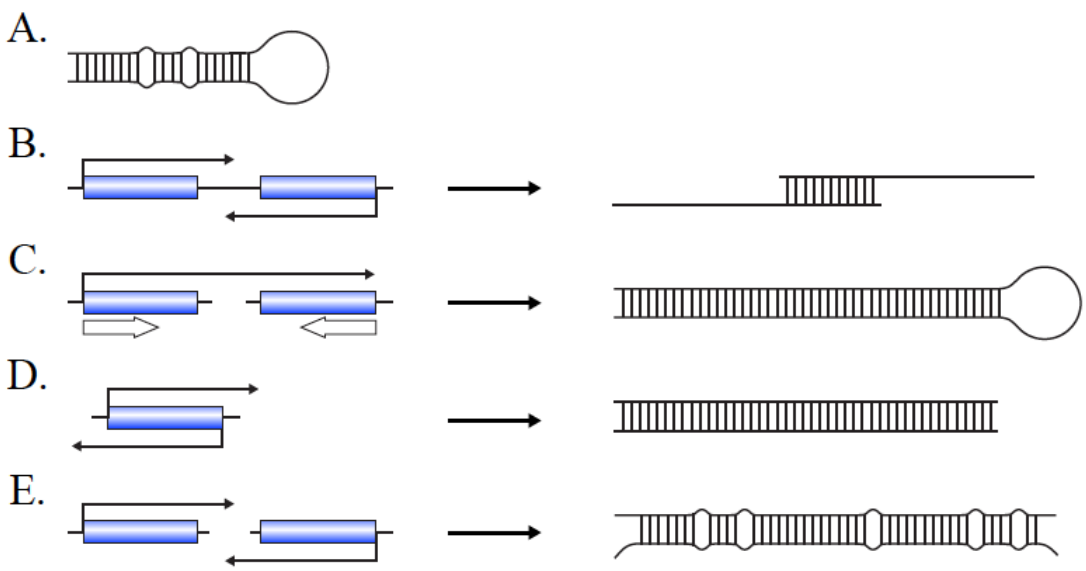

FIGURE 1.13. Endogenous dsRNA triggers for esiRNA biogenesis in *Drosophila*. (A) Structured loci encoded within the genome are processed by Dicer to generate siRNAs. (B) Convergent and (D) bidirectional transcription as well as transcription of transposable elements found in inverted orientation (C), all lead to the generation of dsRNA molecules. (E) Trans-interactions between a gene and its inverted pseudogene also leads to the generation of dsRNA structures. Thin black arrows indicate transcription, whereas white arrows indicate orientation (Redrawn from information contained in Ghildiyal and Zamore, 2009).

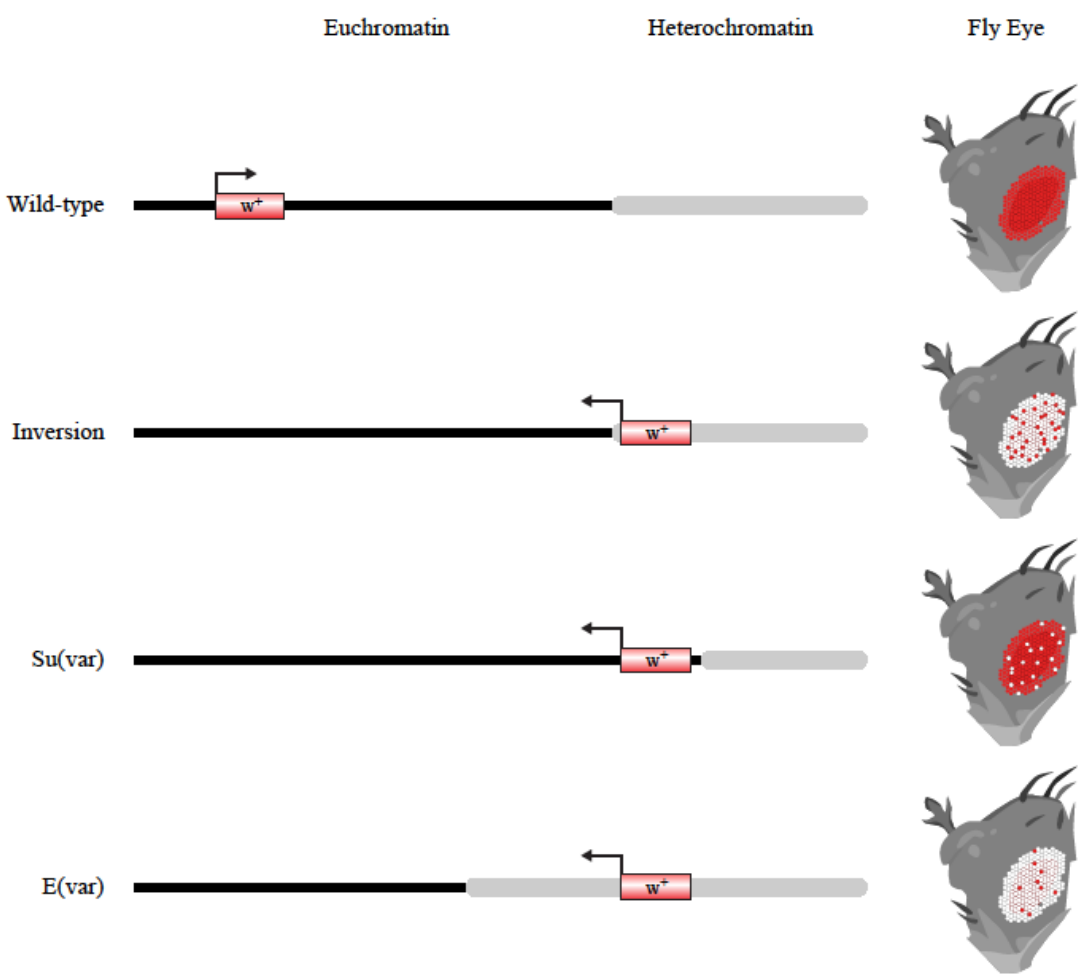

FIGURE 1.14. Diagram illustrating position effect variegation (PEV) in *Drosophila*. When the *white*$^{+}$ reporter gene resides within euchromatin (black), it is fully expressed, resulting in a full red eye phenotype. Juxtaposition of the *white*$^{+}$ gene close to heterochromatin (grey), results in a red and white mosaic eye phenotype. The presence of a suppressor of variegation, Su(var), leads to a less potent silencing effect, giving rise to more pigmented ommatidia in the eye. In contrast, the presence of an enhancer of variegation, E(var), results in a stronger silencing phenotype.

CHAPTER 2:

Engineered Alterations in RNA Editing Modulate Complex Behavior in *Drosophila*

This chapter consists of previous published data. "Engineered Alterations in RNA Editing Modulate Complex Behavior in Drosophila". Authors: James E. C. Jepson*, Yiannis A. Savva*, Chio Yokose, Arthur U. Sugden, Asli Sahin, and Robert A. Reenan. Journal of Biological Chemistry **286** (10): 8325-8337, 2011. (*) These authors contributed equally to this work. My specific contributions to this publication include: (a) I created the *dAdar*^{hyp} allele used in this study using homologous recombination, (b) I created the molecular reported of editing activity used in this study (Figure 2.2A), (c) I performed the molecular analysis on RNA editing sites in the ADAR hypomorph allele (Figure 2.3A-C), I performed the molecular analysis of various editing sites during development (Figure 2.4B-C), and I assisted in the behavioral analysis of ADAR hypomorphs (Figure 2.5A-E).

ABSTRACT

Select proteins involved in electrical and chemical neurotransmission are re-coded at the RNA level via the deamination of particular adenosines to inosine by adenosine deaminases acting on RNA (ADARs). It has been hypothesized that this process, termed RNA editing, acts to "fine-tune" neurophysiological properties in animals and potentially downstream behavioral outputs. However, the extreme phenotypes resulting from deletions of *adar* loci have precluded investigations into the relationship between ADAR levels, target transcripts, and complex behaviors. Here, we engineer *Drosophila* hypomorphic for ADAR expression using homologous recombination. A substantial reduction in ADAR activity (>80%) leads to altered circadian motor patterns and abnormal male courtship, although surprisingly, general locomotor coordination is spared. The altered phenotypic landscape in our *adar* hypomorph is paralleled by an unexpected dichotomous response of ADAR target transcripts, *i.e.* certain adenosines are minimally affected by dramatic ADAR reduction, whereas editing of others is severely curtailed. Furthermore, we use a novel reporter to map RNA editing activity across the nervous system, and we demonstrate that knockdown of editing in *fruitless*-expressing neurons is sufficient to modify the male courtship song. Our data demonstrate that network-wide temporal and spatial regulation of ADAR activity can tune the complex system of RNA-editing sites and modulate multiple ethologically relevant behavioral modalities.

INTRODUCTION

Informational recoding of RNA by the catalytic deamination of adenosine to inosine proceeds through the action of ADARs (Nishikura, 2010). Long double strand RNA duplexes exhibiting perfect complementarity can be modified extensively by promiscuous ADAR activity. However, mRNAs may also serve as site-specific substrates for ADARs via base pairing interactions that generate short imperfect duplexes that generally include the exon destined for editing and a *cis*-acting complementary sequence, usually found in a neighboring intron (Higuchi et al., 1993; Reenan, 2005). Because inosine is recognized by the translation machinery as guanosine (Basillo et al., 1962), A-to-I editing in mRNAs can lead to the incorporation of amino acids differing from those specified by the literal genome.

In *Drosophila*, the spectrum of ADAR substrates is peculiarly specific, consisting primarily of mRNAs encoding an array of voltage- and ligand-gated ion channels, as well as numerous pre-synaptic proteins involved in exo- and endocytosis of synaptic vesicles (Grauso et al., 2002; Hoopengardner et al., 2003; Semenov and Pak, 1999; Smith et al., 1998). Similarly, several mammalian ion channels and G-protein-coupled receptors are also subject to RNA editing (Bhalla et al., 2004; Burns et al., 1997; Higuchi et al., 1993; Hoopengardner et al., 2003; Ohlson et al., 2007). In light of the ontological class and high sequence conservation of ADAR target genes, RNA editing has been invoked as an essential function in controlling synaptic transmission and neurophysiology. Correspondingly, deletion of the single *Drosophila adar* locus (*dAdar*) results in severe adult-stage behavioral abnormalities, including extreme uncoordination, seizures and a complete lack of courtship in *dAdar* null ($dAdar^{5g1}$) males (Palladino et al., 2000a),

whereas mice lacking ADAR2 suffer from seizures and early mortality (Higuchi et al., 2000).

Due to the presence of a single X-linked *adar* locus and more than 100 mRNA sites of dADAR modification, *Drosophila* provides an ideal system to study the correlation between deaminase levels and recoding output. We have previously shown that restoration of editing in the adult nervous system partially rescues the locomotor defect of *dAdar*-deficient males, an effect that appears to be independent of any interactions between *dAdar* and the RNAi pathway (Jepson and Reenan, 2009). However, the pattern of dADAR expression and activity within the fly nervous system is currently unknown. Furthermore, although previous studies have focused on the relationship between dADAR activity and motor control, it is unclear whether complex behaviors require regulated editing and, if so, whether subpopulations of edited proteins contribute to distinct behavioral outputs.

Here, we investigate these issues using homologous recombination and a molecular reporter for RNA editing activity. Although dADAR expression can be detected in almost all neuronal nuclei, significant variation in dADAR activity exists between genetically distinct neurons. Finally, through the generation of a novel hypomorphic *dAdar* allele, we demonstrate an unexpectedly complex relationship between *in vivo* dADAR levels and deamination of specific RNA editing targets.

These data, combined with neuron-specific dADAR knockdown, demonstrate that correct regulation of editing activity at both cell-autonomous and network levels is required for behavioral outputs in *Drosophila* and provide mechanistic insight into the complex landscape of proteomic diversity generated by RNA editing.

MATERIALS AND METHODS

Drosophila Strains and Genetics

For a full list of *Drosophila* strains used, see supplemental Tables S2.1 and S2.2. Flies were raised at a constant 25 °C, on standard molasses food, and under 12-h day/night cycles. Both *dAdar* RNAi transgenes were obtained from the Vienna *Drosophila* RNAi Stock Center. Generation of the double RNAi line was described previously (Jepson and Reenan, 2009). Tissue-specific Gal4 lines were obtained from the Bloomington stock center.

Ends-out Homologous Recombination of the dAdar Locus

We performed ends out homologous recombination using a similar methodology to that reported previously (Maggert et al., 2008). Briefly, we utilized the ends-out targeting vector p [w25.2] that contains the *white*$^{+}$ selectable eye color mini-gene flanked by LoxP sites for subsequent removal by Cre-recombinase. Homology arms were cloned and sequenced in pTOPO (Invitrogen) and then shuttled into the multiple cloning sites of the vector to generate p [w25-dADAR-HA], which was then introduced into the *Drosophila* genome by standard transgenic methods (Genetic Services Inc.).

The cloning strategy is as follows, where all genomic coordinates are given by the *Drosophila melanogaster* draft, BDGP Release 5, with release 5.12 annotation provided by FlyBase at the UCSC Genome Browser. Arm 1 is the 5' arm of p [w25-dADAR-HA] (see Fig. 2.1) and was generated by PCR amplification to incorporate cloning sites as follows: Arm 1, *BsiWI*-1,673,865–1,676,526-*AscI*. Arm 2 is the 3' arm of

P [w25-dADAR-HA] and was generated in two parts by PCR amplification to incorporate cloning sites and an HA epitope tag; Arm2, *Acc65I*-1,676,602–1677784-HA/NheI-1,677,788–1,679,400-NotI. The HA tag sequence was inserted after the terminal glutamate codon of *dAdar* (GAA) ending in an opal (TGA) stop codon and an NheI (gctagc) cutting site as follows: GAAtacccttacgatgttcctgattacgccagcctgTGAgctagc.

Targeting was performed to generate multiple independent targeting events in which the HA tag was incorporated or excluded from the recombination events. Targeted alleles were validated by amplification using primers outside the region of targeting. All targeted alleles were sequenced to verify only the presence of indicated sequences. Subsequent removal of the *white*$^{+}$ mini-gene selectable marker was achieved by performing crosses to animals expressing Cre-recombinase and re-isolation of targeted chromosomes containing a single LoxP site. The recombinant alleles were subsequently backcrossed to Canton-S for five generations.

Behavioral Analysis

Locomotor patterns were recorded using horizontal, single fly activity monitors (TriKinetics). Flies were left to acclimatize for ~12 h before recording was initiated. An average daily pattern was calculated for each fly by averaging data from 3 consecutive days. These values were then further averaged across the experimental population.

Mating assays and song recording were performed in a custom-made chamber. For each assay, 5–7-day-old males and 3–5-day-old virgin females were used, and the time taken for male initiation of courtship (latency) and the courtship index (time spent courting/total time) was recorded over 10 min. All mating assays were performed in a

narrow time window (7–10 a.m.) to minimize circadian influences on experimental outcome, blind to experimental genotype where possible. Mating songs were recorded using a MicroTrack mobile digital recorder (M-Audio) and were analyzed in Audacity. Because *dAdar*^{hyp} males expressed a *white*$^{+}$ mini-gene and *dAdar*^{WTLoxP} did not, we crossed a *white*$^{+}$ mini-gene-containing p [w25.2] vector inserted in the 3rd chromosome into the *dAdar*^{WTLoxP} background to restore eye pigment expression.

RNA Editing Analysis

RNA extractions from *Drosophila* heads (15–20 per sample) were performed using TRIzol reagent (Invitrogen). Edited cDNAs were amplified via RT-PCR using target-specific primers (Jepson and Reenan, 2009). Levels of editing were determined by measuring the area under A- and G-peaks in individual electropherogram traces using ImageJ. The percent editing is expressed at G/(A + G) X 100.

Western Blotting

Protein samples were prepared in buffer containing SDS and β-mercaptoethanol and electrophoresed on a 10% gel (Amresco). Anti-HA antibody (Covance) was used at 1:500; anti-actin (Millipore) was used at 1:20,000–80,000. Band intensities were quantified on a Kodak Image Station following background subtraction. For adult heads, 20-heads/100 μl of buffer were used per sample. For developmental analysis, we used 250 1st instar larvae, 10 3rd instar larvae, and 10 whole adult males per 100 μl of buffer.

Confocal Microscopy and Immunohistochemistry

A Zeiss LSM 510 meta-confocal microscope was used to obtain all images. Samples for immunohistochemistry were prepared as described previously (Wu and Luo, 2006). Primary antibodies were used at the following concentrations: mouse anti-Lamin, anti-Elav, anti-Repo, and anti-Dachshund (Developmental Studies Hybridoma Bank) were all used at 1:50; mouse anti-HA and rabbit anti-HA (Santa Cruz Biotechnology) were used at 1:50. Alexa-Fluor secondary antibodies (goat anti-mouse Cy3 and goat anti-mouse and anti-rabbit FITC (Invitrogen) were used at 1:200. DAPI (Invitrogen) was used at 1:1000. Confocal images were obtained at subsaturation levels of fluorescent intensity. Images were contrast-enhanced in Adobe Photoshop. Each image shown is a representative example of $n \geq 5$.

Online Supplementary Material

The supplemental material includes seven figures, three tables, and a movie. Supplementary figure 1 (S2.1) shows the expression of dADAR-HA in the male brain and thoracic ganglion. Supplementary figure 2 (S2.2) shows that the exon skipping of the *syt-T* reporter does not account for neuron-specific differences in editing. Supplementary figure 3 (S2.3) shows the frequency distribution of the reduction in editing levels observed at 68 dADAR target adenosines amplified from $dAdar^{hyp}$ heads and thoraxes, compared to the same tissue in $dAdar^{WTLoxP}$ males. Supplementary figure 4 (S2.4) shows examples of single-fly profiles of locomotor activity. Supplementary figure 5 (S2.5) shows no sex-specific exon skipping of the *syt-T* reporter when driven by *fru*-Gal4. Supplementary figure 6 (S2.6) shows lack of sexual dimorphism between endogenous

transcripts in male and female heads and thoraxes. Supplementary figure 7 (S2.7) shows that inhibition of dADAR activity in *fruitless* neurons does not alter circadian rhythms. Supplementary table 1 (S2.1) describes the *Drosophila* strains used in this study. Supplementary table 2 (S2.2) shows the editing levels at two sites, site 3 and site 4, of the *syt-T* molecular reporter expressed in discrete neuronal sub-populations. Supplementary table 3 (S2.3) shows the editing levels at 68 target adenosines in $dAdar^{WTLoxP}$ and $dAdar^{hyp}$ in male head and thorax. The supplementary movie shows that the locomotor activity of $dAdar^{hyp}$ males is relatively robust, despite the severe reduction in dADAR expression. All the online supplementary figures, tables and movie is available at http://www.jbc.org/content/early/2010/11/15/jbc.M110.186817/suppl/DC1

RESULTS

dADAR Is Localized to the Neuronal Nucleus in the *Drosophila* Brain

The endogenous dADAR protein expression pattern within the adult *Drosophila* nervous system has not been determined. To remedy this, we used ends-out homologous recombination (Rong et al., 2002) to generate three independent recombinant lines, two with HA epitope-tagged sequences at the 3' end of the *dAdar* locus (Fig. 2.1A and B) and one without. Editing levels did not significantly differ between both $dAdar^{HA}$ lines and w^{1118} controls (supplementary Fig. S2.1).

During homologous recombination, screening for recombinant flies is facilitated by the insertion of an ~5-kb $white^{+}$ mini-gene eye color selection cassette within an intron of the *dAdar* locus, subsequently removed via a Cre-recombinase step (Rong and Golic, 2000; Rong et al., 2002). Western blotting using an anti-HA antibody revealed robust expression of an HA-immunoreactive protein at the predicted size of dADAR in both recombinant lines lacking the $white^{+}$ mini-gene (Fig. 2.1C). We used these lines to detail the expression pattern of dADAR. Because dADAR-HA levels and endogenous editing were indistinguishable between the two independent lines, we use them interchangeably throughout all subsequent experiments. Confocal microscopy revealed broad expression of dADAR in the brain and thoracic ganglion (supplementary Fig. S2.1). Co-immunostaining for HA and the nuclear envelope protein Lamin showed that dADAR expression was prominent only within nuclei (Fig. 2.1D). No significant dADAR localization to the cytoplasmic, axonal, or dendritic compartments was observed. In addition, dADAR co-localized with Elav (a marker for neuronal nuclei) but not Repo (a

glial nuclear marker), indicating that nuclear dADAR expression is widespread and enriched in the neuronal nucleus (Fig. 2.1E).

Editing Activity Varies Widely between Neuronal Subpopulations

Our initial analysis of dADAR localization revealed clear differences in dADAR protein expression even between neighboring neurons (Fig. 2.1D and E), suggesting that dADAR expression is under spatial control in the *Drosophila* brain, as is the case in mammals (Jacobs et al., 2009). To investigate how dADAR activity varies in genetically defined neurons, we used a molecular reporter of editing activity based on *syt-1*, which contains four editing sites in exon 9, of which sites 3 and 4 are edited most robustly (Fig. 2.2A) (Hoopengardner et al., 2003; Reenan, 2005). The reporter (termed *syt-T*) consists of the edited exon flanked by the upstream and downstream introns and exons cloned into a pUAS vector (Jepson and Reenan, 2009), allowing targeted expression using the UAS-Gal4 binary expression system (Brand and Perrimon, 1993).

We used 21 neuronal Gal4 lines to drive two independent insertions of *syt-T* (see supplemental Table S2.2) and observed production of full-length transcripts with all Gal4 drivers. Sequence analysis confirmed that all full-length transcripts were the result of accurate splicing. In certain cases, a minor band corresponding to exon 9 skipping was observed. However, alterations in editing of the reporter did not correlate with alternative splicing of the edited exon (supplementary Fig. S2.2). Editing at site 4 was detected in all neurons defined by the library of Gal4 lines but varied widely from 27 to 82% (Fig. 2.2B–D). In contrast, editing at site 3 was either undetectable or <10% in 16/21 driver lines tested, and it was only observed at robust levels (>20%) in the five subpopulations

that yielded the highest editing at site 4, suggesting that although low dADAR levels are sufficient for robust editing of site 4, editing at site 3 only occurs once a certain threshold of dADAR expression has been exceeded.

To test whether dADAR expression correlated with editing of the *syt-T* reporter, we examined dADAR expression in two neuronal subtypes representing high and low levels of dADAR activity indicated by the *syt-T* reporter, glutamatergic (*ok371*) and mushroom body neurons, respectively (see supplemental Table S2.2). Robust dADAR levels were detected in many glutamate-releasing neurons labeled with a nuclear red fluorescent protein (Fig. 2.2E) (Barolo et al., 2004). In contrast, mushroom body cells labeled with the nuclear marker Dachshund showed strikingly lower dADAR expression levels relative to surrounding neurons (Fig. 2.2F). These data suggest that cell-autonomous regulation of dADAR expression contributes to neuron-to neuron variation in editing of the molecular reporter.

Stringent Reduction of dADAR Expression Reveals Differential Affinities of Edited Substrates

Initially, the two pre-Cre recombinant lines generated contain a *white*$^{+}$ mini-gene inserted in an inverse orientation relative to *dAdar* transcription. Western blots revealed that prior to removal of this *white*$^{+}$ mini-gene insertion, dADAR-HA staining was reduced by 80 ± 5% and 87 ± 7% relative to post-Cre counterparts (Fig. 2.1C and D). Thus, insertion of *white*$^{+}$ serendipitously generated independent hypomorphic alleles of *dAdar* (which we refer to as *dAdar*^{hyp}; control flies harboring a single LoxP site in intron 7 of *dAdar* are referred to as *dAdar*^{WTLoxP}).

The substantial reduction in dADAR expression also led to a tissue-specific decrease in auto-editing of the *dAdar* transcript, a developmentally regulated event that acts to down-regulate dADAR activity by re-coding a conserved serine residue to glycine near the active site (Keegan et al., 2005). Amplification of the *dAdar* transcript revealed that auto-editing was slightly but significantly reduced in $dAdar^{hyp}$ heads relative to $dAdar^{WTLoxP}$ (*WTLoxP*, 53.8%; *hyp,* 49.1%, $n = 8$ RT-PCRs, $p < 0.005$, Mann-Whitney *U* test). In contrast, auto-editing in thorax tissue dropped from 38.1% in $dAdar^{WTLoxP}$ controls to 23.1% in $dAdar^{hyp}$ thoraxes ($n = 5–8$, $p < 0.005$). The decrease in ADAR protein production by the $dAdar^{hyp}$ allele results in comparable or only slightly reduced levels of the less active (edited) form of *Drosophila* ADAR protein. Thus, any system-wide changes in target deamination should be largely due to changes in ADAR levels rather than effects due to misregulated auto-editing.

Complete loss of A-to-I RNA editing in *Drosophila* results in multifaceted adult-stage behavioral abnormalities (Palladino et al., 2000a), consistent with the functional pleiotropy of dADAR. However, the extreme uncoordination exhibited by $dAdar^{5g1}$ null flies has made investigations into the relation between A-to-I editing activity and complex behavior impossible. Surprisingly, despite the severe reduction in dADAR expression in $dAdar^{hyp}$ males, locomotor activity appeared relatively robust under casual observation (supplemental movie), and no obvious uncoordination was apparent. These observations suggested that editing might perdure in a behaviorally relevant subpopulation of adenosines in *dAdar* hypomorphs, despite the severe reduction in dADAR protein expression. We tested this hypothesis by comparing editing in 68 target adenosines in the hypomorph and control backgrounds. Like editing in the $dAdar^{HA}$

genetic background (supplemental Fig. S2.1), *dAdar*^{WTLoxP} males did not significantly differ from wild-type Canton-S (data not shown). In *dAdar*^{hyp} heads and thoraxes, however, editing was reduced by an average of 68 ± 4% and 56 ± 4%, respectively, relative to the post-Cre control (Fig. 2.3A). We observed a similar reduction in editing in *dAdar*^{HA} males in which the *white*$^{+}$ mini-gene was not removed (data not shown).

Intriguingly, the reduction in specific editing of targets was highly nonuniform (Fig. 2.3A and supplemental Fig. S2.3A and B). Editing at a substantial fraction of sites was reduced by 70–100% in hypomorph heads and thoraxes. In contrast, despite the extreme curtailing of wild-type dADAR levels, a subpopulation of adenosines was modified at nearly wild-type levels (Fig. 2.3A and supplemental Table S2.3). For example, in the male thorax, *syt-1* site 4 and site 2 of the *ard* acetylcholine receptor (also known as Dβ1) are edited at similar levels (95 ± 1% and 94 ± 2%, respectively) (supplemental Table S2.3). However, in *dAdar*^{hyp} thoraxes, editing at *syt-1* site 4 was reduced by 12% relative to *dAdar*^{WTLoxP}, while *ard* site 2 was reduced by 71%. A further striking example is site 4 of *eag* and the single site in *Caα1T*. Site 4 of *eag* is slightly reduced from 84 ± 0.6% to 79 ± 0.4% in *dAdar*^{hyp} heads, while editing in *Caα1T* is completely abolished in *dAdar*^{hyp} heads, despite its high level of editing in *dAdar*^{WTLoxP} heads (87 ± 0.7%).

Based upon these data, we classified dADAR substrates into two groups according to their sensitivity to dADAR protein levels, which we term “high and low efficiency” (HE and LE) sites. We defined HE sites as those reduced by <30% in *dAdar*^{hyp} thoraxes, while LE sites are reduced by >70%. Importantly, HE and LE sites also exhibited similar responses to dADAR reduction in male *dAdar*^{hyp} head samples,

although these were shifted toward slightly lower reductions in HE sites and greater reductions in LE sites (supplemental Fig. S2.3). Many dADAR targets are edited at higher levels in the thorax relative to head tissue (average increase, 16 ± 6% for all sites edited >10%; Fig. 2.3A), although notable exceptions such as *shab* site 5 and *Caα1T* were apparent. This trend may reflect increased dADAR activity in the thoracic ganglion relative to the head, perhaps due to lower levels of auto-editing in $dAdar^{hyp}$ thoraxes.

We took advantage of the $dAdar^{5g1}$ null and hypomorphic $dAdar^{hyp}$ alleles to generate females with a graded range of dADAR expression, and we examined editing at 10 HE and 8 LE sites in head samples from four genetic backgrounds: *hyp*/*hyp*, *5g1*/*FM7* (where *FM7* is a balancer chromosome with a wild-type copy of $dAdar^{+}$), *hyp*/*FM7,* and *WTLoxP*/*WTLoxP*. These genotypes have predicted relative dADAR expression levels of ~ 20, 50, 60, and 100%, respectively. As expected, all LE sites exhibited very low levels of editing in *hyp*/*hyp* heads (0–23%), in contrast to HE sites (30–84%) (Fig. 2.3B and C). Every HE site tested showed wild-type levels of editing in *5g1*/*FM7* heads, and the mean reduction in *hyp*/*hyp* heads relative to wild-type controls was only 26 ± 4%. Thus, only a minimal concentration of dADAR is sufficient to yield robust editing of HE sites.

In contrast, the mean reduction in LE sites in *hyp*/*hyp* heads relative to wild-type controls was 80 ± 4%. However, within the LE sites we examined, we could delineate two subpopulations. Five of the eight sites tested (*ard* sites 1–3, *DSC1* and *Caα1T*) showed wild-type editing levels in *5g1*/*FM7* heads, despite severely reduced editing in the $dAdar^{hyp}$ background. The remaining three sites (*unc-13*, *Caα1D* site 1, and site 6 of the Dα6 acetylcholine receptor) showed sequentially increased editing in proportion to higher dADAR levels and did not reach wild-type levels of editing in either *5g1*/*FM7* or

hyp/*FM7* heads. We also examined five HE and LE sites in *hyp*/*hyp*, *5g1*/*FM7*, *hyp*/*FM7,* and *WTLoxP*/*WTLoxP* thoraxes, with similar results (supplemental Fig. S2.3C and D). Finally, Western blotting indicated that there was no significant up-regulation of expression from a wild-type *dAdar* locus in *dAdarHA*/*5g1* trans-heterozygote females (supplemental Fig. S2.3E), indicating that there does not appear to be a compensatory mechanism counteracting decreased ADAR production.

The unexpectedly complex relationship between dADAR concentration and editing levels appears to vary on a site-by-site basis. One possible explanation for the variation in the sensitivity of edited adenosines to dADAR concentration is a differential ratio of substrate mRNA to dADAR enzyme, *i.e.* LE sites are present in mRNAs with high steady-state expression levels, although the converse is true for HE sites. However, this explanation is not consistent with the close proximity of HE and LE sites within transcripts from a single gene, which was observed for several mRNAs, including Caα1D and Dα6 (Fig. 2.3B and C), as well as *shaker*, *shab*, and *eag* (supplemental Table S2.3). For example, sites 5 and 6 of *shaker* are separated by just six nucleotides yet exhibit strikingly different reductions in editing in $dAdar^{hyp}$ heads, with site 5 reduced by 22% and site 6 by 76% (supplemental Table S2.3). In addition, proteins re-coded by dADAR that function in the same sub-cellular compartment also exhibited drastically divergent responses in $dAdar^{hyp}$. *Synaptotagmin-1* (*syt-1*) and *unc-13* both act to promote vesicle release at pre-synaptic nerve terminals. Nonetheless, site 4 of *syt-1* is robustly edited in $dAdar^{hyp}$, although editing of *unc-13* is almost abolished in both $dAdar^{hyp}$ heads and thoraxes (Fig. 2.3). Therefore, our data strongly suggest that the sensitivity of editing sites to changes in dADAR levels is a function of inherent primary sequence and/or

structural properties specific to the double strand RNA structural intermediates required for ADAR-mediated deamination.

High and Low Efficiency Editing Sites Exhibit Distinct Patterns of Developmental Regulation

Editing at many, but not all, dADAR substrates is under strong temporal control, appearing predominantly at the pupal and adult stages of *Drosophila* development. Edited adenosines exhibiting differential developmental regulation may even be found within the same transcript (Ingleby et al., 2009; Jones et al., 2009), yet how this is achieved remains unknown. Previous data has shown that *dAdar* transcription is low during the larval stages and rapidly peaks at the late pupal and adult stages (Palladino et al., 2000b). We hypothesized that adenosines showing high levels of editing throughout development represent HE sites and require low levels of dADAR expression for robust editing. Conversely, pupae/adult-specific sites would require higher concentrations of dADAR for efficient modification and populate the LE class.

We assessed whether temporal changes in *dAdar* transcription result in similar alterations in dADAR protein levels by comparing dADAR expression in the adult thoracic ganglion and the ventral nerve cord of 3rd instar larvae (L3) (Fig. 2.4A). Although strong dADAR expression was observed in neuronal nuclei in the adult thoracic ganglion, dADAR was largely undetectable by immunohistochemistry in the larval ventral nerve cord. Furthermore, Western blotting revealed robust bands corresponding to dADAR-HA isoforms in adult male tissue, which were undetectable in samples prepared from the 1st instar (L1) and L3 larval stages (Fig. 2.4B, *inset*). Thus, the increase in

dAdar mRNA between the larval and adult stages is mirrored by a similar change in detectable dADAR protein expression.

We next investigated whether HE and LE sites show distinct patterns of developmental regulation, in keeping with the above hypothesis. We measured editing at the same HE and LE sites examined above (Fig. 2.3B and C), amplified from Canton-S L1, L3, and adult-stage cDNAs. Editing sites representing HE and LE classes showed strikingly different developmental regulation (Fig. 2.4B and C). As predicted, all LE sites tested showed clear increases in editing between the L3 and adult stages (Fig. 2.4B). Across the eight sites studied, editing levels at the L3 stage averaged only 8 ± 3% of the corresponding adult values. In contrast, HE sites were enriched for adenosines that were robustly edited in the early and late larval stages (Fig. 2.4C), with the mean values at L3 averaging 53 ± 10% of adult levels. Three of the four HE adenosines that did show developmental regulation mapped to the same transcript, encoding the Caα1D voltage-gated calcium channel. Thus, although deamination of particular transcripts may be developmentally modulated by factors distinct from dADAR itself, editing site-specific responses to dADAR protein levels explains a significant proportion of the temporal variation in editing and correlates well with our functional definition of HE and LE classes.

Reduction of dADAR Expression Affects Complex Behavior

The lack of severe uncoordination in $dAdar^{hyp}$ males allowed us to examine, for the first time, whether complex adult-stage behaviors are altered in a genetic background

with an engineered alteration in editing levels.

Under light-dark (12:12 h) conditions, wild-type *Drosophila* exhibit diurnal peaks of activity centered on the lights-on (dawn) and lights-off (dusk) transitions. Importantly, spikes in activity are preceded by anticipatory increases in locomotion that are driven by an endogenous circadian clock (Allada and Chung, 2010). We examined rhythmic locomotor patterns using automated, single-fly activity monitors. $dAdar^{WTLoxP}$ males displayed peaks of activity at subjective morning and evening, as well as anticipation of both dark-light and light-dark transitions (Fig. 2.5A and supplemental Fig. S2.4). Under constant dark conditions, $dAdar^{WTLoxP}$ males displayed anticipation of subjective morning and night (data not shown), illustrating that the circadian clock remains intact in our control genotype. In $dAdar^{hyp}$ males, peaks of morning and evening activity were present but reduced in amplitude relative to $dAdar^{WTLoxP}$ (Fig. 2.5B), and anticipation of morning, but not night, was completely abolished. Importantly, this pattern of locomotor activity was distinct from $dAdar^{5g1}$ males, which lack coordinated locomotor patterns (Fig. 2.5C and supplemental Fig. S2.4) (Palladino et al., 2000a). We quantified the degree of morning anticipation in the above three genotypes (defined as the number of beam breaks in the 3 h before lights-on normalized to the 6 h before lights-on). $dAdar^{WTLoxP}$ males exhibited a 60 and 45% increase respectively in the degree of morning anticipation relative to $dAdar^{hyp}$ and $dAdar^{5g1}$ males, respectively (Fig. 2.5D). Thus, although limited expression of dADAR (~20%) is sufficient to restore a degree of locomotor coordination and activity, including startle responses to changes in light stimuli, more robust dADAR expression is required for the manifestation of circadian anticipation of morning, a complex behavior. Analysis of total locomotor activity revealed that locomotion in

dAdar^{hyp} males and females was reduced by 52–58% relative to control genotypes (Fig. 2.5E). Interestingly, hetero-allelic females revealed that a very modest increase of dADAR expression (from ~50% in *5g1*/*FM7* to ~60% in *hyp*/*FM7* females) was sufficient to completely restore wild-type locomotor levels (Fig. 2.5E).

Temperature-sensitive paralysis and circling behavior, other hallmarks of *dAdar*^{5g1} males (Palladino et al., 2000a), were not observed in *dAdar*^{hyp} males, although sporadic seizures were clearly apparent (see supplemental movie). Most surprisingly, hypomorphic males exhibited robust courtship toward wild-type females, a behavioral pattern completely absent in *dAdar*^{5g1} males (Palladino et al., 2000a). Because the relationship between RNA editing and mating behavior is unclear, we compared several courtship parameters in *dAdar*^{WTLoxP} and *dAdar*^{hyp} males. Although males from both genotypes court wild-type females, *dAdar*^{hyp} males exhibited an ~ 4-fold increase in the time taken to initiate courtship (latency) relative to *dAdar*^{WTLoxP} males (p 0.00025, Mann-Whitney U test; Fig. 2.6A). Despite this, the overall length of time spent courting did not significantly differ between either genotype (p 0.33; Fig. 2.6B and C).

During mating, males produce a species-specific “love song” via unilateral wing vibration, which is proposed to both facilitate female acceptance and to act as an indicator of correct species identity during courtship. Mutations in several loci that also undergo RNA editing have been shown to alter the song waveform (Peixoto and Hall, 1998). This suggested the possibility that RNA editing in neuronal mRNAs might modulate song properties. To test this, we recorded the pulse songs of *dAdar*^{WTLoxP} and *dAdar*^{hyp} males.

Courting *dAdar*^{WTLoxP} males generated robust pulse songs with highly stereotyped

waveforms similar to previously published examples from wild-type *Drosophila* (n = 26, Fig. 2.6D) (Peixoto and Hall, 1998; Zehring et al., 1984). In contrast, pulse songs from $dAdar^{hyp}$ males often exhibited abnormal waveforms characterized by polycyclic pulses and additional peaks (Fig. 2.6E). Of the 44 songs analyzed from $dAdar^{hyp}$ males, only 7 were similar to the $dAdar^{WTLoxP}$ pulse pattern. The change in waveform was accompanied by alterations in several other song parameters, including a reduced number of pulses per song train, an increased pulse frequency, and a small but highly significant increase in the inter-pulse interval ($dAdar^{WTLoxP}$, 38.6 ms ± 0.4, n = 312; $dAdar^{hyp}$, 40.8 ms ± 0.4, n = 281; p <0.0001, Mann-Whitney U test) (Fig. 2.6F–H). In addition, we observed striking variability in the $dAdar^{hyp}$ pulse waveforms, even between distinct song trains from the same male (Fig. 2.6E). The coefficient of variation (defined as the S.D divided by the mean) of the pulse frequency increased from 0.121 in $dAdar^{WTLoxP}$ to 0.265 in $dAdar^{hyp}$, but it was similar when comparing the inter-pulse intervals of the two genotypes ($dAdar^{WTLoxP}$, 0.175; $dAdar^{hyp}$, 0.155). Thus, in addition to influencing multiple song parameters, robust editing also appears to be required for maintaining aspects of male song pulse stereotypy.

Inhibition of RNA Editing in a Small Subset of Neurons Is Sufficient to Alter Complex Behavior

In *Drosophila,* the male-specific isoform of the transcription factor *Fruitless* (Fru^M) is a key mediator of male-specific behaviors, and the output of *fruitless* (*fru*)

neurons is known to be essential for correct courtship behavior and generation of the mating song (Clyne and Miesenbock, 2008; Manoli et al., 2005; Stockinger et al., 2005). Because both of these behavioral parameters were altered in *dAdar*^{hyp} males, we examined the pattern and function of A-to-I editing in this behaviorally important subset of neurons.

fru neurons are present in both the male and female central brain and thoracic ganglion, composing ~2% of the total neuronal population. Although the distribution and projection patterns of *fru* neurons are broadly similar between male and female *Drosophila* (Demir and Dickson, 2005; Manoli et al., 2005; Stockinger et al., 2005), subpopulations of *fru* neurons have been shown to exhibit sexual dimorphism in both number and wiring (Datta et al., 2008; Kimura et al., 2008; Kimura et al., 2005). We initially tested whether editing activity in *fru* neurons also showed sexual dimorphism by driving the two independent insertions of the *syt-T* reporter (Fig. 2.2) using *fru*-Gal4 and analyzing editing at *syt-T* sites 3 and 4 following RT-PCR amplification from male and female head and thorax cDNA. Interestingly, editing at site 4, which is more robustly edited than site 3, indeed showed subtle but significant sexual dimorphism. Site 4 exhibited a relative increase of ~20% in male *versus* female head cDNA (p = 0.004, Mann-Whitney *U* test). This trend was reversed in thorax cDNA, where site 4 editing in *fru* neurons was reduced by ~10% in males relative to females (p = 0.03; Fig. 2.7A and B,). Editing at site 3 showed a similar trend, albeit at lower levels (Fig. 2.7B). Furthermore, site 4 editing was statistically unchanged between *fru* neurons in male heads and thoraxes (p = 0.94) but increased by 30.5% between female head and thorax samples (p = 0.003; Fig. 2.7B). No sex-specific alternative splicing of the *syt-T* reporter

was observed in either head or thorax tissues (supplemental Fig. S2.5).

Because *dAdar* is X-linked, our results could potentially reflect sex-specific differences in dADAR expression throughout the nervous system. Thus, we examined editing of the endogenous *syt-1* transcript in male and female whole head and thorax cDNA and found no significant sexual dimorphism at either site (supplemental Fig. S2.6). We next measured editing at a further five LE and eight HE sites (Fig. 2.3) in the same tissues. In this combined data set of 15 editing sites, we found a small but significant reduction in overall editing in female relative to male heads (mean reduction, 9%, $p = 0.0013$, paired t test). However, in contrast to editing of the *syt-T* reporter, there was no significant alteration in editing of endogenous mRNAs when comparing male and female thoraxes ($p = 0.198$) nor a significant difference in editing of the 15 sites between female head and thorax samples ($p = 0.68$) (supplemental Fig. S2.6). Thus, the female tissue-specific differences in editing of *syt-T* cannot be explained in terms of a global alteration in editing activity. Collectively, these data suggest that dADAR activity is differentially controlled in male and female *fru* neurons.

The existence of sexually dimorphic editing activity suggested a functional role in dADAR activity in *fru* neurons. Robust dADAR expression was detected in many *fru* neurons in both the male brain and the thoracic ganglion (Fig. 2.7C). Importantly, dADAR is expressed in *fru* neurons in the mesothoracic segment of the ventral nerve cord, which are thought to be a key component of the song pattern generator (Fig. 2.7C) (Hall, 1979; von Schilcher and Hall, 1979). We made use of a previously validated double-RNAi line (adr-IR1 + 2) directed against the 3’ region of the *dAdar* transcript and under the control of the upstream activation sequence promoter (Jepson and Reenan,

2009) to selectively reduce dADAR expression in *fru* neurons. Knockdown of dADAR solely in *fru* neurons did not significantly alter male locomotor activity, latency to court, or total time spent courting (supplemental Fig. S2.7). Male-male courting, a hallmark of *fruitless* mutants, was not observed in *fru*-Gal4 > adr-IR1 + 2 males (data not shown). This, as well as the robust courtship of females, indicates that the development and wiring of *fru* neurons are unlikely to be adversely affected by dADAR knockdown.

We next examined the mating song in the experimental and both control genotypes. Song waveforms from control males containing driver or transgenes alone were indistinguishable from $dAdar^{WTLoxP}$ (Fig. 2.7D and E). In contrast,

12/27 song trains from males with dADAR expression inhibited in *fru* neurons exhibited polycyclic waveforms and/or additional peaks that were not observed in either genetic control (Fig. 2.7F), as was also observed in $dAdar^{hyp}$ males (albeit in a higher proportion of songs). This was accompanied by an increase in the average number of pulses per song train (*fru*-Gal4 > adr-IR1 + 2, 12.9 ± 1.7; *fru*-Gal4/+, 6.6 ± 1; adr-IR1 + 2/+ , 8 ± 1.3; $p <$ 0.005, Mann-Whitney *U* test) but no significant alteration in either pulse frequency or inter-pulse interval relative to both control genotypes. Thus, knockdown of dADAR in *fru* neurons can partially phenocopy a discrete subset of the multifaceted alterations in courtship behavior observed in $dAdar^{hyp}$ males, namely the generation of mating songs with abnormal, often polycyclic, waveforms.

DISCUSSION

Using a novel hypomorphic allele of *dAdar* generated through homologous recombination coupled with cell-specific dADAR knockdown, we have demonstrated that RNA editing serves a modulatory role in multiple adaptive behaviors in *Drosophila*. In short, we provide linkage between the loss of conserved and taxa-specific amino acid re-coding sites and alterations in wild-type ethological outputs that directly impinge on organismal fitness. Importantly, the behavioral defects observed in $dAdar^{hyp}$ males correlate with the severe loss of a particular subset of edited adenosines, namely those that are preferentially edited at the adult stage (Fig. 2.4B).

Our molecular analysis of *dAdar* hypomorphs revealed a striking diversity in the response of edited adenosines to changes in endogenous dADAR levels (Fig. 2.3). Both the local sequence surrounding edited adenosines and their predicted secondary structures vary widely between dADAR substrates, providing a potential mechanism to generate differential affinities for dADAR binding and deamination (Bhalla et al., 2004; Hall, 1979; Reenan, 2005). This finding has important implications as follows. First, it provides a explanatory basis for the developmental regulation of a select population of editing sites (Fig. 2.4), a phenomenon common to both *Drosophila* and mammals (Hanrahan et al., 2000; Ingleby et al., 2009; Jones et al., 2009; Rula et al., 2008). Second, cell-specific variation in dADAR expression (Fig. 2.2) may allow spatial control of LE sites while simultaneously maintaining robust network-wide editing of HE sites, thus providing a means to fine-tune neuronal physiology through the diversification of a constrained population of proteins (see Fig. 2.8, for model).

We have previously shown that pan-neuronal expression of the two hairpin RNAi

constructs used in this study reduces locomotor activity by ~90% (Jepson and Reenan, 2009), and this effect could not be phenocopied by dADAR knockdown in any particular neuronal subset tested. Furthermore, dADAR knockdown under these conditions was robust enough to strongly reduce editing even at HE sites such as *syt-1* site 4. Although knockdown is subject to the level of hairpin expression and efficiency of RNAi in particular neurons, the abrogation of ADAR expression by transgenic knockdown was clearly effective. In contrast, editing at HE sites is still maintained in our purely genetic model using $dAdar^{hyp}$ mutant males and females (Fig. 2.3), as is coordinated locomotion (albeit at lower levels; Fig. 2.5). Indeed, even $dAdar^{hyp}/dAdar^{5g1}$ trans-heterozygote females, predicted to express dADAR at ~10% of wild-type levels, do not appear uncoordinated. Collectively, these data imply that network-wide editing of HE sites is sufficient to provide motor tone and prevent the extreme uncoordination observed in *dAdar* null flies.

Conversely, it is tempting to speculate that developmentally regulated LE sites modulate adult-specific behaviors. Indeed, we examined two ethologically relevant behaviors in $dAdar^{hyp}$ males, which show a severe disruption of developmentally regulated editing (Fig. 2.4), and we found both to be defective (Figs. 2.5 and 2.6). $dAdar^{hyp}$ males did not show the circadian anticipation of lights-on seen in wild-type *Drosophila* (Fig. 2.5), and multiple aspects of courtship behavior were abnormal in $dAdar^{hyp}$ males, including the time required to initiate courtship and the waveform of the mating song (Fig. 2.6). It should be stressed that defects in both of the above parameters are likely to be severely detrimental to reproductive fitness under competitive conditions in the wild.

Although our data lead us to hypothesize that loss of adult stage LE sites may underlie the locomotor and courtship defects exhibited by *dAdar* hypomorphs, we cannot currently link the loss of particular editing sites to the behavioral defects seen in $dAdar^{hyp}$ males due to the large number of characterized dADAR substrates. Over 100 editing sites in 24 mRNAs have been identified either serendipitously or through comparative genomics approaches (Hoopengardner et al., 2003), although a recent bioinformatic screen identified a further potential 27 mRNAs subject to re-coding (Stapleton et al., 2006). The existence of functionally epistastic interactions between editing sites also makes it unlikely that any particular phenotype observed in $dAdar^{hyp}$ males can be fully mapped to the loss of a single editing site (Ingleby et al., 2009; Jones et al., 2009). Rather, the relationship between re-coding and behavior can instead be viewed through the prism of the pleiotropic actions of dADAR on a wide range of RNA substrates, with many edited proteins simultaneously contributing to the total phenotype of interest.

We mapped the cellular foci for behavioral abnormalities associated with stringent loss of dADAR expression using transgenic RNAi (Dietzl et al., 2007). Knockdown of dADAR specifically in *fruitless*-expressing neurons partially recapitulated the polycyclic songs observed in $dAdar^{hyp}$ males (Fig. 2.7) but did not phenocopy alterations in other song properties or mating behavior, suggesting that these highly specific phenotypic components are influenced by editing in other *fru*-negative neurons and/or muscle tissue. Surprisingly, targeted expression of a molecular reporter for editing activity suggests that male and female *fru* neurons within both the brain and thoracic ganglion may differ in terms of dADAR activity (Fig. 2.7). Because only small subpopulations of *fru* neurons exhibit morphological sexual dimorphism, it has been

hypothesized that expression of the male-specific isoform of Fruitless (Fru^M) may modify the physiological properties of *fru* neurons (Clyne and Miesenbock, 2008; Demir and Dickson, 2005; Manoli et al., 2005; Stockinger et al., 2005). Given the large number of transcripts re-coded by A-to-I editing (Hoopengardner et al., 2003), an alteration of dADAR expression or activity by Fru^M could hypothetically provide a means of enabling functional modulation of a wide range of ion channels and synaptic release proteins. Further experiments will be required to test whether the alterations in editing observed between male and female *fru* neurons represent large differences in a subset of *fru* neurons, subtle alterations across the *fru* neuron network, or are due to numerical sexual dimorphism in the *fru* neuron population.

That RNA editing can modulate song properties is particularly intriguing, because editing sites are not static throughout insect evolution (Grauso et al., 2002; Jin et al., 2007; Reenan, 2005). Indeed, even within the *Drosophila* lineage, we have observed species-specific changes in the magnitude of editing at orthologous adenosines in several ion channels (Hanrahan et al., 2000; Hoopengardner et al., 2003). Therefore, our data open the possibility that alterations in RNA editing may contribute to species-specific song waveforms, a key mechanism implicated in the reproductive isolation between *Drosophilids*. More broadly, our data suggest that, in principle, evolutionary divergences in RNA editing may contribute to the generation of adult-stage species-specific behavioral patterns.

REFERENCES

Allada, R., and Chung, B.Y. (2010). Circadian organization of behavior and physiology in Drosophila. Annual review of physiology *72*, 605-624.

Barolo, S., Castro, B., and Posakony, J.W. (2004). New Drosophila transgenic reporters: insulated P-element vectors expressing fast-maturing RFP. BioTechniques *36*, 436-440, 442.

Basillo, C., Wahba, A., Lengyel, P., Speyer, J., and Ochoa, S. (1962). Synthetic polynucleotides and the amino acid code. V. Proceedings of the National Academy of Sciences of the United States of America *48*, 613-616.

Bhalla, T., Rosenthal, J.J., Holmgren, M., and Reenan, R. (2004). Control of human potassium channel inactivation by editing of a small mRNA hairpin. Nature structural & molecular biology *11*, 950-956.

Brand, A.H., and Perrimon, N. (1993). Targeted gene expression as a means of altering cell fates and generating dominant phenotypes. Development (Cambridge, England) *118*, 401-415.

Burns, C.M., Chu, H., Rueter, S.M., Hutchinson, L.K., Canton, H., Sanders-Bush, E., and Emeson, R.B. (1997). Regulation of serotonin-2C receptor G-protein coupling by RNA editing. Nature *387*, 303-308.

Clyne, J.D., and Miesenbock, G. (2008). Sex-specific control and tuning of the pattern generator for courtship song in Drosophila. Cell *133*, 354-363.

Datta, S.R., Vasconcelos, M.L., Ruta, V., Luo, S., Wong, A., Demir, E., Flores, J., Balonze, K., Dickson, B.J., and Axel, R. (2008). The Drosophila pheromone cVA activates a sexually dimorphic neural circuit. Nature *452*, 473-477.

Demir, E., and Dickson, B.J. (2005). fruitless splicing specifies male courtship behavior in Drosophila. Cell *121*, 785-794.

Dietzl, G., Chen, D., Schnorrer, F., Su, K.C., Barinova, Y., Fellner, M., Gasser, B., Kinsey, K., Oppel, S., Scheiblauer, S.*, et al.* (2007). A genome-wide transgenic RNAi library for conditional gene inactivation in Drosophila. Nature *448*, 151-156.

Grauso, M., Reenan, R.A., Culetto, E., and Sattelle, D.B. (2002). Novel putative nicotinic acetylcholine receptor subunit genes, Dalpha5, Dalpha6 and Dalpha7, in Drosophila melanogaster identify a new and highly conserved target of adenosine deaminase acting on RNA-mediated A-to-I pre-mRNA editing. Genetics *160*, 1519-1533.

Hall, J.C. (1979). Control of male reproductive behavior by the central nervous

system of Drosophila: dissection of a courtship pathway by genetic mosaics. Genetics *92,*, 437–457.

Hanrahan, C.J., Palladino, M.J., Ganetzky, B., and Reenan, R.A. (2000). RNA editing of the Drosophila para Na(+) channel transcript. Evolutionary conservation and developmental regulation. Genetics *155*, 1149-1160.

Higuchi, M., Maas, S., Single, F.N., Hartner, J., Rozov, A., Burnashev, N., Feldmeyer, D., Sprengel, R., and Seeburg, P.H. (2000). Point mutation in an AMPA receptor gene rescues lethality in mice deficient in the RNA-editing enzyme ADAR2. Nature *406*, 78-81.

Higuchi, M., Single, F.N., Kohler, M., Sommer, B., Sprengel, R., and Seeburg, P.H. (1993). RNA editing of AMPA receptor subunit GluR-B: a base-paired intron-exon structure determines position and efficiency. Cell *75*, 1361-1370.

Hoopengardner, B., Bhalla, T., Staber, C., and Reenan, R. (2003). Nervous system targets of RNA editing identified by comparative genomics. Science (New York, NY *301*, 832-836.

Ingleby, L., Maloney, R., Jepson, J., Horn, R., and Reenan, R. (2009). Regulated RNA editing and functional epistasis in Shaker potassium channels. The Journal of general physiology *133*, 17-27.

Jacobs, M.M., Fogg, R.L., Emeson, R.B., and Stanwood, G.D. (2009). ADAR1 and ADAR2 expression and editing activity during forebrain development. Developmental neuroscience *31*, 223-237.

Jepson, J.E., and Reenan, R.A. (2009). Adenosine-to-inosine genetic recoding is required in the adult stage nervous system for coordinated behavior in Drosophila. The Journal of biological chemistry *284*, 31391-31400.

Jin, Y., Tian, N., Cao, J., Liang, J., Yang, Z., and Lv, J. (2007). RNA editing and alternative splicing of the insect nAChR subunit alpha6 transcript: evolutionary conservation, divergence and regulation. BMC evolutionary biology *7*, 98.

Jones, A.K., Buckingham, S.D., Papadaki, M., Yokota, M., Sattelle, B.M., Matsuda, K., and Sattelle, D.B. (2009). Splice-Variant- and Stage-Specific RNA Editing of the Drosophila GABA Receptor Modulates Agonist Potency. J Neurosci *29*, 4287-4292.

Keegan, L.P., Brindle, J., Gallo, A., Leroy, A., Reenan, R.A., and O'Connell, M.A. (2005). Tuning of RNA editing by ADAR is required in Drosophila. The EMBO journal *24*, 2183-2193.

Kimura, K., Hachiya, T., Koganezawa, M., Tazawa, T., and Yamamoto, D. (2008). Fruitless and doublesex coordinate to generate male-specific neurons that can initiate courtship. Neuron *59*, 759-769.

Kimura, K., Ote, M., Tazawa, T., and Yamamoto, D. (2005). Fruitless specifies sexually dimorphic neural circuitry in the Drosophila brain. Nature *438*, 229-233.

Maggert, K.A., Gong, W.J., and Golic, K.G. (2008). Methods for homologous recombination in Drosophila. Methods in molecular biology (Clifton, NJ *420*, 155-174.

Manoli, D.S., Foss, M., Villella, A., Taylor, B.J., Hall, J.C., and Baker, B.S. (2005). Male-specific fruitless specifies the neural substrates of Drosophila courtship behaviour. Nature *436*, 395-400.

Nishikura, K. (2010). Functions and regulation of RNA editing by ADAR deaminases. Annual review of biochemistry *79*, 321-349.

Ohlson, J., Pedersen, J.S., Haussler, D., and Ohman, M. (2007). Editing modifies the GABA(A) receptor subunit alpha3. RNA (New York, NY *13*, 698-703.

Palladino, M.J., Keegan, L.P., O'Connell, M.A., and Reenan, R.A. (2000a). A-to-I pre-mRNA editing in Drosophila is primarily involved in adult nervous system function and integrity. Cell *102*, 437-449.

Palladino, M.J., Keegan, L.P., O'Connell, M.A., and Reenan, R.A. (2000b). dADAR, a Drosophila double-stranded RNA-specific adenosine deaminase is highly developmentally regulated and is itself a target for RNA editing. RNA (New York, NY *6*, 1004-1018.

Peixoto, A.A., and Hall, J.C. (1998). Analysis of temperature-sensitive mutants reveals new genes involved in the courtship song of Drosophila. Genetics *148*, 827-838.

Reenan, R.A. (2005). Molecular determinants and guided evolution of species-specific RNA editing. Nature *434*, 409-413.

Rong, Y.S., and Golic, K.G. (2000). Gene targeting by homologous recombination in Drosophila. Science (New York, NY *288*, 2013-2018.

Rong, Y.S., Titen, S.W., Xie, H.B., Golic, M.M., Bastiani, M., Bandyopadhyay, P., Olivera, B.M., Brodsky, M., Rubin, G.M., and Golic, K.G. (2002). Targeted mutagenesis by homologous recombination in D. melanogaster. Genes & development *16*, 1568-1581.

Rula, E.Y., Lagrange, A.H., Jacobs, M.M., Hu, N., Macdonald, R.L., and Emeson, R.B. (2008). Developmental modulation of GABA(A) receptor function by RNA editing. J Neurosci *28*, 6196-6201.

Semenov, E.P., and Pak, W.L. (1999). Diversification of Drosophila chloride channel gene by multiple posttranscriptional mRNA modifications. Journal of neurochemistry *72*, 66-72.

Smith, L.A., Peixoto, A.A., and Hall, J.C. (1998). RNA editing in the Drosophila DMCA1A calcium-channel alpha 1 subunit transcript. Journal of neurogenetics *12*, 227-240.

Stapleton, M., Carlson, J.W., and Celniker, S.E. (2006). RNA editing in Drosophila melanogaster: New targets and functional consequences. RNA (New York, NY *12*, 1922-1932.

Stockinger, P., Kvitsiani, D., Rotkopf, S., Tirian, L., and Dickson, B.J. (2005). Neural circuitry that governs Drosophila male courtship behavior. Cell *121*, 795-807.

von Schilcher, F., and Hall, J.C. (1979). Neural topography of courtship song in sex mosaics of Drosophila melanogaster. Journal of Comparative Physiology [A], 85-95.

Wu, J.S., and Luo, L. (2006). A protocol for dissecting Drosophila melanogaster brains for live imaging or immunostaining. Nature protocols *1*, 2110-2115.

Zehring, W.A., Wheeler, D.A., Reddy, P., Konopka, R.J., Kyriacou, C.P., Rosbash, M., and Hall, J.C. (1984). P-element transformation with period locus DNA restores rhythmicity to mutant, arrhythmic Drosophila melanogaster. Cell *39*, 369-376.

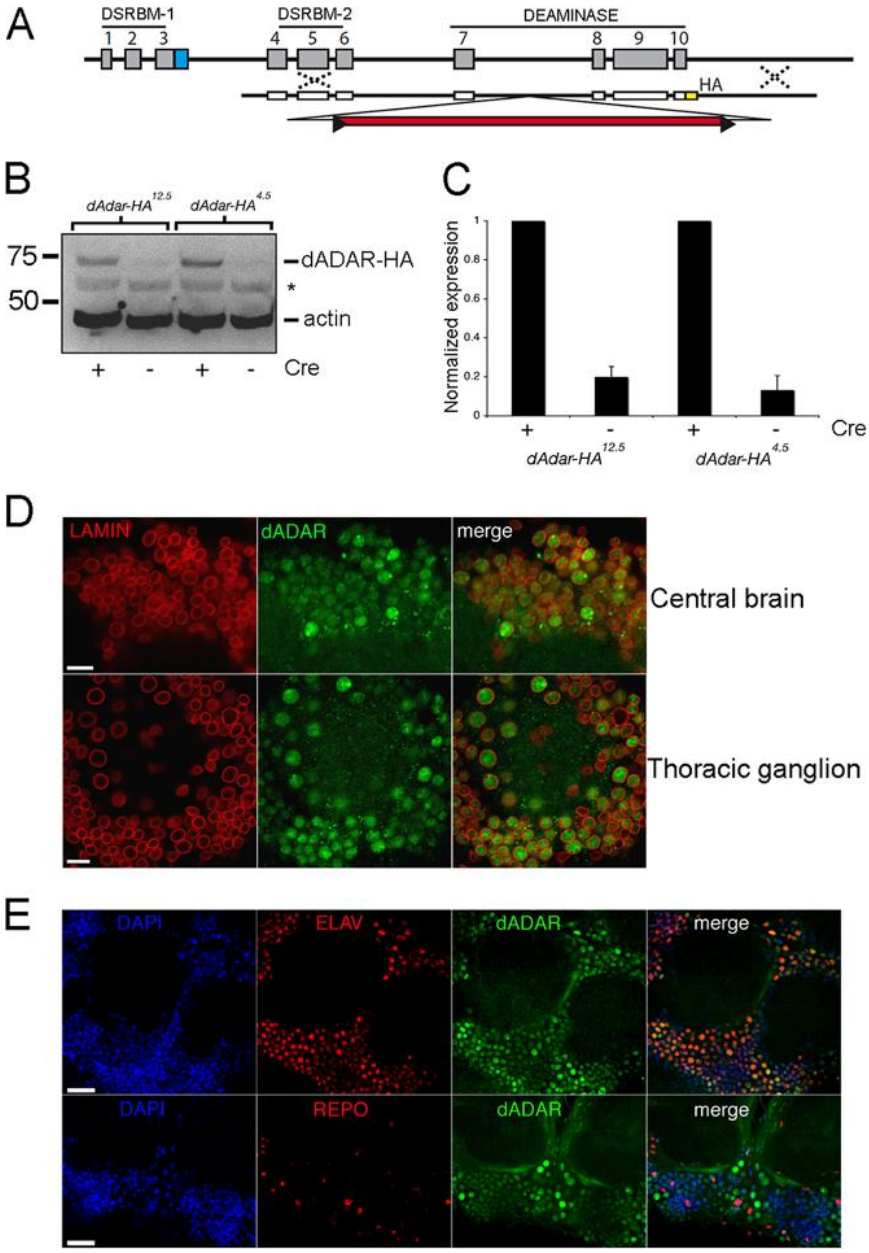

FIGURE 2.1. Visualization of dADAR expression using ends-out homologous recombination. (A) Schematic representation of the targeting construct used to insert an HA epitope tag at the 3' of the *dAdar* locus. (B) Representative Western blot showing HA-positive bands in two independent lines lacking the *white*$^{+}$ mini-gene. Actin was used as a loading control. *, nonspecific labeling. This is likely to be a head/brain-specific cross-reaction because it is not observed when using whole fly tissue (see Fig. 2.4B). (C) Quantification of relative dADAR-HA levels (normalized to actin) before and after Cre expression. Values are expressed relative to the mean of each post-Cre *dAdarHA* line (n = 6 Western blots, three independent samples). *Error bars*, S.E. values. (D) Lamin and dADAR-HA staining in the male brain and thoracic ganglion. *Scale bar,* 10 μm. *E*, dADAR-HA co-localizes with DAPI-stained nuclei and Elav, but not Repo, inthe male brain. *Scale bar,* 20 μm.

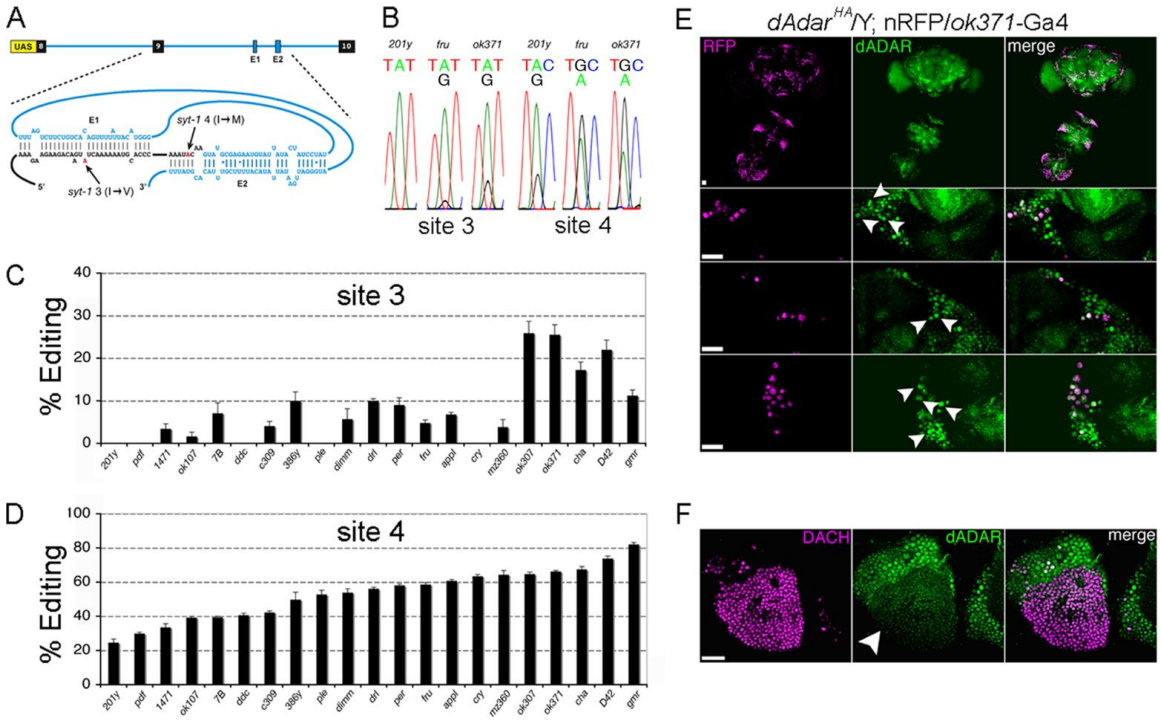

FIGURE 2.2. Molecular reporter of RNA editing reveals neuron-specific patterns of dADAR activity**. (**A) Design of the reporter, termed *syt-T*. Exons 8–10 of *syt-1*, along with the intervening introns, were cloned into the pUAS expression vector. Upon transcription, the E1 and E2 elements form a pseudo-knot structure by base pairing with coding sequences in exon 9 (Reenan, 2005), leading to formation of a dADAR substrate and editing of sites 3 and 4. (B) Example electropherograms showing editing of sites 3 and 4 in three genetically distinct cell types as follows: mushroom body neurons (*201y*), *fruitless*-positive (*fru*), and glutamatergic (*ok371*) neurons. Average editing of site 3 and 4 in 21 classes of neurons, defined by distinct Gal4 drivers, is shown in C and D. Each value is the mean of 4–6 RT-PCRs derived from males carrying each Gal4 driver and one of two independent insertions of *syt-T*. *Error bars*, S.E. values. (E) dADAR expression in glutamatergic neurons. dADAR-HA and the nuclear red fluorescent protein *red-stinger* (Barolo et al., 2004) driven by *ok371*-Gal4 are shown in the male brain and thoracic ganglion (*upper panel*), and at higher magnification in the central brain (*middle*) and thoracic ganglion (*lower panel*). (F) dADAR-HA expression in Dachshund-positive Kenyon cells is clearly reduced relative to the surrounding nuclei. *Scale bars,* 20 μm.

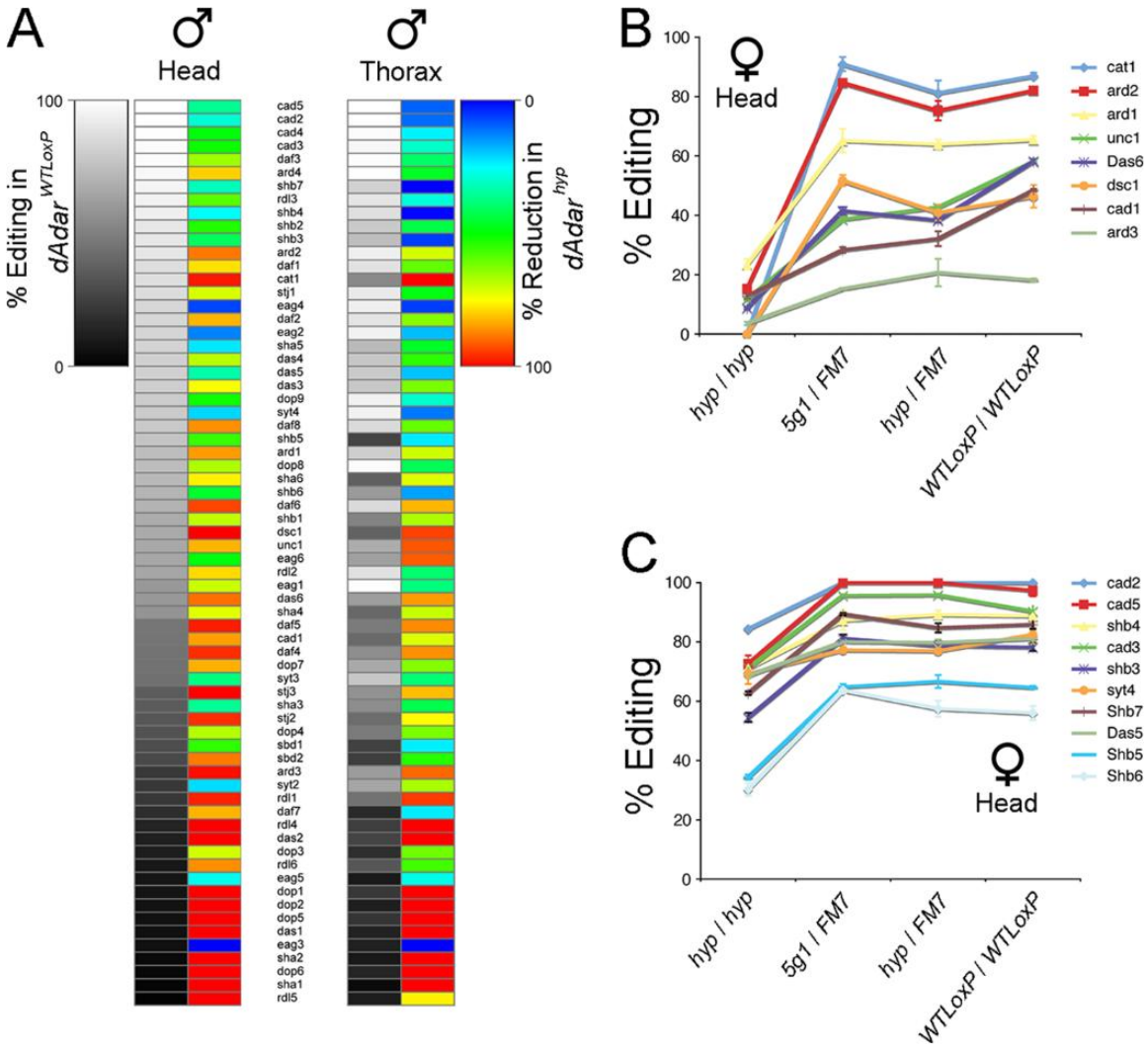

FIGURE 2.3. Varied impacts on mRNA re-coding following reduction of dADAR expression. **(**A) Heat map representation of editing levels at 68 sites in *dAdar*^{WTLoxP} heads and thoraxes, and the corresponding reduction of editing in the same tissue from *dAdar*^{hyp} males. Each editing site is represented by a four-symbol code (see supplemental Table S2.3 for details). (B) and (C) Editing levels in female heads for 8 LE sites (B) and 10 HE sites (C). The homozygotic and heterozygotic backgrounds containing various *dAdar* alleles are noted *below* each graph. Each value is the mean of ≥3 RT-PCRs. *Error bars*, S.E. values.

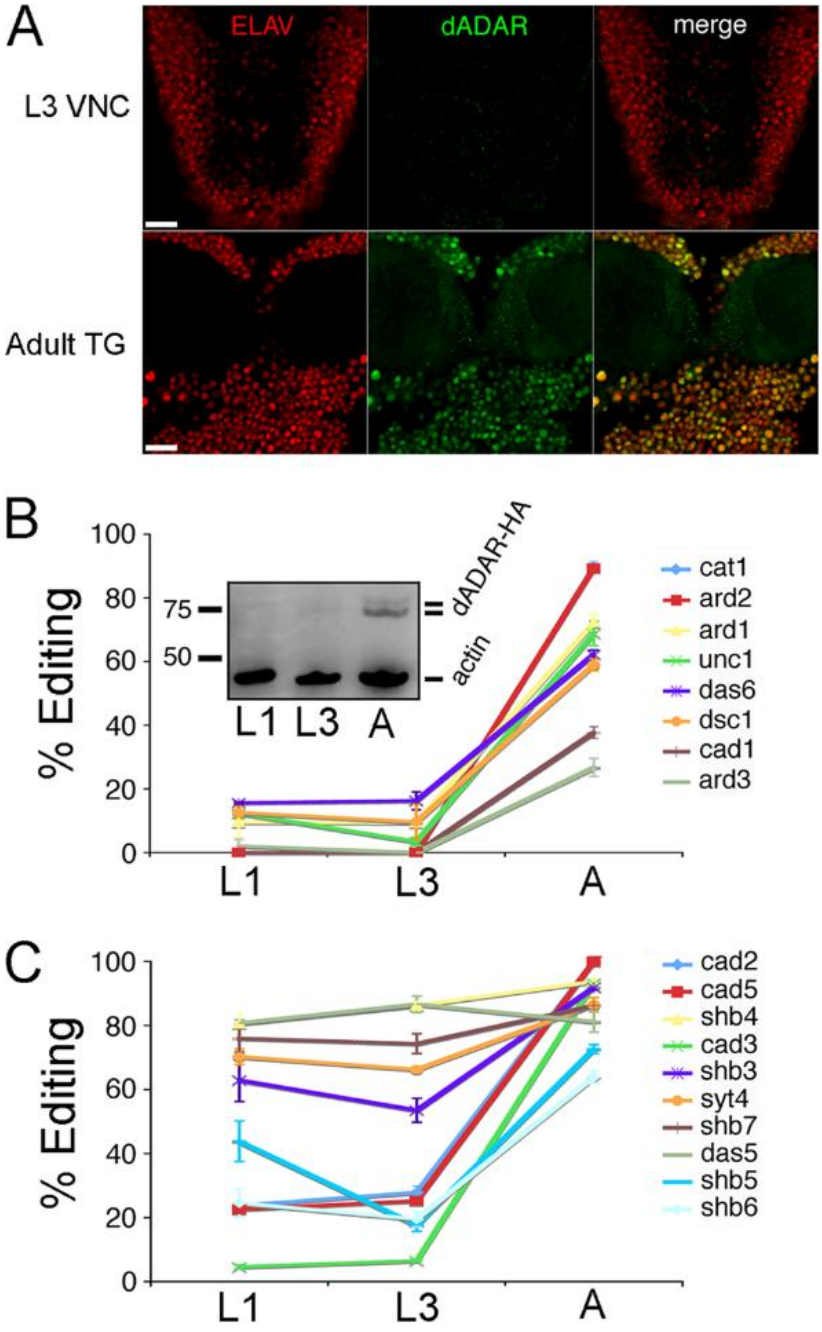

FIGURE 2.4. Dynamic control of dADAR expression underlies developmental patterns of editing at low efficiency sites. **(**A) dADAR and Elav expression in the L3 ventral nerve chord (*VNC*) and the adult thoracic ganglion (*TG*). *Scale bar,* 20 μm. (B) LE sites are subject to strong developmental regulation. Editing at eight LE sites was examined at two larval stages (L1 and L3) and in adult males (A). *Inset,* representative example of $n = 4$ Western blots showing a strong increase in dADAR expression at the male adult stage relative to L1 and L3. The two dADAR-HA bands likely represent dADAR proteins containing or lacking the alternatively spliced 3a exon, which is included at a higher level in the abdomen relative to the head and thorax. (C) Developmental profiles of 10 HE sites in L1, L3, and adult (A) males. *Error bars*, S.E. values.

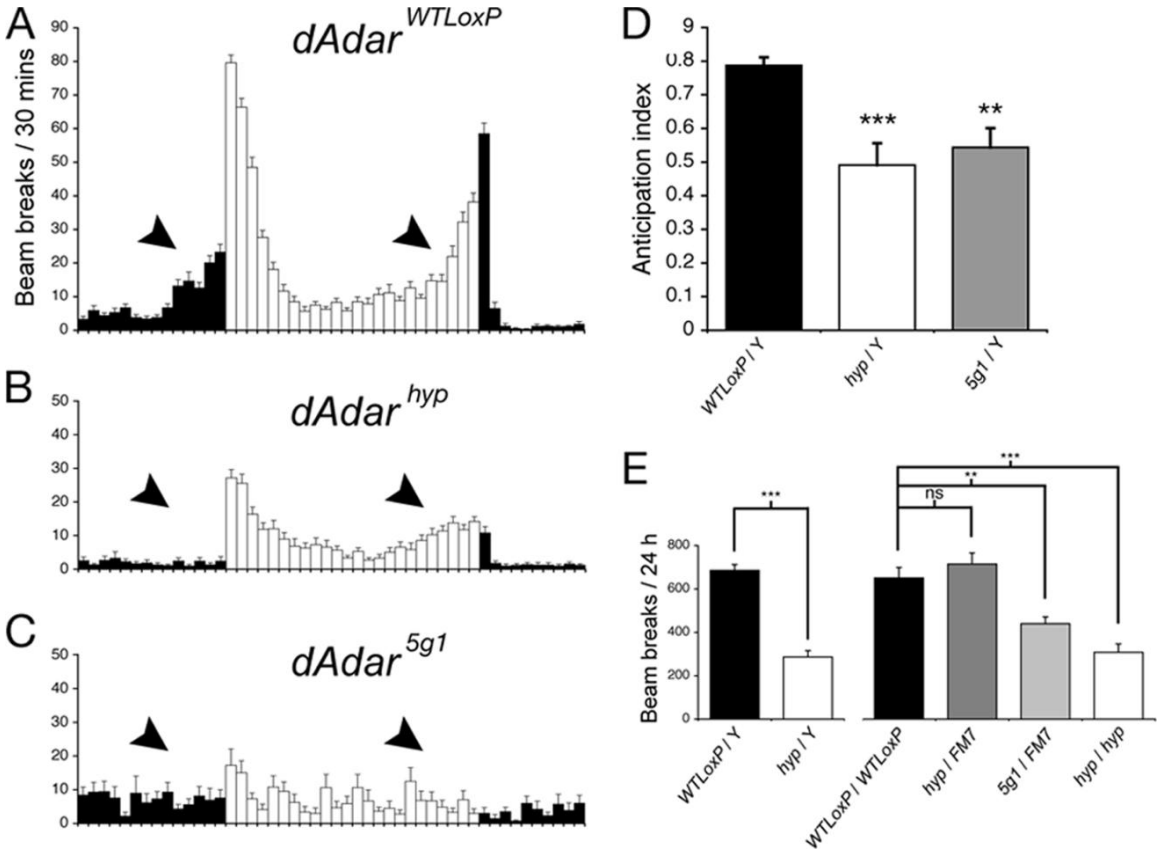

FIGURE 2.5. Global reduction in dADAR activity leads to altered patterns of locomotor activity. **(**A–C) Mean activity profile of *dAdar*^{WTLoxP} (A, n = 30), *dAdar*^{hyp} (B, n = 30), and *dAdar*^{5g1} males (C, n = 16) under 12-h light-dark cycles (*white* and *black bars*). Each *bar* is an average value of time points from three consecutive days. In *dAdar*^{WTLoxP}, but not dAdar^{hyp} or *dAdar*^{5g1} males, anticipation of morning and evening can be observed under both environmental conditions (*arrowheads*). (D) Quantification of morning anticipation in the three experimental genotypes. (E) Mean locomotor activity in male and female *dAdar* allelic backgrounds. *Error bars*, S.E. values. **, $p < 0.005$; ***, $p < 0.0005$; not significant (*ns*): $p > 0.05$ (Mann-Whitney *U* test).

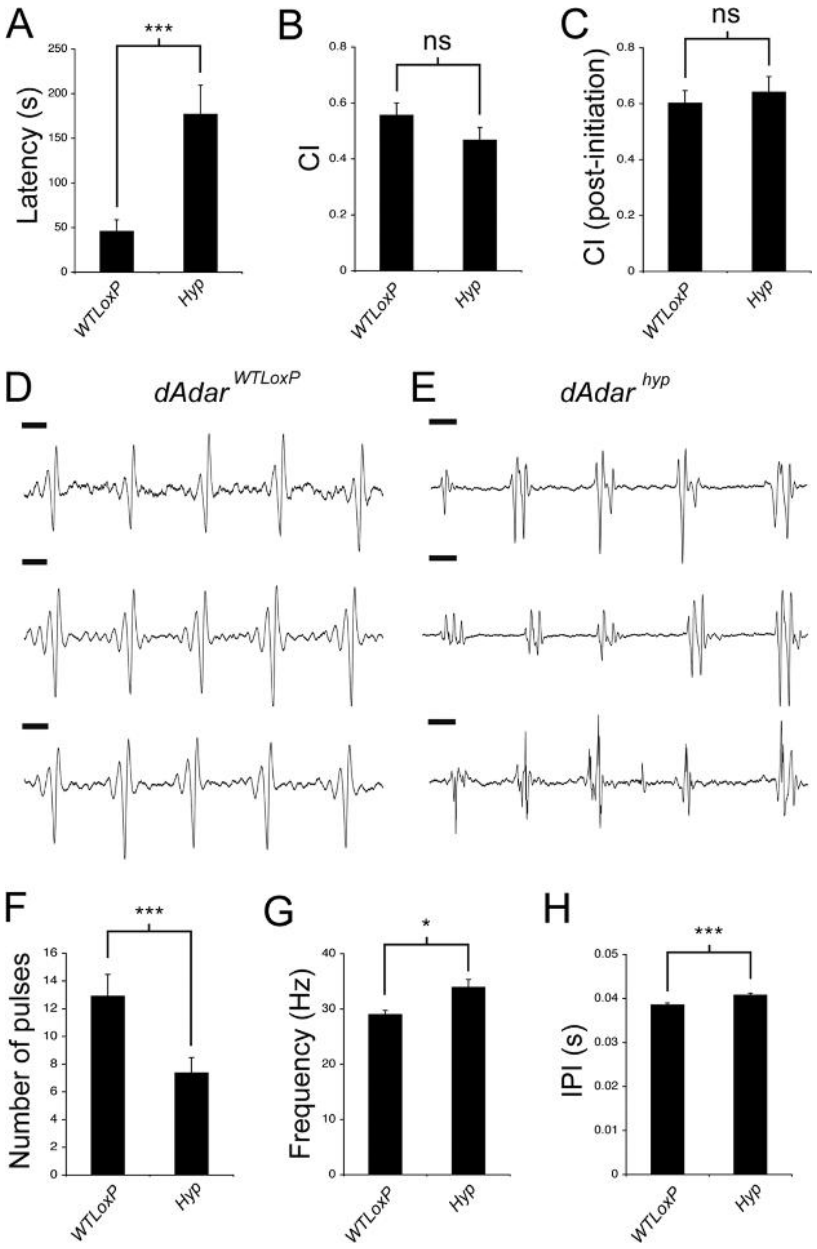

FIGURE 2.6. RNA editing is required for appropriate male courtship. **(**A) Time taken to initiate courtship (latency) is significantly higher in *dAdar*^{hyp} males (n = 20) relative to *dAdar*^{WTLoxP} controls (n = 15), yet the total time spent courting virgin females over a 10-min period (courtship index, *CI*) is not significantly different between either genotype (B and C). Courtship index was either calculated over the whole 10 min (B) or following initiation of courtship (C). Examples of three separate song trains are shown from a single *dAdar*^{WTLoxP} (D) or *dAdar*^{hyp} male (E). Note that although the trains from the *dAdar*^{WTLoxP} male are highly stereotyped, trains from even a single *dAdar*^{hyp} male show striking variability in waveform pattern. *Scale bar,* 10 ms. F–H, song parameters in *dAdar*^{WTLoxP} (n = 26 songs, 5 males) and *dAdar*^{hyp} (n = 44 songs, 9 males). *Error bars*, S.E. values. *, $p < 0.05$; ***, $p < 0.0005$; not significant (*ns*): $p > 0.05$(Mann-Whitney U test).

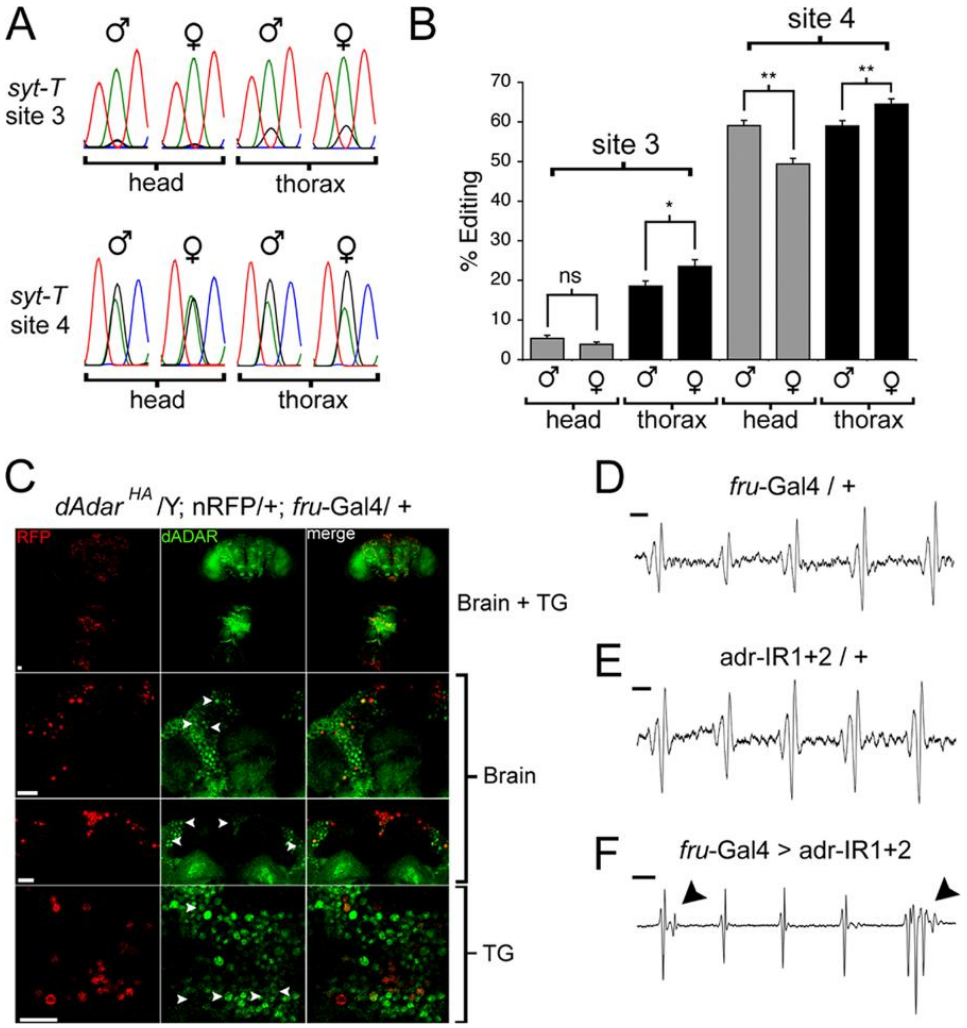

FIGURE 2.7. Knockdown of dADAR in *fruitless*-expressing neurons alters the male courtship song. **(**A) Example of electropherograms showing editing of *syt-T* site 3 and 4 expressed in *fruitless*-positive (*fru*) neurons within the male and female head or thorax. (B) Quantification of editing of two independent insertions of *syt-T* (n = 6–7 RT-PCRs for each value). (C) dADAR expression was examined specifically in *fru* neurons by expressing a nuclear red fluorescent protein using the *fru*-Gal4 driver line, in a $dAdar^{HA}$ background. Nuclei of *fru* neurons can be detected throughout the brain and thoracic ganglion (*upper panel*). Examples of dADAR expression in *fru* neurons in the dorsal anterior segment and pars intercerebralis (*middle panels*) and meso-thoracic ganglion (*lower panel*) are shown at higher magnification below. (D and E) Example of song trains from control males heterozygous for driver (w^+; + ; *fru*-Gal4/+ , n = 26 song trains, 10 males) or RNAi transgenes (w^+; adr-IR1/+ ; adr-IR2/+ , n = 30 song trains, 10 males). Note the similarity in waveform between song trains shown in D and E compared with those from $dAdar^{WTLoxP}$ males (Fig. 2.6D). (F) Example of song trains from males with reduced dADAR expression in *fru* neurons (w^+; adr-IR1/+ ; *fru*-Gal4/adr-IR2) (n = 27 song trains, 11 males). Note the extra spike in the first pulse and the polycyclic waveform in the last pulse. *Scale bar,* 10 ms. *Error bars*, S.E. values. *, $p < 0.05$; **, $p < 0.005$; not significant (*ns*): $p > 0.05$ (Mann-Whitney *U* test).

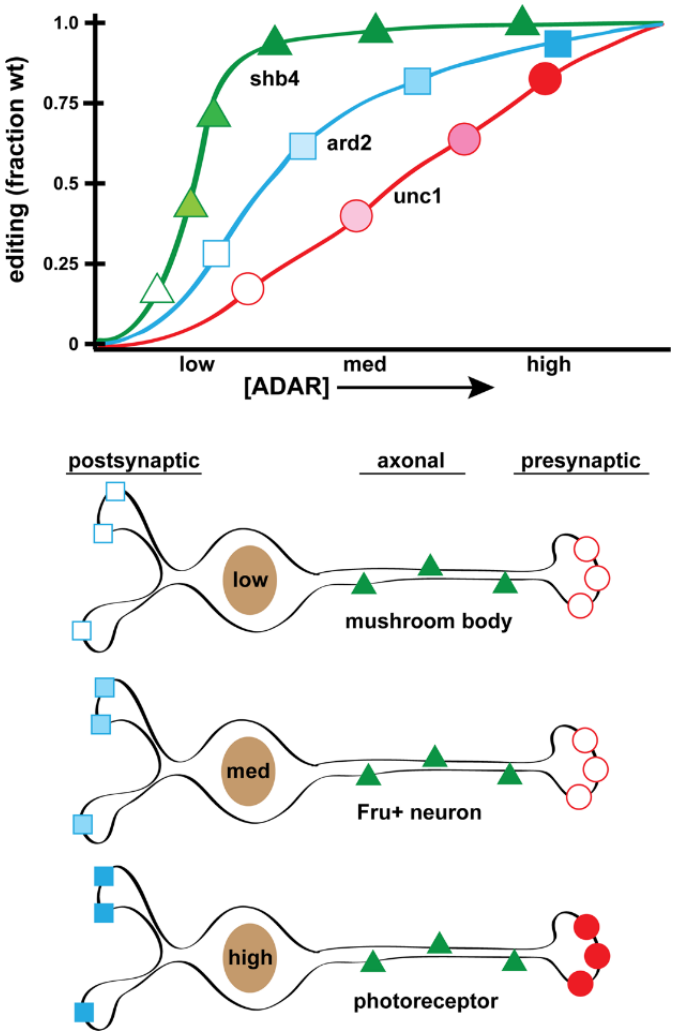

FIGURE 2.8. Model for neuron-to-neuron variation in editing levels within the *Drosophila* nervous system. *Top panel* shows a graphical representation of the change in editing of one HE site (*shab* site 4; shb4) and two LE sites (*ard* site 2; ard2, and *unc-13*; unc1). *Shab* site 4 is edited at almost wildtype levels even in genotypes with very low dADAR expression, as is the case for all HE sites (Fig. 2.3). Thus, editing at this, and similar sites, is unlikely to vary widely from neuron to neuron, even though dADAR activity is highly variable in different neuronal populations (Fig. 2.2). In contrast, editing at LE sites is likely to vary substantially in neurons with differing levels of dADAR expression. Certain LE sites only required 50% of wild-type dADAR expression for achieving wild-type editing levels, while the others required more robust dADAR expression (Fig. 2.3). The *bottom panel* shows a diagrammatic representation of three distinct neuronal subtypes (derived from Fig. 2.2), with low, medium (*med*), and high relative expression of dADAR. In neurons with low dADAR activity (such as mushroom body neurons), only HE sites such as *shab* site 4 are likely to be strongly edited. At slightly higher levels (for example, *fru* neurons), both *shab* site 4 and *ard* site 2 (*i.e.* the "higher efficiency" LE sites) will show editing but not weak LE sites such as *unc-13*. Finally, in neurons with high dADAR expression (such as photo- receptors; supplemental Table S2.2), all subclasses may be open to robust editing.

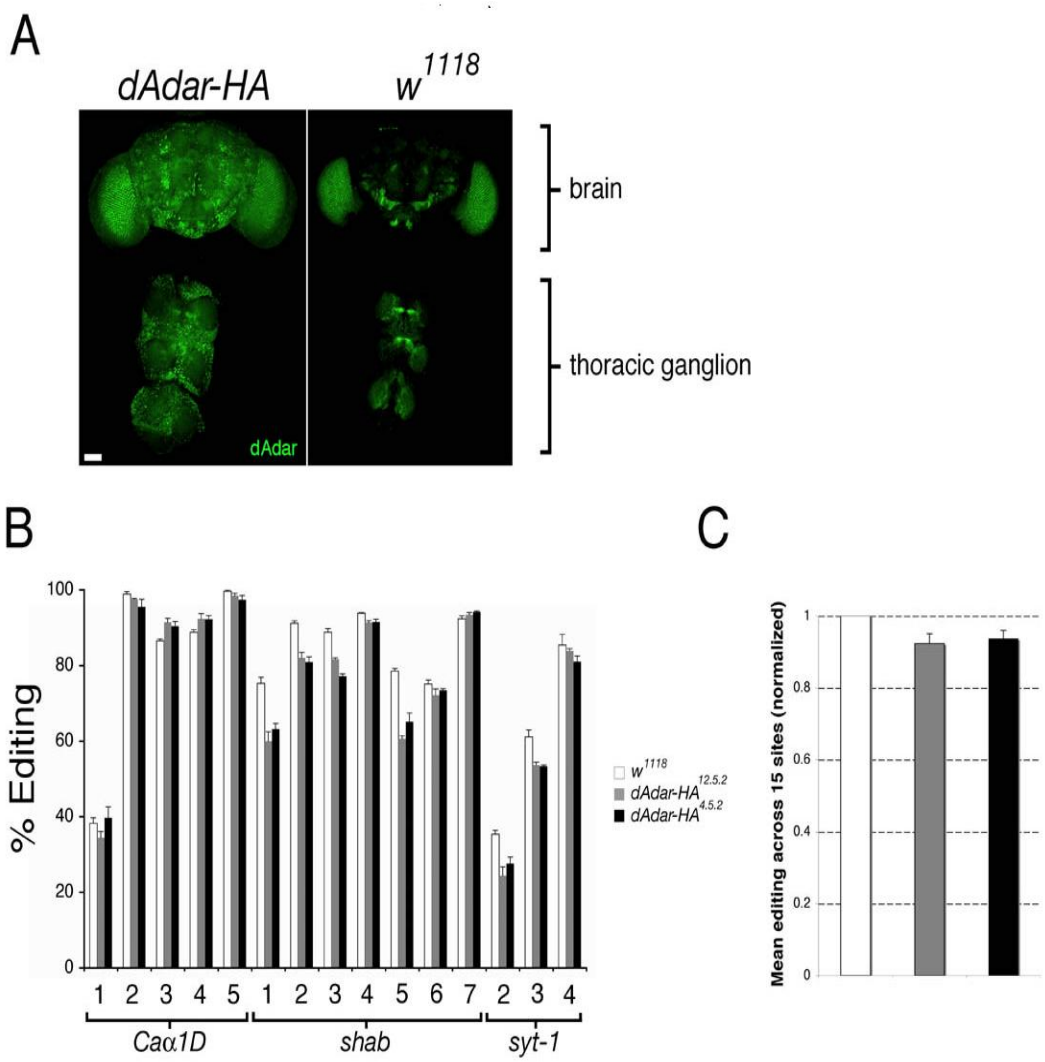

FIGURE S2.1. (A) Expression of dADAR-HA in the male brain and thoracic ganglion (TG). Punctate HA-positive staining was observed in nuclear regions throughout both the brain and thoracic ganglion (TG) in *dAdar*^{HA} males but not w^{1118} negative controls. Scale bar = 50 μm. (B) Editing levels at 15 adenosines in three different transcripts were not affected by addition of the HA-tag to the *dAdar* locus. Two independent *dAdar*^{HA} alleles (12.5.2 and 4.5.2) were compared to w^{1118} males. Mean values for the population of editing sites are shown in C, after normalization to w^{1118}. *Error bars*, S.E values.

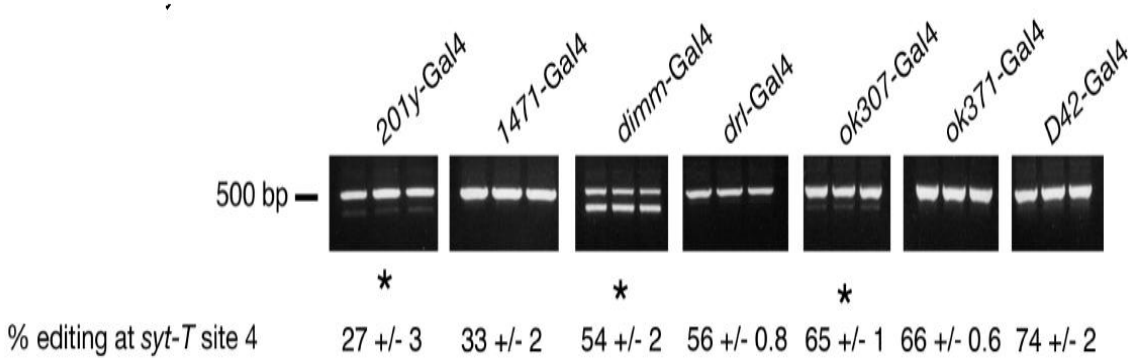

FIGURE S2.2. Exon skipping of the *syt-T* reporter does not account for neuron-specific differences in editing. Only in a minority of the 21 neuronal sub-types in which the reporter was expressed (supplemental Table S2.2), did we observe skipping of the edited exon (exon 9, Figure 2.2) in RT-PCR products (three independent PCR reactions are shown for each Gal4 line). However, the degree of skipping did not correlate with the level of editing at either editing site in the *syt-T* construct. For example, when *syt-T* was driven using both *201*y- and *ok307*-Gal4, we observed a small degree of skipping, yet these two neurons exhibit contrasting levels of editing at *syt-T* site 4. In adult heads, robust skipping only occurred when *syt-T* was driven in one neuronal subtype (peptidergic neurons) by *dimm*-Gal4. In this neuronal subtype, editing at site 4 is not significantly different from that seen when *syt-T* is driven by *drl*-Gal4 (MB and CC expression, Supp. Table S2.2), yet we observed no alternative splicing using this driver.

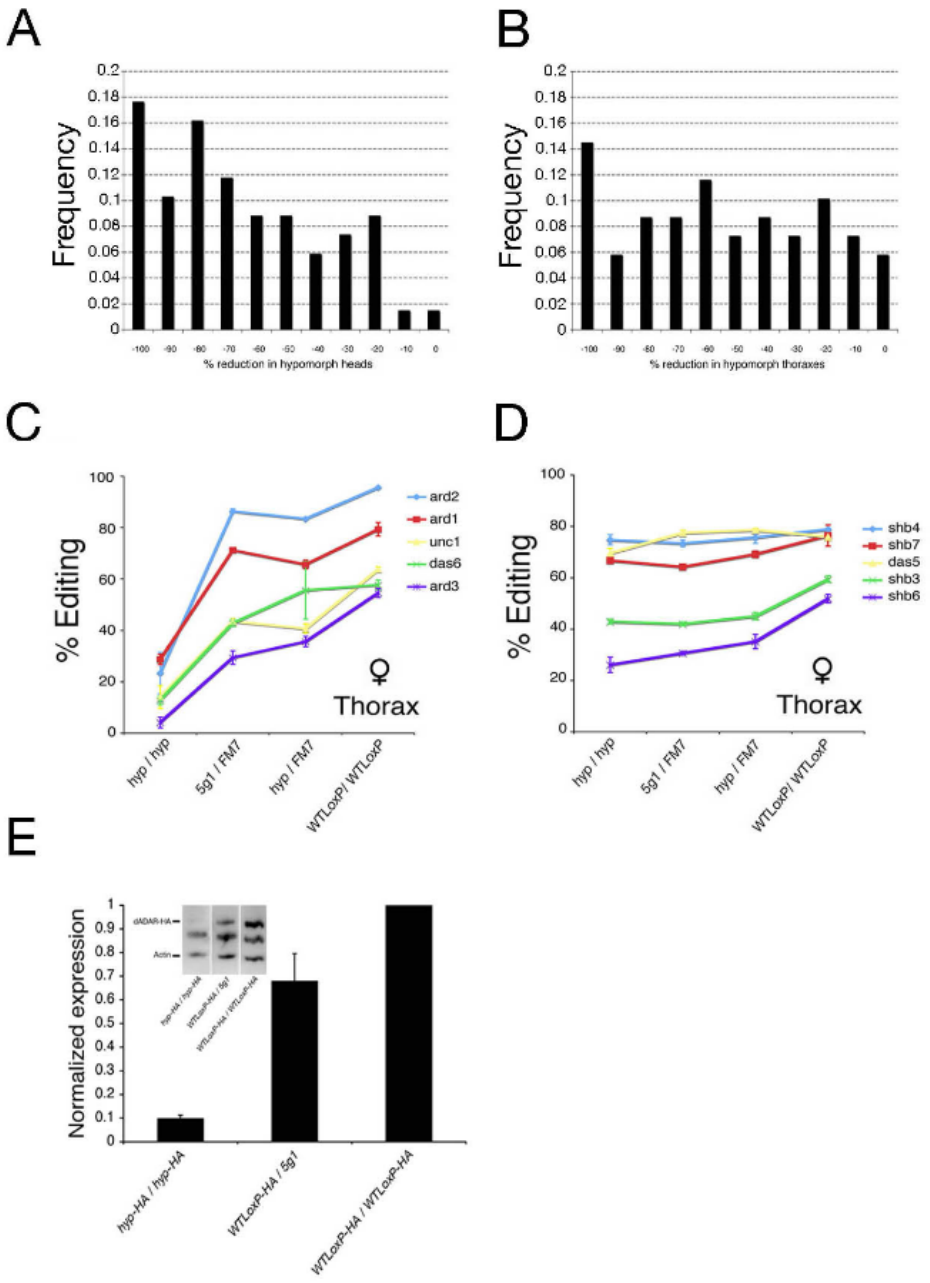

FIGURE S2.3. Frequency distribution of the reduction in editing levels observed at 68 dADAR target adenosines amplified from *dAdar*^{hyp} heads (A) and thoraxes (B), compared to the same tissue in *dAdar*^{WTLoxP} males. (C-D) Editing levels in female thoraxes for five 'low efficiency' (LE) sites (C) and high-efficiency (HE) sites (D). The female genetic backgrounds are noted below each graph. Each mean was calculated from ≥ 3 RT-PCRs. (E) dADAR-HA expression levels in *hyp*^{HA}, *WTLoxPHA*/*5g1* and *WTLoxPHA* females. Inset shows example western blot from the above genotypes. We did not observe signs of any substantial feedback loop indicating increased expression from the single wild-type *dAdar* locus in*WTLoxP*^{HA}/*5g1* female (n = 3 western blots). *Error bars*, S.E values.

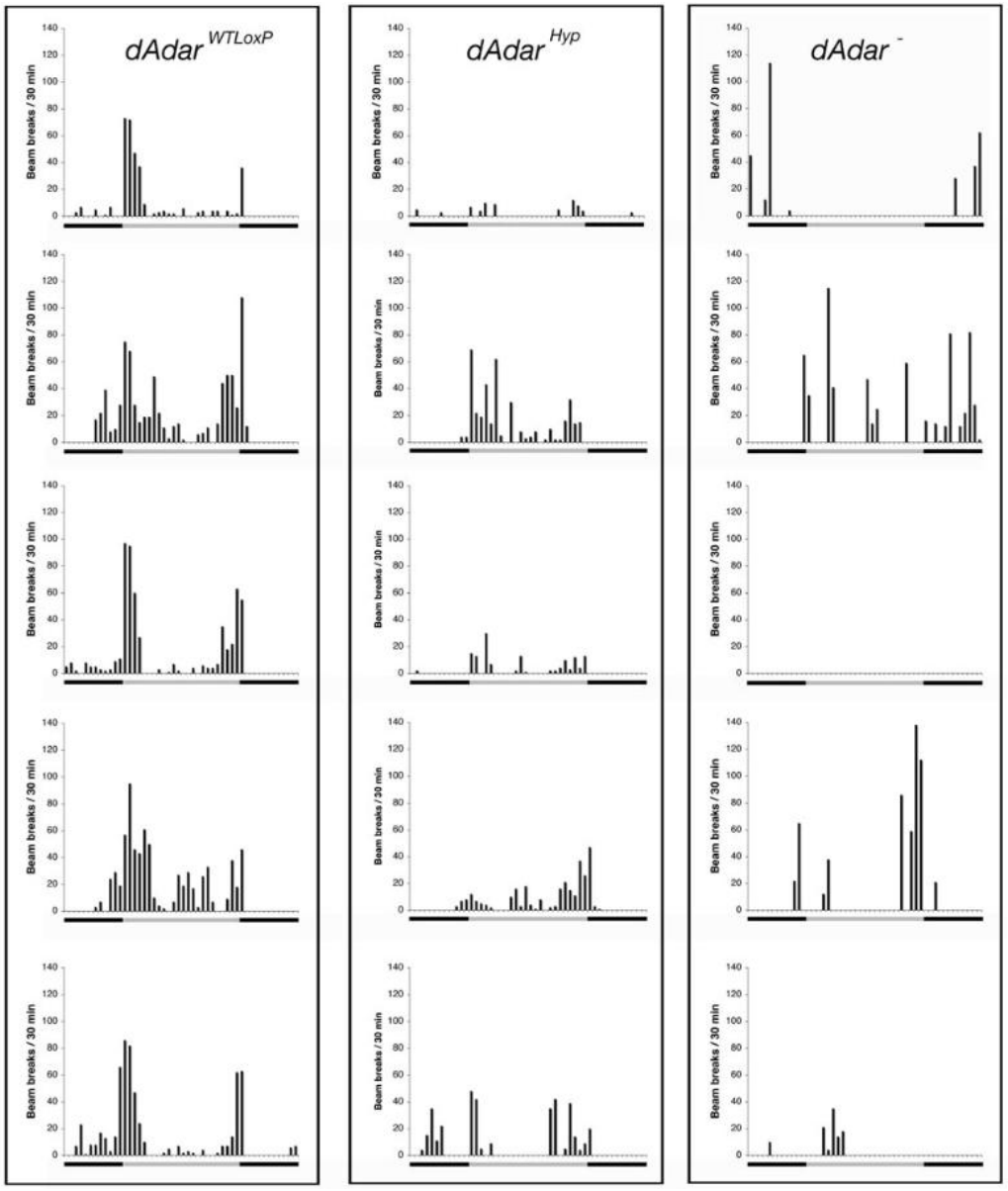

FIGURE S2.4. Examples of single-fly profiles of locomotor activity. For each genotype, five individual traces are shown across a single 24 h period. Dark bars represent lights-off and grey bars lights-on. Locomotion in *dAdar*^{WTLoxP} males is highly stereotyped, with peak levels of activity occurring at lights-on and lights-off in all cases, and very little activity observed under dark conditions. *dAdar* hypomorphs also show peaks at lights-on and lights-off, but the peaks are reduced in magnitude relative to *dAdar*^{WTLoxP}. In addition, the increase in activity preceding lights-on, which can be observed in *dAdar*^{WTLoxP} males, is not generally present in *dAdar* hypomorphs. In contrast to *dAdar* hypomorphs, *dAdar* null (*dAdar*^{5g1}) males exhibit an essentially random pattern of activity, with brief increases in beam breaks even observed in dark conditions. In some cases, no activity is observed over a 24 h period (third example). In the example given, locomotor activity was detected in the next 24 h period, indicating that the fly was not simply dead, but inactive.

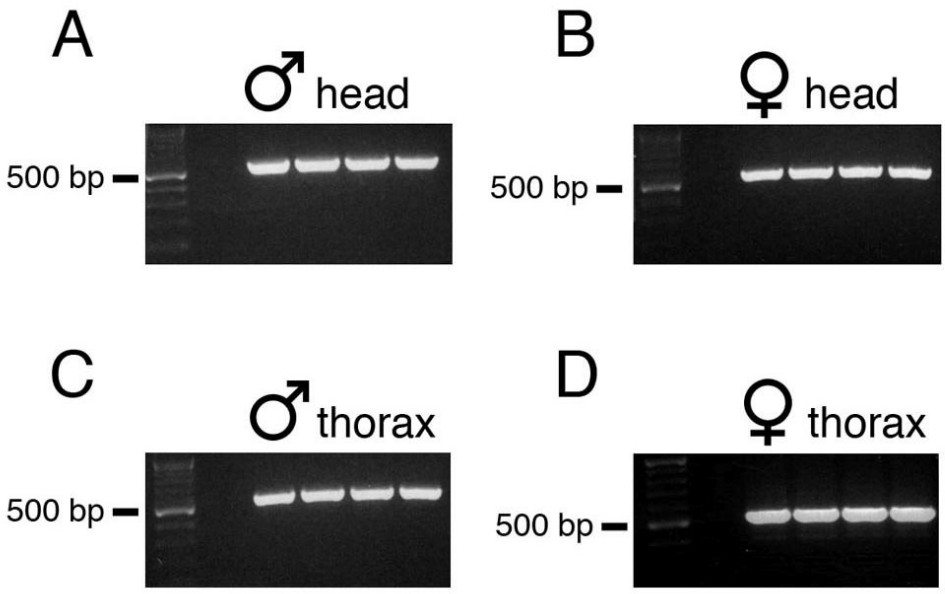

FIGURE S2.5. No sex-specific exon skipping of the *syt-T* reporter when driven by *fru*-Gal4. Four independent PCR products of *syt-T* amplified from male (A, C) or female (B, D) head and thorax are shown. No difference *syt-T* splicing in male head vs. thorax or male vs. female head tissue was observed. We noticed a slight degree of skipping in female thoraxes (D), but this was insignificant relative to the full length PCR product which was subjected to sequence analysis.

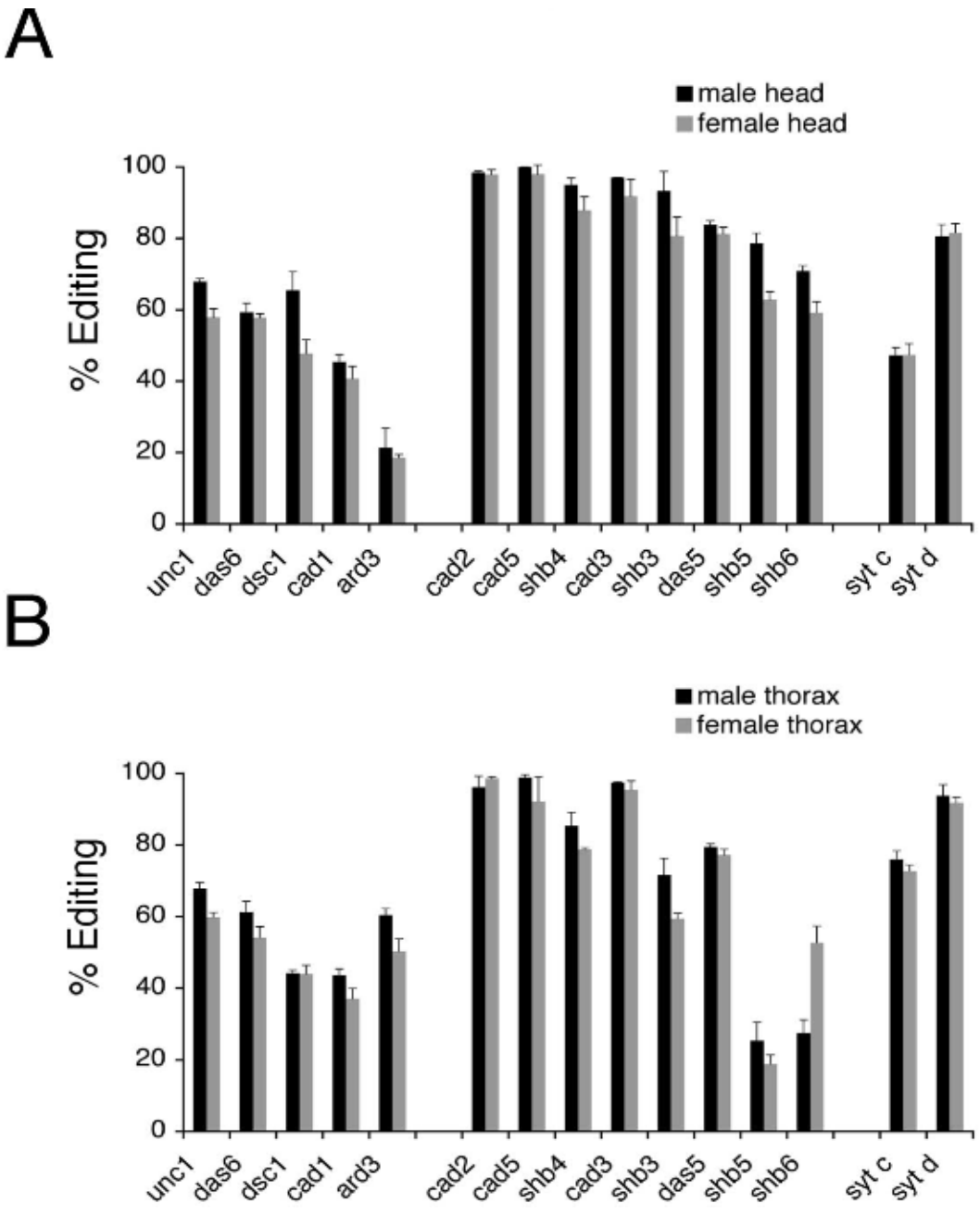

FIGURE S2.6. Lack of sexual dimorphism between endogenous transcripts in male and female heads (A) and thoraxes (B). Five LE sites and eight HE sites were examined (see Figures 2.3B and 2.3C), as well as the *syt-1* transcript that is the basis for the *syt-T* reporter. Importantly, there was no significant difference between editing at either site in *syt-1* amplified from either male or female tissue. Small reductions in female heads and thoraxes were observed relative to the corresponding male transcripts at several other sites. Notably, at only one site (*shab* site 6) was there an increase in females relative to males, but only in the female thorax. n > 3 RTPCRs for each data point. *Error bars*, S.E values.

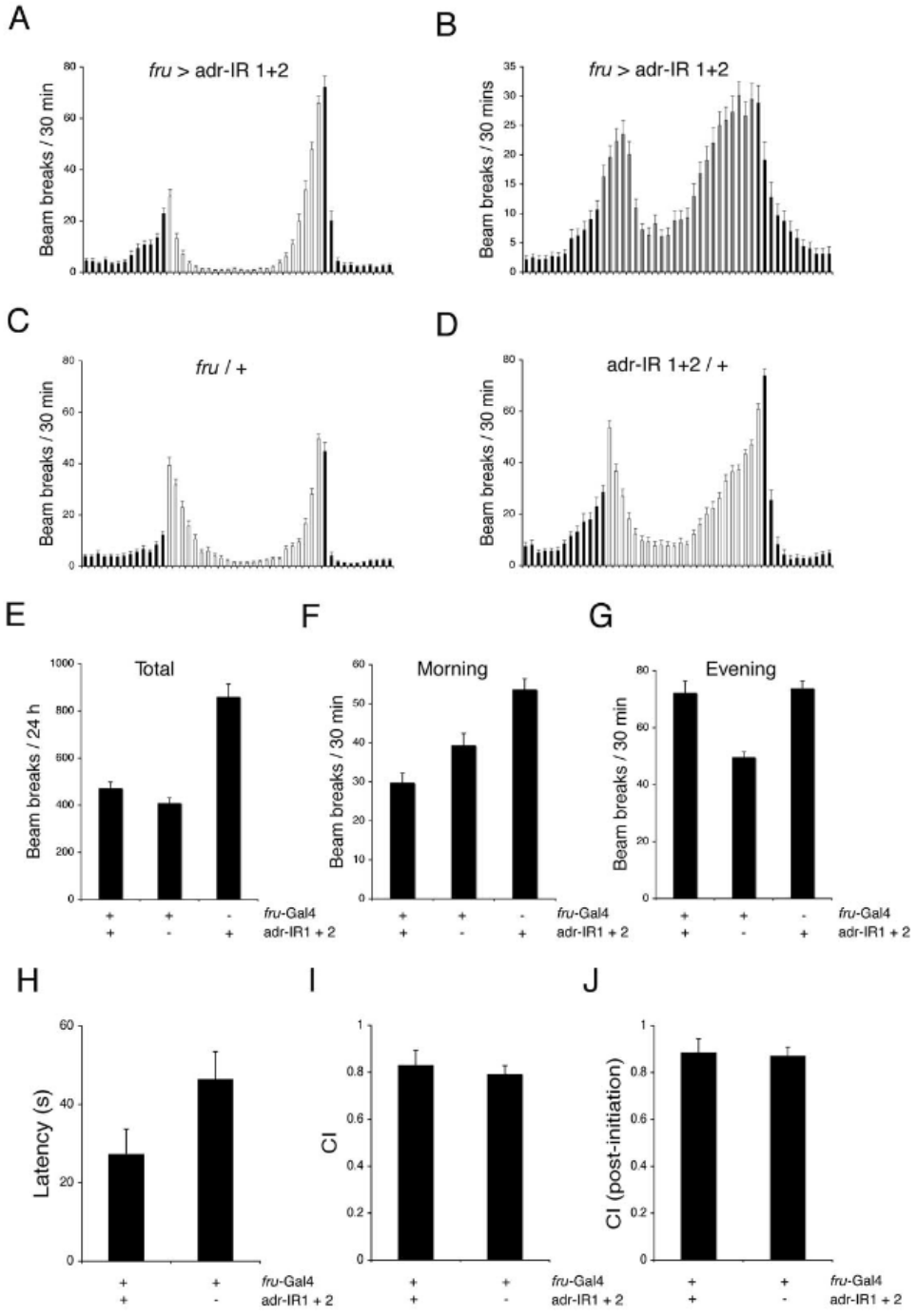

FIGURE S2.7. Inhibiting dADAR activity in *fruitless* neurons does not alter circadian rhythms. (A-C) Average locomotor activity profiles for the three genotypes used in Figure 2.7. All genotypes showed anticipation of both lights on (morning) and lights of (evening) (n = 32 for each genotype). Black bars represent lights-off, white bars represent lights-on. (D) Under constant-dark conditions, males with reduced dADAR expression in *fru*-positive neurons still exhibit anticipation of lights-on and lights-off, illustrating that the circadian clock is intact under these conditions. (E-F) Average locomotion over 24 h (E), and for morning (F) and evening (G) peaks of activity. *Error bars*, S.E values.

Drosophila strain	Homologous recombinant, mutant allele or transgene?	Description
$dAdar^{5g1}$	Null allele of *dAdar*	P-element derived deletion of the *dAdar* locus
$dAdar^{WTLoxP}$	Recombinant *dAdar* allele	Control allele of *dAdar* containing a single loxP site in intron 7 of the *dAdar* locus
$dAdar^{hyp}$	Recombinant *dAdar* allele	Wild-type *dAdar* locus with the addition of a ~ 5 kb $white^{+}$ mini-gene cassette in intron 7, leading to a stringent loss of dADAR expression
$dAdar^{HA}$	Recombinant *dAdar* allele	In addition to the loxP site in intron 7, contains a HA epitope-tag sequence at the 3' of the *dAdar* locus
Syt-T	Transgene under control of UAS promoter	Vector contains exons 8-10 of the *syt-1* locus and the intervening intronic regions containing cis-elements directing RNA editing at site 3 and 4 of *syt-1*
w^{1}; *adr-IR1*; *adr-IR2* (adr-IR1+2)	Double transgene RNAi line	Contains two independent insertions (one chromosomes II and III) of inverted repeat sequences directed to the 3' of the *dAdar* locus
w^{1}; *red-stinger*/CyO	Transgene insertion	Drives a modified RFP fluorophore localized to the nuclear compartment
Canton-S		Control stock
w^{1118}		Control stock

TABLE S2.1. Description of *Drosophila* strains used in this study.

Driver	Predominant cell-type	Site 3 (mean ± s.e.m)	Site 4 (mean ± s.e.m)
201y	mushroom bodies	7 ± 3	27 ± 3
pdf	circadian neurons	0	30 ± 0.8
1471	mushroom bodies	3 ± 1	33 ± 2
Ok107	mushroom bodies	1.6 ± 1	39 ± 0.8
7B	mushroom bodies	7 ± 2	39 ± 0.8
ddc	dopaminergic neurons	0	41 ± 1
c309	mushroom bodies	4 ± 1	42 ± 1
386y	peptidergic neurons	10 ± 2	50 ± 4
ple	dopaminergic neurons	0	53 ± 2
dimm	peptidergic neurons	6 ± 2	54 ± 2
drl	mushroom bodies and central complex	10 ± 0.6	56 ± 0.8
per	circadian neurons	9 ± 2	58 ± 0.8
fru	*fruitless* neurons	5 ± 0.7	59 ± 1
appl	pan-neuronal	7 ± 0.5	61 ± 0.7
cry	circadian neurons	0	63 ± 1
mz360	serotonergic neurons	4 ± 2	64 ± 2
ok307	giant descending neuron	26 ± 2	65 ± 1
ok371	glutamatergic neurons	26 ± 2	66 ± 0.6
cha	cholinergic neurons	17 ± 2	67 ± 2
D42	motor neurons	22 ± 2	74 ± 2
gmr	eye	11 ± 1	82 ± 0.1

TABLE S2.2. Expression of a molecular reporter for RNA editing in discrete neuronal sub-populations. Mean values from two independent lines expressed using each driver are shown for both site 3 and 4 of the ectopically expressed region of *syt-1* (termed *syt-T*).

CG number	Gene	Chromosome	Coordinate	Editing site	name	*dAdar*^{WTLexP} head % editing (mean ± s.e.m)	*dAdar*^{hyp} head % editing	*dAdar*^{WTLexP} thorax % editing	*dAdar*^{hyp} thorax % editing
10537	*rdl*	3L	9144936	site 5	rdl5	1 ± 0.7	0	11 ± 0.7	0.3 ± 0.02
12348	*shaker*	X	17846750	site 1	sha1	2 ± 0.7	0	4 ± 1	0
18314	*DopEcR*	3L	4369207	site 7	dop7	3 ± 0.9	0	14 ± 1	0
12348	*shaker*	X	17846749	site 2	sha2	4 ± 0.1	0	10 ± 0.9	0
10952	*eag*	X	14893953	site 3	eag3	7 ± 0.7	9 ± 0.7	13 ± 0.6	14 ± 0.3
4128	*Dα6*	2L	9809367	site 1	das1	7 ± 0.5	0	14 ± 0.9	0
18314	*DopEcR*	3L	4369208	site 6	dop6	7 ± 0.4	0	21 ± 1	0
18314	*DopEcR*	3L	4369455	site 2	dop2	8 ± 0.7	0	12 ± 0.1	0
18314	*DopEcR*	3L	4369459	site 1	dop1	8 ± 0.6	0	22 ± 0.9	0
10952	*eag*	X	14893971	site 5	eag5	8 ± 0.9	6 ± 2	10 ± -/5	7 ± 0.6
10537	*rdl*	3L	9144935	site 6	rdl6	9 ± 0.6	1.3 ± 1.3	34 ± 1	15 ± 0.5
18314	*DopEcR*	3L	4369445	site 3	dop3	12 ± 1	3 ± 0.9	18 ± 1	7 ± 0.8
4128	*Dα6*	2L	9809365	site 2	das2	13 ± 0.6	0	27 ± 0.7	0
10537	*rdl*	3L	9148285	site 4	rdl4	14 ± 0.4	0	25 ± 4	0
32975	*Dα5*	2L	14089233	site 7	daf7	18 ± 1	3 ± 0.3	16 ± 0.2	13 ± 0.6
10537	*rdl*	3L	9156024	site 1	rdl1	22 ± 1	0.7 ± 0.7	45 ± 0.5	3 ± 0.1
3139	*syt-1*	2L	2785621	site 2	syt2	22 ± 1	17 ± 1	65 ± 1	22 ± 1
11348	*ard*	3L	4433319	site 3	ard3	22 ± 1	0.3 ± 0.3	61 ± 0.7	6 ± 0.2
6798	*sbd*	3R	20337373	site 2	sbd2	29 ± 1	4 ± 0.4	25 ± 0.1	12 ± 0.4
6798	*sbd*	3R	20337378	site 1	sbd1	30 ± 0.6	14 ± 0.6	26 ± 0.8	20 ± 0.8
18314	*DopEcR*	3L	4369313	site 4	dop4	32 ± 0.9	10 ± 1	48 ± 2	18 ± 0.6
12295	*stj*	2R	9697112	site 2	stj2	34 ± 0.6	2 ± 0.3	43 ± 1	11 ± 0.1
12348	*shaker*	X	17844090	site 3	sha3	36 ± 0.6	23 ± 1	55 ± 1	32 ± 0.3
12295	*stj*	2R	9697467	site 3	stj3	37 ± 2	0	57 ± 0.3	11 ± 2
3139	*syt-1*	2L	2785610	site 3	syt3	44 ± 4	16 ± 0.2	78 ± 1	48 ± 1
18314	*DopEcR*	3L	4369185	site 8	dop8	45 ± 1	8 ± 1	66 ± 0.5	25 ± 2
32975	*Dα5*	2L	14089207	site 4	daf4	45 ± 2	2 ± 0.4	56 ± 2	8 ± 0.5
4894	*Caα1D*	2L	16174116	site 1	cad1	46 ± 0.4	7 ± 0.2	41 ± 1	12 ± .06
32975	*Dα5*	2L	14089212	site 5	daf5	46 ± 8	1 ± 0.3	48 ± 0.2	7 ± 0.2
12348	*shaker*	X	17824766	site 4	sha4	58 ± 16	16 ± 0.3	41 ± 1	12.5 ± 1
4128	*Dα6*	2L	9807941	site 6	das6	60 ± 2	7 ± 0.2	62 ± 0.2	10 ± .6
10952	*eag*	X	14890707	site 1	eag1	60 ± 0.9	18 ± 2	1	62 ± 2
10537	*rdl*	3L	9156017	site 2	rdl2	65 ± 0.9	14 ± 0.5	88 ± 0.5	54 ± 2
10952	*eag*	X	14894656	site 6	eag6	65 ± 2	33 ± 2	63 ± 1	6 ± 0.1
2999	*unc-13*	4	895009	site 1	unc1	66 ± 1	12 ± 1	68 ± 0.5	6 ± 0.4
34405	*DSC1*	2R	20800371	site 1	dsc1	67 ± 2	0	39 ± 2	3 ± 2
1066	*shab*	3L	2941131	site 1	shb1	67 ± 3	21 ± 2	52 ± 1	17 ± 0.4
32975	*Dα5*	2L	14089221	site 6	daf6	70 ± 0.6	5 ± 0.3	85 ± 0.3	15 ± 1
1066	*shab*	3L	2941425	site 6	shb6	71 ± 1	39 ± 1	61 ± 1	51 ± 0.1
12348	*shaker*	X	17824684	site 6	sha6	72 ± 1	17 ± 0.7	37 ± 0.3	11 ± 1
18314	*DopEcR*	3L	4369184	site 9	dop9	74 ± 0.2	25 ± 2	99 ± 0.1	58 ± 0.5

11348	*ard*	3L	4432486	site 1	ard1	74 ± 0.2	11 ± 0.4	81 ± 0.7	24 ± 3
1066	*shab*	3L	2941396	site 5	shb5	77 ± 0.8	34 ± 0.1	27 ± 2	21 ± 1
32975	*Dα5*	2L	14089236	site 8	daf8	79 ± 0.8	11 ± 0.2	86 ± 0.3	34 ± 1
3139	*syt-1*	2L	2785542	site 4	syt4	79 ± 4	64 ± 0.3	95 ± 1	84 ± 1
18314	*DopEcR*	3L	4369162	site 10	dop10	80 ± 1	39 ± 2	95 ± 0.5	67 ± 2
4128	*Dα6*	2L	9809350	site 3	das3	81 ± 0.8	21 ± 0.7	79 ± 1	30 ± 2
4128	*Dα6*	2L	9809297	site 5	das5	82 ± 1	54 ± 0.9	79 ± 1	64 ± 1
4128	*Dα6*	2L	9809349	site 4	das4	82 ± 0.3	26 ± 0.7	78 ± 1	36 ± 1
12348	*shaker*	X	17824691	site 5	sha5	83 ± 6	64 ± 0.3	73 ± 0.6	39 ± 1
10952	*eag*	X	14893901	site 2	eag2	84 ± 0.3	73 ± 0.4	95 ± 0.2	77 ± 2
32975	*Dα5*	2L	14083517	site 2	daf2	84 ± 0.3	15 ± 1	89 ± 1	33 ± 1
10952	*eag*	X	14893957	site 4	eag4	84 ± 1	79 ± 0.4	94 ± 0.6	88 ± 0.6
12295	*stj*	2R	9697052	site 1	stj1	86 ± 0.4	25 ± 2	92 ± 0.4	47 ± 4
15899	*Cα1T*	X	6009458	site 1	cat1	87 ± 0.7	2 ± 1	54 ± 3	0
32975	*Dα5*	2L	14083516	site 1	daf1	87 ± 0.4	19.2 ± 0.1	89 ± 0.9	36 ± 1
11348	*ard*	3L	4432487	site 2	ard2	90 ± 0.6	11 ± 3	94 ± 2	27 ± 2
1066	*shab*	3L	2941312	site 3	shb3	90 ± 3	54 ± 1	75 ± 2	70 ± 0.6
1066	*shab*	3L	2941132	site 2	shb2	91 ± 0.5	42 ± 0.8	79 ± 3	45 ± 0.8
1066	*shab*	3L	2941364	site 4	shb4	94 ± 0.9	70 ± 2	88 ± 0.4	87 ± 0.9
10537	*rdl*	3L	9148318	site 3	rdl3	95 ± 0.2	39 ± 2	90 ± 2	64 ± 0.9
1066	*shab*	3L	2941426	site 7	shb7	96 ± 1	66 ± 0.7	82 ± 2	84 ± 1
11348	*ard*	3L	4433320	site 4	ard4	97 ± 0.1	20 ± 0.1	1	54 ± 2
32975	*Dα5*	2L	14089204	site 3	daf3	98 ± 0.8	34 ± 2	99 ± 0.5	60 ± 0.2
4894	*Cα1D*	2L	16174152	site 3	cad3	99 ± 1	48 ± 1	97 ± 0.1	68 ± 2
4894	*Cα1D*	2L	16174153	site 4	cad4	99 ± 0.5	51 ± 1	99 ± 0.1	75 ± 0.9
4894	*Cα1D*	2L	16174138	site 2	cad2	100	71 ± .9	100	89 ± 3
4894	*Cα1D*	2L	16174194	site 5	cad5	100	64 ± 0.5	100	90 ± 0.6

TABLE S2.3. Editing levels at 68 target adenosines in dADAR^{WTLoxP} and dADAR^{hyp} male head and thorax.

CHAPTER 3:

Fine-tuning of mRNA Re-coding and Complex Behavior by Auto-regulatory RNA Editing in *Drosophila*

This chapter consists of data that was presented in a manuscript and submitted for peer review. "Fine-tuning of mRNA Re-coding and Complex Behavior by Auto-regulatory RNA Editing in *Drosophila*". Authors: Yiannis A. Savva*, James E.C. Jepson*, Asli Sahin, Arthur U. Sudgen, Ryan Bell, Lauren Alpert, Charles Lawrence, and Robert A. Reenan, 2011. (*) These authors contributed equally to this work. My specific contributions to this manuscript include: (a) I created the $dAdar^{WTLoxP}$, $dAdar^{S}$, $dAdar^{S\text{-}HA}$ alleles used in this study using ends-out homologous recombination. (b) I performed the molecular analysis on 100 RNA editing sites from all the alleles used in this study (Figure 3.1C-G; Figure 3.2; Supplementary Figures S3.2-12). (c) I performed immuno-histochemistry of 3rd instar larval salivary glands (Supplementary Figures S3.13-14).

ABSTRACT

Auto-regulatory feedback loops are a common molecular strategy for optimizing protein activity. In *Drosophila*, many mRNAs involved in neuro-transmission are re-coded at the RNA level by the RNA editing enzyme, dADAR, leading to the incorporation of amino acids that are not directly encoded by the genome. dADAR self-edits its own transcript, but the consequences of this auto-regulation *in vivo* are unclear. Using homologous recombination to bi-directionally interfere with dADAR regulation, we show that dADAR auto-editing dramatically remodels the landscape of re-coding events in a site-specific manner. These molecular phenotypes correlate with altered localization of dADAR within the nuclear compartment. Finally, we demonstrate that the nervous system-wide control of dADAR auto-editing is necessary for adaptive complex behaviors. Our results reveal the *in vivo* relevance of homeostatic control over post-transcriptional mRNA re-coding events.

INTRODUCTION

ADARs (adenosine deaminases acting on RNA) act to facilitate amino acid re-coding through the deamination of adenosine (A) to inosine (I) in dsRNA templates (Nishikura, 2010). Intriguingly, mRNAs that encode proteins involved in electrical and chemical neuro-transmission are highly over-represented in the population of mRNAs known to undergo editing (Hoopengardner et al., 2003; Seeburg and Hartner, 2003). In these cases, editing is mediated by the presence of *cis*-acting complementary sequences that bind the region surrounding the edited adenosine after transcription to form a dsRNA intermediate (Higuchi et al., 1993; Reenan, 2005). Furthermore, since inosine is interpreted as guanosine by the ribosome, editing in coding regions often leads to amino acid re-coding, and thus the translation of proteins that are not literally encoded by genomic DNA (Basillo et al., 1962).

Both mammalian ADAR2 and the single *Drosophila* ADAR (dADAR) edit specific adenosines within their own transcripts (Palladino et al., 2000b; Rueter et al., 1999). ADAR2 auto-editing acts as a negative feedback mechanism by generating a novel AI splicing acceptor site, leading to a N-terminal frame-shift and translation of a truncated ADAR2 isoform at reduced levels (Rueter et al., 1999). Correspondingly, abolition of ADAR2 auto-editing *in vivo* increases ADAR2 expression and editing at several target adenosines (Feng et al., 2006).

In contrast, dADAR auto-editing results in a serine to glycine coding change in the C-terminal catalytic domain (Palladino et al., 2000b). Auto-editing is highly developmentally regulated, occurring predominantly at the pupal and adult stages, and is mediated by a complementary sequence within the edited exon (Keegan et al., 2005;

Palladino et al., 2000b). The genomic serine residue is conserved throughout metazoan ADARs and structurally maps to a loop near the active site in the human ADAR2 crystal structure (Macbeth et al., 2005) (supplementary Fig. S3.1). *In vitro* experiments using two dADAR substrates indicate that auto-editing acts to reduce dADAR activity, suggesting an evolutionary convergence in function of dADAR and ADAR2 auto-regulation (Keegan et al., 2005). However, it is unknown whether dADAR auto-editing acts generically to reduce editing at all target adenosines *in vivo* or, rather, to modify particular sites in a substrate-specific manner.

MATERIALS AND METHODS

Drosophila Stocks and Ends-out Homologous Recombination of the *dAdar* Locus

Flies were raised at 25°C, on standard molasses food and under 12 h day/night cycles. Extensive details of the constructs used to manipulate the *dAdar* locus using homologous recombination have been published previously (Jepson et al. 2010). Briefly, we cloned two arms encompassing exons 4-7 (arm 1) and 8-10 (arm 2) of the *dAdar* genomic sequence into the p[w25.2] vector (Rong et al., 2002) (Fig. 3.1A). The auto-edited adenosine in the *dAdar* transcript resides towards the 3' end of arm 1 (Fig. 3.1A). We used mutagenic primers to convert the endogenous AGT serine codon to a synonymous TCT codon or a GGT glycine codon. An arm 1 with an AGT codon served as a control. Arm 2 contains a HA epitope-tag immediately after the last coding amino acid of dADAR, and prior to an opal (TGA) stop codon. Following recombination with the endogenous *dAdar* locus, we isolated recombinants which either had incorporated the HA epitope-tag or had not, depending on the site of recombination, using the *white*$^{+}$ eye-color mini-gene as a selection marker. This was followed by molecular validation and determination of the presence or absence of both the HA tag and the desired mutation at the auto-editing site using direct sequencing and restriction digest analysis. The *white*$^{+}$ mini-gene was subsequently removed via cre-recombinase and each recombinant strain was then back-crossed into a Canton-S control stock for at least five generations.

RT-PCR and Computational Calculation of Editing Levels

RNA extractions from *Drosophila* tissues were performed using Tri Reagent (MRC). Edited cDNAs were amplified via RT-PCR using target-specific primers (Jepson and Reenan, 2009). To computationally calculate editing ratios of the chosen 100 sites of the inosinome, editing sites were initially selected from RT-PCR electropherograms via an automated search for the local sequence surrounding the edited adenosine. All sequential peaks were then fit with a Gaussian mixture model (GMM; supplementary Fig. S3.16A). This prevents errors in which neighboring peaks of the same nucleotide artificially inflate the area under the curve. A grid search determines the relative positions of the peaks and a Markov Chain Monte Carlo process is used to find the best values for height (h), width (w), and standard deviation (c), as determined by the minimum chi-square of the sum of the areas of the predicted peaks and the chromatogram data (supplementary Fig. S3.16B). The program may be found at http://grapheasy.org. A minimum of three independent PCR amplicons were used to derive the editing levels of each adenosine. To determine the degree of auto-editing in male hemizygotes and females heterozygous for various engineered *dAdar* alleles, we used the following methodology: $dAdar^{S}$ and $dAdar^{G}$ males and females were assumed to have auto-editing levels of 0% and 100% respectively. For the remaining genotypes, auto-editing was calculated using bulk RT-PCR electropherograms of the *dAdar* mRNA from male and female heads, with the % auto-editing calculated as G/(A+G) x 100. For $dAdar^{S}/dAdar^{WTLoxP}$ females, harboring both TCT and AGT serine alleles, the total level

of un-edited *dAdar* was calculated by summating the A and T peaks. The auto-editing level was then derived as G/(A+T+G) x 100.

Microscopy, Immuno-histochemistry and Analysis of dADAR Punctae

All confocal images were obtained on a Zeiss LSM 510 meta confocal microscope. Adult brain and 3rd instar larval salivary gland samples for immuno-histochemistry were prepared as described previously (Wu and Luo, 2006). Primary antibodies were used at the following concentrations: rabbit anti-HA (Santa Cruz Biotech) - 1:50; goat anti-human fibrillarin – 1: 200. Mouse anti-Lamin (Developmental Studies Hybridoma Bank) – 1:40; DAPI (Invitrogen) was used at 1:1000. To quantify the degree of extranucleolar punctal dADAR, cells were split by hand into individual images, using DAPI as a marker for nuclear location. In each image, the brightest point of fibrillarin staining was found and the computer expanded outward in steps, determining all contiguous pixels greater than 1/4 of the maximum. This area was taken to be the nucleolus, N. The brightest point of dADAR was found similarly, marking the center of dADAR staining, and the computer determined the brightest point of dADAR staining to be all contiguous pixels greater than 1/2 of the maximum, P. Because this program was designed to measure extranucleolar, point-like dADAR staining, any staining not matching both of these criteria was ignored; if the center of dADAR staining lay inside the nucleolus, N, then the nuclear concentration of dADAR was judged to be intranucleolar and P was set to 0. If the area of P exceeded that of N, it was determined not point-like and P was set to 0.

Western Blotting

Protein samples were prepared as described previously (Jepson et al. 2010). Anti-HA antibody (Covance) was used at 1:500, and anti-actin (Millipore) was used at 1:20000. Band intensities were quantified on a Kodak Image Station following background subtraction. 20 adult heads / 100 μL of buffer were used per sample.

Behavioral Analysis

Locomotor patterns were recorded using horizontal single fly or vertical population activity monitors (TriKinetics). Flies were left for ~ 12h before data collection. For single-fly monitors, mean locomotor patterns were calculated for each fly by averaging data from three consecutive days, which were then further averaged across the experimental population. To quantify geotaxis using vertical population monitors, we took advantage of the presence of three concentric infra-red beams at the bottom, middle and top portions of the vial. We calculated the total number of beam breaks for all levels, and solely for the top level (close to the top of the vial). Relative geotaxis was calculated by dividing the number of beams breaks in the top ring by the total for all three rings, for each vial. Mating assays and song recording were observed or recorded in a custom made chamber using 5-7 day old males and 3-5 day old virgin females. The time taken for male initiation of courtship (latency) and the courtship index (time spent courting / total time) were recorded over 10 min. Mating events were observed over a narrow time window (7-10 am) to minimize circadian influences on experimental outcome. Courtship songs were

recorded using a MicroTrack mobile digital recorder (M-Audio). Subsequently, songs were computationally divided into trains by testing for pulses greater than four inter-pulse intervals apart (supplementary Fig. S3.17A, red line). Pulses are determined by finding regions where intensities reach outside a 2 standard deviation threshold (supplementary Fig. S3.17B, red horizontal lines). Then, extrema, or cycles, are measured to determine the number of cycles per pulse. Each extremum is marked on the graph with a green line and the first major cycle is marked in magenta. The cycles are computationally counted and the IPI is measured as the time between first major cycles.

Online Supplementary Material

The supplementary material includes 17 figures and a table. Supplementary figure 1 (S3.1) shows the domain structure of the dADAR protein. Supplementary figure 2 (S3.2) shows examples of edited adenosines that exhibit no alteration, mono-, or bidirectional changes in editing levels in the same mRNA. Supplementary figure 3 (S3.3) shows a heat map representation of alterations in editing levels at 100 adenosines in male thorax from $dAdar^{S}$, $dAdar^{WTLoxP}$, and $dAdar^{G}$. Supplementary figure 4 (S3.4) shows a heat map representation of alterations in editing levels at 100 adenosines in male eye from $dAdar^{S}$, $dAdar^{WTLoxP}$, and $dAdar^{G}$. Supplementary figure 5 (S3.5) shows a heat map representation of alterations in editing levels at 100 adenosines in male antennae from $dAdar^{S}$, $dAdar^{WTLoxP}$, and $dAdar^{G}$. Supplementary figure 6 (S3.6) illustrates a heat map showing levels of editing at 100 adenosines in mRNAs amplified from $dAdar^{S/S}$,

dAdar$^{S/L}$, *dAdar*$^{S/G}$, *dAdar*$^{L/L}$, *dAdar*$^{G/L}$, and *dAdar*$^{G/G}$ female heads. Supplementary figure 7 (S3.7) illustrates a heat map showing levels of editing at 100 adenosines in mRNAs amplified from *dAdar*$^{S/S}$, *dAdar*$^{S/L}$, *dAdar*$^{S/G}$, *dAdar*$^{L/L}$, *dAdar*$^{G/L}$, and *dAdar*$^{G/G}$ female thoraxes. Supplementary figure 8 (S3.8) shows a comparison of editing levels at 100 adenosines in mRNAs amplified from male and female head/thorax cDNA. Supplementary figure 9 (S3.9) shows editing levels at 22 adenosines in mRNAs amplified from head tissue derived from *dAdar*$^{S/S}$, *dAdar*$^{S/L}$, *dAdar*$^{S/G}$, *dAdar*$^{L/L}$, *dAdar*$^{G/L}$, and *dAdar*$^{G/G}$ allelic combinations. Supplementary figure 10 (S3.10) shows the rank ordering of editing levels at 100 adenosines amplified from *dAdar*^{S}, *dAdar*^{WTLoxP}, and *dAdar*^{G} male heads and thoraxes. Supplementary figure 11 (S3.11) shows the rank ordering of editing levels at 100 adenosines in females amplified from *dAdar*$^{S/S}$, *dAdar*$^{S/L}$, *dAdar*$^{S/G}$, *dAdar*$^{L/L}$, *dAdar*$^{G/L}$, and *dAdar*$^{G/G}$ heads and thoraxes. Supplementary figure 12 (S3.12) shows editing levels at novel editing sites detected in the *dAdar*^{S} genetic background. Supplementary figure 13 (S3.13) shows that dADAR transgenes expressed in larval salivary gland nuclei localize within the nucleolus. Supplementary figure 14 (S3.14) shows that dADAR transgenes and endogenous dADAR localize within the nuclear envelope. Supplementary figure 15 (S3.15) shows a model that illustrates neuron-to-neuron variation in the regulation of editing levels at four adenosines by *dAdar* auto-editing. Supplementary figure 16 (S3.16) illustrates the computational method used for analysis of editing levels. Supplementary figure 17 (S3.17) illustrates the computational method used for analysis of courtship song waveforms. Supplementary table 1 (S3.1) describes the nomenclature for the 23 transcripts analyzed in various *dAdar* allelic backgrounds.

RESULTS

In order to determine the *in vivo* significance of auto-editing, we performed ends-out homologous recombination (Rong et al., 2002) on the endogenous *dAdar* locus to generate *Drosophila* with either constitutive serine (S) or glycine (G) residues (Fig. 3.1A). An allele producing only auto-edited dADAR protein ($dAdar^{G}$) was engineered by mutating the edited adenosine of the serine codon (AGT) to guanosine (GGT), converting it to a glycine codon. Conversely, a $dAdar^{S}$ allele, producing only un-edited dADAR, was generated by altering the same serine codon to its degenerate counterpart (TCT), rendering A-to-I modification impossible. A *dAdar* allele containing a single intronic loxP site but with no alteration at the edited serine residue ($dAdar^{WTLoxP}$) served as a wild-type control. In addition, we generated recombinant flies with the above alleles and an HA-epitope tag at the 3' terminus of the *dAdar* coding sequence (Fig. 3.1A), allowing us to compare expression levels and localization of wild-type, edited and un-edited dADAR. We have previously shown that the HA-tag has no effect on dADAR activity on several known targets (Jepson et al. 2010), and Western blot analyses revealed that modifying auto-editing has no significant effect on levels of dADAR protein expression (Fig. 3.1B).

Drosophila possesses a large population of mRNAs subject to specific A-to-I editing, which encode voltage- and ligand-gated ion channels and regulators of exo- and endocytosis (Hoopengardner et al., 2003). To comprehensively determine the influence of *dAdar* auto-editing on mRNA re-coding, we examined editing levels at 100 adenosines in 23 mRNAs amplified from $dAdar^{WTLoxP}$, $dAdar^{S}$ and $dAdar^{G}$ male head cDNA (Fig. 3.1C-E, Fig. 3.2).

Comparative analysis of editing in the three X-linked *dAdar* alleles revealed a complex relationship between the editing status of dADAR and re-coding output. We were able to delineate three categories of editing sites from our initial dataset: adenosines that were completely insensitive to the edited state of *dAdar* (Fig. 3.1C); adenosines where elimination of auto-editing was ineffectual upon maximal editing levels, yet exhibited a significant reduction upon hard-wiring of *dAdar* auto-editing (Fig. 3.1D); and finally, adenosines which exhibited a bi-directional response to elimination or hard-wiring of auto-editing (Fig. 3.1E). Importantly, the above classes were not biased towards adenosines with particular levels of editing, and comprise diverse mRNAs. Examples of each class could even be found in the same mRNA (supplementary Fig. S3.2). Thus, *dAdar* auto-editing acts as a negative auto-regulatory feedback mechanism to selectively modulate dADAR activity on particular target adenosines in the male *Drosophila* head (Fig. 3.2).

Previous *in vitro* experiments have suggested that *dAdar* mRNA is efficiently deaminated by unedited dADAR (S) protein, but the edited version (G) is far less effective (*10*). This observation provided a clear prediction that the presence of either of our modified *dAdar* alleles should shift the auto-editing of a wild-type allelic counterpart in the opposite direction. We therefore generated females carrying all possible allelic combinations of $dAdar^{WTLoxP}$, $dAdar^{S}$ and $dAdar^{G}$ (Fig. 3.1F). Curiously, we found that wild-type *dAdar* mRNA appears insensitive to the editing status of a modified *dAdar* locus *in vivo* (Fig. 3.1F): auto-regulation does not regulate auto-regulation.

To test whether the selective negative-feedback effect of *dAdar* auto-editing observed in male heads was tissue- and/or sex-specific, we analyzed the same set of 100

adenosines using mRNA derived from three separate *dAdar*^{WTLoxP}, *dAdar*^{S} and *dAdar*^{G} male tissues (thorax, eye and antennae; supplementary Figs. S3.3-5), and head and thorax cDNA from all six female allelic combinations (supplementary Figs. S3.6-7). From this dataset, we discerned multiple instances of tissue- and sex-specific editing states (Fig. 3.1G, supplementary Fig. S3.8), demonstrating that the previously described spatio-temporal control of editing in the *Drosophila shaker* potassium channel mRNA applies generically to much of the *Drosophila* inosinome (Ingleby et al., 2009).

Layered onto these complex regulatory events, we found that *dAdar* auto-editing itself is sexually dimorphic in the thorax, but not the head (supplementary Fig. S3.8). Furthermore, in some cases, auto-editing of *dAdar* only exerted an influence in particular tissue- and/or sex-specific contexts (Fig. 3.1G). Broadly, however, in head tissue, substrate adenosines generally show similar responses to alterations in *dAdar* auto-editing, independent of sex (Fig. 3.1C-E and supplementary Fig. S3.9A-C).

Comparison of the editing levels across 100 adenosines in head and thorax tissue from the three male and six female genotypes comprehensively demonstrates that the *dAdar*^{S} allele dominates endogenous dADAR activity *in vivo* (supplementary Fig. S3.10-11). In addition, we observed novel editing sites that were only apparent in bulk RT-PCR from *dAdar*^{S} backgrounds (supplementary Fig. S3.12). One of these, a K $\rightarrow$ E substitution in the cyclic nucleotide binding domain of *eag*, is 100 bp from the closest known editing site (Hoopengardner et al., 2003), suggesting the presence of a novel dADAR substrate that is only deaminated in neurons where *dAdar* auto-editing is very low, such as in antennal lobe interneurons.

What is the mechanism by which auto-editing reduces dADAR function given the wide response range of different target adenosines to dADAR auto-editing? We recently engineered a novel hypomorphic allele of *dAdar* (*dAdar*^{hyp}), in which dADAR expression is reduced by ~ 80% (Jepson et al. 2010). In this background, editing at many sites, but not all, is significantly reduced. Males and females hemi- or homozygous for the *dAdar*^{G} allele also show reduced editing at a subset of adenosines (Fig. 3.1 and 3.2, supplementary Fig. S3.3-7 and S3.10-11). If auto-editing is modulating substrate-specificity, there is no *a priori* reason that the *dAdar*^{G} and *dAdar*^{hyp} alleles should exhibit a molecular phenotypic resemblance. However, for the editing sites that showed a significant reduction in *dAdar*^{G} males, we found a strong correlation between the degree of reduction in both *dAdar*^{G} and *dAdar*^{hyp} heads (r = 0.57, P = 0.008, permutation test; Fig. 3.1H) and thoraxes (r = 0.61, P = 0.0061; data not shown). Thus, in essence, auto-editing appears to post- transcriptionally phenocopy a weak hypomorphic allele of *dAdar*.

To explore this further, we examined the localization of dADAR in our various genetic backgrounds using HA-tagged versions of each allele (Fig. 3.1A), with the underlying hypothesis that auto-editing might in some way be lowering the effective concentration of dADAR within the nucleus. Mammalian ADARs have been shown to localize to the nucleolus and alter their localization in response to substrate abundance (Sansam et al., 2003). dADAR transgenes comparable to the *dAdar*^{WTLoxP} and *dAdar*^{S} alleles also localized to the nucleolus when ectopically expressed in 3rd instar larval salivary gland nuclei (supplementary Fig. S3.13).

Since dADAR is strongly expressed throughout the adult nervous system (Jepson et al. 2010), we next examined the endogenous localization of the dADAR isoforms in

neuronal nuclei of the adult brain. Both ectopically expressed dADAR transgenes and all HA-tagged endogenous alleles localized to within the nuclear envelope (supplementary Fig. S3.14), and in the adult nervous system, HA-tagged dADAR co-localized with the nucleolus to a degree that was independent of its auto-editing status (Fig. 3.3A-D). However, we observed that the dADAR$^{G\text{-}HA}$ isoform showed strong additional punctal staining in regions outside the nucleolus (Fig. 3.3C, E; supplementary Fig. S3.14). This pattern was rarely seen in neurons expressing dADAR$^{S\text{-}HA}$, which showed dispersed expression in the non-nucleolar regions of the nucleus (Fig. 3.3A). Interestingly, wild-type dADAR^{HA} exhibited an intermediate phenotype – in a sub-population of neurons, extra-nucleolar punctae were visible, but were reduced in intensity relative to those seen in the dADAR$^{G\text{-}HA}$ background (Fig. 3.3B, F). The variation in dADAR$^{WTLoxP\text{-}HA}$ localization presumably reflects neuron-specific control of auto-editing levels. These results suggest that auto-editing leads to the sequestration of dADAR to a distinct nuclear compartment, perhaps reflecting binding to a form of dsRNA that is not bound by dADAR$^{S\text{-}HA}$ stably enough to be detectable by confocal microscopy. We hypothesize that this localized depot of dADAR^{G} effectively lowers the concentration of total dADAR at active sites of target transcription, generating a molecular phenocopy of a *dAdar* hypomorph.

A common consequence of many ADAR mutations in higher metazoans is the disruption of normal nervous system function (Higuchi et al., 2000; Palladino et al., 2000a; Tonkin et al., 2002). We therefore asked whether the relatively subtle changes in editing observed in *dAdar*^{S} and *dAdar*^{G} could also confer abnormal adult-stage behaviors. We initially assessed locomotor patterns using both automated horizontal single-fly and

vertical population monitors (Fig. 3.4A-D). In constant dark conditions, all genotypes exhibited rhythmic locomotor patterns (data not shown), indicating that the circadian clock is intact in the recombinant lines. However, in 12 h light:dark conditions, we observed a bi-directional change in the degree of morning anticipation, an output of a subset of the circadian neuronal network that is also absent in *dAdar* hypomorphs (Allada and Chung, 2010; Jepson et al. 2010) (Fig. 3.4A). In both single-fly and population settings (Fig. 3.4B-C), altering auto-editing did not significantly change locomotor activity relative to $dAdar^{WTLoxP}$, although $dAdar^{S}$ males were significantly more active than $dAdar^{G}$ under horizontal conditions (Fig. 3.4B). In addition, in the vertical assay, the proportion of time $dAdar^{S}$ males spent towards the top of the vial was significantly lower compared to $dAdar^{WTLoxP}$ and $dAdar^{G}$ males, suggesting that loss of auto-editing impairs normal climbing ability and/or geotaxis while sparing general locomotor activity (Fig. 3.4C).

Finally, we investigated male courtship behavior. We noted alterations in length of the mating song and the strength of the song waveform in both experimental genetic backgrounds (Fig. 3.4E-H). Also, while the total time spent courting was equivalent to wild-type, $dAdar^{G}$ males initiated courtship significantly slower than $dAdar^{WTLoxP}$ controls or $dAdar^{S}$ males (Fig. 3.4I-J). Thus, homeostatic control of dADAR function through auto-regulation modulates ethologically relevant behavioral modalities that are subject to intense natural selection.

DISCUSSION

In summary, we have investigated the role of auto-regulatory RNA editing using homologous recombination, allowing us to assess molecular and behavioral consequences while keeping the remaining endogenous control of dADAR expression intact. Auto-editing is developmentally synchronized with a robust increase in dADAR expression at the pupal and adult stages (Palladino et al., 2000b). Surprisingly, however, auto-editing is not greatly reduced in *dAdar* hypomorphs (Jepson et al. 2010). Thus, spatio-temporal changes in auto-editing are not simply a response to synchronous alterations in dADAR protein levels. Rather, we propose that auto-editing levels are set on a neuron-to-neuron basis to fine-tune cellular physiology (supplementary Fig. S3.15). We envision that such regulation could be necessary for appropriate behavioral outputs, since recent studies have shown that manipulation of the firing properties of a single neuron can alter global behavioral states (Li et al., 2009). Indeed, in our accompanying paper, we infer differential control of auto-editing even between spatially close neuronal subtypes within the *Drosophila* mushroom bodies. Our results elaborate the complex nature of A-to-I RNA editing in the *Drosophila* nervous system and the multi-layered regulatory mechanisms that control mRNA re-coding, neuronal physiology and behavior.

REFERENCES

Allada, R., and Chung, B.Y. (2010). Circadian organization of behavior and physiology in Drosophila. Annual review of physiology *72*, 605-624.

Basillo, C., Wahba, A., Lengyel, P., Speyer, J., and Ochoa, S. (1962). Synthetic polynucleotides and the amino acid code. V. Proceedings of the National Academy of Sciences of the United States of America *48*, 613-616.

Feng, Y., Sansam, C.L., Singh, M., and Emeson, R.B. (2006). Altered RNA editing in mice lacking ADAR2 autoregulation. Molecular and cellular biology *26*, 480-488.

Higuchi, M., Maas, S., Single, F.N., Hartner, J., Rozov, A., Burnashev, N., Feldmeyer, D., Sprengel, R., and Seeburg, P.H. (2000). Point mutation in an AMPA receptor gene rescues lethality in mice deficient in the RNA-editing enzyme ADAR2. Nature *406*, 78-81.

Higuchi, M., Single, F.N., Kohler, M., Sommer, B., Sprengel, R., and Seeburg, P.H. (1993). RNA editing of AMPA receptor subunit GluR-B: a base-paired intron-exon structure determines position and efficiency. Cell *75*, 1361-1370.

Hoopengardner, B., Bhalla, T., Staber, C., and Reenan, R. (2003). Nervous system targets of RNA editing identified by comparative genomics. Science (New York, NY *301*, 832-836.

Ingleby, L., Maloney, R., Jepson, J., Horn, R., and Reenan, R. (2009). Regulated RNA editing and functional epistasis in Shaker potassium channels. The Journal of general physiology *133*, 17-27.

Jepson, J.E., and Reenan, R.A. (2009). Adenosine-to-inosine genetic recoding is required in the adult stage nervous system for coordinated behavior in Drosophila. The Journal of biological chemistry *284*, 31391-31400.

Jepson, J.E., Savva, Y.A., Yokose, C., Sugden, A.U., Sahin, A., and Reenan, R.A. (2010). Engineered alterations in RNA editing modulate complex behavior in Drosophila: regulatory diversity of adenosine deaminase acting on RNA (ADAR) targets. The Journal of biological chemistry.

Keegan, L.P., Brindle, J., Gallo, A., Leroy, A., Reenan, R.A., and O'Connell, M.A. (2005). Tuning of RNA editing by ADAR is required in Drosophila. The EMBO journal *24*, 2183-2193.

Li, C.Y., Poo, M.M., and Dan, Y. (2009). Burst spiking of a single cortical neuron modifies global brain state. Science (New York, NY *324*, 643-646.

Macbeth, M.R., Schubert, H.L., Vandemark, A.P., Lingam, A.T., Hill, C.P., and Bass, B.L. (2005). Inositol hexakisphosphate is bound in the ADAR2 core and required for RNA editing. Science (New York, NY *309*, 1534-1539.

Nishikura, K. (2010). Functions and regulation of RNA editing by ADAR deaminases. Annual review of biochemistry *79*, 321-349.

Palladino, M.J., Keegan, L.P., O'Connell, M.A., and Reenan, R.A. (2000a). A-to-I pre-mRNA editing in Drosophila is primarily involved in adult nervous system function and integrity. Cell *102*, 437-449.

Palladino, M.J., Keegan, L.P., O'Connell, M.A., and Reenan, R.A. (2000b). dADAR, a Drosophila double-stranded RNA-specific adenosine deaminase is highly developmentally regulated and is itself a target for RNA editing. RNA (New York, NY *6*, 1004-1018.

Reenan, R.A. (2005). Molecular determinants and guided evolution of species-specific RNA editing. Nature *434*, 409-413.

Rong, Y.S., Titen, S.W., Xie, H.B., Golic, M.M., Bastiani, M., Bandyopadhyay, P., Olivera, B.M., Brodsky, M., Rubin, G.M., and Golic, K.G. (2002). Targeted mutagenesis by homologous recombination in D. melanogaster. Genes & development *16*, 1568-1581.

Rueter, S.M., Dawson, T.R., and Emeson, R.B. (1999). Regulation of alternative splicing by RNA editing. Nature *399*, 75-80.

Sansam, C.L., Wells, K.S., and Emeson, R.B. (2003). Modulation of RNA editing by functional nucleolar sequestration of ADAR2. Proceedings of the National Academy of Sciences of the United States of America *100*, 14018-14023.

Seeburg, P.H., and Hartner, J. (2003). Regulation of ion channel/neurotransmitter receptor function by RNA editing. Current opinion in neurobiology *13*, 279-283.

Tonkin, L.A., Saccomanno, L., Morse, D.P., Brodigan, T., Krause, M., and Bass, B.L. (2002). RNA editing by ADARs is important for normal behavior in Caenorhabditis elegans. The EMBO journal *21*, 6025-6035.

Wu, J.S., and Luo, L. (2006). A protocol for dissecting Drosophila melanogaster brains for live imaging or immunostaining. Nature protocols *1*, 2110-2115.

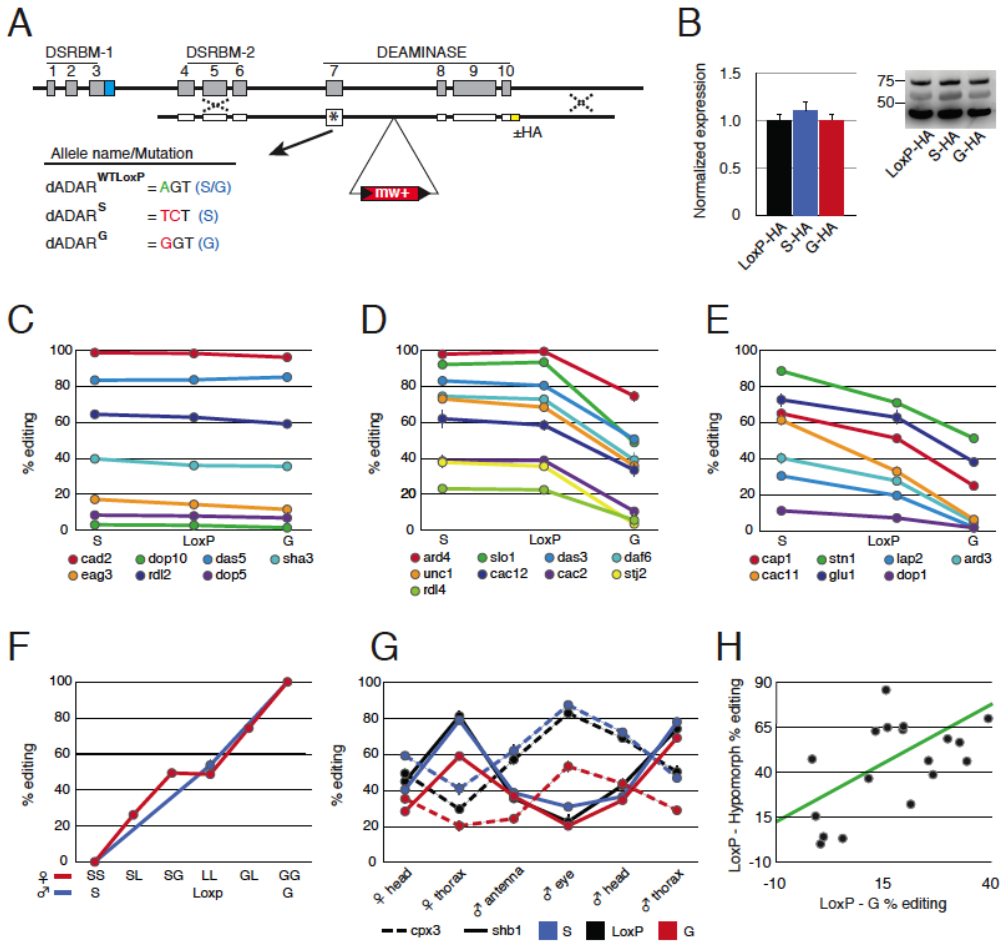

FIGURE 3.1. (A) Schematic of the *dAdar* locus illustrating targeting arm design to induce homologous recombination, and nomenclature for the three *dAdar* alleles used in this study. (B) Modification of *dAdar* auto-editing does not affect dADAR protein levels (n = 5-6 Western blots from 3 separate head-protein samples for each HA-tagged allele; *P* = 0.383, Kruskall-Wallis Rank Sum test). Top band - dADAR-HA; middle band - non-specific; lower band – actin. Values are presented as dADAR/actin. (C-E) Examples of edited adenosines that show no alteration (C), a mono- (D) or bi-directional (E) shift in editing levels in $dAdar^{S}$ and $dAdar^{G}$ when compared to $dAdar^{WTLoxP}$. All RT-PCRs were performed using mRNA isolated from male heads. See Supplementary Table 1 for description of mRNA target annotations. (F) Total auto-editing levels at a wild-type *dAdar* locus in combination with engineered mutations in *dAdar* auto-editing. $dAdar^{S}$ hemi- and homozygotes are defined as having 0 % auto-editing, while $dAdar^{G}$ is 100 %. Auto-editing levels in the remaining allelic combinations were determined experimentally. The data is consistent with a model where the auto-editing levels of each *dAdar* allele are determined independently. The LoxP wild-type allele is indicated by L. (G) Pattern of editing levels of site 3 of *complexin* (cpx3) and site 1 of *shab* (shb1) mRNAs amplified from various tissues in male and female *dAdar* allelic backgrounds. (H) Correlation between the reduction in editing at 18 adenosines in $dAdar^{G}$ and $dAdar^{hyp}$ male heads. Error bars: standard error.

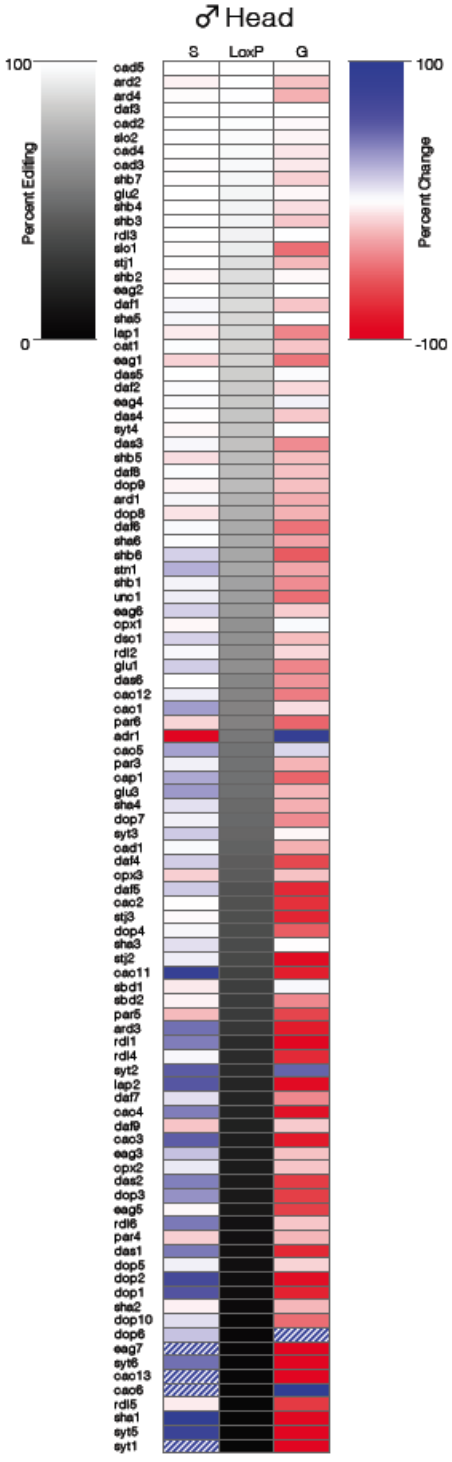

FIGURE 3.2. Heat map representation of alterations in editing at 100 adenosines in *dAdar*^{S} and *dAdar*^{G} males relative to *dAdar*^{WTLoxP} controls, amplified from male head cDNA. Data are derived from ≥ 3 RT-PCRs for each adenosine, and are presented in rank order relative to the endogenous editing levels in *dAdar*^{WTLoxP}. Dashed boxes indicate a > 100% increase.

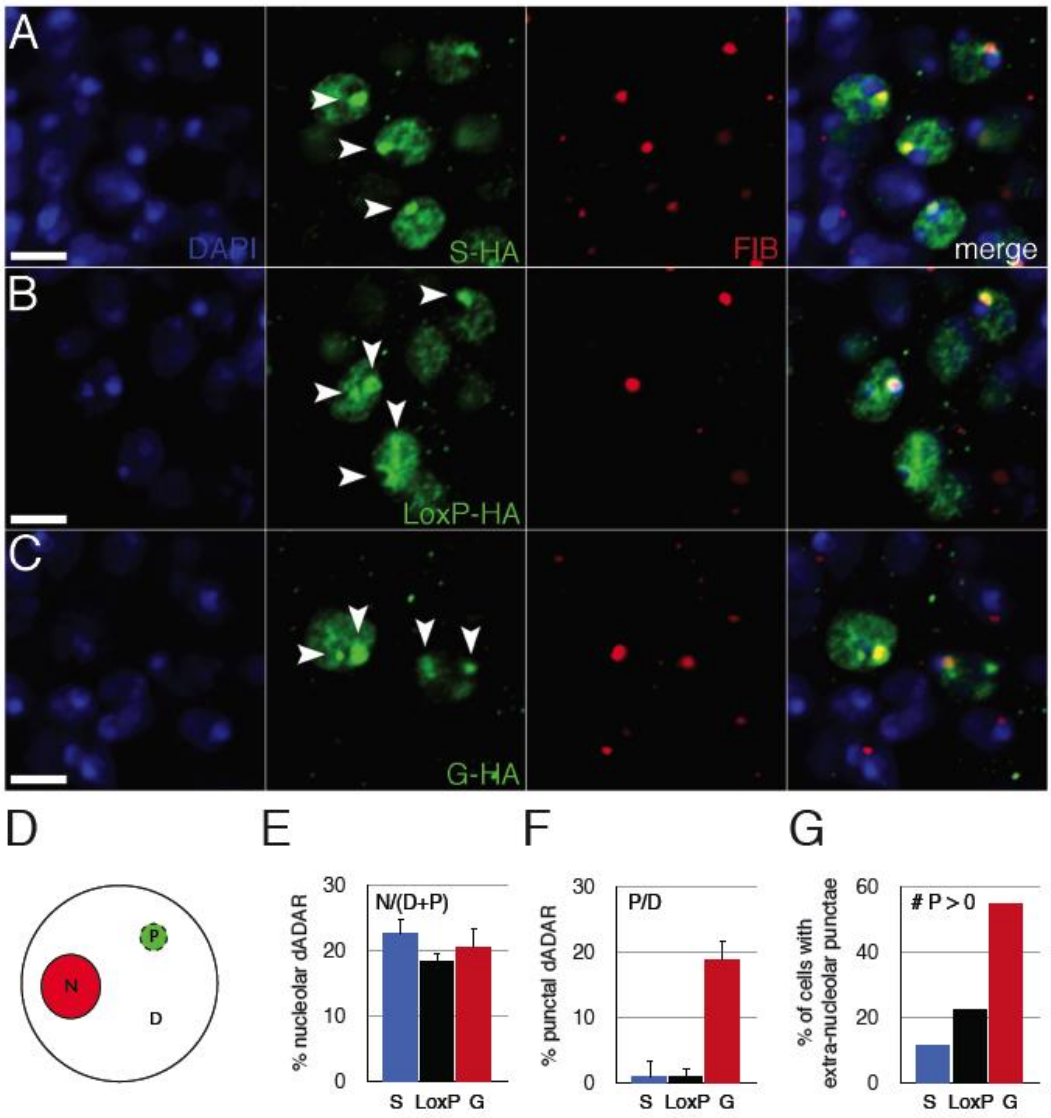

FIGURE 3.3. Auto-editing modifies the sub-nuclear localization of dADAR. We examined the nuclear localization of HA-tagged control and experimental dADAR alleles (A-C) in the adult male nervous system. To control for spatial differences in dADAR localization, confocal slices were obtained from nuclei surrounding the antennal lobes. All dADAR alleles co-localized with DAPI-stained DNA (blue) and the nucleolus (stained with fibrillarin, red). (D-G) Quantification of the relative dADAR signal intensity in the nucleolus (N) compared to dispersed (D) or punctate (P, arrowheads) extra-nucleolar staining between WTLoxP-HA, S-HA and G-HA dADARs. Number of cells used for computational analysis: dADAR$^{WTloxP\text{-}HA}$ – 36; dADAR$^{S\text{-}HA}$ – 26; dADAR$^{G\text{-}HA}$ – 33. Images were derived from ≥ 5 brains for each genotype. Scale bar = 5 μm.

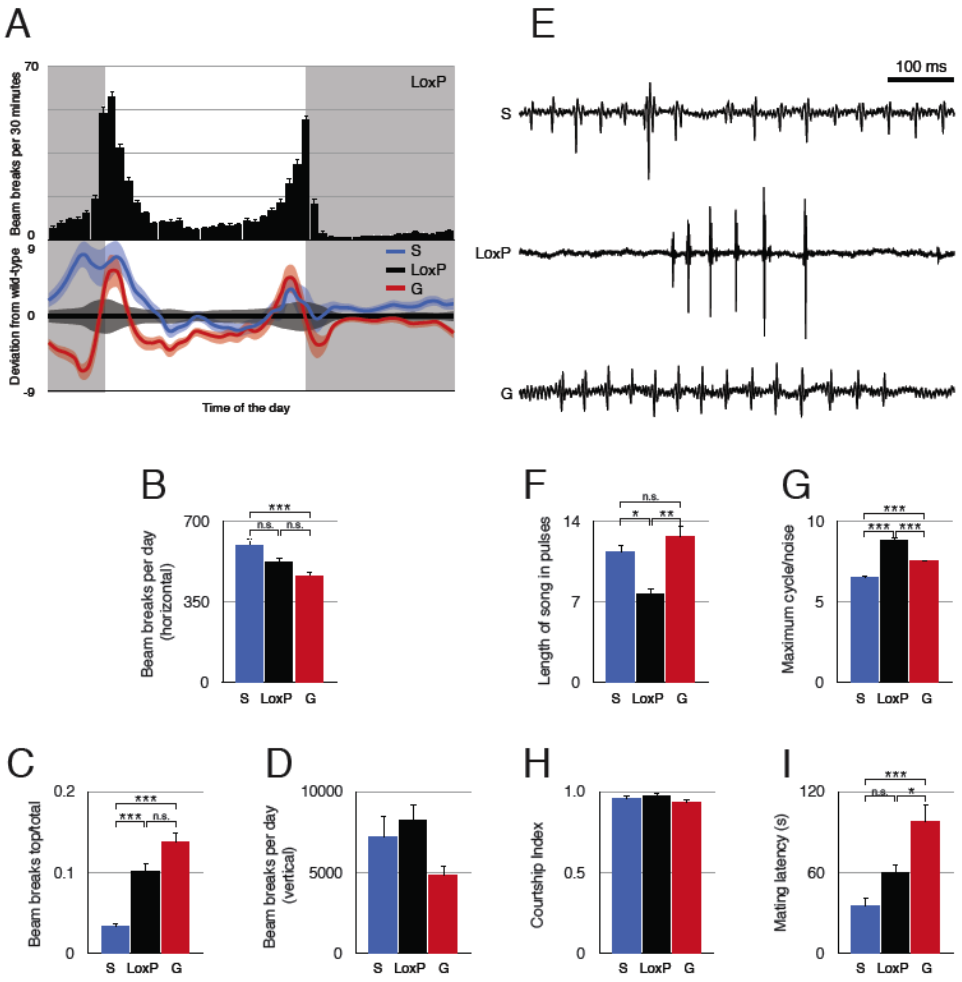

FIGURE 3.4. Dysregulation of *dAdar* auto-editing alters complex behaviors. (A) Locomotor profile of control and experimental male under 12 h light: dark (LD) conditions. Top panel – bar graph showing mean LD activity in $dAdar^{WTLoxP}$ control males (n = 65). Note that circadian anticipatory increases in locomotion preceding morning and night are present. Lower panel –mean locomotion in $dAdar^{S}$ (n = 67) and $dAdar^{G}$ (n = 77) males normalized to $dAdar^{WTLoxP}$. Light bars indicate standard error of the mean. (B) Total locomotor levels derived from single-fly activity data. (C-D) Relative geotaxis and total locomotor levels derived from vertical population activity monitors. $dAdar^{WTLoxP}$: n = 15 vials each containing 5 male flies; $dAdar^{S}$: n = 14; $dAdar^{G}$: n = 14. (E-I) Courtship song and mating parameters in $dAdar^{WTLoxP}$, $dAdar^{S}$ and $dAdar^{G}$ males. Representative pulse-song traces are shown in (E). Both auto-editing mutants exhibit longer pulse-song lengths (F) and reduced song strength (G) relative to $dAdar^{WTLoxP}$ controls. $dAdar^{WTLoxP}$: n = 63 songs, 510 waveforms; $dAdar^{S}$: n = 136, 1534; $dAdar^{G}$: n = 126, 1599. (H) Total time spent courting virgin females in a 10 min window (courtship index) did not differ between control and experimental genotypes. However, $dAdar^{G}$ males (n = 49) took significantly longer to initiate courtship relative to $dAdar^{WTLoxP}$ (n = 41) or $dAdar^{S}$ (n = 30) males (I). *: $P < 0.05$; **: $P < 0.005$; ***: $P < 0.0005$, one-way ANOVA with Tukey's HSD post-hoc test. Error bars: standard error.

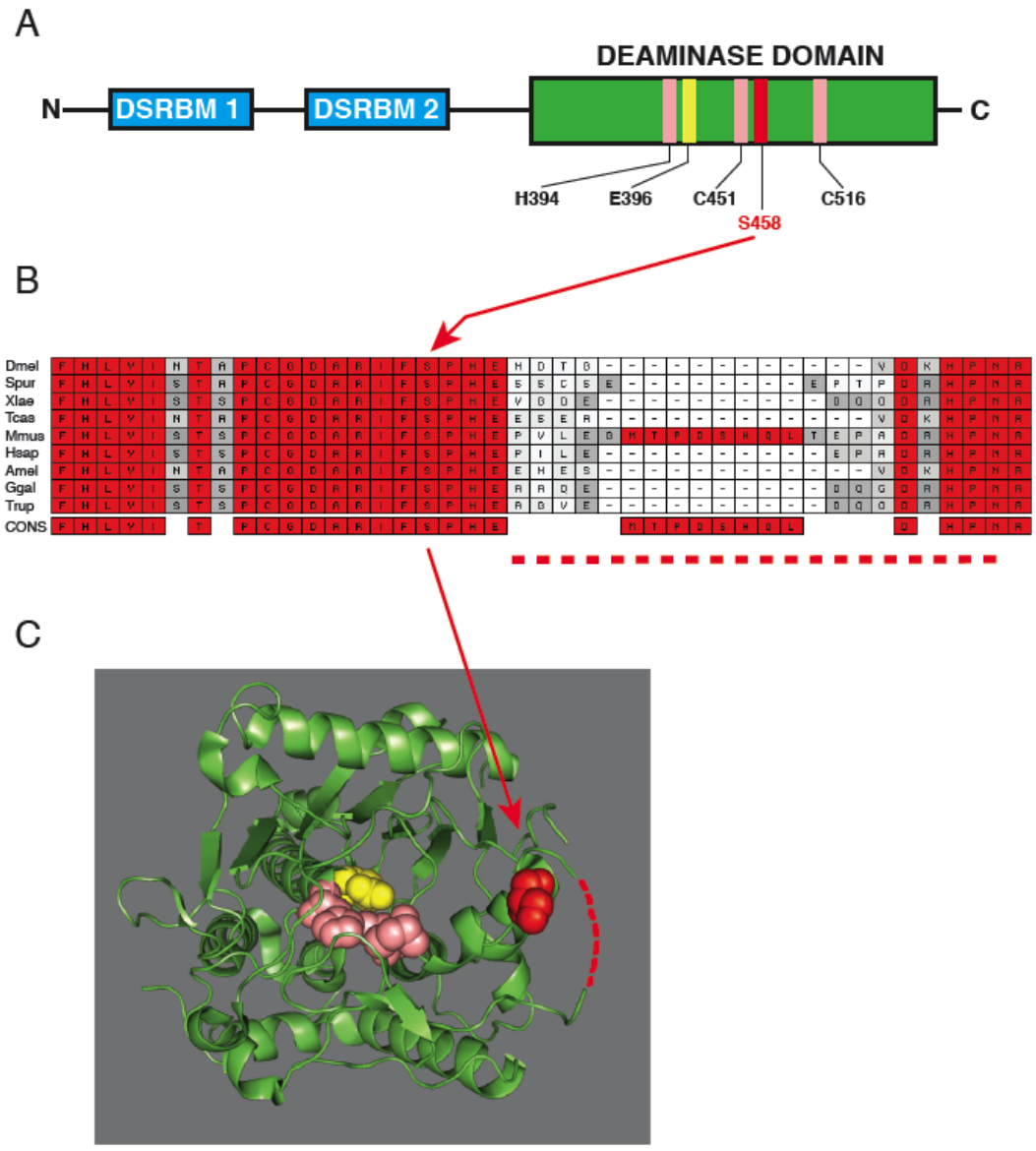

FIGURE S3.1. (A) Domain structure of the dADAR protein. The auto-edited residue resides within the C-terminal catalytic deaminase domain, which is downstream of the two double-strand RNA binding motifs (DSRBMs). Zinc ion coordinating residues (H394, C541, and C516) are shown in pink and the proton shuttling residue (E396) is shown in yellow. Auto-editing results in an amino acid substitution (serine → glycine) at a residue that is completely conserved between ADARs from highly divergent species (B), and the orthologous position in the human ADAR2 crystal structure is close to the active site of the deaminase domain (C).

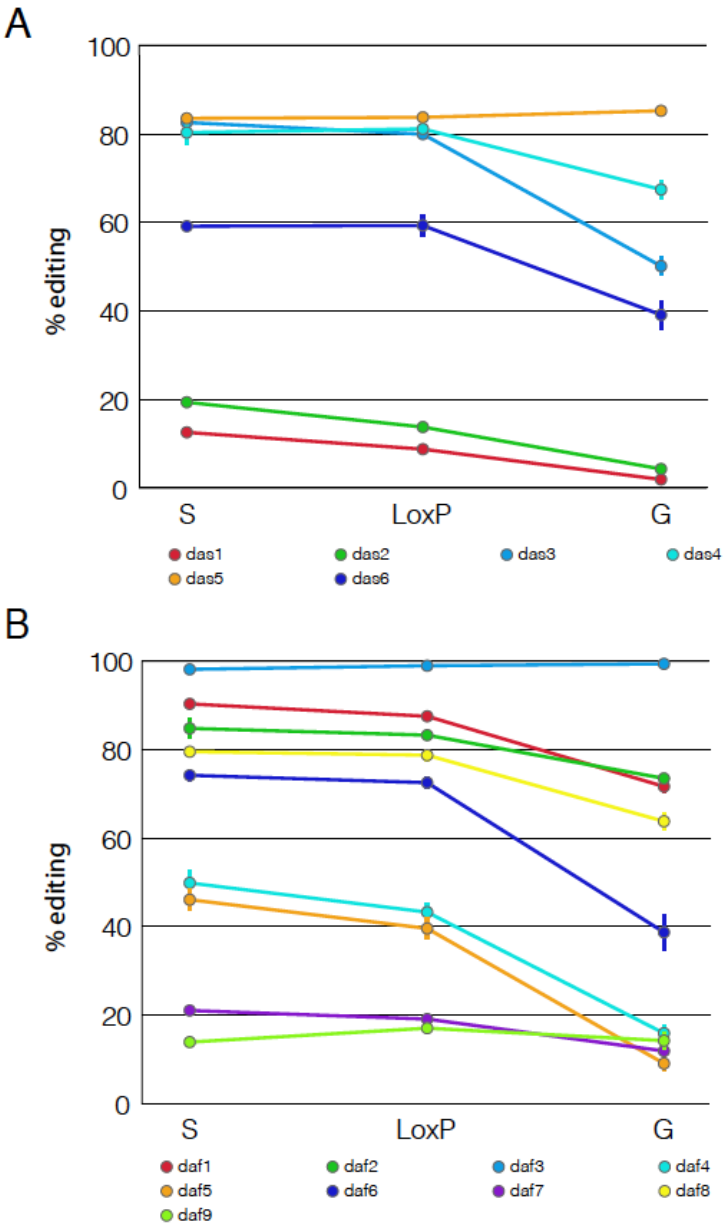

FIGURE S3.2. Examples of edited adenosines that exhibit no alteration, mono-, or bi-directional changes in editing levels in the same mRNA. (A) Six editing sites in the *Da6* acetylcholine receptor transcript show differential regulation in $dAdar^{S}$ and $dAdar^{G}$ when compared to $dAdar^{WTLoxP}$. One site in *Da6* shows no alteration, three sites show a mono-directional alteration, and two sites show a bi-directional alteration in response to abolishing or hard-wiring *dAdar* auto-editing. (B) Nine editing sites in the *Da5* acetylcholine receptor transcript show differential regulation in $dAdar^{S}$ and $dAdar^{G}$ when compared to $dAdar^{WTLoxP}$. Two sites in *Da5* show no alteration, five sites show a mono-directional, and two sites a bi-directional alteration upon changes in *dAdar* auto-editing. mRNAs were amplified from male head cDNA. Data are derived from ≥ 3 RT-PCR amplicons for each adenosine.

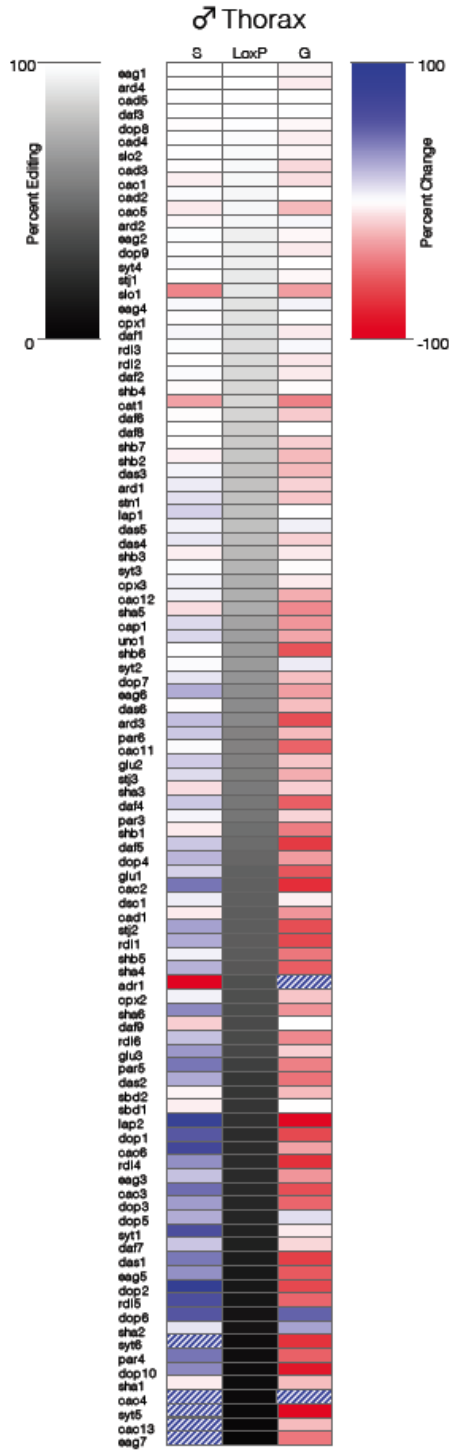

FIGURE S3.3. Heat map representations of alterations in editing at 100 adenosines (presented in four digit annotations – see Supplementary Table 1 for nomenclature) in male thorax from *dAdar*^{S}, *dAdar*^{WTLoxP}, and *dAdar*^{G}. Data are derived from ≥ 3 RT-PCRs for each adenosine, and are presented in rank order relative to the endogenous editing levels in *dAdar*^{WTLoxP}. Dashed boxes indicate a > 100% increase.

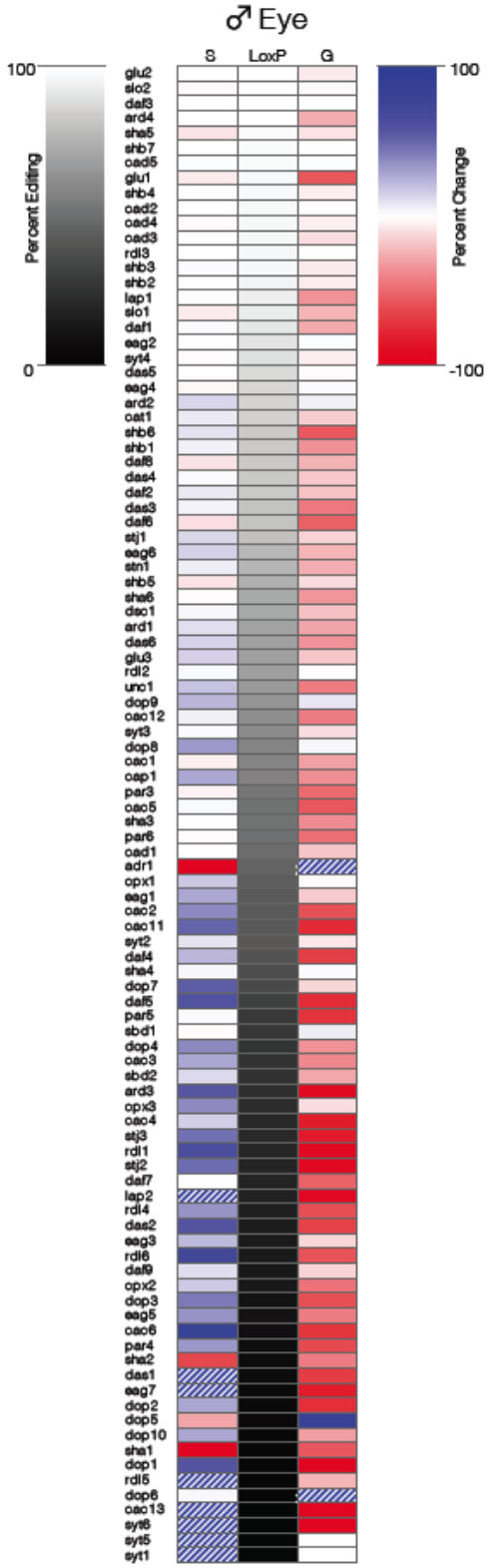

FIGURE S3.4. Heat map representations of alterations in editing in *dAdar*^{S}, *dAdar*^{WTLoxP}, and *dAdar*^{G} male eye cDNA. Data are derived from ≥ 3 RT-PCRs for each adenosine.

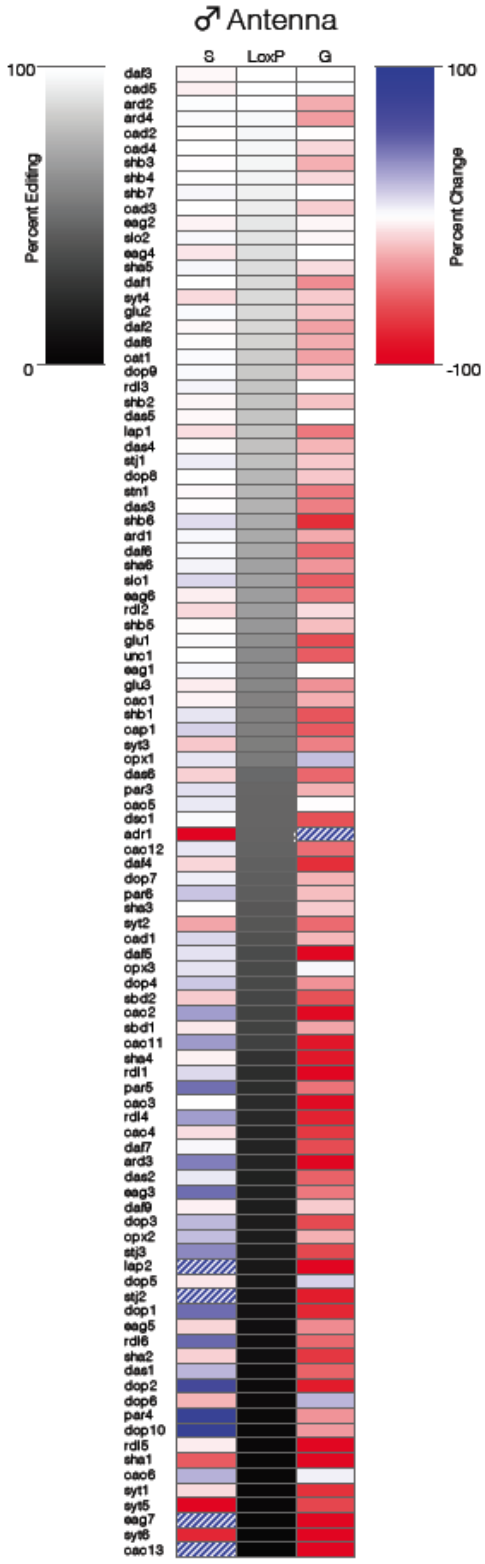

FIGURE S3.5. Alterations in editing in *dAdar*^{S}, *dAdar*^{WTLoxP}, and *dAdar*^{G} male antennae. Data are derived from ≥ 3 RT-PCRs for each adenosine.

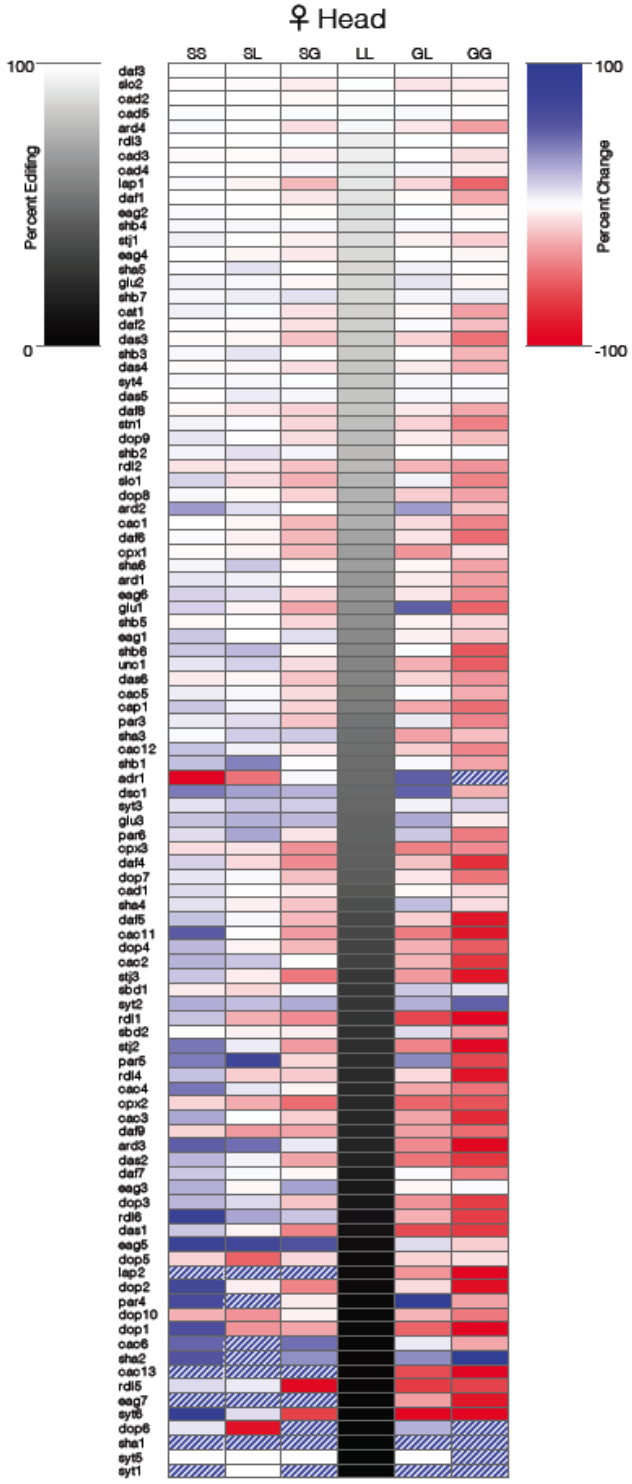

FIGURE S3.6. Heat map showing levels of editing at 100 adenosines in mRNAs amplified from $dAdar^{S/S}$, $dAdar^{S/L}$, $dAdar^{S/G}$, $dAdar^{L/L}$, $dAdar^{G/L}$, and $dAdar^{G/G}$ female heads. Data are derived from ≥ 3 RT-PCRs for each adenosine, and are presented in rank order relative to the endogenous editing levels in $dAdar^{L/L}$. L indicates the $dAdar^{WTLoxP}$ allele. Dashed boxes indicate a > 100% increase.

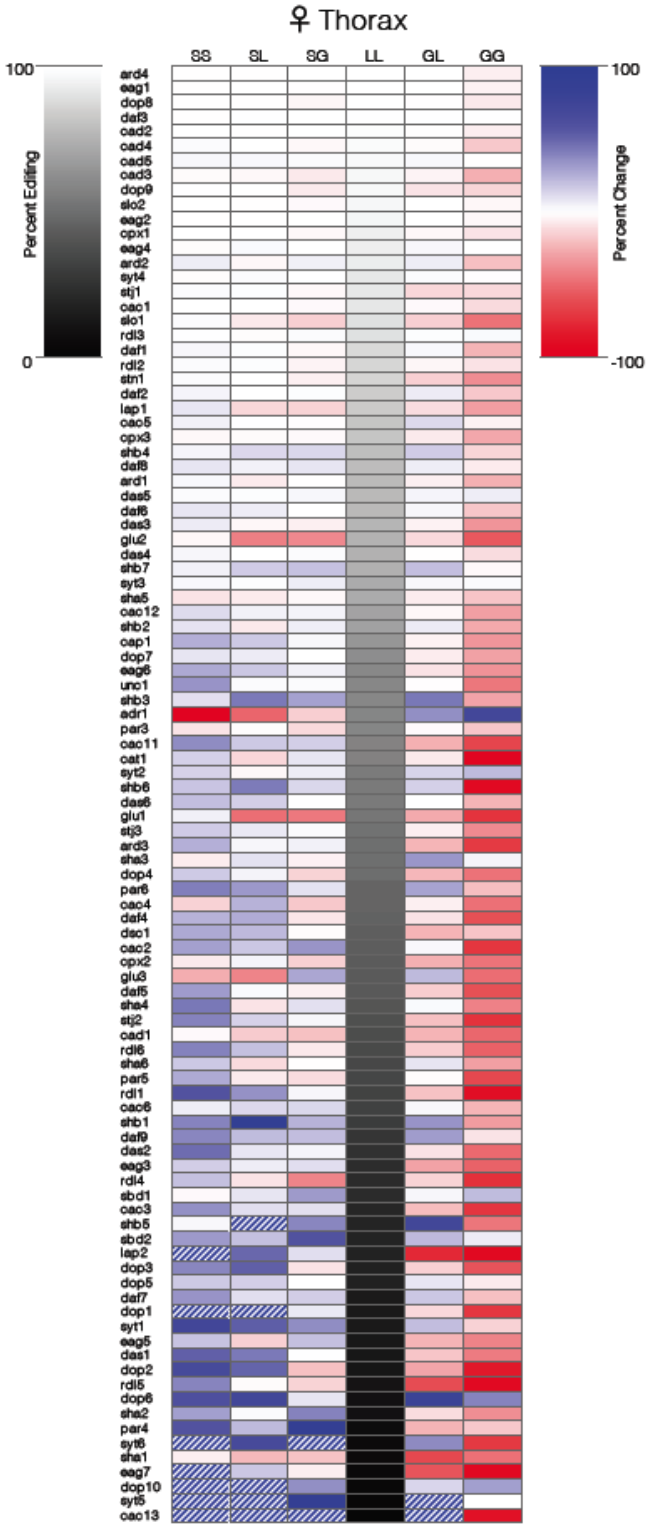

FIGURE S3.7. Editing levels at 100 adenosines in mRNAs amplified from $dAdar^{S/S}$, $dAdar^{S/L}$, $dAdar^{S/G}$, $dAdar^{L/L}$, $dAdar^{G/L}$, and $dAdar^{G/G}$ female thorax cDNA. Data are derived from ≥ 3 RT-PCRs for each adenosine, and are presented in rank order relative to the endogenous editing levels in $dAdar^{L/L}$.

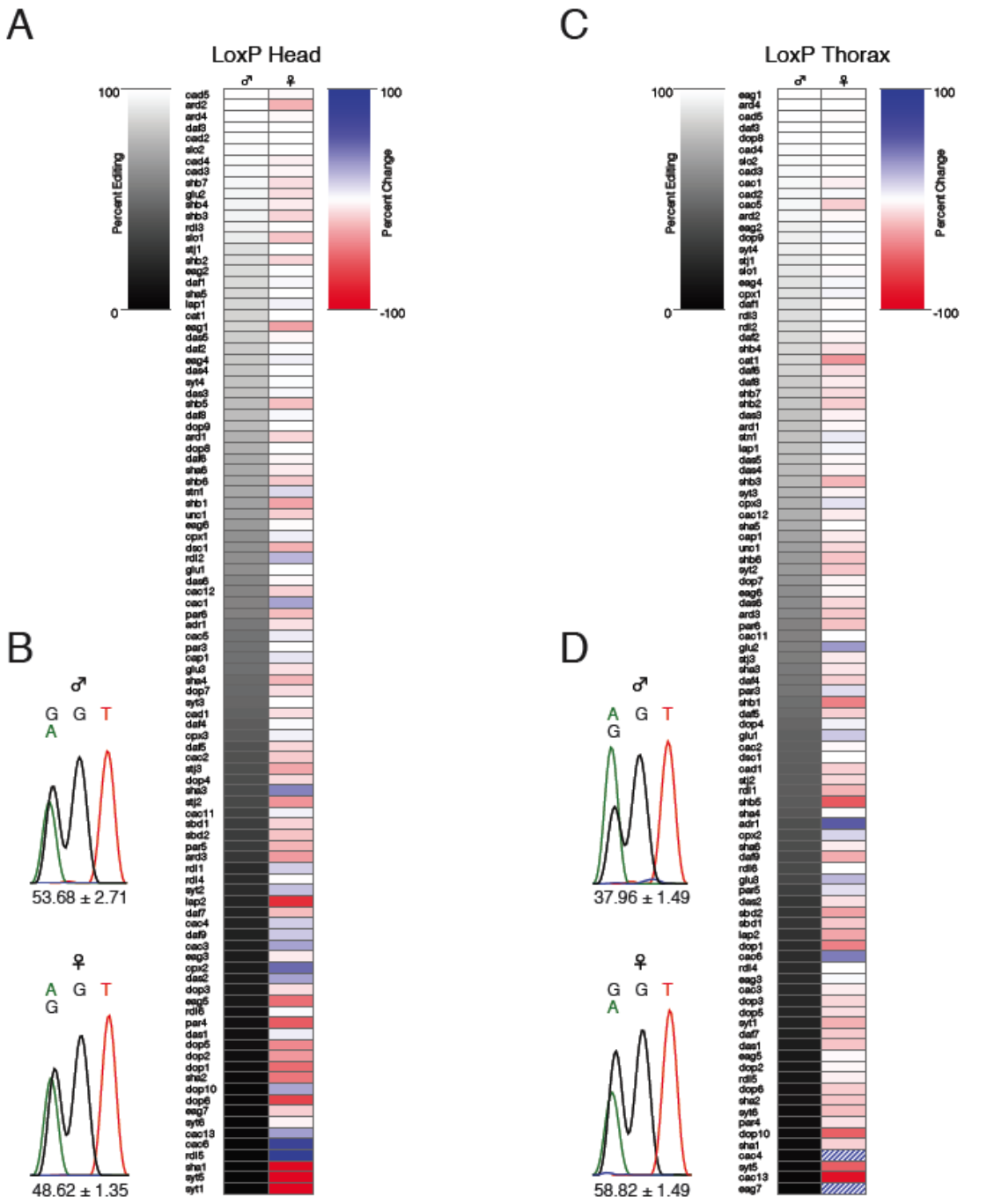

FIGURE S3.8. Comparison of editing levels at 100 adenosines in mRNAs amplified from male and female head cDNA (A) and thorax cDNA (C). Data are derived from ≥ 3 RT-PCRs for each adenosine, and are presented in rank order relative to the endogenous male editing levels in *dAdar*^{WTLoxP} head and thoraxes. Example electropherograms depicting the auto-editing state of *dAdar* in male and female head (B) and thoraxes (D).

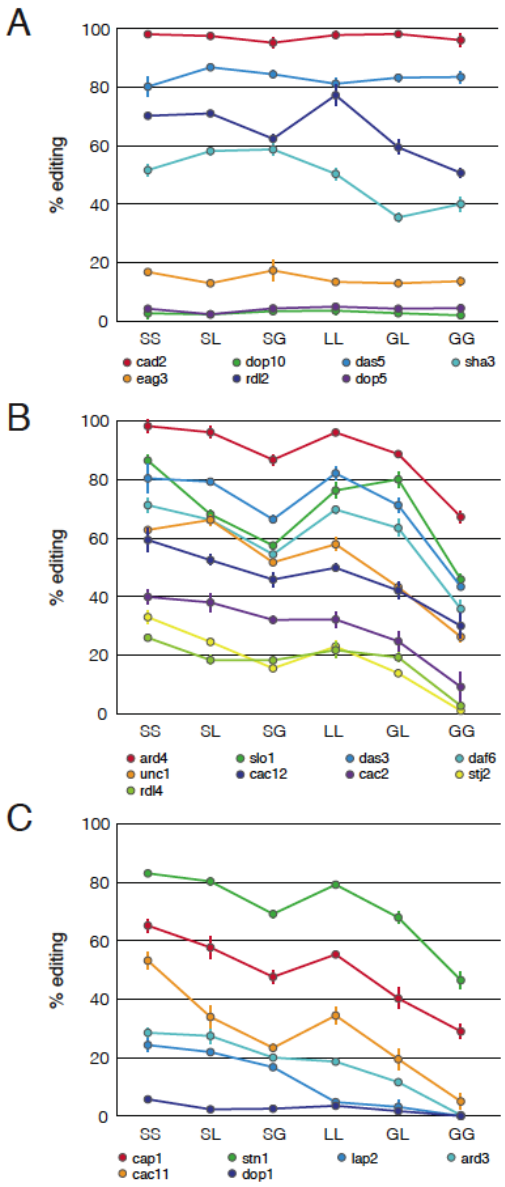

FIGURE S3.9. Editing levels at 22 adenosines in mRNAs amplified from head tissue derived from six different female *dAdar* allelic combinations, which show a graded shift in auto-editing levels. In male heads, the same adenosines either exhibit no response (A), a mono-directional (B) or bi-directional change (C) in editing in response to reducing or increasing *dAdar* auto-editing levels (Fig. 3.1C-E). Similar responses to alterations in *dAdar* auto-editing were generally observed when comparing male and female head samples. However, there were exceptions: editing at *rdl* site 2 (rdl2) and *shaker* site 3 (sha3) were not reduced in $dAdar^{G}$/Y males relative to wild-type controls (Fig. 3.1C), yet editing at both sites was robustly reduced in $dAdar^{G}/dAdar^{G}$ females relative to $dAdar^{WTLoxP}$ homozygotes (A). Conversely, editing at *stoned-B* site 1 (stn1) was significantly higher in $dAdar^{G}$/Y males relative to controls, yet was unchanged in $dAdar^{G}$/ $dAdar^{G}$ females relative to $dAdar^{WTLoxP}$ homozygotes (C). These results emphasize the context-specific nature of the molecular effects of *dAdar* auto-editing. The LoxP wild-type allele is indicated by L.

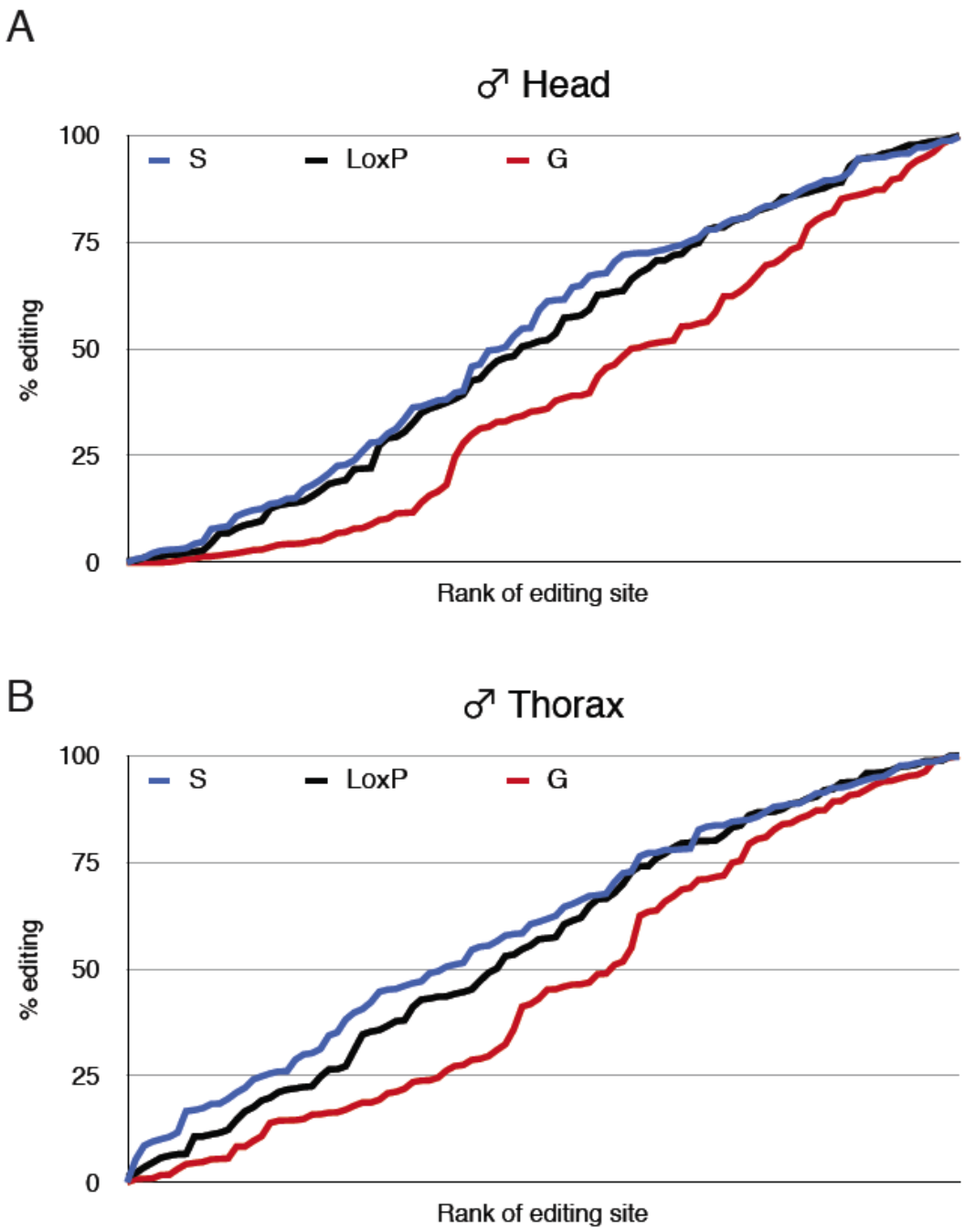

FIGURE S3.10. Rank-ordered editing levels at 100 adenosines amplified from *dAdar*^{G}/Y, *dAdar*^{WTLoxP}/Y and *dAdar*^{S}/Y male heads (A) and thoraxes (B). Each population is rank-ordered independently. Overall, the change in editing levels in *dAdar*^{S}/Y heads and thoraxes (in terms of absolute values) is relatively subtle, particularly in the head. However, in both tissues, hard-wiring *dAdar* auto-editing significantly reduces editing across the inosinome.

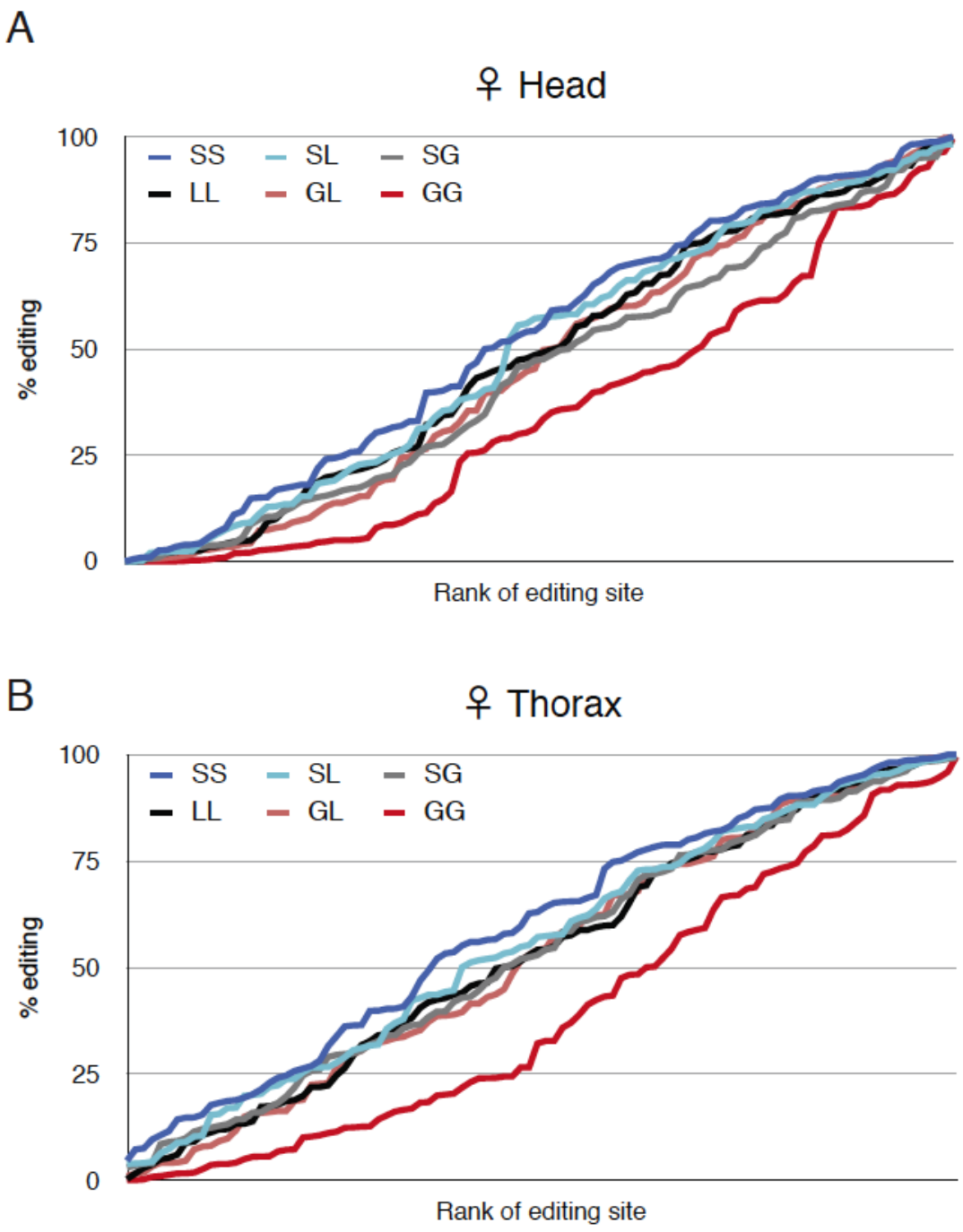

FIGURE S3.11. Rank-ordered editing levels at 100 adenosines amplified from female head (A) and thorax (B) cDNA from six allelic *dAdar* combinations. As in male heads and thoraxes (fig. S3.10), editing in $dAdar^{G}$/ $dAdar^{G}$ homozygote females is robustly reduced across almost all of the inosinome relative to all other possible allelic combinations. Importantly, the introduction of just a single wild-type *dAdar* allele (reducing auto-editing by ~ 25%) is sufficient to restore broad editing levels to approximately wild-type levels in both head and thoraxes. The LoxP wild-type allele is indicated by L.

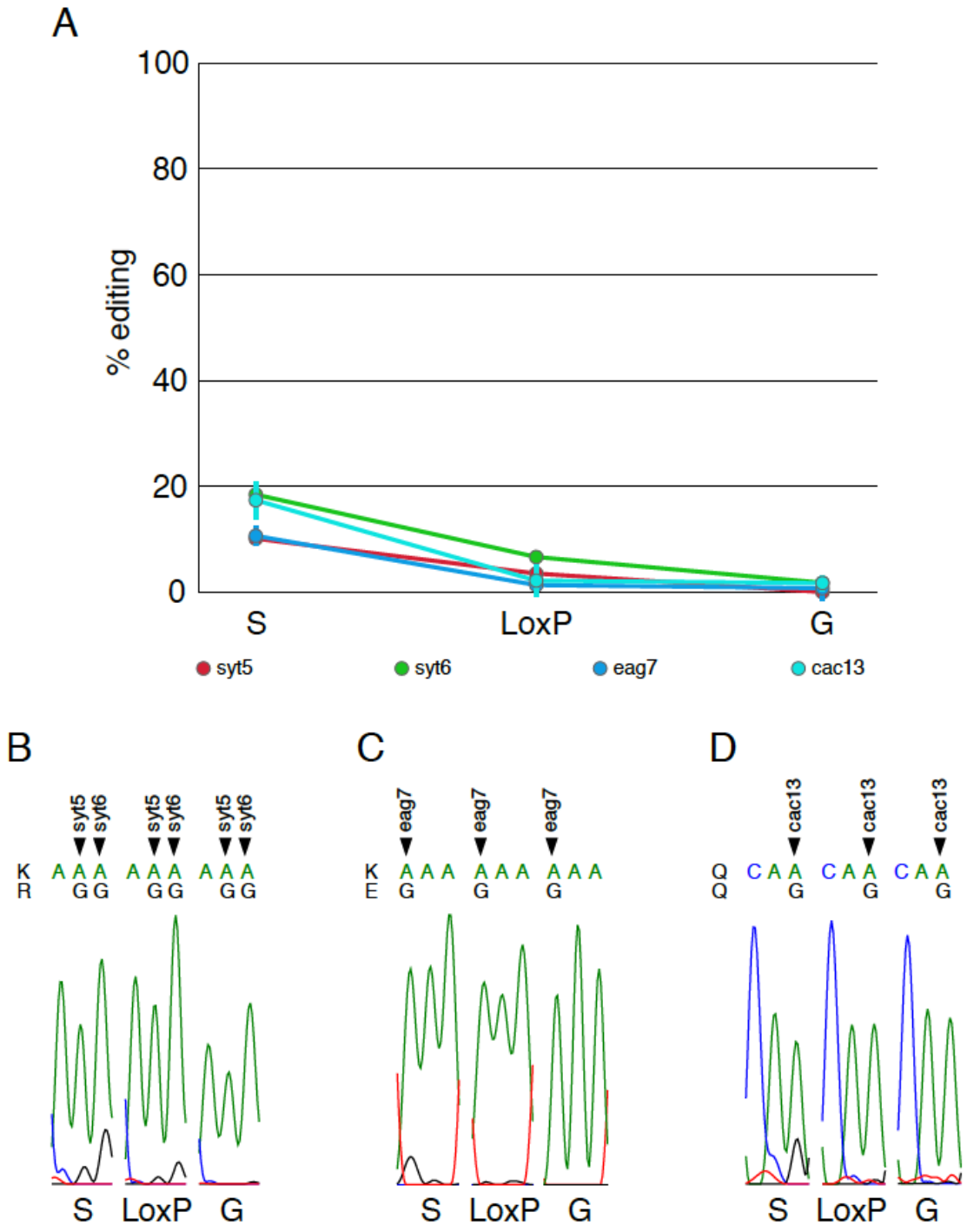

FIGURE S3.12. (A) Editing levels at novel editing sites which were only detected in the *dAdar*^{S} background. Editing at *Synaptotagmin-1* site 5 (syt5) and *eag* site 7 (eag7) lead to the amino acid substitutions K → R and K → E respectively. RNA editing at *synaptotagmin-1* site 6 (syt6) and *cacophony* site 13 (cac13) leads to synonymous changes. (B-D) Example electropherograms showing editing of the novel editing sites in three genetically distinct *dAdar* backgrounds: *dAdar*^{S}, *dAdar*^{WTLoxP}, and *dAdar*^{G}.

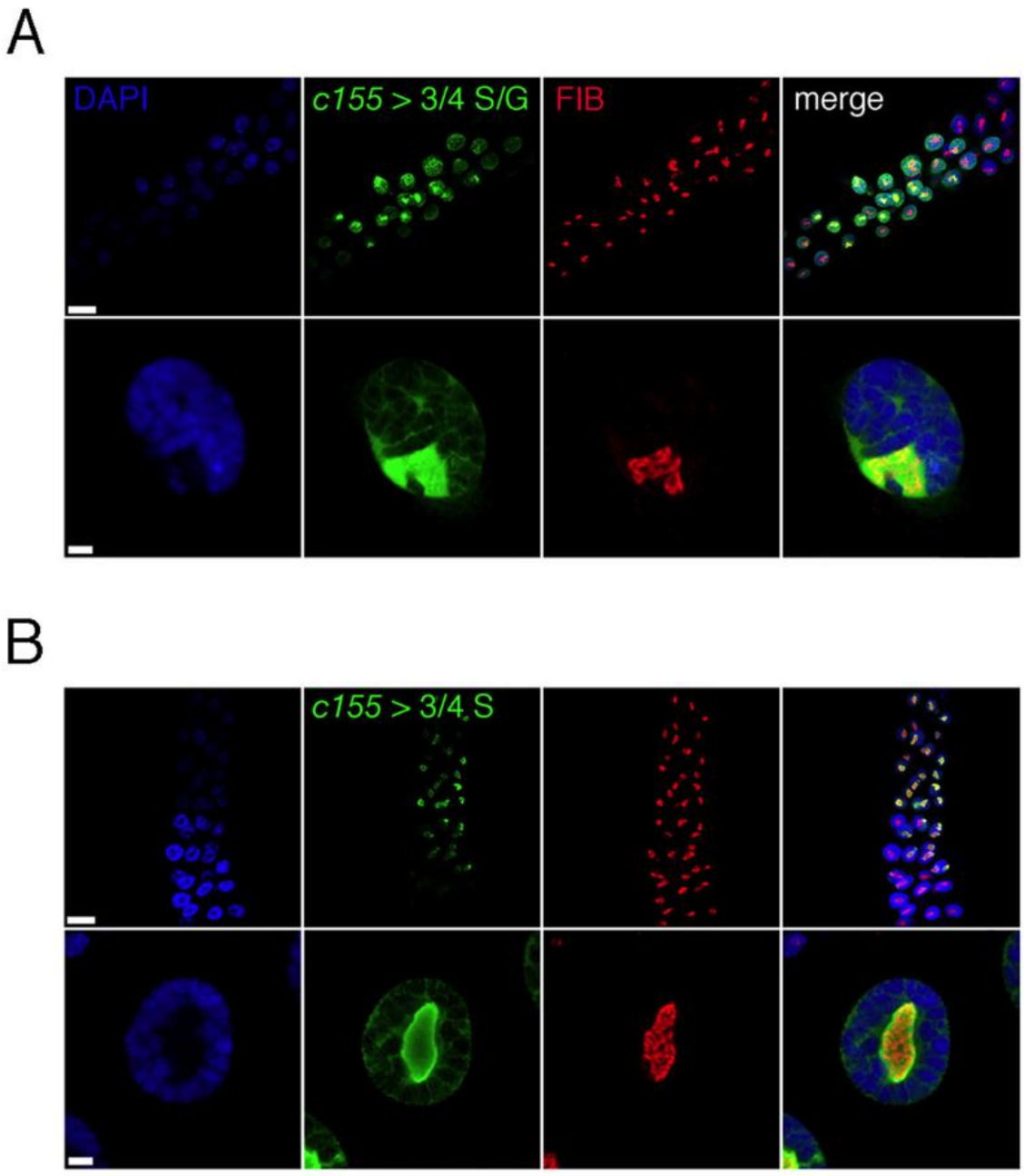

FIGURE S3.13. dADAR transgenes expressed in 3rd instar larval salivary gland nuclei co-localize with the nucleolus. Two separate transgenes representing the predominant adult-stage isoform of dADAR, which lacks the alternatively spliced 3a exon (termed '3/4') were expressed in larval salivary glands using the *c155*-Gal4 driver. At the auto-editing site, the serine codon was either wild-type (AGT) ('S/G') and is capable of being edited by the dADAR transgene, or was mutated to an un-editable synonymous TCT codon ('S'). In the adult nervous system, the wild-type dADAR transgene is robustly edited. Both the 3/4 S/G (A) and the 3/4 S transgene (B) primarily co-localized with the nucleolus, labeled with an anti-fibrillarin antibody. Upper panels: scale bar = 50 μm. Lower panels: scale bar = 5 μm.

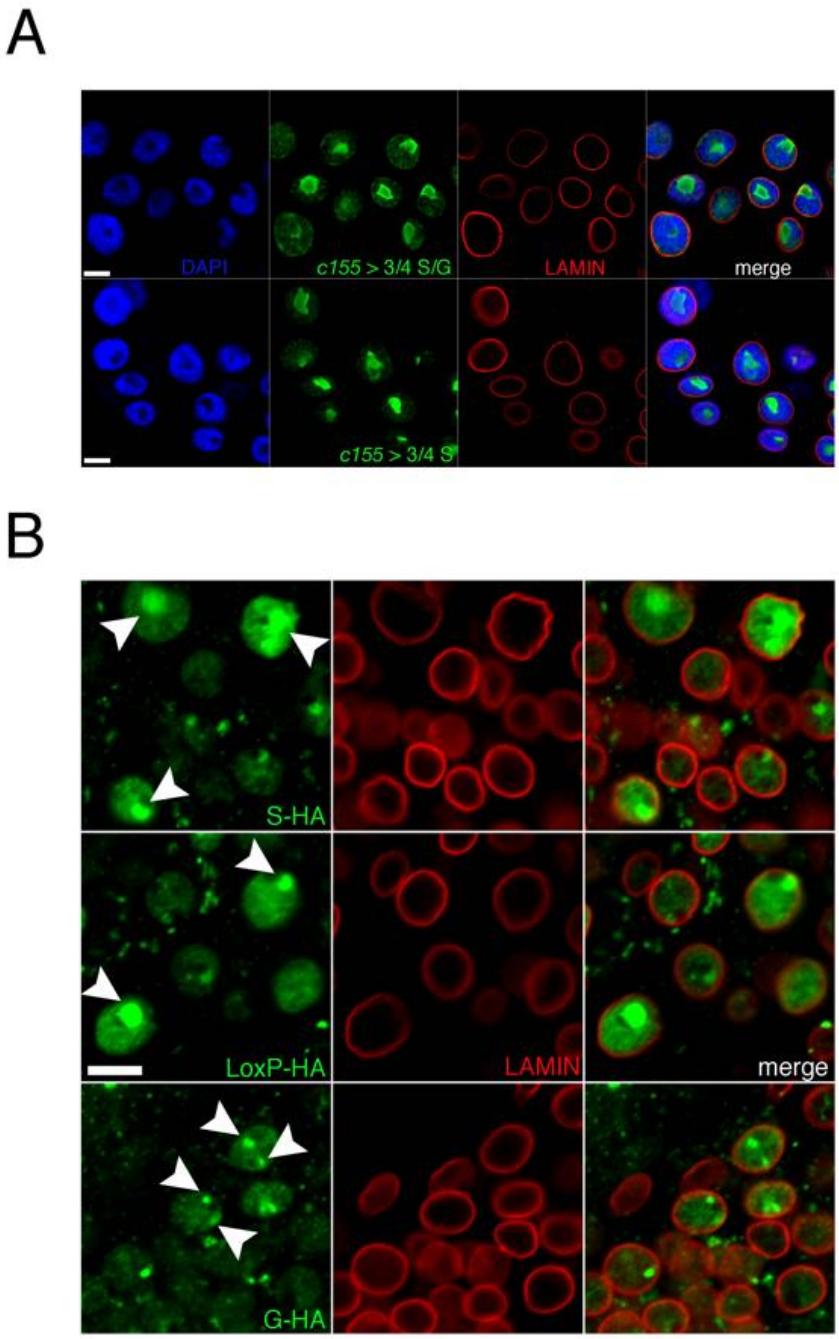

FIGURE S3.14. dADAR transgenes and endogenous dADAR localize to within the nuclear envelope irrespective of the auto-editing state. (A) Ectopically expressed dADAR transgenes either capable of auto-editing (3/4 S/G) or with a hard-wired serine codon (3/4 S) localize internally to the nuclear envelope (labeled with an anti-Lamin antibody) in 3rd instar larval salivary glands. Scale bars = 20 μm. (B) In adult neuronal nuclei, WTLoxP-HA, S-HA and G-HA dADARs also localize to within the nuclear envelope. Arrows indicate the primary concentrations of nuclear dADAR. Note the presence of multiple punctae within the nucleus in neurons expressing G-HA dADAR, but not S-HA dADAR (Fig. 3.3). Scale bar = 5 μm.

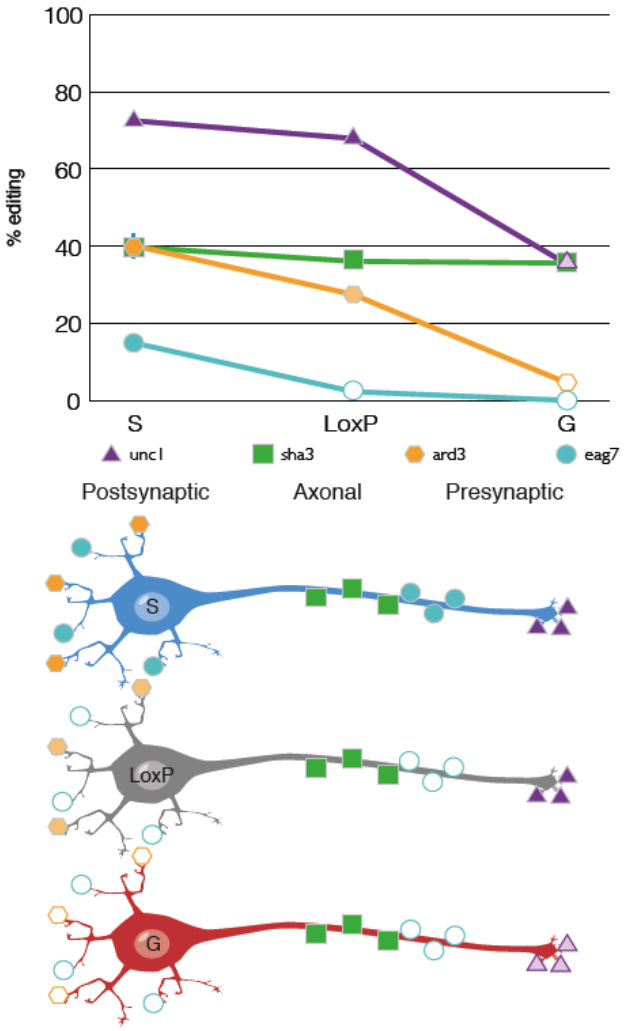

FIGURE S3.15. Top panel illustrates a graphical representation of the change in editing of four substrate adenosines in the *dAdar*^{WTLoxP}, *dAdar*^{S}, and *dAdar*^{G} genetic backgrounds. *Unc-13* site 1 (unc1) belongs to the category of editing sites that displayed no effect upon elimination of auto-editing, but exhibited a significant reduction upon hard-wiring of *dAdar* auto-editing (Fig. 3.1D). *Shaker* site 3 (sha3) belongs to the category of editing sites that was insensitive to the edited status of *dAdar* (Fig. 3.1C), while *ard* site 3 (ard3) belongs to the category of editing sites that displayed a bi-directional change upon elimination or hard-wiring of auto-editing (Fig. 3.1E). Finally, *eag* site 7 (eag7) is a novel RNA editing site that only appears upon elimination of auto-editing (supplementary Fig. S3.9). The bottom panel illustrates a diagrammatic representation of three distinct neuronal subtypes: a neuron in which *dAdar* auto-editing is lacking (S), a neuron in which edited and unedited states of *dAdar* are present at wild-type levels (LoxP), and a neuron in which *dAdar* auto-editing is at maximum (G). *dAdar* auto-editing regulates the editing levels of the four adenosines in a site-specific manner. While the levels of editing of *shaker* site 3 are the same between the three different neuronal subtypes, *ard* site 3 and *unc-13* site 1 exhibit differential editing levels depending on the degree of *dAdar* auto-editing. Finally, *eag* site 7 is only edited in neurons where auto-editing is absent, or possibly very low.

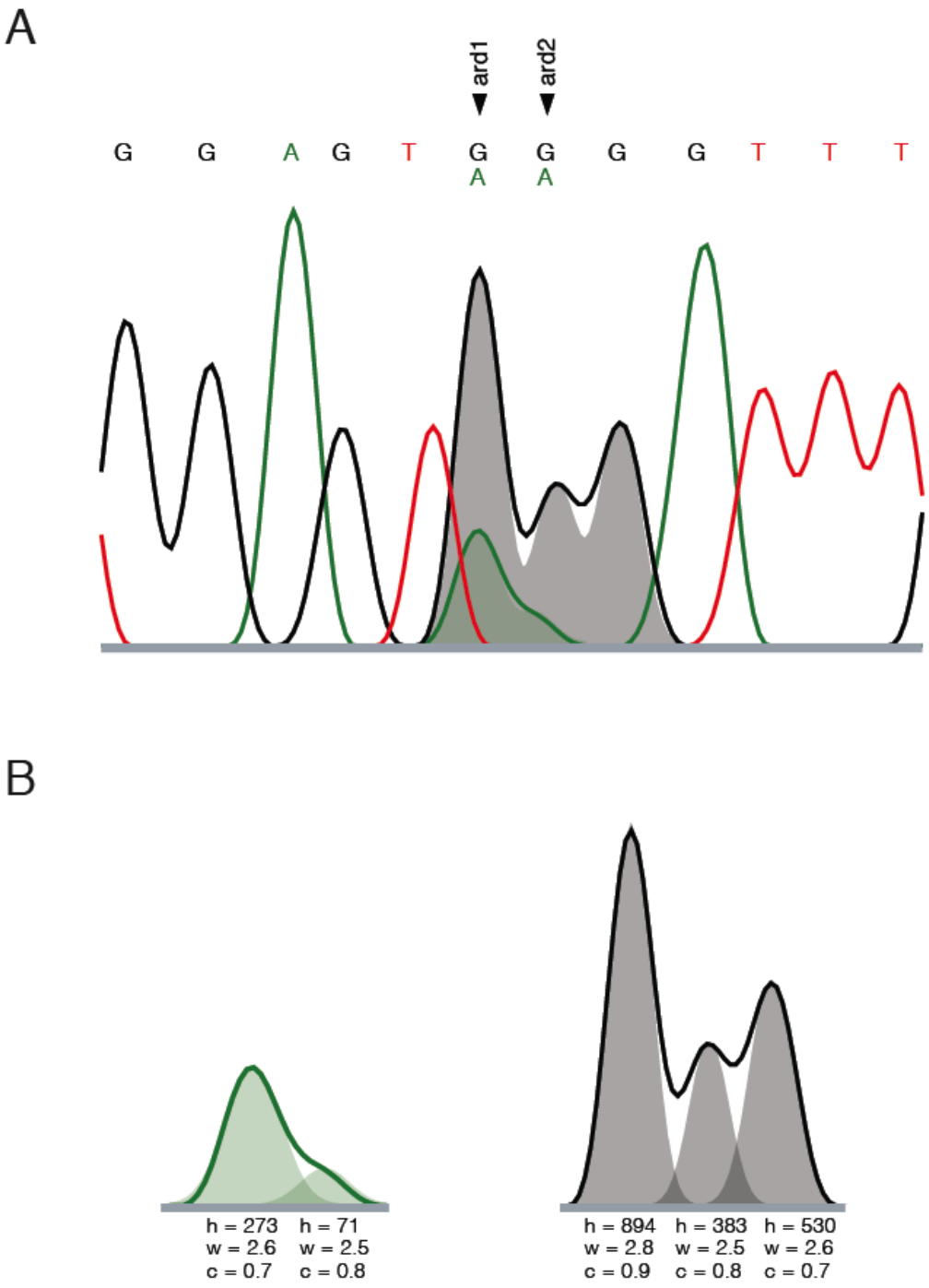

FIGURE S3.16. (A) Example electropherogram showing the edited adenosines ard1 and ard2 (sites 1 and 2 of the *ard* acetylcholine receptor), in which the best fit Gaussian curves for the A and G residues are shown as filled green and black, respectively. (B) A and G chromatograms on the left and right in which each best fit Gaussian curve and its parameters are shown.

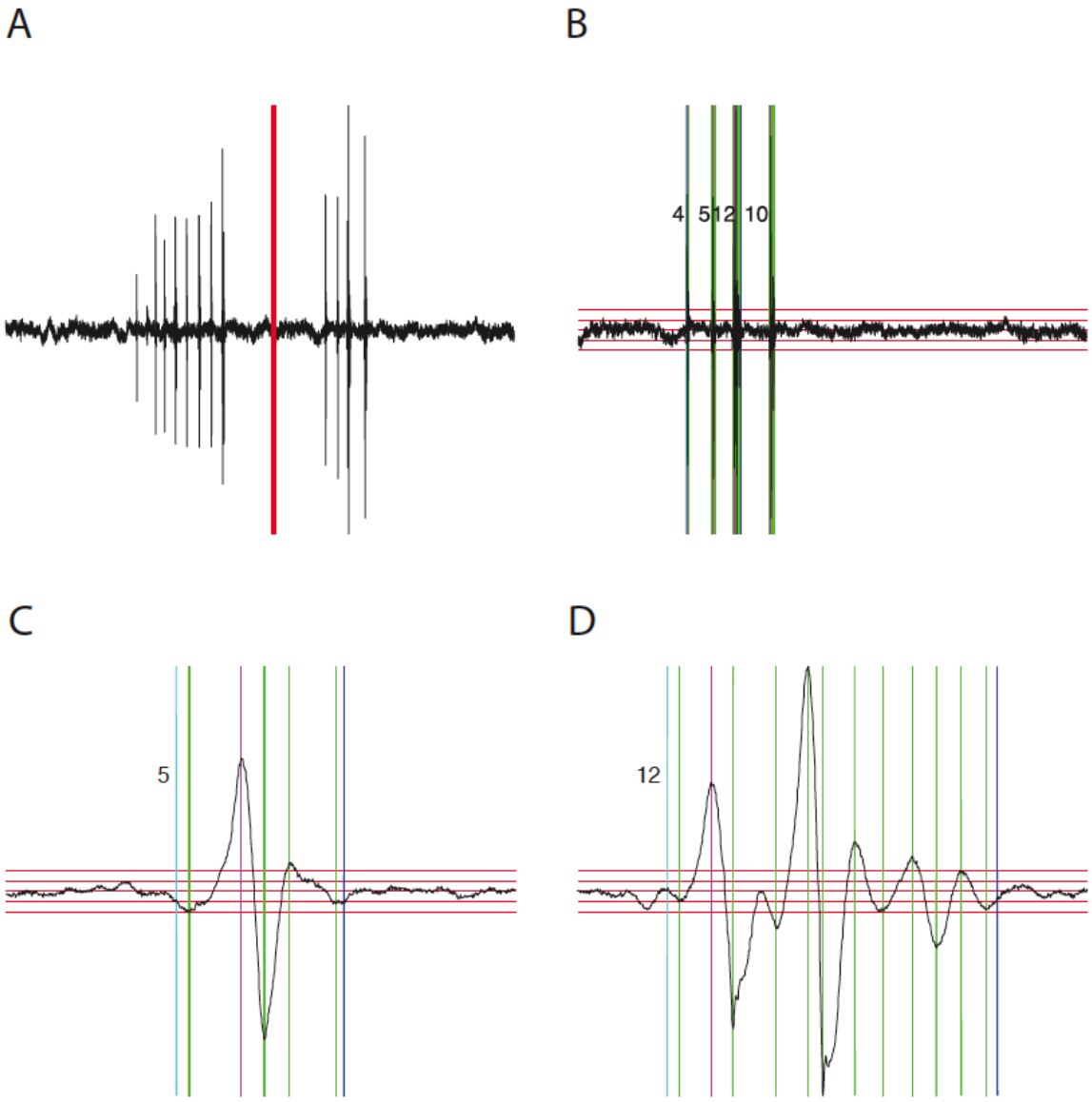

FIGURE S3.17. (A) The waveform of a full courtship song with a red line showing where the computer split the song. (B) The waveform of one train: that of the latter part of the song in (A). Green vertical lines show the positions of each pulse and red horizontal lines show the error from -2 to 2 standard deviations. Magenta vertical lines show the first major cycle in a pulse. (C) A normal pulse from the train in (B). Similar colors apply. Cycles are judged as extrema that lie outside the noise threshold. (D) An unusual song containing many cycles.

Abbreviation	Locus	Synonyms/ full name	Molecular function
adr	*dAdar*	*Drosophila adenosine deaminase acting on RNA*	RNA editing enzyme
ard	*ard*	nAcRβ-64B	Nicotinic acetylcholine receptor β-subunit
cac	*cacophony*	Dmcα1A	Voltage-gated calcium channel α-subunit
cad	*Ca-alpha1D*	Dmcα1D	Voltage-gated calcium channel α-subunit
cap	*caps*	Calcium activated protein for secretion	Regulator of exocytosis
cat	*Ca-alpha1T*	Dmcα1T	Voltage-gated calcium channel α-subunit
cpx	*complexin*		Regulator of exocytosis
daf	*Dα5*	nAcRα-34E	Nicotinic acetylcholine receptor α-subunit
das	*Dα6*	nAcRα-30D	Nicotinic acetylcholine receptor α-subunit
dop	*DopEcR*		Dopamine/Ecdysteroid receptor
dsc	*dsc1*	NaCP60E	Voltage-gated sodium channel
eag	*eag*	Ether-a-go-go	Voltage-gated potassium channel α-subunit
glu	*GluClα*		Glutamate-gated chloride channel
lap	*lap*	like-AP180	Regulator of endocytosis
par	*para*	*paralytic*	Voltage-gated sodium channel α-subunit
rdl	*rdl*	*resistance to dieldrin*	GABA receptor α-subunit
sbd	*sbd*	nAcRβ-96A	Nicotinic acetylcholine receptor β-subunit
sha	*shaker*		Voltage-gated potassium channel α-subunit
shb	*shab*		Voltage-gated potassium channel α-subunit
slo	*slowpoke*		Ca^{2+}-activated potassium channel
stj	*straightjacket*	α2δ	Voltage-gated calcium channel
stn	*stoned-B*		Regulator of endocytosis
syt	*synaptotagmin-1*		Regulator of exocytosis
unc	*unc-13*		Regulator of exocytosis

Table S3.1: Nomenclature for the 23 transcripts analyzed in various *dAdar* allelic backgrounds. Sites (1, 2...) are labeled in a 5' to 3' order within the transcript.

CHAPTER 4:

Visualizing inter-individual variation in adenosine-to-inosine RNA editing

This chapter consists of data that was presented in a manuscript and submitted for peer review. “Visualizing inter-individual variation in adenosine-to-inosine RNA editing” Authors: James E.C Jepson, Kyle A. Jay, Yiannis A. Savva and Robert A. Reenan. My specific contributions to this manuscript include: (a) I created the *dAdar*^{WTLoxP}, *dAdar*^{S} and *dAdar*^{hyp} alleles used in this study using ends-out homologous recombination.

ABSTRACT

Informational recoding by adenosine-to-inosine (A-to-I) RNA editing functionally diversifies neuronal proteomes by chemically modifying structured messenger RNAs (mRNAs) (Bass and Weintraub, 1988; Keegan et al., 2001; Nishikura, 2010). However, techniques for analyzing editing activity on substrates within defined neuronal populations *in vivo* are lacking. Here, guided by comparative genomics, we reverse-engineer a fluorescent reporter sensitive to *Drosophila* adenosine deaminase acting on RNA (dADAR) activity and auto-regulation. While the reporter demonstrates spatially relevant expression, we also found measurable non-stereotypy of RNA editing activity in the nervous system between individuals. Our results demonstrate the feasibility of structurally mimicking ADAR substrates as a means to regulate protein expression and, potentially, therapeutically repair mutant mRNAs. In addition, our data suggest differential RNA editing as a credible molecular mechanism for mediating individual-to-individual variation in neuronal physiology and behavior.

INTRODUCTION

A-to-I RNA editing results when deamination of adenosine to inosine occurs within double-stranded (ds) RNA substrates (Bass and Weintraub, 1988), catalyzed by ADARs (adenosine deaminases acting on RNA) (Keegan et al., 2001; Nishikura, 2010). In animals, a variety of mRNAs encoding proteins involved in fast electrical and chemical neuro-transmission are subject to A-to-I editing (Grauso et al., 2002; Higuchi et al., 1993; Hoopengardner et al., 2003; Seeburg and Hartner, 2003), and ADAR activity is crucial for neuronal integrity and behavior in several model genetic organisms (Higuchi et al., 2000; Mombereau et al., 2010; Palladino et al., 2000a; Singh et al., 2009; Tonkin et al., 2002).

Editing levels in mRNAs are generally studied as a bulk property via RT-PCR followed by analysis of cDNA clones or electropherograms. However, robust PCR amplification from smaller tissues such as sub-populations of neurons is technically demanding. An alternative strategy that can be exploited lies in ADAR's ability to edit the amber (U**A**G) stop codon to tryptophan (U**I**G). Such a read-through approach has previously been used to generate molecular reporters for editing activity by linear coupling of a modified ADAR substrate containing an editable amber codon to a downstream output, such as b-galactosidase or luciferase (Gommans et al., 2010; Pokharel and Beal, 2006). However, no reporter system for editing activity has been validated in the primary site of ADAR activity *in vivo*, namely, the nervous system.

MATERIALS AND METHODS

In vitro expression studies

Transformation into *Drosophila* S2 cells was performed as previously described (Reenan, 2005). Briefly, transformations of the various reporter constructs were performed with 1 mg of pCoBLAST::reporter construct and 0.2 mg of pCoBLAST (empty vector) or pCoBLAST::dADAR to assess dADAR dependence. Cells were transfected, allowed to recover for 24 h, and then induced with copper. Cells were imaged at 24 h post-induction.

Drosophila stocks and genetics

For all epi-fluorescence and confocal images, we used 1-2 day old male *Drosophila* raised at a constant 25°C, on standard molasses food and under 12 h day/night cycles. The *dAdar* and *indy* RNAi transgenes were obtained from the VDRC stock center and have been validated previously (Jepson and Reenan, 2009). For experiments involving *dAdar* null males, we used the $dAdar^{5g1}$ allele, previously shown to lack all detectable RNA editing activity (Palladino et al., 2000a). The $dAdar^{WTLoxP}$, $dAdar^{S}$, $dAdar^{G}$ and $dAdar^{hyp}$ alleles were generated using ends-out homologous recombination, described previously for $dAdar^{hyp}$ (Jepson et al. 2010). The *tubulin*-Gal4 line was obtained from the Bloomington stock center.

For experiments involving analysis of variation in YFP^{splice} and GFP^{edit} expression, we used 2-3 independent transgenic insertions of each construct to control for position

effects on the stability of expression. A single copy of two independent YFP^{splice} transgenes (both located on chromosome III) was sufficient to yield robust fluorescence in whole-mount and confocal imaging experiments (see below) when driven with *tubulin*-Gal4. Since only a fraction of GFP^{edit} transcripts generate functional GFP due to the requirement for successful A-to-I editing, we found that generally, lines expressing multiple insertions of GFP^{edit} were optimal for robust GFP fluorescence. The insertions used in this study were located on chromosome X (and thus up-regulated relative to autosomal copies), homozygosed on chromosome II, or a single copy on chromosome III, all in conjunction with *tubulin*-Gal4. In figures showing multiple examples of GFP^{edit} or YFP^{splice} expression/fluorescence, all examples are from males expressing the same transgene insertion.

RNA editing analysis

RNA was extracted from the heads of 1-3 day old male *Drosophila* (15-20 per sample) were performed using TRIzol reagent (Invitrogen). The GFP^{edit} construct was amplified via RT-PCR using the following primer sets: for the RT reaction, we used a reverse primer specific to the UAS construct (UAS-R1: 5' GTCACACCACAGAAGTAAGGTTCC 3'). The following primers were used for PCR: forward – 5' GCGAGGAGCTGTTCACTGGGGTGG 3'; reverse – 5' GTCTAGATTACTTGTACAGCTCGT 3'. Sequencing primer: 5' CATCCTGGTCGAGCTGGACGGCGA 3'. Primers for amplifying and sequencing *unc-13* were described previously (Jepson and Reenan, 2009). Levels of editing were

determined by measuring the area under A- and G-peaks in individual electropherogram traces using Image J. The % editing is expressed at G/(A+G) x 100.

Microscopy and immuno-histochemistry

To quantify variation in YFP^{splice} and GFP^{edit}, we used different approaches depending on whether the imaging was epi-fluorescent or confocal. A Zeiss LSM 510 meta was used to obtain all confocal z-stacks and slices, while a Zeiss AX10 Imager.M1 was used for epi-fluorescent whole-mount imaging. For epi-fluorescent imaging of heads and forelegs, fluorescence of YFP^{splice} or GFP^{edit} was measured directly via excitation at 488nm. Fluorescence in the clypeus or forelegs was subsequently quantified using Image J. For confocal immune-histochemistry, adult and larval brains were prepared as described previously (Ingleby et al., 2009). Primary antibodies were used at the following concentrations: mouse anti-nc82 and anti-Dachshund (Developmental studies hybridoma bank) were all used at 1:40. We labeled both GFP and YFP using a rabbit anti-GFP primary (Invitrogen) at 1:200, followed by a cy5-tagged secondary to avoid excitation of the fluorophore itself. Alexa-fluor secondary antibodies (goat anti-mouse Cy3 and goat anti-rabbit cy5 (Invitrogen Molecular Probes)) were used at 1:200. Confocal images were obtained at sub-saturation levels of fluorescent intensity. Images were contrast-enhanced in Adobe Photoshop.

Since we re-used primary antibodies for consecutive batches, we controlled for any potential reduction in anti-GFP concentration by normalizing anti-GFP intensity to the nc82 counter-stain signal (for antennal lobe fluorescence, YFP or GFP glomerular

staining was normalized to nc82 staining in the same glomeruli; for the mushroom body α/β and g-lobes, YFP and GFP staining was normalized to nc82 staining in ipsi-lateral g-lobe, which were easily identifiable). We next normalized the GFP/nc82 or YFP/nc82 values in each batch of brains to the batch mean; if the mean absolute GFP or YFP staining was not significantly different between separate batches ($P > 0.05$, Mann-Whitney U-test), batches were pooled. Mushroom body α- and β-lobes were analyzed separately and pooled following normalization. To rule out any contribution of differences in signal/noise ratios between YFP^{splice} and GFP^{edit}, we only compared batches of YFP^{splice} and GFP^{edit} that did not significantly differ in cy5 fluorescent intensity ($P > 0.05$, Mann-Whitney U-test).

Online Supplementary Material

The supplementary material includes 7 figures. Supplementary figure 1 (S4.1) shows the molecular design of the GFP^{edit} reporter. Supplementary figure 2 (S4.2) shows GFP^{edit} fluorescence in S2 cells is dependent on dADAR expression. Supplementary figure 3 (S4.3) shows the cell-types responsible for GFP^{edit} expression in the antennal lobe (AL) and mushroom bodies (MB). Supplementary figure 4 (S4.4) shows that expression of GFP^{edit} *in vivo* is dependent on dADAR expression. Supplementary figure 5 (S4.5) shows the expression of GFP^{edit} in $dAdar^{hyp}$ allele. Supplementary figure 6 (S4.6) shows the developmentally regulated spatial control of dADAR activity. Supplementary figure 7 (S4.7) shows representative examples of YFP^{splice} driven by *tubulin*-Gal4 in male heads and forelegs.

RESULTS

To generate a more natural *in vivo* reporter for dADAR activity, we made use of structural information gleaned from comparative genomics (Reenan, 2005). The *Drosophila synaptotagmin-1* (*syt-1*) mRNA is edited at four positions (A-D), of which editing at site D is most robust (Hoopengardner et al., 2003). The structure that directs editing at sites C and D has been partially solved, is ultra-conserved amongst *Drosophilids*, and consists of a complex pseudoknoted interaction between the edited exon and two complementary and conserved non-coding elements (E1 and E2) located in the downstream intron (Reenan, 2005). Importantly, the duplex structure that directs editing at site D has the property of consisting largely of intronic sequence (Reenan, 2005) (supplementary Fig. S4.1A). Utilizing this fact, we generated a chimeric gene construct that would express full-length wild-type green fluorescent protein (GFP) only when acted upon by correct RNA splicing and dADAR modification. First, we inserted the entire intron 9 of *syt-1,* containing all splicing signals and the E2 cis-element directing editing at site D, directly into the GFP coding sequence, artificially generating two GFP 'exons' (Fig. 4.1A and supplementary Fig. S4.1B). The GFP sequences were arranged such that the second position guanosine of a conserved GFP tryptophan codon (U**G**G) would be positioned at the normally edited third position adenosine of the isoleucine codon (AU**A**) within the RNA structure of *syt-1*. This tryptophan residue is the only such position in the *Aequorea victoria* GFP gene and resides very near the chromophore. By then mutating this tryptophan to an amber stop codon (U**G**G → U**A**G), we re-created a potentially editable adenosine at the same conceptual position as *syt-1*

site D. Finally, we re-engineered element E2 with structurally compensatory changes (as well as a single synonymous change in GFP coding sequence) to mimic the normal base-paired structure between E2 and *syt-1* site D (Fig. 4.1A, supplementary Fig. S4.1C-D). We term this construct GFP^{edit}. A separate construct based on YFP was also generated, which contained a tryptophan residue in place of the amber stop codon to serve as a splicing control (YFP^{splice}).

We inserted the above constructs into the pMT and pUAS plasmids to allow both inducible expression in *Drosophila* S2 tissue culture cells and cell-specific expression *in vivo* using the Gal4-UAS binary expression system, respectively (Brand and Perrimon, 1993). As predicted, transient expression of GFP^{edit} in S2 cells resulted in detectable GFP fluorescence only upon co-transfection of a dADAR transgene (supplementary Fig. S4.2A). The wild-type chimera with the amber stop codon, but without structural mutations to mimic the *syt-1* structure, showed no fluorescence (data not shown). Thus, the intended structure reverse-engineered into the reporter clearly directs coupled splicing and editing to produce functional GFP protein utilizing a jellyfish/fruitfly chimera and a structural mimic of a natural dADAR substrate.

To visually probe A-to-I editing in *Drosophila,* irrespective of tissue-type, we expressed constructs using a ubiquitous driver (*tubulin*-Gal4). Global expression of the YFP^{splice} control yielded fluorescence in the anterior and dorsal regions of the head capsule, as well as the clypeus, labellum, and legs (Fig. 4.1B,C). When GFP^{edit} was driven using the same driver, GFP fluorescence was observed in a similar pattern to YFP^{splice}, albeit with higher fluorescence intensity in the clypeus and labellum, likely due to the fact that YFP is only partially excited at the optimal excitation wavelength for

GFP. Furthermore, fluorescence was not observed in any tissue when GFP^{edit} was driven by *tubulin*-Gal4 in a *dAdar* null (*dAdar*^{5g1}) background (Fig. 4.1B,C). Thus, GFP^{edit} fluorescence is limited to areas in which the transcript is accurately spliced, and is dependent on dADAR activity *in vitro* and *in vivo*.

In the adult *Drosophila* nervous system, YFP^{splice} and GFP^{edit} expression was limited primarily to three neuronal centers: the αβ- and γ-lobes of the mushroom bodies (MBs), antennal lobe (AL) glomeruli, and the central complex (CC) (Fig. 4.1D,E). For both YFP^{splice} and GFP^{edit}, MB and AL fluorescence was deduced to originate from Dachsund-positive Kenyon cells and local AL interneurons respectively (supplementary Fig. S4.3). No YFP^{splice} expression was detected in the thoracic ganglion or non-neuronal cell types (upplementary Fig. S4.2B), possibly due to splicing regulatory elements within the *syt-1* intron that only allow correct splicing in a nervous system and cell-specific manner. When expressed in adult heads, GFP^{edit} was edited at ~ 25% - less than the endogenous *syt-1* site D but at a similar (or higher) level to a significant proportion of the *Drosophila* inosinome (Jepson and Reenan, 2009; Jepson et al. 2010) (supplementary Fig. S4.4A). In a *dAdar*^{5g1} background, the GFP^{edit} transgene was successfully edited upon co-expression of dADAR transgenes representing two distinct splice-forms of dADAR (supplementary Fig. S4.4B,C). Co-expression of GFP^{edit} with RNAi constructs targeted to dADAR (Jepson and Reenan, 2009), or in a background containing a hypomorphic allele of *dAdar*, further confirmed that GFP^{edit} fluorescence in the adult brain is dADAR-dependent and responsive to dADAR levels (supplementary Fig. S4.4D-G and supplementary Fig. S4.5).

Interestingly, while the adult nervous system patterns of YFP^{splice} and GFP^{edit}

expression largely overlapped, this was not the case at earlier stages of development, where dADAR protein levels are relatively low (Jepson et al. 2010). In the 3rd instar larval brain, YFP^{splice} expression was observed in both the MB γ-lobes and the larval AL (supplementary Fig. S4.6). In contrast, GFP^{edit} was limited solely to the γ-lobes, illustrating that our *in vivo* reporter system is capable of detecting spatio-temporal alterations in dADAR expression and activity during development.

To analyze the response of GFP^{edit} to more subtle modifications of dADAR activity, we next determined the response of GFP^{edit} expression to changes in dADAR auto-editing. At the pupal and adult stages of *Drosophila*, dADAR edits its own transcript, leading to a serine (S) to glycine (G) substitution close to motif II of the catalytic domain (Keegan et al., 2005; Palladino et al., 2000b). *In vivo*, auto-editing reduces dADAR's catalytic activity on a subset of edited adenosines. Expression of GFP^{edit} in a genetic background lacking auto-editing ($dAdar^{S}$) significantly increased editing measured on GFP^{edit} transcripts by 17.5% relative to $dAdar^{WTLoxP}$ controls (absolute value; $p = 0.004$, Kruskal-wallis test, $n = 6$ PCRs for all genotypes), while editing of GFP^{edit} transcripts in males containing a constitutively edited allele of *dAdar* ($dAdar^{G}$) was reduced by 2.5% ($p = 0.006$). Intriguingly, the changes in editing of the GFP^{edit} transgene in RNA isolated from whole head tissue was not reflected by corresponding uniform spatial changes in MB or AL fluorescence (Fig. 4.2). In AL glomeruli, GFP^{edit} expression did not increase in a $dAdar^{S}$ background compared to $dAdar^{WTLoxP}$ controls, but was significantly reduced in $dAdar^{G}$ males, suggesting that *dAdar* mRNAs expressed in neurons contributing to AL fluorescence are largely un-edited. In contrast, in both the α/β- and γ-lobes of the MBs, fluorescence significantly

increased in *dAdar*^{S} males. We also observed a reduction in γ-lobe fluorescence in *dAdar*^{G} males, but not in α/β-lobes (Fig. 4.2D), suggesting that *dAdar* auto-editing may be spatially regulated even within distinct Kenyon cell subtypes.

The above results comprehensively demonstrate that the GFP^{edit} reporter is sensitive to alterations in dADAR expression and catalytic activity in an *in vivo* setting. Previous analyses of epitope tagged endogenous dADAR expression indicated substantial neuron-to-neuron variation in expression levels (Jepson et al. 2010). We thus used our novel reporter system to address a fundamental question not easily answered using standard molecular techniques: how stereotyped is editing activity between individuals within a population, both at the tissue and cellular levels?

When examining fluorescence of GFP^{edit} in *Drosophila* heads, we noticed a surprising degree of spatial variation in fluorescent intensity within the head capsule between 1-2 day old male flies (Fig. 4.3A). We then quantified the degree of variation in GFP^{edit} and YFP^{splice} epi-fluorescence in the clypeus and leg tissues. Although a slight increase in the proportion of outliers from the mean fluorescence in the clypeus could be detected when driving GFP^{edit} relative to YFP^{splice} (Fig. 4.3A), GFP^{edit} fluorescence in the clypeus was, on average, highly stereotyped and the variance in fluorescence did not significantly differ from YFP^{splice} (p = 0.48, F-test) (Fig. 4.3C; for examples of YFP^{splice} see supplementary Fig. S4.7A). In contrast, while YFP^{splice} expression in the femur of the prothoracic legs was also highly stereotyped (s.d = 0.21), we observed a robust increase in the degree of variation in GFP^{edit} fluorescence in the same tissue type (s.d = 0.44, p = 1.1 x 10^{-7}, F-test) (Fig. 4.3B, D and supplementary Fig. S4.7B). This significant increase in the standard deviation of GFP^{edit} relative to YFP^{splice} fluorescence indicates that the

variability of GFP^{edit} fluorescence is not due to either RNA splicing or the *tub*-Gal4 driver, but instead is a function of dADAR activity.

We next investigated two aspects of variation in YFP^{splice} and GFP^{edit} fluorescence in behaviorally relevant neuronal structures (Fig. 4.4A,B). For the control fluorophore, YFP^{splice}, variation within and between batches can occur via stochastic differences in driver strength and technical issues relating to immune-histochemistry (re-use of antibodies etc.). In these cases, however, fluorescence in distinct neurons within a single brain should co-vary, rather than varying independently. This was indeed the case when comparing YFP^{splice} fluorescence in the α- and β-lobes of the MB (which share a common cell body) (Lee et al., 1999) and between the MB γ-lobes and ALs (which do not) (Fig. 4.4C,D). In contrast, while as expected, GFP^{edit} fluorescence still strongly co-varied between MB α- and β-lobes (Fig. 4.4E), fluorescence in the MB γ-lobes and ALs was only weakly correlated (Fig. 4.4F), demonstrating that RNA editing in distinct regions of the *Drosophila* brain can be autonomously controlled.

Finally, we tested for non-stereotypical patterns of GFP^{edit} fluorescence in the MBs and ALs. To avoid signal: noise differences between populations, we only analyzed batches of brains with mean fluorescent signals that were not significantly different for each neuronal structure, blind to the variance within batches. Consistent with Figure 4.3, in both the MB and the AL, we observed a significant increase in the standard deviation of normalized GFP^{edit} versus YFP^{splice} fluorescence within batches (see methods) when comparing multiple aged-matched male *Drosophila* (α/β-lobes: s.d increase = 35%, $p = 7.8 \times 10^{-5}$, F-test; γ-lobes: 57%, $p = 0.0001$; AL: 49%, $p = 0.0027$) (Fig. 4.4G-L). Thus, dADAR activity as measured by fluorescence output of an editing-dependent reporter

exhibits non-stereotypical patterns within neuronal populations controlling complex adult-stage behaviors such as the processing of olfactory information and memory formation.

DISCUSSION

In summary, we have reverse-engineered a novel dADAR substrate that generates full-length GFP only following successful splicing and A-to-I editing, thus demonstrating the capacity of ADARs to repair mutant mRNAs in the presence of engineered cis-acting (and hypothetically, trans-acting) RNA elements. We have used this *in vivo* reporter system not only to infer neuron-specific control of *dAdar* auto-editing and dADAR activity (Figs. 4.2 and 4.4), but to document significant spatial variation in dADAR activity within behaviorally important tissues and neuronal sub-types (Figs. 4.3 and 4.4). Particularly intriguing is our observation of variable dADAR activity within Kenyon cells and AL interneurons, as recent work has revealed significant electrophysiological non-stereotypy in both of these cell types (Chou et al., 2010), as well as in behavioral outputs associated with mushroom body function (Murthy et al., 2008).

In our accompanying paper, we demonstrate that even subtle modifications of dADAR activity may have profound effects on several adaptive behavioral outputs. Taken together, our data suggests that differential modification of the functional properties of ion channels and synaptic release proteins through variable RNA editing (Claridge-Chang et al., 2009; Hoopengardner et al., 2003) could provide a plausible mechanism for neuro-physiological and behavioral variability.

REFERENCES

Bass, B.L., and Weintraub, H. (1988). An unwinding activity that covalently modifies its double-stranded RNA substrate. Cell *55*, 1089-1098.

Brand, A.H., and Perrimon, N. (1993). Targeted gene expression as a means of altering cell fates and generating dominant phenotypes. Development (Cambridge, England) *118*, 401-415.

Chou, Y.H., Spletter, M.L., Yaksi, E., Leong, J.C., Wilson, R.I., and Luo, L. (2010). Diversity and wiring variability of olfactory local interneurons in the Drosophila antennal lobe. Nature neuroscience *13*, 439-449.

Claridge-Chang, A., Roorda, R.D., Vrontou, E., Sjulson, L., Li, H., Hirsh, J., and Miesenbock, G. (2009). Writing memories with light-addressable reinforcement circuitry. Cell *139*, 405-415.

Gommans, W.M., McCane, J., Nacarelli, G.S., and Maas, S. (2010). A mammalian reporter system for fast and quantitative detection of intracellular A-to-I RNA editing levels. Analytical biochemistry *399*, 230-236.

Grauso, M., Reenan, R.A., Culetto, E., and Sattelle, D.B. (2002). Novel putative nicotinic acetylcholine receptor subunit genes, Dalpha5, Dalpha6 and Dalpha7, in Drosophila melanogaster identify a new and highly conserved target of adenosine deaminase acting on RNA-mediated A-to-I pre-mRNA editing. Genetics *160*, 1519-1533.

Higuchi, M., Maas, S., Single, F.N., Hartner, J., Rozov, A., Burnashev, N., Feldmeyer, D., Sprengel, R., and Seeburg, P.H. (2000). Point mutation in an AMPA receptor gene rescues lethality in mice deficient in the RNA-editing enzyme ADAR2. Nature *406*, 78-81.

Higuchi, M., Single, F.N., Kohler, M., Sommer, B., Sprengel, R., and Seeburg, P.H. (1993). RNA editing of AMPA receptor subunit GluR-B: a base-paired intron-exon structure determines position and efficiency. Cell *75*, 1361-1370.

Hoopengardner, B., Bhalla, T., Staber, C., and Reenan, R. (2003). Nervous system targets of RNA editing identified by comparative genomics. Science (New York, NY *301*, 832-836.

Ingleby, L., Maloney, R., Jepson, J., Horn, R., and Reenan, R. (2009). Regulated RNA editing and functional epistasis in Shaker potassium channels. The Journal of general physiology *133*, 17-27.

Jepson, J.E., and Reenan, R.A. (2009). Adenosine-to-inosine genetic recoding is required in the adult stage nervous system for coordinated behavior in Drosophila. The Journal of biological chemistry *284*, 31391-31400.

Jepson, J.E., Savva, Y.A., Yokose, C., Sugden, A.U., Sahin, A., and Reenan, R.A. (2010). Engineered alterations in RNA editing modulate complex behavior in Drosophila: regulatory diversity of adenosine deaminase acting on RNA (ADAR) targets. The Journal of biological chemistry. *In press*.

Keegan, L.P., Brindle, J., Gallo, A., Leroy, A., Reenan, R.A., and O'Connell, M.A. (2005). Tuning of RNA editing by ADAR is required in Drosophila. The EMBO journal *24*, 2183-2193.

Keegan, L.P., Gallo, A., and O'Connell, M.A. (2001). The many roles of an RNA editor. Nat Rev Genet *2*, 869-878.

Lee, T., Lee, A., and Luo, L. (1999). Development of the Drosophila mushroom bodies: sequential generation of three distinct types of neurons from a neuroblast. Development (Cambridge, England) *126*, 4065-4076.

Mombereau, C., Kawahara, Y., Gundersen, B.B., Nishikura, K., and Blendy, J.A. (2010). Functional relevance of serotonin 2C receptor mRNA editing in antidepressant- and anxiety-like behaviors. Neuropharmacology.

Murthy, M., Fiete, I., and Laurent, G. (2008). Testing odor response stereotypy in the Drosophila mushroom body. Neuron *59*, 1009-1023.

Nishikura, K (2010). Functions and regulation of RNA editing by ADAR deaminases. Annual review of biochemistry *79*, 321-349.

Palladino, M.J., Keegan, L.P., O'Connell, M.A., and Reenan, R.A. (2000a). A-to-I pre-mRNA editing in Drosophila is primarily involved in adult nervous system function and integrity. Cell *102*, 437-449.

Palladino, M.J., Keegan, L.P., O'Connell, M.A., and Reenan, R.A. (2000b). dADAR, a Drosophila double-stranded RNA-specific adenosine deaminase is highly developmentally regulated and is itself a target for RNA editing. RNA (New York, NY *6*, 1004-1018.

Pokharel, S., and Beal, P.A. (2006). High-throughput screening for functional adenosine to inosine RNA editing systems. ACS chemical biology *1*, 761-765.

Reenan, R.A. (2005). Molecular determinants and guided evolution of species-specific RNA editing. Nature *434*, 409-413.

Seeburg, P.H., and Hartner, J. (2003). Regulation of ion channel/neurotransmitter receptor function by RNA editing. Current opinion in neurobiology *13*, 279-283.

Singh, M., Zimmerman, M.B., Beltz, T.G., and Johnson, A.K. (2009). Affect-related behaviors in mice misexpressing the RNA editing enzyme ADAR2. Physiology & behavior *97*, 446-454.

Tonkin, L.A., Saccomanno, L., Morse, D.P., Brodigan, T., Krause, M., and Bass, B.L. (2002). RNA editing by ADARs is important for normal behavior in Caenorhabditis elegans. The EMBO journal *21*, 6025-6035.

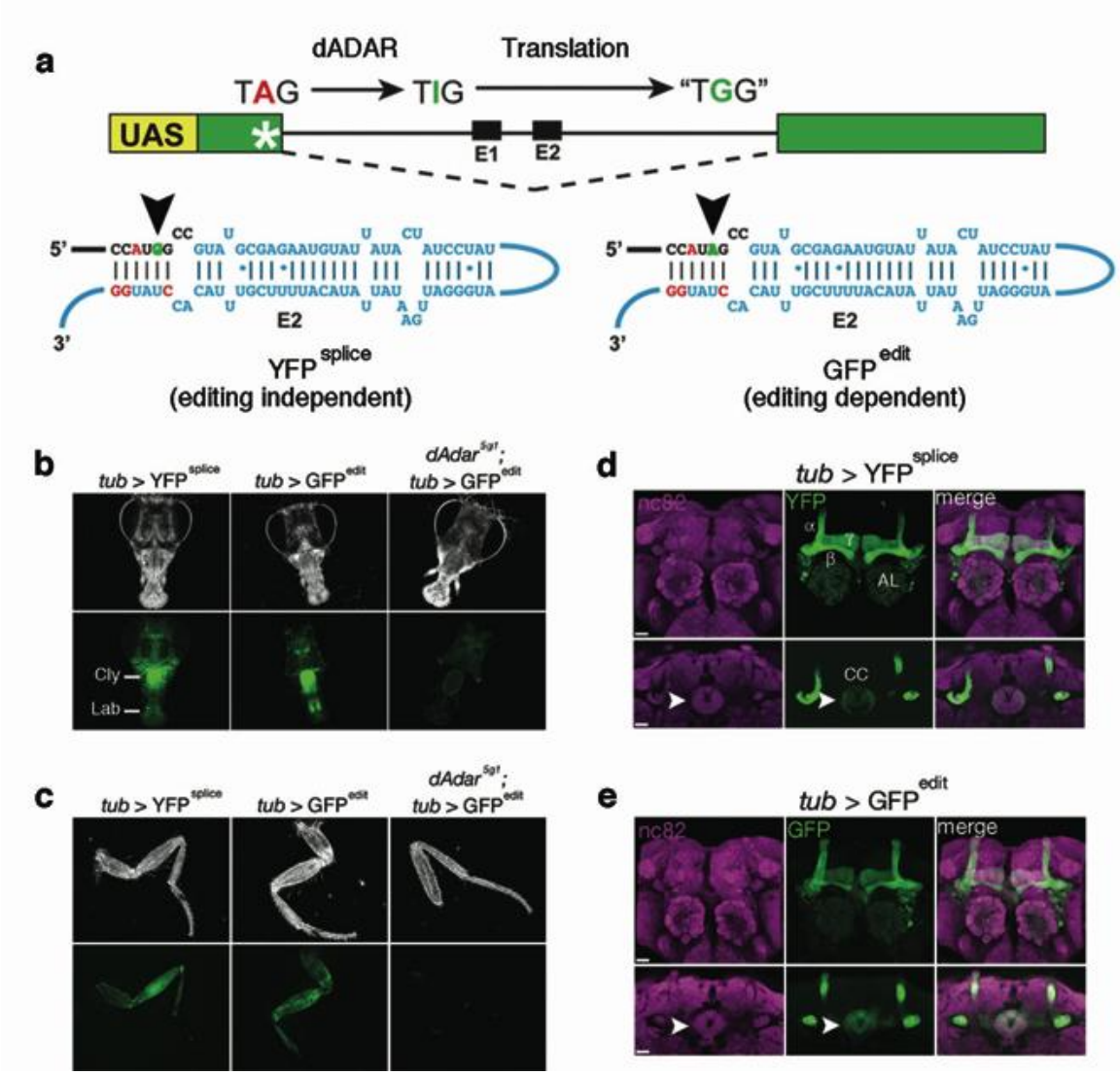

FIGURE 4.1. Design and validation of a fluorescent reporter of A-to-I editing**.** (a) Schematic illustration strategy used to generate full length GFP only in the presence of active dADAR, and the dsRNA structure directing editing of the GFP^{edit} construct. (b-c) Epi-fluorescent whole-mount images of 1-2 day old male heads (b) and forelegs (c) expressing the YFP^{splice} control (left panel), or GFP^{edit} in a wild-type (middle) or *dAdar* null (*dAdar*^{5g1}; right) background, driven by *tubulin*-Gal4 (*tub*). Top panel – bright-field image (La – labellum; Cly – clypeus). Lower panel - excitation at 488nm. Middle and right panels were exposed to the same fluorescent intensity. In the adult nervous system, both the YFP^{splice} (d) and GFP^{edit} (e) constructs exhibit a similar expression pattern when driven by *tub*-Gal4. YFP and GFP were visualized using an anti-GFP antibody and a fluorescent cy5-conjugated secondary antibody (see methods). Top panel: z-stacks showing expression in the mushroom body lobes (α/β, γ) and antennal lobes (ALs). Bottom panel: confocal slices detailing expression in the central complex (CC). Scale bar, 20 μm.

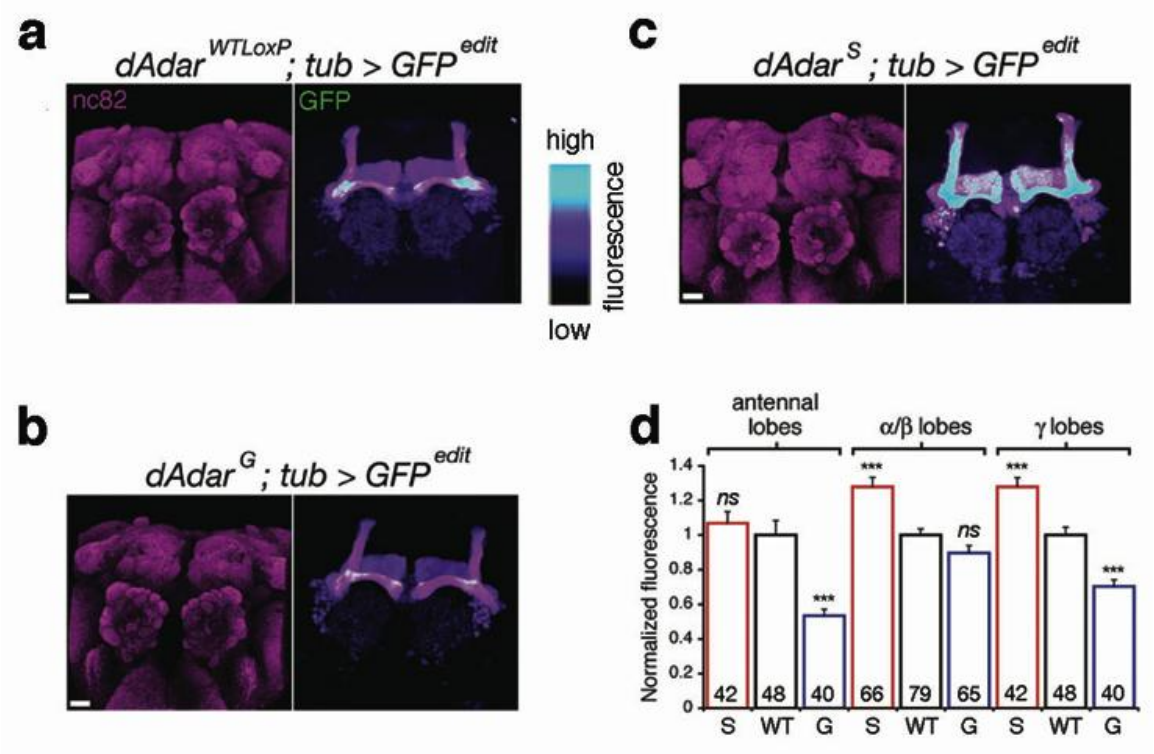

FIGURE 4.2. Neuron-specific modulation of GFP^{edit} fluorescence by alterations in dADAR auto-editing. (a-c) Representative confocal z-stacks of GFP^{edit} expression in the mushroom bodies and antennal lobes of *dAdar*^{WTLoxP} (WT) control males (a) and experimental males generated through homologous recombination in which auto-editing of the *dAdar* transcript is either abolished (*dAdar*^{S}; S) (b) or constitutively hard-wired (*dAdar*^{G}; G) (c). (d) Quantification of GFP^{edit} fluorescence in α/β- and γ-lobes of the mushroom bodies, and the antennal lobes in *dAdar*^{S} and *dAdar*^{G} males, normalized to *dAdar*^{WTLoxP} controls. *n*-values for each neuronal sub-population are indicated. ***: $p < 0.0001$; ns: $p > 0.05$, one-way ANOVA with Dunnett post-hoc test. Scale bars, 20 μm.

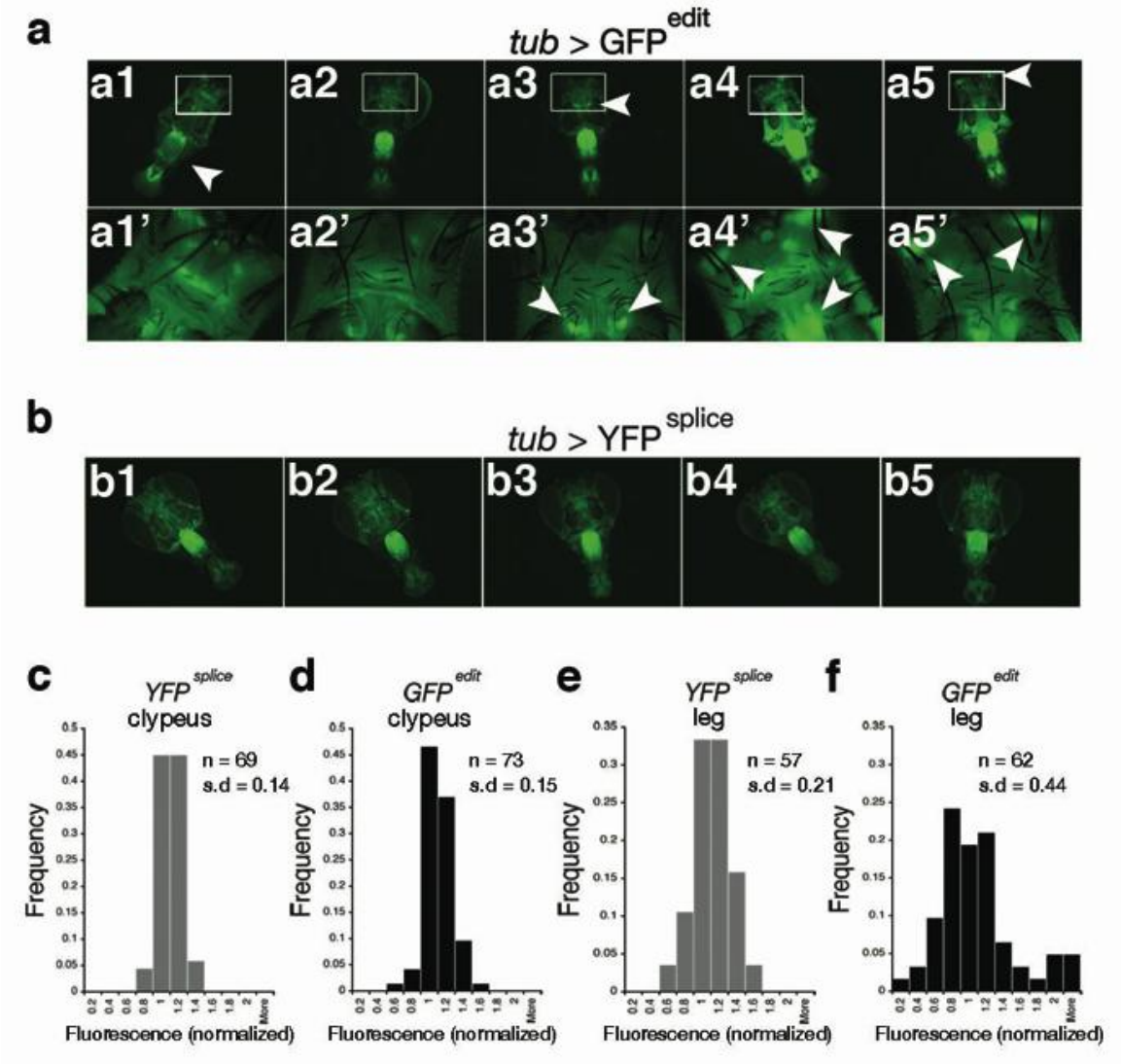

FIGURE 4.3. Variability in dADAR activity between individual male *Drosophila*. (a) Examples of GFP^{edit} fluorescence in individual adult male heads. Upper panel: whole head fluorescence, illustrating differential GFP^{edit} expression within the head capsule (magnified in lower panels). Note the differential fluorescence in regions corresponding to the antennal lobes and the Kenyon cells (for example, compare a2' and a4'). (b) Examples of GFP^{edit} fluorescence in adult male forelegs. (c-d), Histograms illustrating variation in YFP^{splice} (c) or GFP^{edit} (d) fluorescence in the clypeus. Values for the population studied are normalized such that the average fluorescence = 1. *n*-values and standard deviation of the mean (s.d) are shown. (e-f) Variability in YFP^{splice} or GFP^{edit} fluorescence in the large segment of adult forelegs.

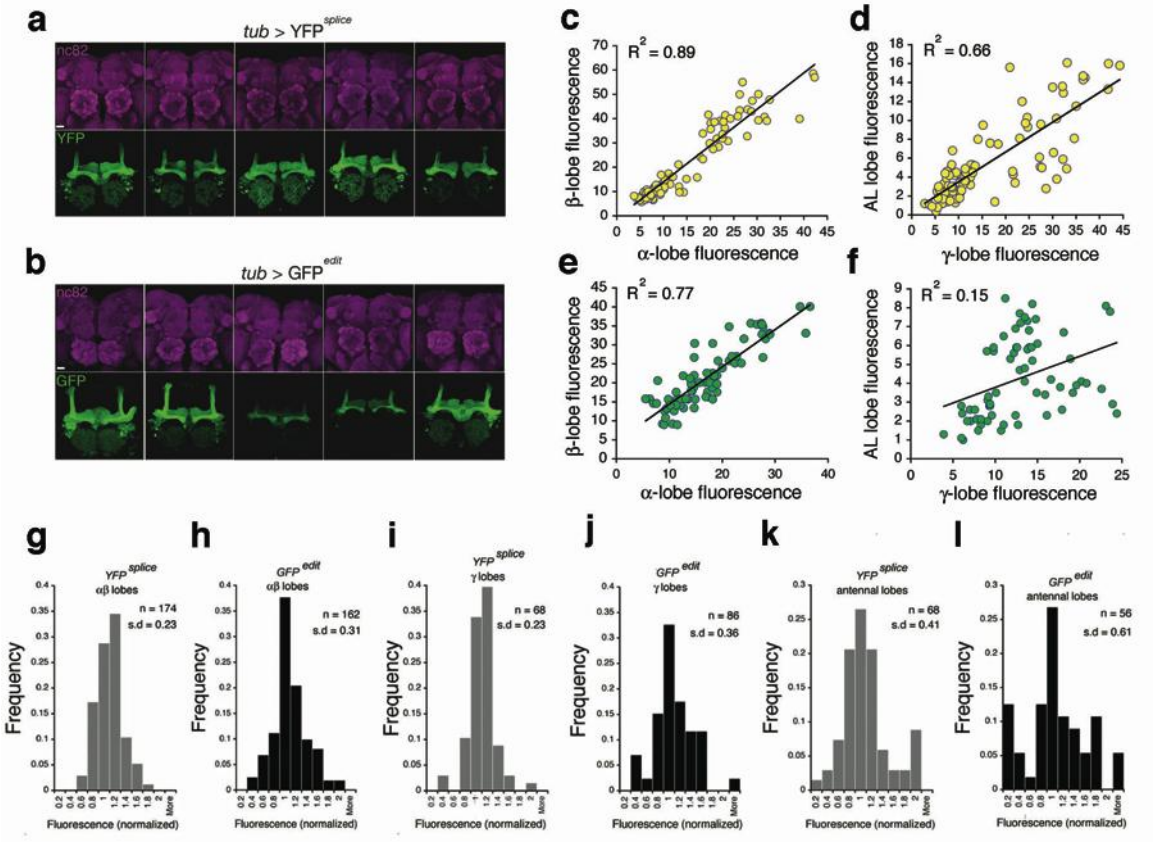

FIGURE 4.4 Non-stereotypical patterns of RNA editing in *Drosophila* neurons. (a-b) Example images of variation in YFP^{splice} and GFP^{edit} fluorescence in the MBs and ALs. Scale bars, 20 μm. (c-d) Variation in YFP^{splice} fluorescence between ipsi-lateral MB α- and β-lobes (c) and γ-lobes and ALs (d) is highly correlated. In contrast, while GFP^{edit} fluorescence in the MB α- and β-lobes strongly co-varies (as would be expected, given their shared cell bodies) (e) only a weak relationship between γ-lobes and AL fluorescence was observed (f). (g-i) Histograms detailing variation in YFP^{splice} expression within the α/β- and γ-lobes of the mushroom bodies, and the antennal lobes. (j-l) Corresponding histograms detailing variation in GFP^{edit} expression in the same tissues. *n*-values and s.d are shown.

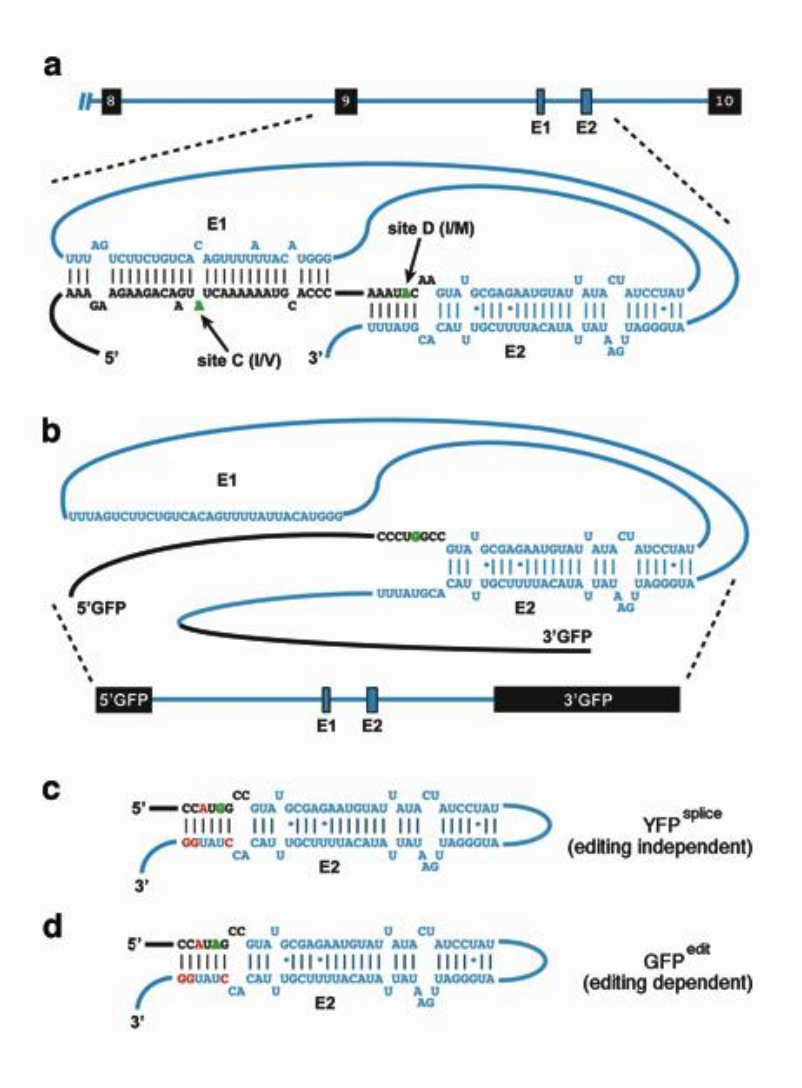

FIGURE S4.1. Molecular design of the GFP^{edit} reporter. (a) The organization of the endogenous *dsyt-1* is shown (above) with the experimentally verified dsRNA secondary structures in the pre-mRNA (below). Exonic sequences (black) base pair with intronic sequences (blue) to generate this structure. Editing site D is shown in green. E1 and E2 represent the highly conserved intronic elements that direct dADAR-mediated modification. (b) The structure depicted here represents the insertion of *dsyt-1* intron-9 into the open reading frame of GFP in such a way that the second-position guanosine (G, in green) of a tryptophan codon (T**G**G) is positioned at precisely the same position as the edited adenosine of site D. However, the natural dsRNA structure is obviously disrupted. (c) Mutations were introduced into the construct in part (b) shown in red, that restore the secondary structure (but not primary sequence) of the endogenous *dsyt-1* dADAR substrate, while the tryptophan codon is wild-type (T**G**G). Thus, while this construct requires splicing to produce emGFP protein, it is editing independent. (d) The structure shown is the same as in part (c), except that the tryptophan codon has been converted to an amber (T**A**G) nonsense codon. Correct production of emGFP protein requires both ADAR modification of the adenosine of the amber codon, and correct splicing.

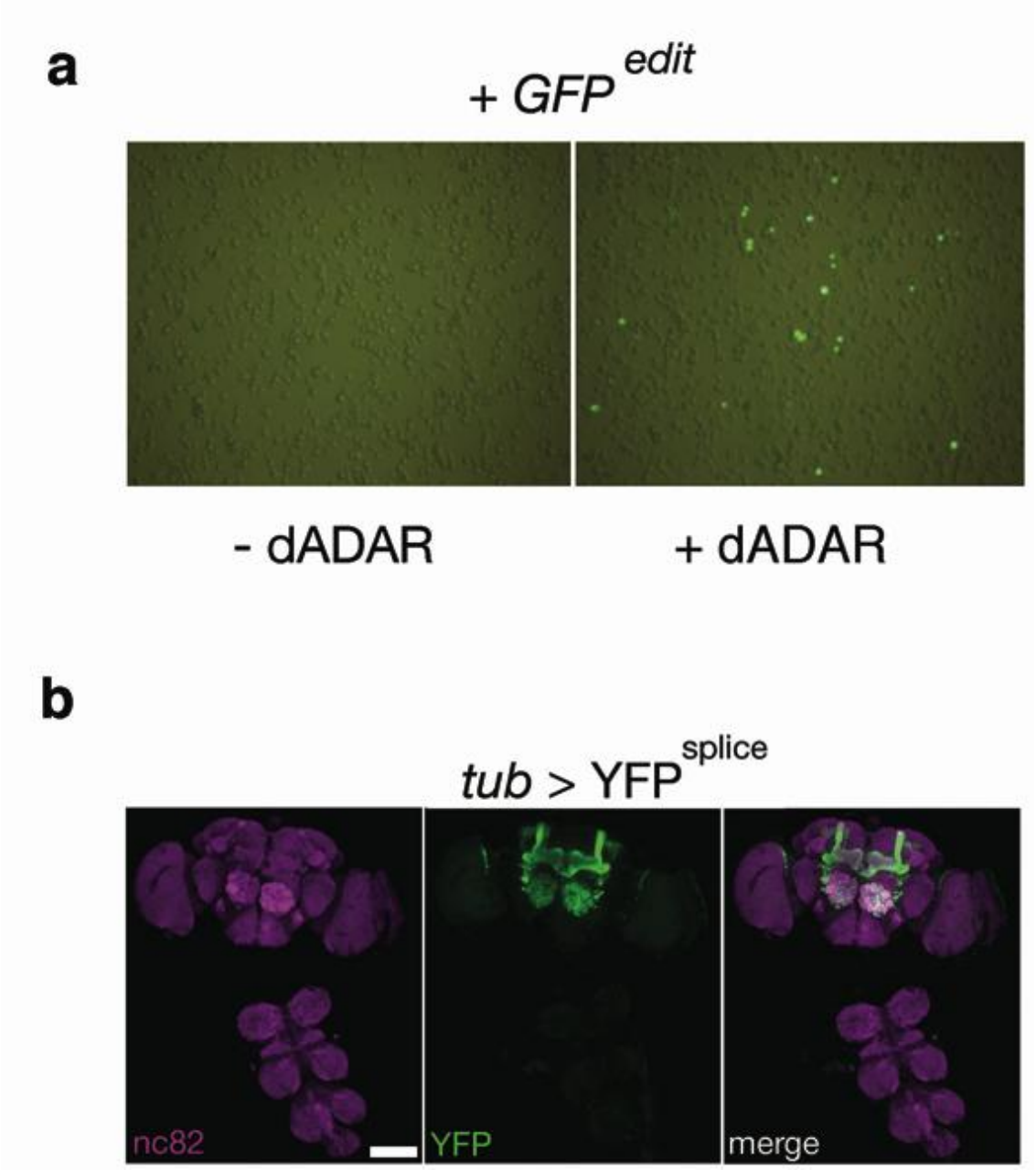

FIGURE S4.2. GFP^{edit} fluorescence in S2 cells is dependent on dADAR expression. (a) The pCoBLAST::GFP^{edit} construct was transfected into *Drosophila* S2 cells and induced with copper in the absence (left) or presence (right) of pCoBLAST::dADAR. Shown are representative cell fields 24 h after induction demonstrating robust emGFP protein production only when exogenous dADAR is supplied. (b) Expression of YFP^{splice} under the control of *tubulin*-Gal4 in the male brain and thoracic ganglion. Although *tubulin*-Gal4 is a ubiquitous driver, we only observed YFP fluorescence in the central brain. No fluorescence was observed either in the optic lobes, the medulla, or the thoracic ganglion. A cluster of YFP-positive cell bodies can also be observed in the dorsal portion of the lobula. Scale bar, 100 μm.

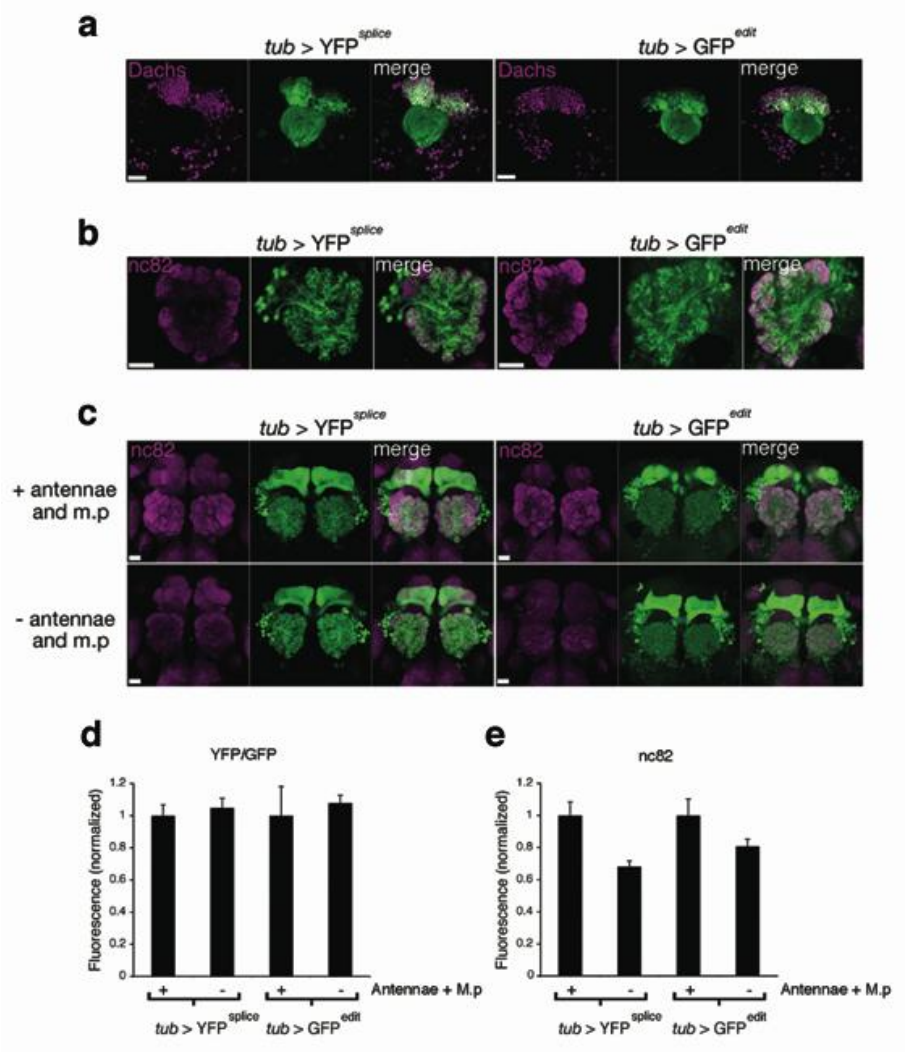

FIGURE S4.3. Elucidating the cell-types responsible for GFP^{edit} expression in the AL and MB. (a) YFP^{splice} and GFP^{edit} expression in the mushroom bodies is localized to dachshund-expressing Kenyon cells (representative images of $n > 6$). We did not observe any YFP^{splice} and GFP^{edit} positive innervations of the MBs from non-Kenyon cell bodies. AL fluorescence could arise from either pre-synaptic sensory neurons innervating the AL from the antennae and maxillary palps, local interneurons, or post-synaptic projection neurons (PNs). Since we did not observe any GFP-positive projections to the lateral horn, we ruled out PNs as a likely source of GFP^{edit} (Fig. 4.1). In contrast, two lines of evidence point to local interneurons as the source of GFP^{edit}. Firstly, GFP-positive cell bodies surround the AL, and axons from these cell-bodies clearly innervate the AL (b), consistent with previously described morphological and arborization characteristics of pan-glomerular interneurons. Secondly, removing the antennae and maxillary palps did not reduce AL expression of either YFP^{splice} ($p = 0.63$, Mann-Whitney U-test) or GFP^{edit} ($p = 0.31$) in age-matched controls, ruling out a contribution from sensory neurons (c, d). n = 8-14 per genotype. As expected following sensory synapse retraction, pre-synaptic bruchpilot (nc82) intensity in the antennal lobe is reduced in both experimental populations (YFP^{splice}: 31.8% reduction; GFP^{edit}: 20% reduction) (**e**). Scale bars, 20 μm.

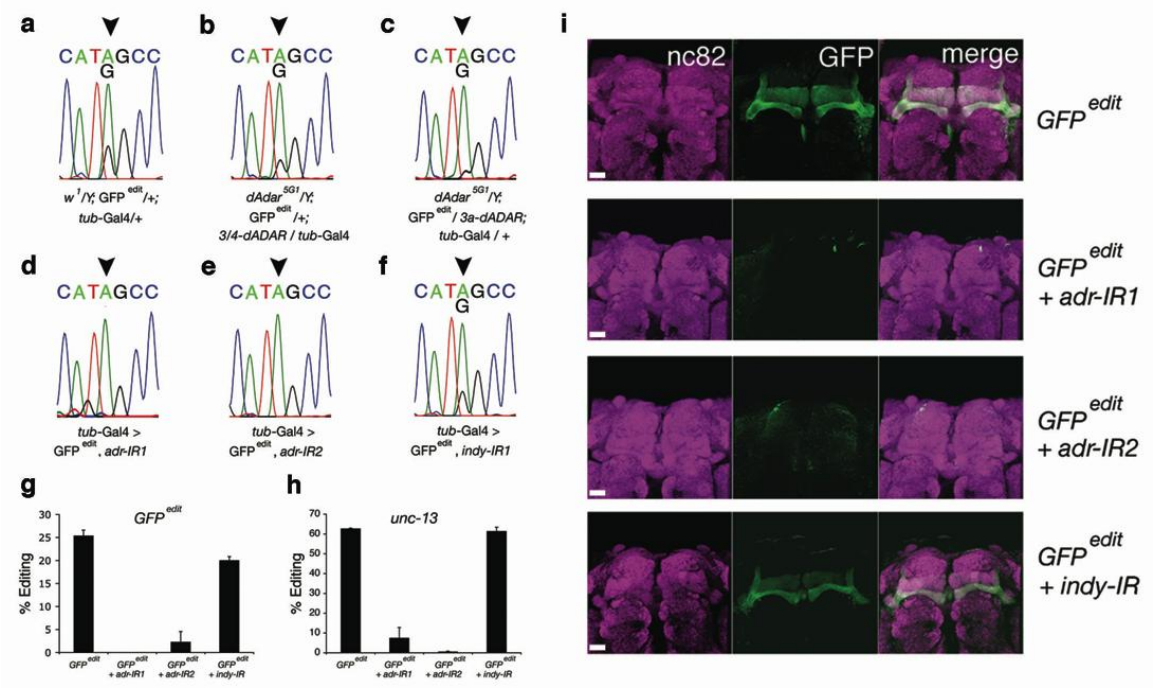

FIGURE S4.4. GFP^{edit} fluorescence *in vivo* requires dADAR expression**. (**a-c) Expression of one copy of GFP^{edit} (driven by *tubulin*-Gal4) in a wild-type (w^{1118}) (a) or a *dAdar* null ($dAdar^{5g1}$) background co-expressing transgenes encoding two of the predominant dADAR isoforms lacking (3/4 – b) or containing (3a – c) the alternatively spliced 3a exon, results in detectable editing at the adenosine of the amber stop codon within the GFP^{edit} open reading frame. In w^{1118} male heads, editing levels at the GFP^{edit} stop codon were 25.4% ± 1.2 (n = 3 PCRs). (d-h) Co-expression of two separate RNAi transgenes directed against dADAR (adr-IR1 and adr-IR2) abolishes editing of the GFP^{edit} stop codon. In contrast, co-expression of a control RNAi construct targeting the *indy* transcript had no effect on editing of GFP^{edit}. Example electropherograms are shown in (d-f). (g-h) Quantification of editing in GFP^{edit} (g) and the endogenous *unc-13* transcript (h) following co-expression of GFP^{edit} with experimental or control RNAi transgenes (n = 3 PCRs for all genotypes). (i) Knockdown of dADAR using transgenic RNAi abolishes fluorescence of GFP^{edit} in the adult mushroom bodies. When dADAR activity is reduced using transgenic RNAi, fluorescence of a single copy of GFP^{edit} is inhibited in the mushroom bodies (expressing a single autosomal copy of GFP^{edit} does not result in robust fluorescence in the antennal lobes or central complex, which requires expression of two copies of the GFP^{edit} construct – see methods). Expression of an *indy* RNAi transgene had no effect on GFP^{edit} fluorescence. Thus, fluorescence of GFP^{edit} in the adult brain correlates with the degree of editing at the amber stop codon. Figure shows a representative image of $n \geq 5$ male brains. Scale bar, 20 μm.

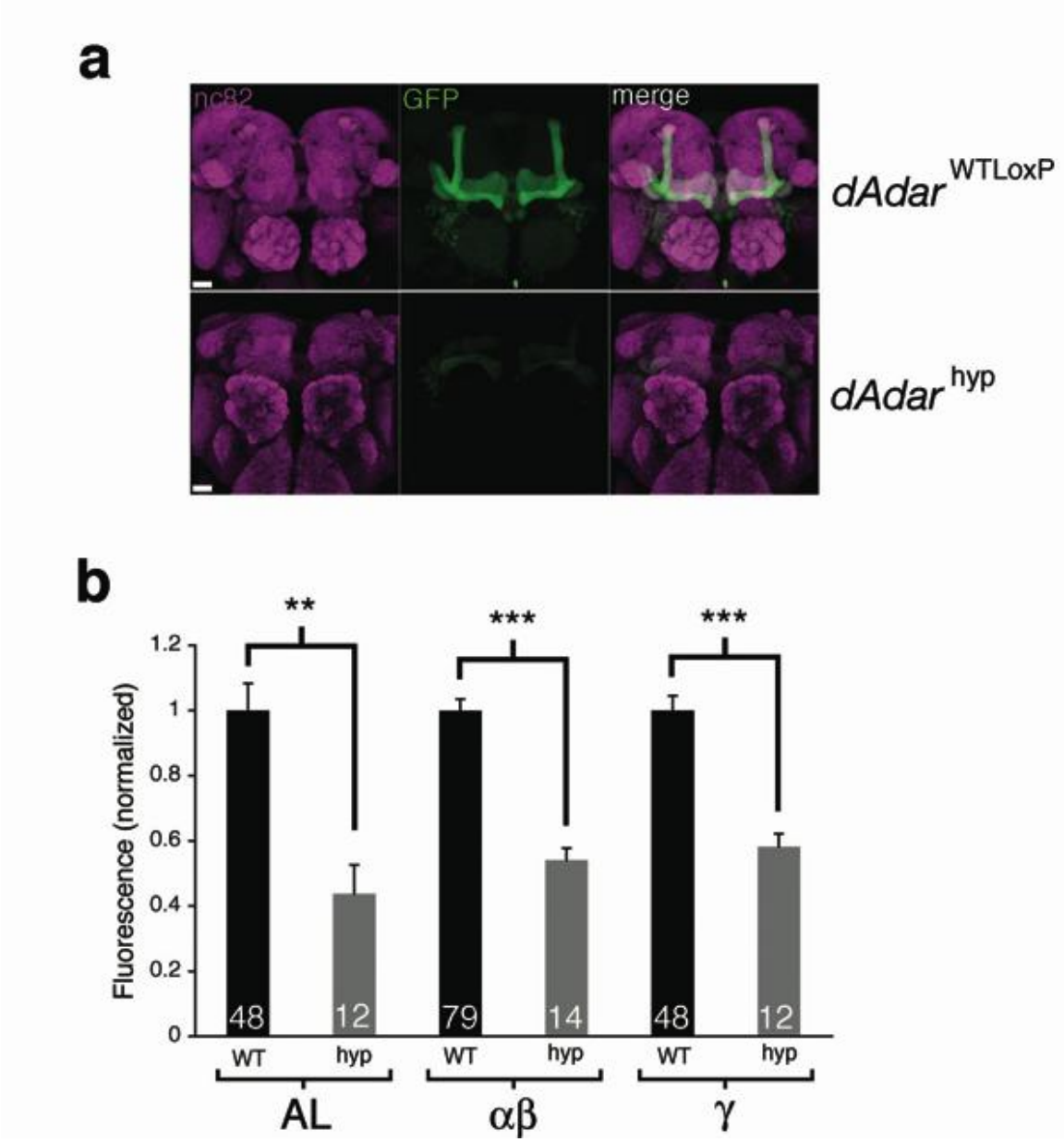

FIGURE S4.5. Expression of GFP^{edit} in a genetic background carrying a hypomorphic *dAdar* allele leads to decreased reporter fluorescence. (a) Example confocal images of GFP^{edit} expressed in either *dAdar*^{WTLoxP} controls of *dAdar*^{hyp} males. (b) Quantification of GFP^{edit} fluorescence, normalized to bruchpilot (nc82), in the antennal lobes (AL), MB α/β-lobes, and MB γ-lobes. Stringent loss of dADAR expression leads to significant reductions in GFP^{edit} fluorescence in all neuronal subtypes examined (AL: 56% reduction; α/β-lobes: 46%; γ-lobes: 42%). *n*-values are indicated in white. **: $p < 0.005$; ***: $p < 0.0005$, Mann-Whitney U-test. Scale bar, 20 μm.

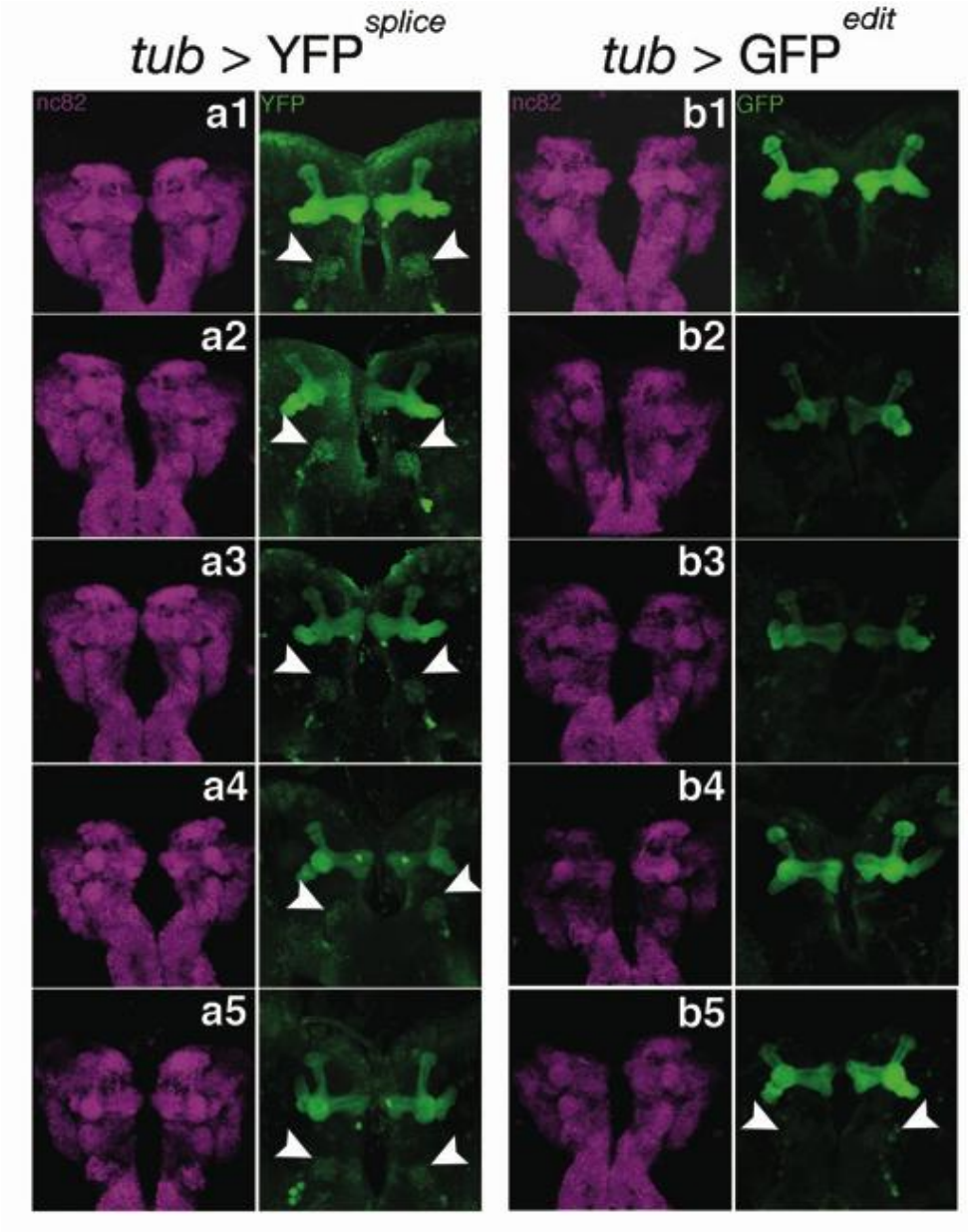

FIGURE S4.6. YFP^{splice} and GFP^{edit} fluorescence in the 3rd instar larval nervous system reveals developmentally regulated spatial control of dADAR activity. In 36/36 wandering 3rd instar larval brains expressing YFP^{splice} using *tubulin*-Gal4, we observed YFP staining in the larval mushroom body γ-lobes and the larval antennal lobe (LAL). In contrast, 25/26 larval brains expressing GFP^{edit} only exhibited fluorescence in the γ-lobes, with no GFP staining observable in the LAL. Five representative examples of YFP^{splice} and four of GFP^{edit} are shown (a1-5 and b1-4). Only 1/26 larval brains expressing GFP^{edit} exhibited weak GFP expression in the LALs (b5). This suggests that, while previous studies testing for developmental regulation of dADAR transcript and protein levels have indicated that dADAR expression is significantly lower at the 3rd instar larval, subsets of neurons may still exhibit robust dADAR activity at the larval stages of development. Scale bar, 20 μm.

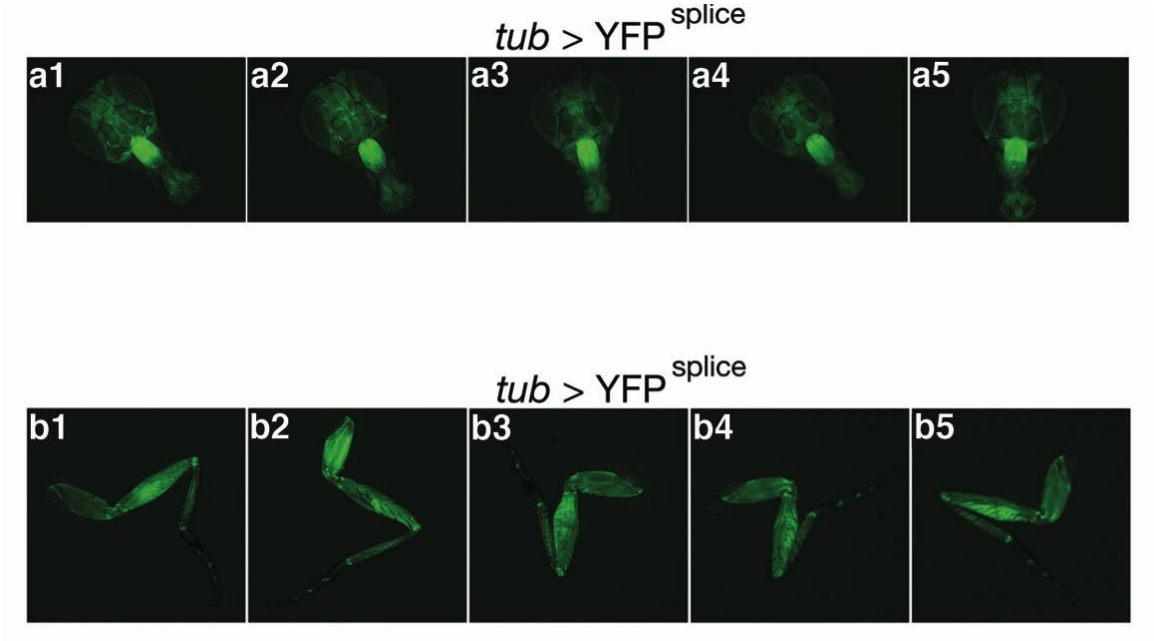

FIGURE S4.7. Representative examples of YFP^{splice} driven by *tubulin*-Gal4 in 1-2 day old adult male heads (a) and forelegs (b).

CHAPTER 5:

RNA Editing Generates a Natural Regulator of Heterochromatic Gene Silencing

ABSTRACT

Heterochromatic gene silencing and RNA interference (RNAi) are widely proposed to functionally converge in defending against nucleic acid parasites. Here, we utilize the binding activity of adenosine deaminases acting on RNAs (ADARs) to visualize the *in vivo* production, by transposons, of long double-stranded RNA (dsRNA) at the *Hoppel killer* locus (*Hok*). Using homologous recombination to interfere with *d*ADAR binding, we show that *Hok* deletions dramatically alter the chromatin architecture of the fourth chromosome of *Drosophila melanogaster*. Furthermore, we demonstrate that *d*ADAR can act as an enhancer or suppressor of position effect variegation (PEV) and this action can be bi-directionally modulated by an auto-regulatory editing event that alters a single amino acid. Together, our findings indicate that the dosage of long dsRNA from *Hok*, as well as ADAR's role in determining long dsRNA fate, are key regulators of heterochromatin formation.

INTRODUCTION

In eukaryotic cells, informational recoding and RNA interference (RNAi) proceed through structurally diverse double-stranded (ds) RNA molecules (Bass, 2002). Highly conserved sequences within exclusive pre-mRNAs involved in neurotransmission, generate short (~20-50bp) imperfect dsRNAs that are modified selectively through the action of ADARs (Nishikura, 2010). In these dsRNA molecules, hydrolytic deamination of adenosine to inosine (A-to-I) usually results in amino acid substitutions because an inosine in mature mRNAs is interpreted as guanosine by the translation machinery, leading to novel protein coding potential (Basillo et al., 1962). However, perfectly paired long (~100-1000bp) dsRNAs that enter the RNAi pathway may also serve as ADAR substrates. In this scenario, ADAR activity is promiscuous resulting in the deamination of up to 50% of the adenosines within the dsRNA; a process that affects both small interfering RNA (siRNA) biogenesis and activity (Nishikura, 2006).

In somatic tissues, nuclear pools of siRNAs ranking from 18-22nt in length guide RNA induced silencing complexes (RISCs) to discrete regulatory targets for initiation of a sequence-specific silence mechanism known as RNAi (Chapman and Carrington, 2007; Peters and Meister, 2007). The biogenesis of siRNAs, including endogenous small interfering RNAs (esiRNAs), microRNAs (miRNAs), and repeat-associated small RNAs (rasi-RNAs), proceeds through the action of Dicer on dsRNAs transcribed from distinct genomic sources (Ghildiyal and Zamore, 2009). In *Drosophila*, the majority of esiRNAs derive from read-though transcription of transposable elements (TE) that are widely distributed throughout the fly genome (Kawamura et al., 2008). Mutations in Dicer-2, the

ribonuclease involved in the biogenesis of esiRNAs, result in elevated TE transcript levels, suggesting that this RNAi pathway operates to inhibit transposon activation in somatic cells (Chung et al., 2008; Czech et al., 2008; Ghildiyal et al., 2008; Kawamura et al., 2008).

In the *Drosophila* germ line a different class of small RNAs, piwi-interacting RNA (piRNAs), facilitate the silencing of transposons (Aravin et al., 2007a; Aravin et al., 2007b). piRNAs are thought to be generated from single-stranded (ss) RNA transcripts derived form transposon-rich loci through a Dicer-independent pathway (Brennecke et al., 2007). Given that TEs represent a threat to the genome in which they reside because of their mutagenic potential as mobile genetic elements, TEs sequences have been proposed to serve as targets for silencing through heterochromatin formation (Riddle et al., 2009).

Heterochromatin is considered to contain both high levels of TEs and low gene density, resulting in a compact DNA organization compared to euchromatin (Grewal and Elgin, 2007). Genes that are normally reside in euchromatin are silenced when juxtaposed nearby or into heterochromatin (Schulze and Wallrath, 2007). In *Drosophila*, these differences in chromatin organization are exemplified by position effect variegation (PEV) (Grewal and Elgin, 2007; Locke et al., 1988). Using PEV in various screens for suppressors of silencing, at a variegating reporter, resulted in the characterization of multiple loci that are involved in the initiation of heterochromatin formation. Interestingly, mutations in proteins that encode RNAi components result in a loss of silencing suggesting that heterochromatin formation is directed by siRNAs. In *Drosophila*, mutations in proteins that direct the piRNA pathway result in reduction of

H3 Lys^9 methylation, a heterochromatic modification marker, as well as aberrant localization of heterochromatin protein 1 (HP1). These molecular phenotypes correlate with loss of silencing at a variegating reporter (Pal-Bhadra et al., 2004). Mutations in components of the esiRNAi pathway lead to suppression of heterochromatic silencing in a similar fashion to piRNAi pathway (Fagegaltier et al., 2009). These results suggest that nuclear pools of esiRNAs initiate heterochromatin formation in somatic tissues in *Drosophila*.

Sequence analysis of esiRNAs from *Drosophila* S2 cultured cells revealed that a large number of these small RNAs contain adenosine to guanosine single mismatches relative to the genomic sequence, suggesting that dsRNA structures that enter this RNAi pathway serve as ADAR substrates (Kawamura et al., 2008). However, it is unknown whether dADAR regulates heterochromatin formation or whether A-to-I RNA editing is involved in the regulation of transposon transcripts in the nervous system of *Drosophila*.

MATERIALS AND METHODS

Drosophila Stocks and Ends-out Homologous Recombination of the *caps* Locus

Flies were raised at 25°C, on standard molasses food and under 12 h day/night cycles. We performed ends out homologous recombination using a similar methodology to that reported previously (Maggert et al., 2008). Briefly, we utilized the ends-out targeting vector p [w25.2] that contains the *white*$^{+}$ selectable eye color mini-gene flanked by LoxP sites for subsequent removal by Cre-recombinase. Homology arms were cloned and sequenced in pTOPO (Invitrogen) and then shuttled into the multiple cloning sites of the vector to generate p [w25-dADAR-HA], which was then introduced into the *Drosophila* genome by standard transgenic methods (Genetic Services Inc.).

Targeting was performed to generate multiple independent targeting events in which the HA tag was incorporated or excluded from the recombination events. Targeted alleles were validated by amplification using primers outside the region of targeting. All targeted alleles were PCR validated for the deletion of the *Hoppel* elements. Subsequent removal of the *white*$^{+}$ mini-gene selectable marker was achieved by performing crosses to animals expressing Cre-recombinase and re-isolation of targeted chromosomes containing a single LoxP site. The recombinant alleles were subsequently backcrossed to Canton-S for five generations.

RNA Editing Analysis

RNA extractions from 3rd instar salivary glands (20-30 per sample) were

performed using TRIzol reagent (Invitrogen). Edited cDNAs were amplified via RT-PCR using target-specific primers (Jepson and Reenan, 2009).

Imaging and Eye-pigmentation Measurements

A zeiss LSM 510 meta was used to obtain all confocal z-stacks and slices of salivary gland nuclei and adult brains. A Zeiss AX10 Imager.M1 was used for polytene chromosomes. For confocal immune-histochemistry, adult brains and salivary glands were prepared as described previously (Wu and Luo, 2006). To measure eye pigmentation, the heads of 20 male flies, 2-3 days old and raised at 25^{O}C, of each genotype were homogenized in methanol (1 ml, acidified with 0.1% HCL). Eye pigmentation was represented as the absorbance of the supernatant at 480 nm.

FISH of Polytene Chromosomes

Probes were generated form PCR products with Biotin-dUTP. Larvae were dissected in 45% acetic acid and transferred to a fixative solution for 5 min. Slides were frozen in liquid nitrogen and washed in ethanol and PBS for 10 min each. The chromosomes were placed at 70 ^{O}C in 2X SSC for 45 min. The chromosomal DNA was denatured in 0.14M NaOH/2XSSC for 3 min, and subsequently washed in 70% ethanol for 20 min and 95% ethanol for 10 min. The FISH probe was hybridized to the polytene chromosomes at 37 ^{O}C for 20 hours. An anti-biotin Texas Red secondary antibody was used to detect the FISH probe.

RNAase Treatment of Polytene Chromosomes

RNAase teatment of chromosomes was carried out in situ in the salivary glands. Glands were dissected are room temperature and incubated with RNAase A or RNAase H for 10 min. Glands were then transferred to formaldehyde for fixation.

RESULTS

dADAR auto-editing dramatically affects the level of A-to-I modification of short imperfect duplex double-stranded mRNA targets, dADAR subnuclear localization, and complex behavior (Savva et al., 2011). Our over-expression studies of tagged dADAR-HA in whole salivary glands revealed a surprise; a peculiarly intense site of localization in polytene nuclei, in addition to nucleolar staining (Fig. 5.1A). Chromosome squash preparations of these glands exhibited a concentrated, RNAase-sensitive band of dADAR-HA localization on the fourth chromosome, as well as numerous fainter bands throughout the genome (Fig. 5.1B-D). dADAR auto-editing results in a serine (S) to glycine (G) coding change in the C-terminal catalytic domain (Palladino et al., 2000). Localization of dADAR to the fourth chromosome was independent upon the auto-editing status (supplementary Fig. S5.1A-D), as well as irrespective of the alternative splice form of dADAR (supplementary Fig. S5.1E-F). ADAR(S) protein, produced via expression of auto-editing incompetent transgenes, localizes to the nucleolus and on the fourth chromosome (supplementary Fig. S5.1C-D). Similar localization was observed for auto-editing competent dADAR transgenes, which resulted in the production of ~50% dADAR(G) transcripts after expression in salivary glands (Fig. 5.1B, supplementary Fig. S5.1A-B, G). Furthermore, ectopic expression of an HA-tagged *Hydra magnipapillata* ADAR (hADAR) transgene in salivary gland nuclei, yielded a similar localization pattern as dADAR (Fig. 5.2A), but with additional strong bands throughout the genome (Fig. 5.2B-E). Flock house virus B2 (FHV-B2) protein binds both long and short dsRNA in its role as a natural inhibitor of dicer cleavage and RNAi (Chao et al., 2005; Lingel et al.,

2005; Sullivan and Ganem, 2005). In addition, expression of FHV-B2 has been shown to suppress heterochromatic gene silencing in *Drosophila* by antagonizing the endogenous small interfering RNAi (esiRNAi) pathway that is active in somatic tissues (Fagegaltier et al., 2009). Co-expression of FHV-B2 protein and dADAR resulted in completely overlapping localization patterns (Fig. 5.3). Thus, dADAR efficiently binds to long dsRNA *in vivo*, and could possibly interfere with dsRNA processing and gene silencing in a manner akin to FHV-B2.

In order to better understand the nature of the dADAR binding site on the fourth chromosome, we performed fluorescence in situ hybridization (FISH) for a number of genes on the fourth chromosome coupled with immuno-staining for HA-tagged dADAR. These data suggested that the band of dADAR localization is near the *caps* locus at the telomere of chromosome 4 (Fig. 5.4A-B). In fact, we discovered one undocumented site of dADAR modification in the *caps* mRNA in salivary glands over-expressing dADAR (supplementary Fig. S5.2A). However, we also showed comparably high levels of editing for a known fourth chromosome target of dADAR, *unc-13* (supplementary Fig. S5.2B), without observing a band of dADAR protein localization (data not shown). A careful examination of the genomic region of the *caps* locus revealed a unique sequence feature which could account for the abundant localization of dADAR and FHV-B2 proteins. Nested within the *caps* transcription unit, we observed numerous copies of the transposable element *Hoppel* (a.k.a. *1360*), three of which were tandemly repeated (supplementary Fig. S5.3A). Two copies are a direct inverted repeat capable of forming an extensive (>1kb) nearly perfect dsRNA foldback (supplementary Fig. S5.3B). We scanned the annotated *D.melanogaster* genome for other instances of tandem inverted

repeats of *Hoppel* and found none (data not shown). We then showed that dADAR localization also overlaps with FISH signal for *Hoppel* elements (Fig. 5.5A-B). As a direct test of the potential for *Hoppel* elements to generate a dsRNA capable of binding dADAR, we performed ends-out homologous recombination (HR) to create a deletion mutation of the three tandemly repeated *Hoppels* from the intron within the *caps* locus (supplementary Fig. S5.4, Methods). Indeed, removal of these three elements resulted in complete loss of dADAR binding to the telomeric region of chromosome 4 as demonstrated by FISH for the *white*$^{+}$ gene in the deleted allele and dADAR localization in a deletion heterozygote (Fig. 5.6A-E). We call this locus of dsRNA generation *Hoppel killer* (*Hok*), in keeping with the similarly arranged *Mu killer* (*Muk*) locus in plants (Slotkin et al., 2005).

We then tested the sufficiency of the *Hok* locus to generate an dADAR-binding dsRNA by engineering flies transgenically expressing a UAS-*Hok* mini-gene construct. Expression of this construct inserted at several locations using the Gal4-UAS binary expression system resulted in the generation of robust ectopic sites of dADAR binding (Fig. 5.7A). This expression was dependent upon induction by Gal4, as we did not observ dADAR localization in a promoter-less transgenic construct (Casper-*Hok*, Fig. 5.7B-C). Thus, we demonstrate that *Drosophila* possesses a site of dsRNA production coupled to *caps* expression to an endogenous transposable element and that dADAR is capable of binding to, and possibly regulating the processing of, the *Hok* duplex RNA.

Previous studies have shown that components of the RNAi pathway regulate nucleolar organization. Mutations in dicer-2 result in the formation of extra nucleoli compared to wild-type cells that contain single nucleoli (Peng and Karpen, 2007). When

overexpressing dADAR, hADAR, and FHV-B2 proteins in salivary gland nuclei, we observed a striking change in nucleolar organization accompanied with changes in silencing marks. Staining for fibrillarin, a component of rRNA machinery (Tollervey et al., 1993), revealed that salivary gland nuclei contained multiple nucleoli (supplementary fig. S5.5). In addition, HP1 localization was reduced in FHV-B2, dADAR, and hADAR overexpression (supplementary fig. S5.5). These results suggest that binding of RNAi substrates by FHV-B2 and ADAR proteins results in an inefficient RNAi response leading to disorganization of both nucleoli and chromatin states.

The fourth chromosome in *Drosophila* comprises about 80 genes nestled within ~1.2Mb highly enriched for transposable elements (TEs), including *Hoppel* (Riddle et al., 2009). Because of this genomic organization, chromosome four is considered to have features of both euchromatin and heterochromatin (Riddle et al., 2008). Importantly, *Hoppel* elements on chromosome 4 induce gene silencing (as evidenced by position effect variegation (PEV)) of mini-*white* gene (w^+) reporters in a proximity-dependent manner via a mechanism involving RNAi pathway components (Haynes et al., 2006; Sun et al., 2004). Moreover, siRNAs of a size consistent with dicer function and homologous to *Hoppel* were detected in these studies and mutations in dicer were shown to affect PEV (Haynes et al., 2006). An intermediate in targeting the *Hok* locus for deletion by HR is the insertion of a mini-gene copy of the $white^+$ gene flanked by loxP sites ($Hok^{del.w+}$) (supplementary fig. S5.4). Heterozygotes for this insertion ($Hok^{del.w+}/Hok^+$) displayed robust PEV (Fig 5.8), suggesting that the $white^+$ gene in the vacant *Hok* locus is subject to heterochromatic gene silencing. A similar reporter inserted into the *caps* intron containing Hok^+ was previously reported to show PEV. To our surprise, we observed

striking loss of PEV upon homozygosis of the *white*$^{+}$-containing *Hok* deletion allele (*Hok*$^{del.w+}$/*Hok*$^{del.w+}$) (Fig 5.8). We attribute this loss of silencing to complete absence of the *Hok*$^{+}$ dsRNA.

The organization of the *caps* locus suggests a mechanism for the PEV observed in *Hok*$^{del.w+}$/*Hok*$^{+}$ animals. Given the close proximity (~7kb) of a fourth *Hoppel* element within the *caps* locus, we suggest that dsRNA generated from *Hok*$^{+}$ homologue enters the RNAi pathway and initiates heterochromatization by targeting silencing machinery to the remaining proximate *Hoppel* element remaining on the *Hok*$^{del.w+}$ homologue (supplementary fig. S5.6). This is consistent with previous data that suggests that silencing marks spread effectively to induce PEV of reporters within <10kb of a *Hoppel* element (Sun et al., 2004). Thus, genetic deletion of the *Hok* locus appears to reduce or eliminate the triggering action of *Hok* in establishing the silenced state in the vicinity of a target *Hoppel* element within the *caps* locus.

Numerous P-element reporters for PEV have been generated and characterized with respect to PEV and proximity to *Hoppel* elements on the fourth chromosome (Riddle et al., 2008). We utilized a number of these reporters to characterize the ability of *Hok* dosage to affect PEV at sites distal to the *caps* locus. We found that decreasing the dosage of *Hok* in animals containing a PEV reporter suppressed variegation in two out of three reporters tested. Importantly, the *Hok*$^{del.loxP}$ allele had the largest effect on reporters near a *Hoppel* element as well as on a variegating reporter not under the influence of *Hoppel* (Fig. 5.9). These confirms previous data that suggest the involvement of additional *cis*-acting elements in the formation of heterochromatin (Riddle et al., 2008). Given the increased density and distribution of *Hoppel* elements on the fourth

chromosome, we looked at the effect of *Hok* deletion on chromatin state. In homozygotes for *Hok* deletions, we noticed a change in chromatin architecture by DAPI staining alone. In addition, positioning with respect to the chromocenter was altered homozygotes deleted for *Hok* (Fig 5.10A-C). Furthermore, HP1 localization on the fourth chromosome is severely reduced in both heterozygotes and homozygotes *Hok* deletions (Fig 5.11). These results suggest that in *Hok* deletions the chromatin architecture of the chromosome 4 is altered resulting in loss of silencing at specific domains along the chromosome.

Since the *Hok* locus attracts dADAR, suggesting a functional interaction, we assessed the effect of genetic alterations in dADAR activity on heterochromatic gene silencing. Using HR, we generated endogenous *dAdar* loci hardwired for the production of dADAR(S) or dADAR(G) proteins (Savva et al., 2011). In addition, we generated the wild-type control ($dAdar^{loxP}$) and a *dAdar* null allele ($dAdar^{null}$). In males heterozygous for three independent variegating $white^{+}$ alleles at the *Hok* locus ($Hok^{del.w+}/Hok^{+}$), hemizygosity for the $dAdar^{G}$ allele acted as a complete suppressor of PEV (Su(var)), comparable to complete deletion of the Hok locus (Fig 5.12). In contrast, hemizygosity for either $dAdar^{null}$ or $dAdar^{S}$ alleles (genotypes incapable of producing dADAR(G) protein) in the same three variegating genetic backgrounds resulted in enhancement of PEV (E(var)). The wild type, auto-editing competent control ($dAdar^{loxP}$) displayed robust variegation as expected (Fig 5.12). These results suggest that heterochromatic gene silencing at this variegating reporter is directed by dsRNA intermediates that are regulated in a dADAR dependent manner. More importantly, dADAR auto-editing generates a natural regulator of heterochromatin gene silencing.

Given the effects of dADAR on silencing, we decided to determine whether altering dADAR activity through auto-editing could result in changes of heterochromatic marks in neuronal nuclei. We observed decreased levels of HP1 in neuronal nuclei in the *dAdar*^{G} adult brains when compared to the *dAdar*^{loxP} allele supporting its role as a suppressor of variegation (Fig. 5.13). In complete agreement with previous PEV experiments, neuronal nuclei in the *dAdar*^{S} and *dAdar*^{null} alleles exhibit higher levels of HP1, suggesting that these alleles act as enhancers of variegation

DISCUSSION

Taken together, these data demonstrate that the status of dADAR auto-editing acts as a mechanistic basis for the generation of variegating gene expression (PEV), likely by affecting the rate of entry of dsRNA molecules into downstream processing pathways that lead to the establishment of heterochromatic states. Furthermore, our data support an intersection of dADAR activity with gene silencing pathways very early in the mechanism, at the site of generation of dsRNA molecules destined to enter the RNAi pathway. Interestingly, the $dAdar^{G}$ allele acts as a Su(var) while the $dAdar^{S}$ allele acts as an E(var). The precise mechanism for this bi-directional response of dADAR activity via auto-editing is unclear. However, intervention at this key point by the dADAR(G) protein, acting in a manner similar to viral proteins which mask dsRNA from dicer activity, potentially provides a versatile mechanism for bestowing cell-autonomous tuning of gene silencing (Fig. 5.14). Neuronal cells expressing dADAR at low levels, or only dADAR(S) would experience no diminution of the silencing effect of expressed long dsRNAs. Conversely, cells expressing varying amounts of dADAR(G) and dADAR(S), as in the case of $dADAR^{loxP}$ allele, would lead to moderate antagonistic effects on dsRNAs.

In rodents, recent studies have shown that neuronal genomes are not static because of active transposition that results in the generation of somatic mosaicism (Muotri et al., 2005). Given that ADAR anzymes are highly expressed in the nervous system of metazoans (Nishikura, 2010), RNA editing of dsRNA molecules that enter the RNAi pathway could affect the biogenesis and activity of siRNAs, resulting in the

derepression of TEs. Consequently, this could allow stochastic transposition that could generate novel genomic sequences and chromatin architectures in neuronal cells. Thus, RNA editing could represent a credible molecular mechanism for generating somatic variations in neuronal genomes, which could regulate plasticity and behavior. Hypothetically, such a mechanism could broaden the behavioral phenotypic repertoire that can originate from a single genome.

REFERENCES

Aravin, A.A., Hannon, G.J., and Brennecke, J. (2007a). The Piwi-piRNA pathway provides an adaptive defense in the transposon arms race. Science (New York, NY *318*, 761-764.

Aravin, A.A., Sachidanandam, R., Girard, A., Fejes-Toth, K., and Hannon, G.J. (2007b). Developmentally regulated piRNA clusters implicate MILI in transposon control. Science (New York, NY *316*, 744-747.

Basillo, C., Wahba, A., Lengyel, P., Speyer, J., and Ochoa, S. (1962). Synthetic polynucleotides and the amino acid code. V. Proceedings of the National Academy of Sciences of the United States of America *48*, 613-616.

Bass, B.L. (2002). RNA editing by adenosine deaminases that act on RNA. Annual review of biochemistry *71*, 817-846.

Brennecke, J., Aravin, A.A., Stark, A., Dus, M., Kellis, M., Sachidanandam, R., and Hannon, G.J. (2007). Discrete small RNA-generating loci as master regulators of transposon activity in Drosophila. Cell *128*, 1089-1103.

Chao, J.A., Lee, J.H., Chapados, B.R., Debler, E.W., Schneemann, A., and Williamson, J.R. (2005). Dual modes of RNA-silencing suppression by Flock House virus protein B2. Nature structural & molecular biology *12*, 952-957.

Chapman, E.J., and Carrington, J.C. (2007). Specialization and evolution of endogenous small RNA pathways. Nat Rev Genet *8*, 884-896.

Chung, W.J., Okamura, K., Martin, R., and Lai, E.C. (2008). Endogenous RNA interference provides a somatic defense against Drosophila transposons. Curr Biol *18*, 795-802.

Cordaux, R., and Batzer, M.A. (2009). The impact of retrotransposons on human genome evolution. Nat Rev Genet *10*, 691-703.

Czech, B., Malone, C.D., Zhou, R., Stark, A., Schlingeheyde, C., Dus, M., Perrimon, N., Kellis, M., Wohlschlegel, J.A., Sachidanandam, R.*, et al.* (2008). An endogenous small interfering RNA pathway in Drosophila. Nature *453*, 798-802.

Fagegaltier, D., Bouge, A.L., Berry, B., Poisot, E., Sismeiro, O., Coppee, J.Y., Theodore, L., Voinnet, O., and Antoniewski, C. (2009). The endogenous siRNA pathway is involved in heterochromatin formation in Drosophila. Proceedings of the National Academy of Sciences of the United States of America *106*, 21258-21263.

Ghildiyal, M., Seitz, H., Horwich, M.D., Li, C., Du, T., Lee, S., Xu, J., Kittler, E.L., Zapp, M.L., Weng, Z., *et al.* (2008). Endogenous siRNAs derived from transposons and mRNAs in Drosophila somatic cells. Science (New York, NY *320*, 1077-1081.

Ghildiyal, M., and Zamore, P.D. (2009). Small silencing RNAs: an expanding universe. Nat Rev Genet *10*, 94-108.

Grewal, S.I., and Elgin, S.C. (2007). Transcription and RNA interference in the formation of heterochromatin. Nature *447*, 399-406.

Haynes, K.A., Caudy, A.A., Collins, L., and Elgin, S.C. (2006). Element 1360 and RNAi components contribute to HP1-dependent silencing of a pericentric reporter. Curr Biol *16*, 2222-2227.

Kawamura, Y., Saito, K., Kin, T., Ono, Y., Asai, K., Sunohara, T., Okada, T.N., Siomi, M.C., and Siomi, H. (2008). Drosophila endogenous small RNAs bind to Argonaute 2 in somatic cells. Nature *453*, 793-797.

Lingel, A., Simon, B., Izaurralde, E., and Sattler, M. (2005). The structure of the flock house virus B2 protein, a viral suppressor of RNA interference, shows a novel mode of double-stranded RNA recognition. EMBO reports *6*, 1149-1155.

Locke, J., Kotarski, M.A., and Tartof, K.D. (1988). Dosage-dependent modifiers of position effect variegation in Drosophila and a mass action model that explains their effect. Genetics *120*, 181-198.

Muotri, A.R., Chu, V.T., Marchetto, M.C., Deng, W., Moran, J.V., and Gage, F.H. (2005). Somatic mosaicism in neuronal precursor cells mediated by L1 retrotransposition. Nature *435*, 903-910.

Nishikura, K. (2010) Functions and regulation of RNA editing by ADAR deaminases. Annual review of biochemistry *79*, 321-349.

Nishikura, K. (2006). Editor meets silencer: crosstalk between RNA editing and RNA interference. Nature reviews *7*, 919-931.

Pal-Bhadra, M., Leibovitch, B.A., Gandhi, S.G., Rao, M., Bhadra, U., Birchler, J.A., and Elgin, S.C. (2004). Heterochromatic silencing and HP1 localization in Drosophila are dependent on the RNAi machinery. Science (New York, NY *303*, 669-672.

Palladino, M.J., Keegan, L.P., O'Connell, M.A., and Reenan, R.A. (2000). dADAR, a Drosophila double-stranded RNA-specific adenosine deaminase is highly developmentally regulated and is itself a target for RNA editing. RNA (New York, NY *6*, 1004-1018.

Peng, J.C., and Karpen, G.H. (2007). H3K9 methylation and RNA interference regulate nucleolar organization and repeated DNA stability. Nature cell biology *9*, 25-35.

Peters, L., and Meister, G. (2007). Argonaute proteins: mediators of RNA silencing. Molecular cell *26*, 611-623.

Riddle, N.C., Leung, W., Haynes, K.A., Granok, H., Wuller, J., and Elgin, S.C. (2008). An investigation of heterochromatin domains on the fourth chromosome of Drosophila melanogaster. Genetics *178*, 1177-1191.

Riddle, N.C., Shaffer, C.D., and Elgin, S.C. (2009). A lot about a little dot - lessons learned from Drosophila melanogaster chromosome 4. Biochemistry and cell biology = Biochimie et biologie cellulaire *87*, 229-241.

Schulze, S.R., and Wallrath, L.L. (2007). Gene regulation by chromatin structure: paradigms established in Drosophila melanogaster. Annual review of entomology *52*, 171-192.

Slotkin, R.K., Freeling, M., and Lisch, D. (2005). Heritable transposon silencing initiated by a naturally occurring transposon inverted duplication. Nature genetics *37*, 641-644.

Savva, A.Y., Jepson E.C.J., Sahin, A., Sudgen, A., Bell, R., Alpert, L., Lawrence, C., and Reenan, A.R. (2011). Fine-tuning of mRNA recoding and complex behavior by auto-regulatory RNA editing in *Drosophila*. *Submitted*.

Sullivan, C.S., and Ganem, D. (2005). A virus-encoded inhibitor that blocks RNA interference in mammalian cells. Journal of virology *79*, 7371-7379.

Sun, F.L., Haynes, K., Simpson, C.L., Lee, S.D., Collins, L., Wuller, J., Eissenberg, J.C., and Elgin, S.C. (2004). cis-Acting determinants of heterochromatin formation on Drosophila melanogaster chromosome four. Molecular and cellular biology *24*, 8210-8220.

Tollervey, D., Lehtonen, H., Jansen, R., Kern, H., and Hurt, E.C. (1993). Temperature-sensitive mutations demonstrate roles for yeast fibrillarin in pre-rRNA processing, pre-rRNA methylation, and ribosome assembly. Cell *72*, 443-457.

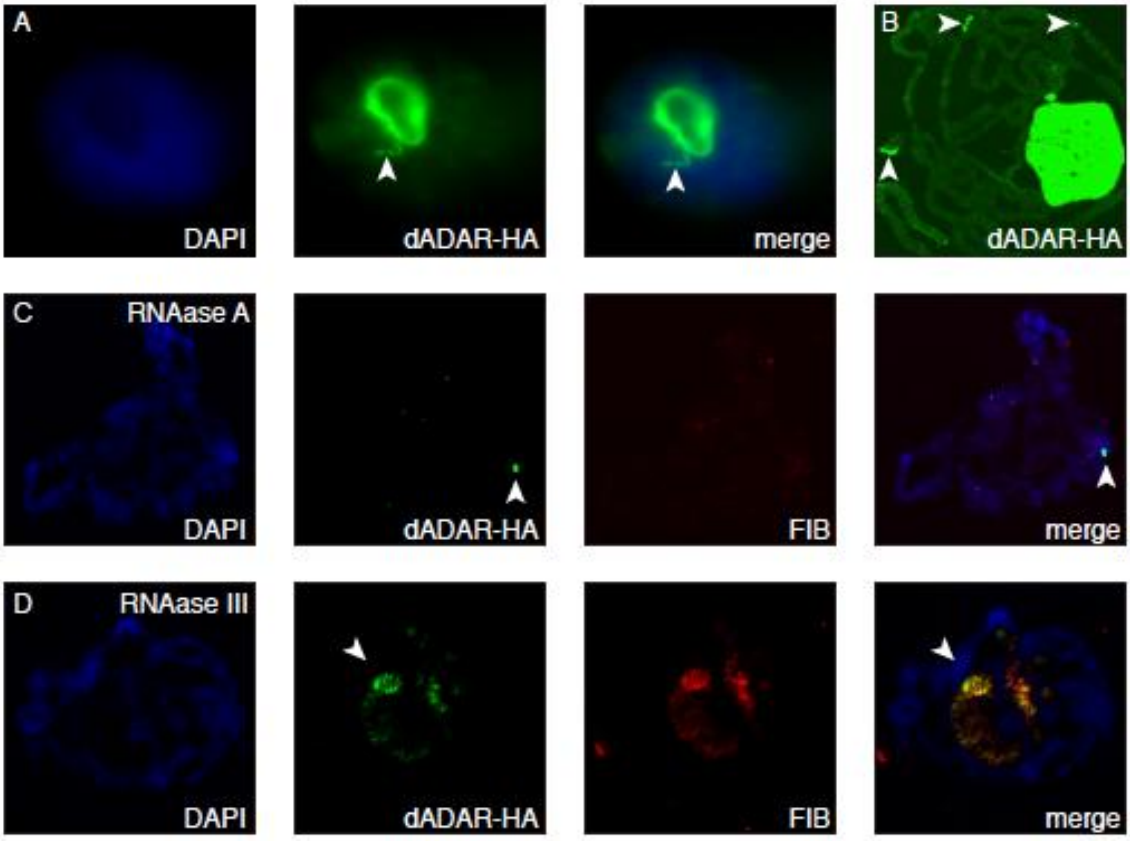

FIGURE 5.1. dADAR-HA transgene expressed in 3rd instar larval salivary gland nuclei and polytene chromosomes. (A) dADAR transgene driven by the *c155*-Gal4 driver revealed an intense site of localization (arrow) in salivary gland nuclei. (B) Chromosome squash preparation of salivary gland nuclei showed dADAR localizes on the fourth chromosome as well as numerous bands throughout the genome (arrows). In addition, dADAR localizes within the nucleolus. (C) dADAR binding on the fourth chromosome is not abolished by RNAase A digestion (arrow). In contrast, dADAR binding in the nucleolus is abolished by RNAase A treatment. (D) RNAase H digestion results in loss of dADAR binding on chromosome 4 (arrow) without abolishing dADAR bound within the nucleolus.

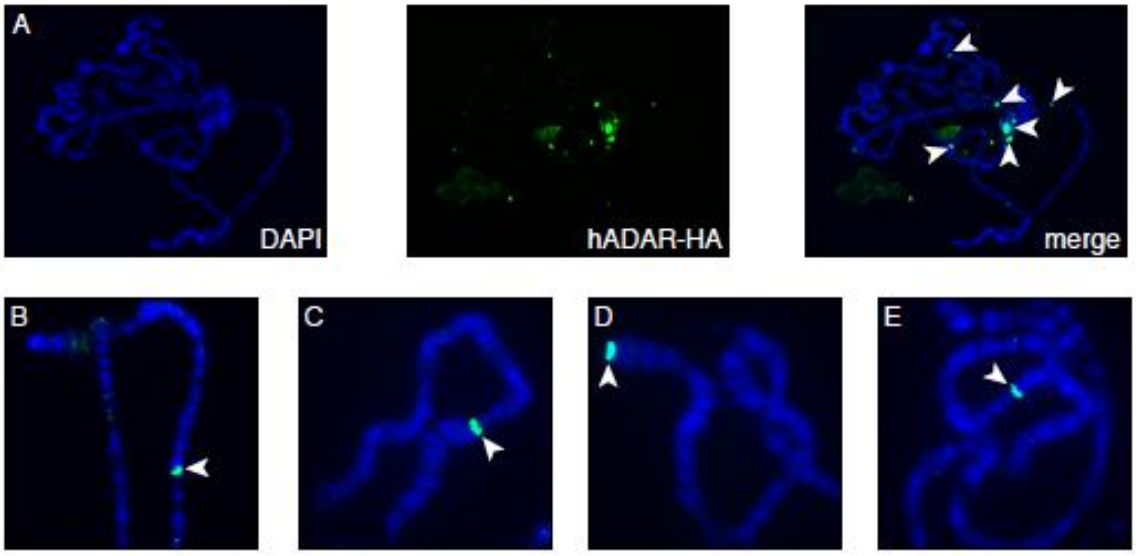

FIGURE 5.2. hADAR transgene localization on polytene chromosomes. (A) Expression of *Hydra magnipapillata* ADAR transgene using the *c155*-Gal4 driver yielded a similar localization pattern as dADAR (arrows). hADAR binds on chromosome 4 as well as on numerous other locations throughout the genome (B-E).

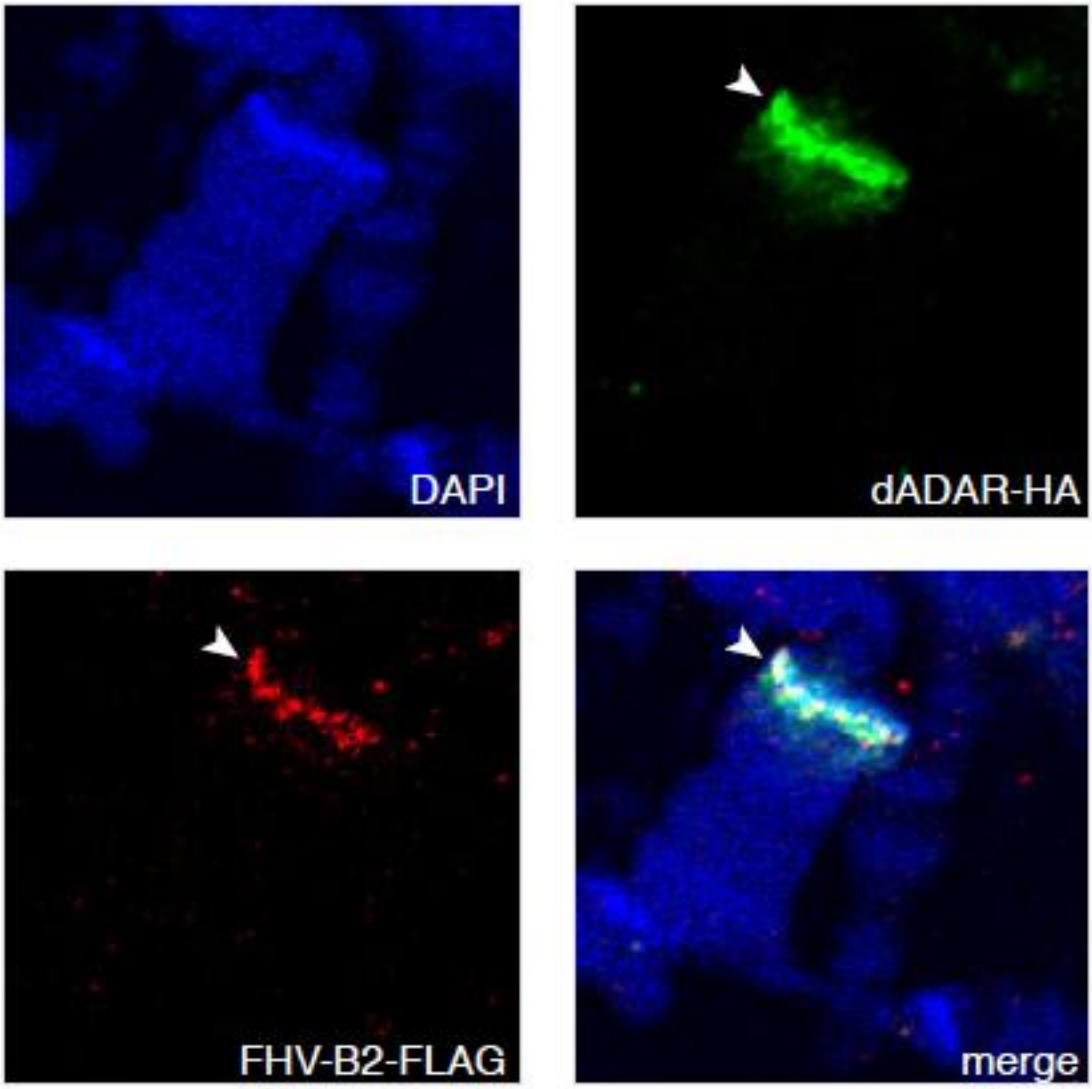

FIGURE 5.3. Flock house virus B2 protein co-localizes with dADAR on chromosome 4. Simultaneous expression of dADAR-HA and FHV-B2-FLAG transgenes using the *c155*-Gal4 driver results in completely overlapping localization pattern.

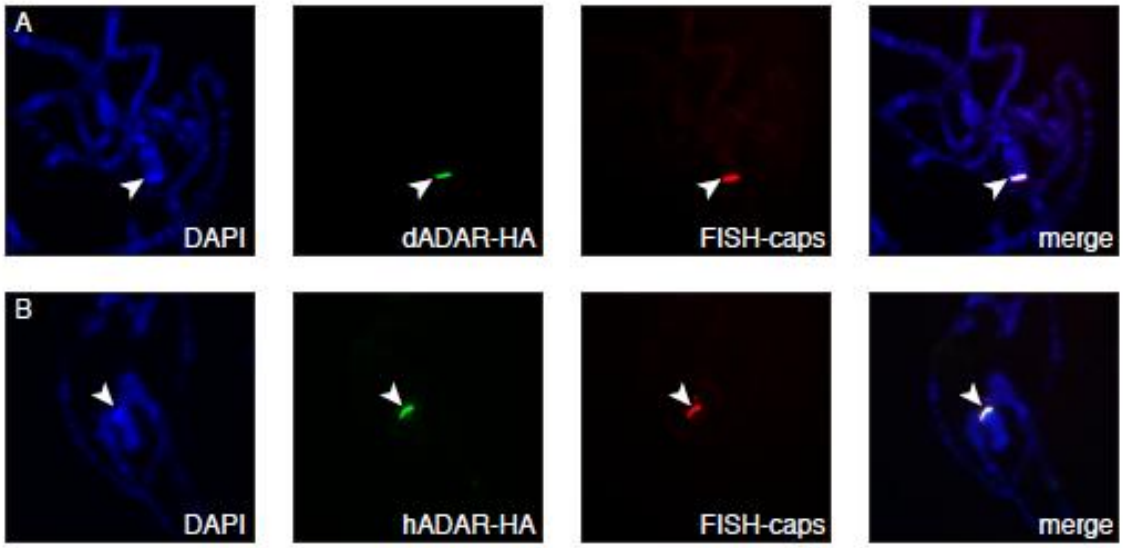

FIGURE 5.4. dADAR and hADAR localize near the *caps* locus on the fourth chromosome. FISH probes generated from PCR products spanning the *caps* locus were hybridized to fixed polytene chromosomes. FISH coupled with immuno-staining for HA-tagged dADAR (A) and hADAR (B) transgenes, showed co-localization of ADAR with the *caps* FISH probe.

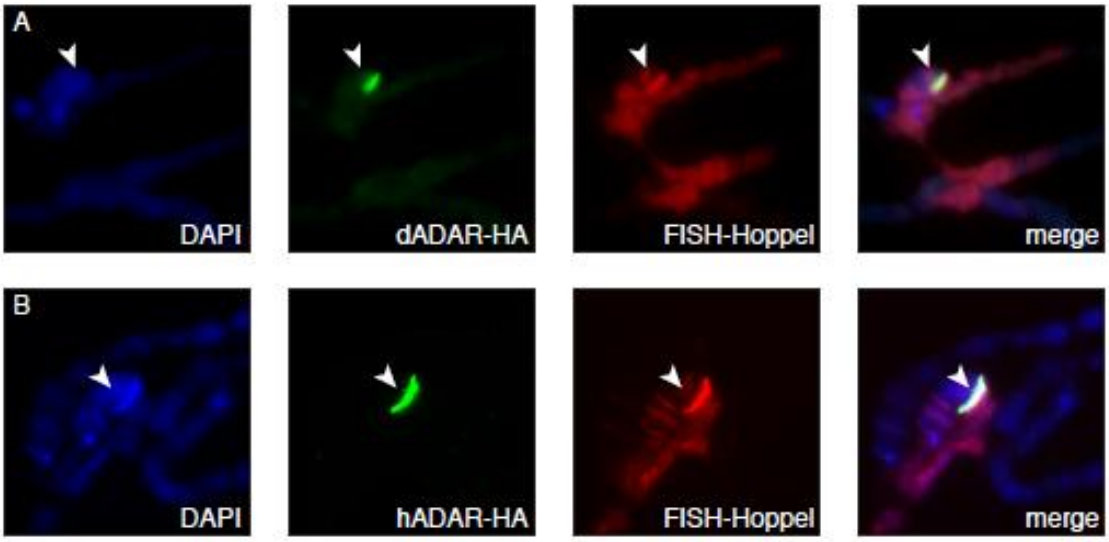

FIGURE 5.5. dADAR and hADAR localize near *Hoppel* elements on the fourth chromosome. FISH probes generated from PCR products spanning a *Hoppel* element were hybridized to fixed polytene chromosomes. FISH coupled with immuno-staining for HA-tagged dADAR (A) and hADAR (B) transgenes, showed co-localization of ADAR with the *Hoppel* FISH probe.

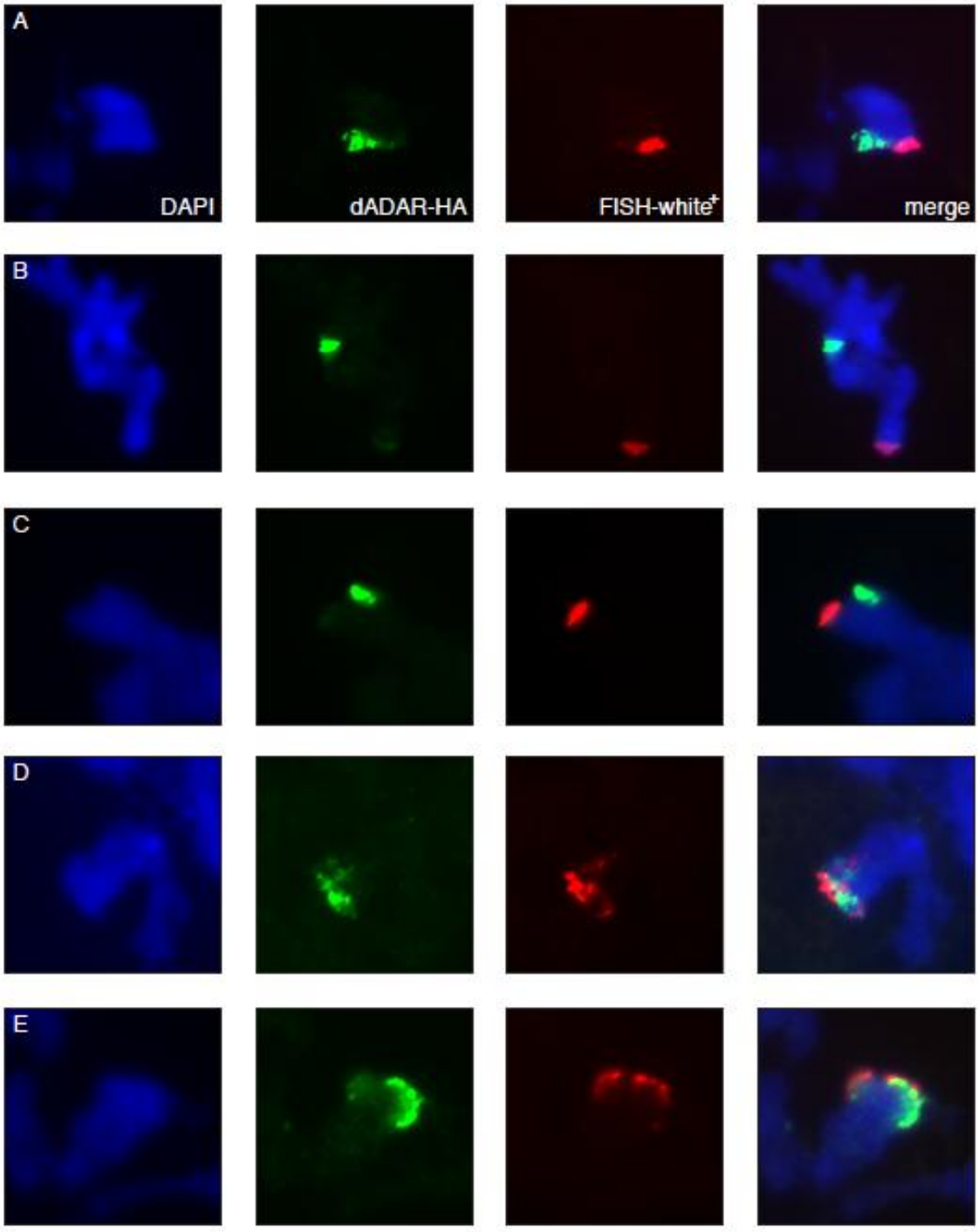

FIGURE 5.6. Removal of *Hoppels* from the intron within the *caps* locus results in complete loss of dADAR binding to the telomeric region of chromosome 4. FISH probes generated from PCR products spanning the *white*$^{+}$ gene were hybridized to fixed polytene chromosomes to identify the deleted allele in a *Hoppel* deletion heterozygote. (A-E) FISH coupled with immuno-staining for HA-tagged dADAR transgene, resulted in a completely non-overlapping localization pattern.

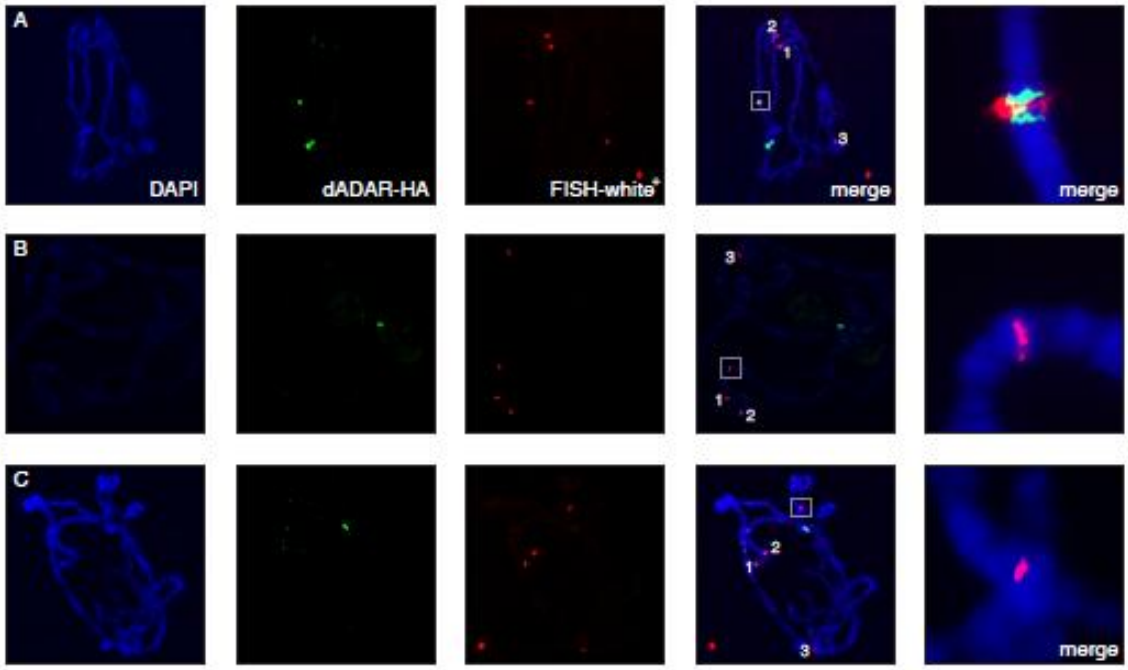

FIGURE 5.7. The *Hok* locus can generate a dADAR-binding dsRNA. FISH probes generated from PCR products spanning the *white*$^{+}$ gene were hybridized to fixed polytene chromosomes to identify the UAS-*Hok* and Casper-*Hok* mini-gene constructs. (A) FISH to identify the UAS-*Hok* construct coupled with immuno-staining for HA-tagged dADAR transgene, resulted in completely overlapping ectopic localization pattern (white box). (B-C) FISH to identify the Casper-*Hok* construct coupled with immuno-staining for HA-tagged dADAR transgene, resulted in no dADAR ectopic localization (white boxes).1-*c155* Gal-4 driver, 2- endogenous *white*$^{+}$ gene, and 3- dADAR-HA transgene.

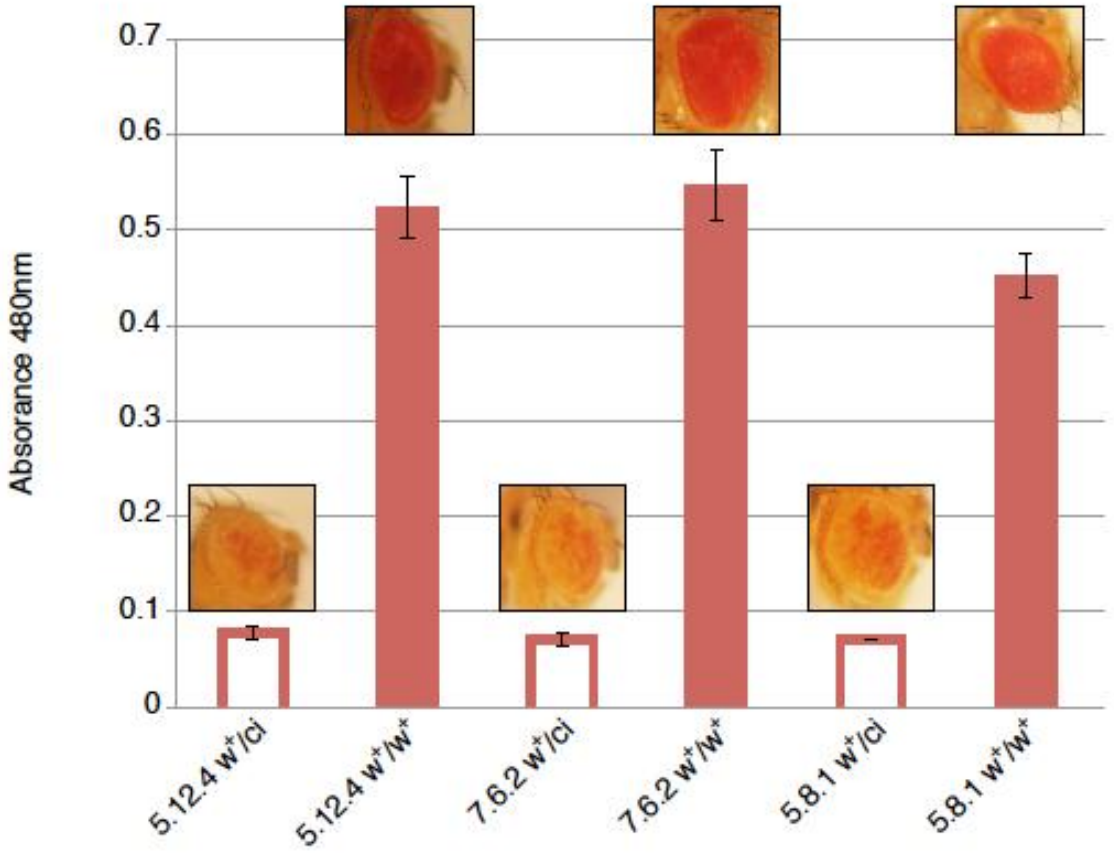

FIGURE 5.8. Homologous recombinants display robust PEV. Heterozygotes for three independent *Hok* deletion alleles displayed robust PEV whereas homozygotes exhibited striking loss of PEV. Eye-pigment levels were determined by measuring absorbance at a wavelength of 480 nm.

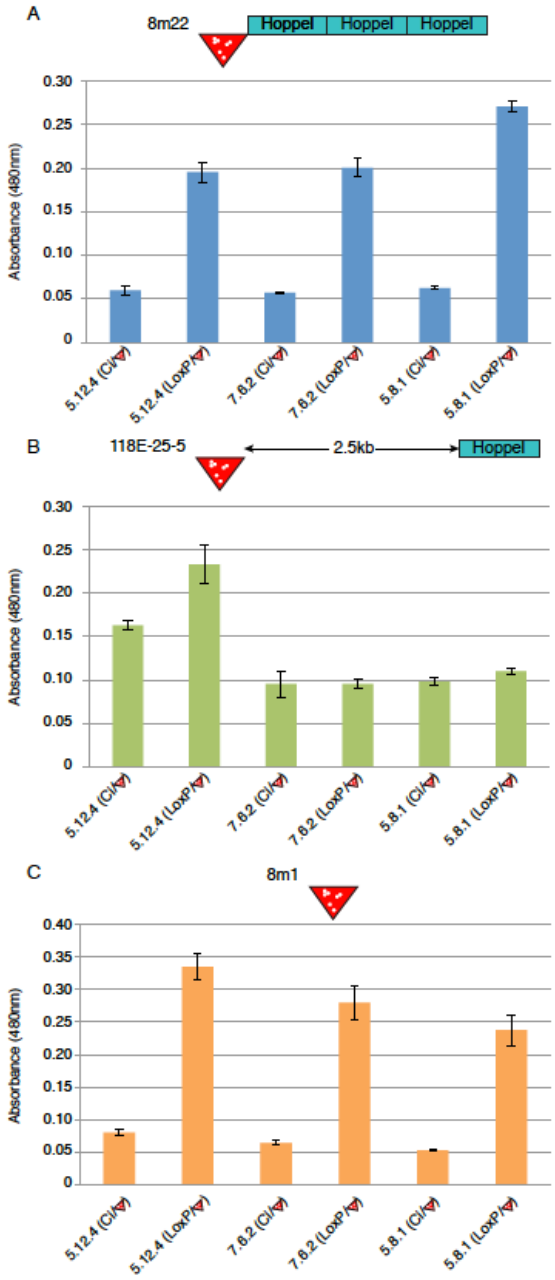

FIGURE 5.9. *Hok* dosage affects PEV at sites distal to the *caps* locus. Three independent variegating reporters were used to characterize the ability of *Hok* dosage to affect PEV. 8m22 is located within the *caps* locus adjacent to the *Hoppel* elements where as the 118E-25-5-variegating reporter is located ~2.5 kb away from a single *Hoppel* element. Conversely, the 8m1-variegating reporter has no *Hoppel* elements near by. (A) Suppression of PEV variegation of 8m22 reporter in three independent *Hok* deletion heterozygote alleles. (B) Decreasing the *Hok* dosage does not affect silencing of the 118E-25-5-variegating reporter. (C) Interestingly, decreasing the *Hok* dosage suppresses the silencing of 8m1-variegating reporter despite the fact that there are no *Hoppel* elements nearby. Eye-pigment levels were determined by measuring absorbance at a wavelength of 480 nm.

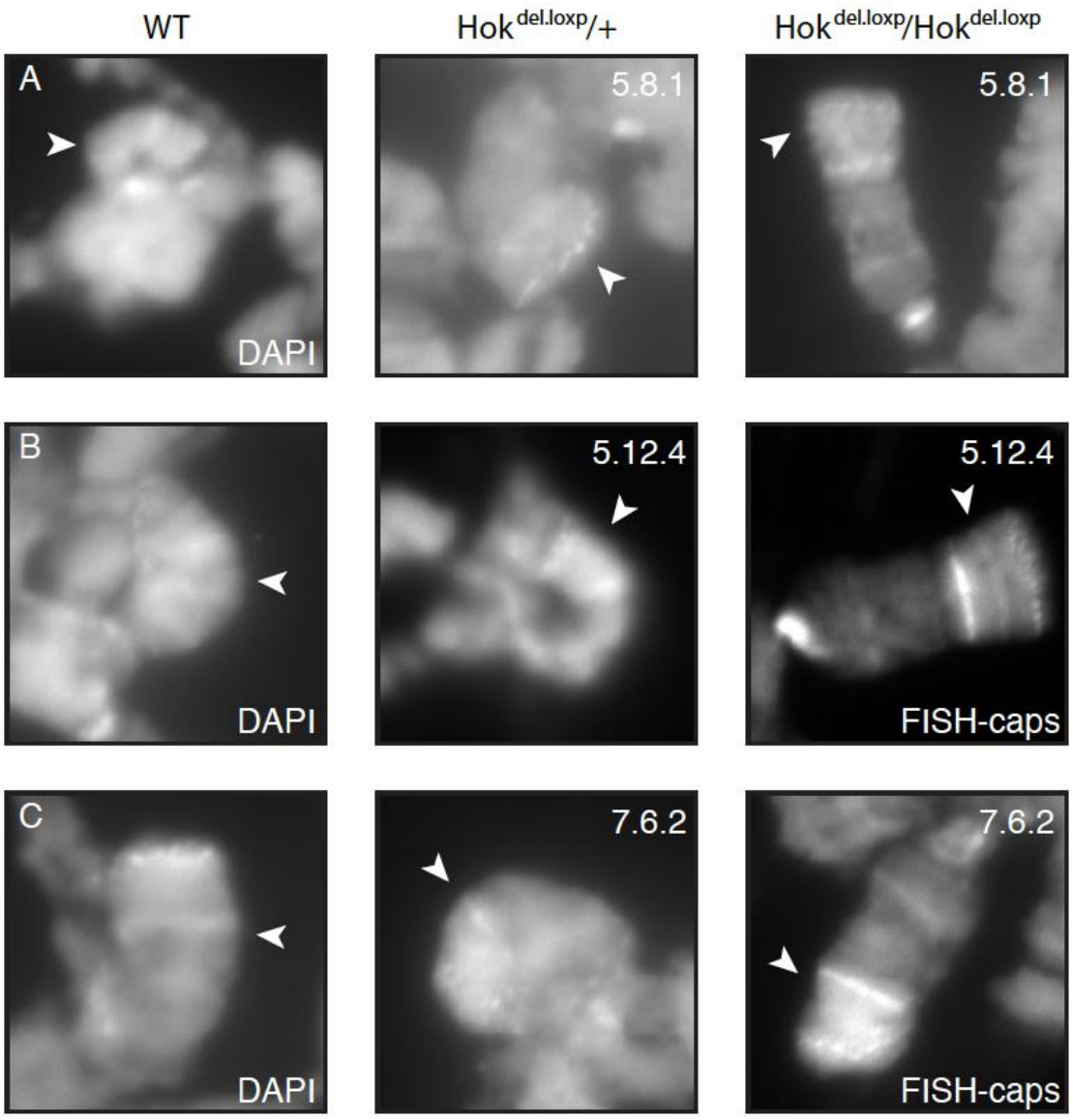

FIGURE 5.10. *Hok* deletions dramatically alter the chromatin architecture of the fourth chromosome. (A-C) DAPI stained fourth chromosomes (arrows) in three independent *Hok* deletion alleles. In homozygote deletion alleles the chromatin architecture of the fourth chromosome is altered when compared to heterozygote and WT alleles.

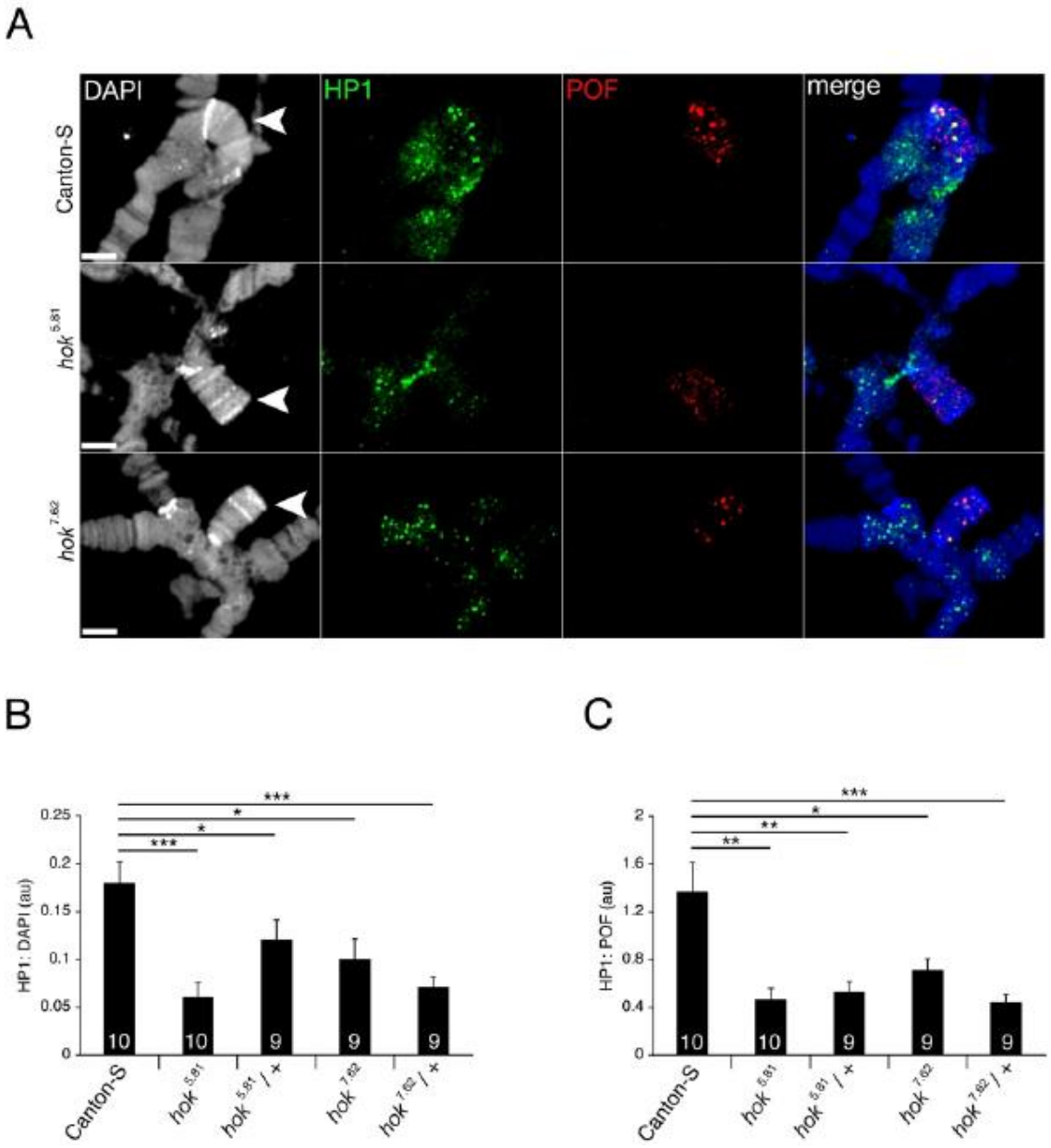

FIGURE 5.11. HP1 localization is reduced in *Hok* deletion alleles. (A) Chromosomes spreads were costained with anti-HP1 and anti-POF in two independent *Hok* deletion alleles. (B-C) Fluorescent intensity ratios between HP1:DAPI and HP1:POF revealed that HP1 localization on chromosome four is severely reduced in *Hok* deletion alleles. *: $P < 0.05$; **: $P < 0.005$; ***: $P < 0.0005$, one-way ANOVA with Tukey's HSD post-hoc test. Error bars: standard error.

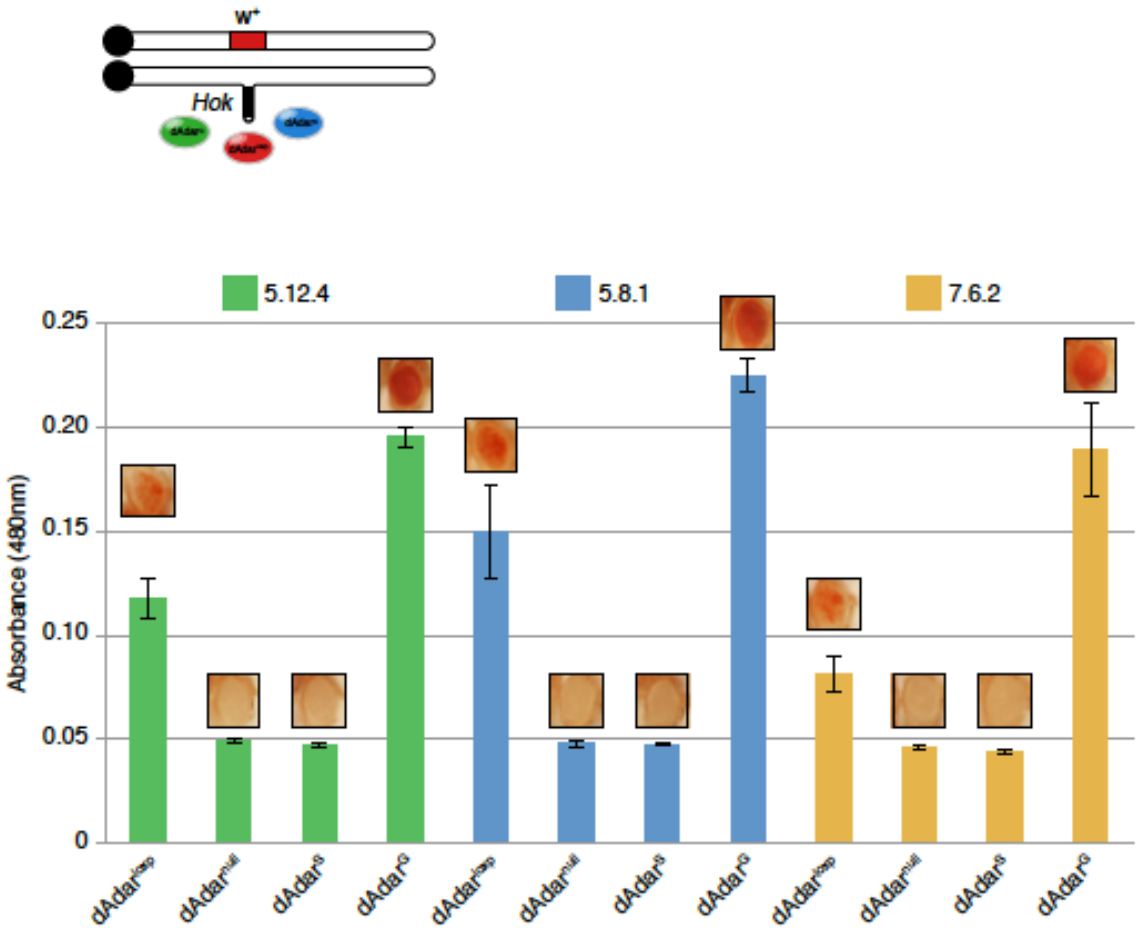

FIGURE 5.12. dADAR auto-editing generates a natural regulator of heterochromatin gene silencing. In males heterozygous for three independent variegating *white*$^{+}$ alleles at the *Hok* locus (*Hok*$^{del.w+}$/*Hok*$^{+}$), hemizygosity for the *dAdar*^{G} allele acted as a complete suppressor of PEV (Su(var)). In contrast, hemizygosity for either *dAdar*^{null} or *dAdar*^{S} alleles (genotypes incapable of producing *d*ADAR(G) protein) in the same three variegating genetic backgrounds resulted in enhancement of PEV (E(var)). The wild type, auto-editing competent control (*dAdar*^{loxP}) displayed robust variegation as expected. Eye-pigment levels were determined by measuring absorbance at a wavelength of 480 nm.

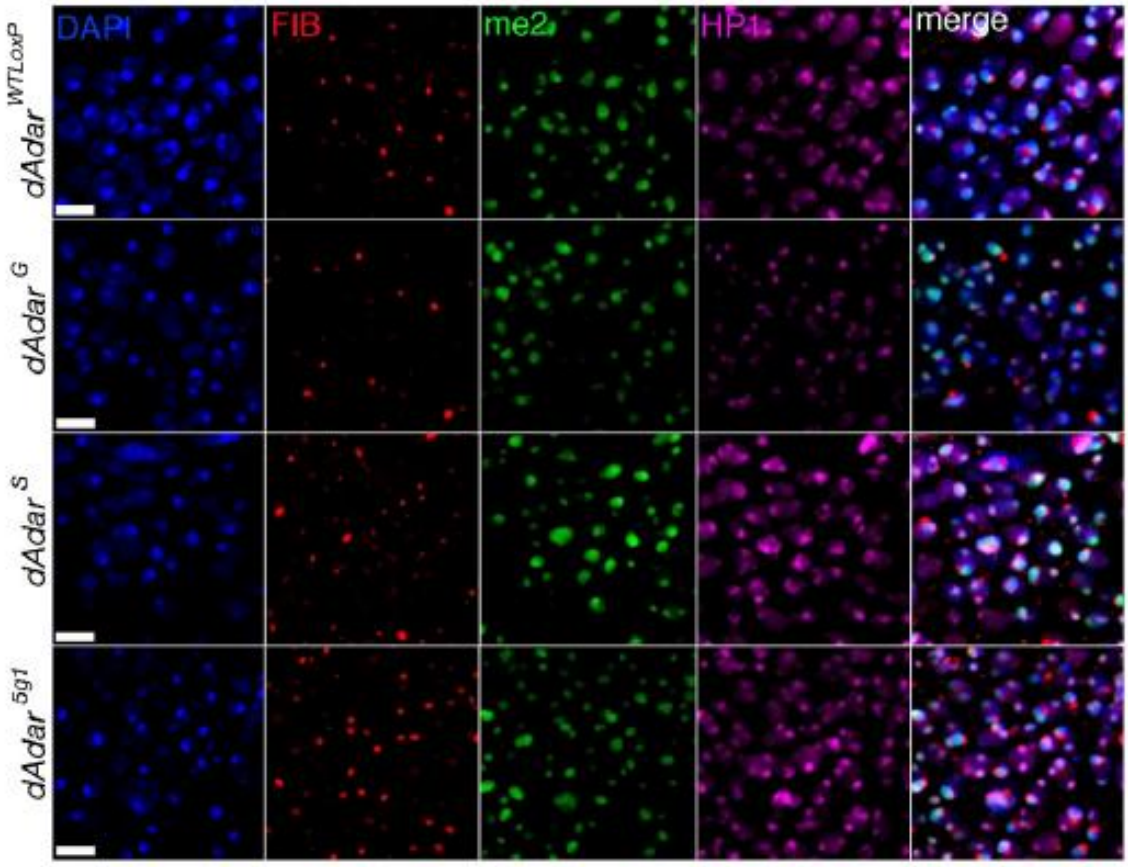

FIGURE 5.13. Alterations in dADAR activity via auto-editing regulate heterochromatin in neuronal nuclei. Male neuronal nuclei were costained with anti-FIB, anti-H3K9me2, and anti-HP1 in *dAdar*^{null}, *dAdar*^{S}, *and dAdar*^{G} alleles. In complete agreement with previous PEV experiments, neuronal nuclei in the *dAdar*^{S} and *dAdar*^{null} alleles exhibit higher levels of HP1. Conversely, HP1 levels are reduced in neuronal nuclei in the *dAdar*^{G} adult brains when compared to the *dAdar*^{loxP} allele supporting its role as a suppressor of variegation.

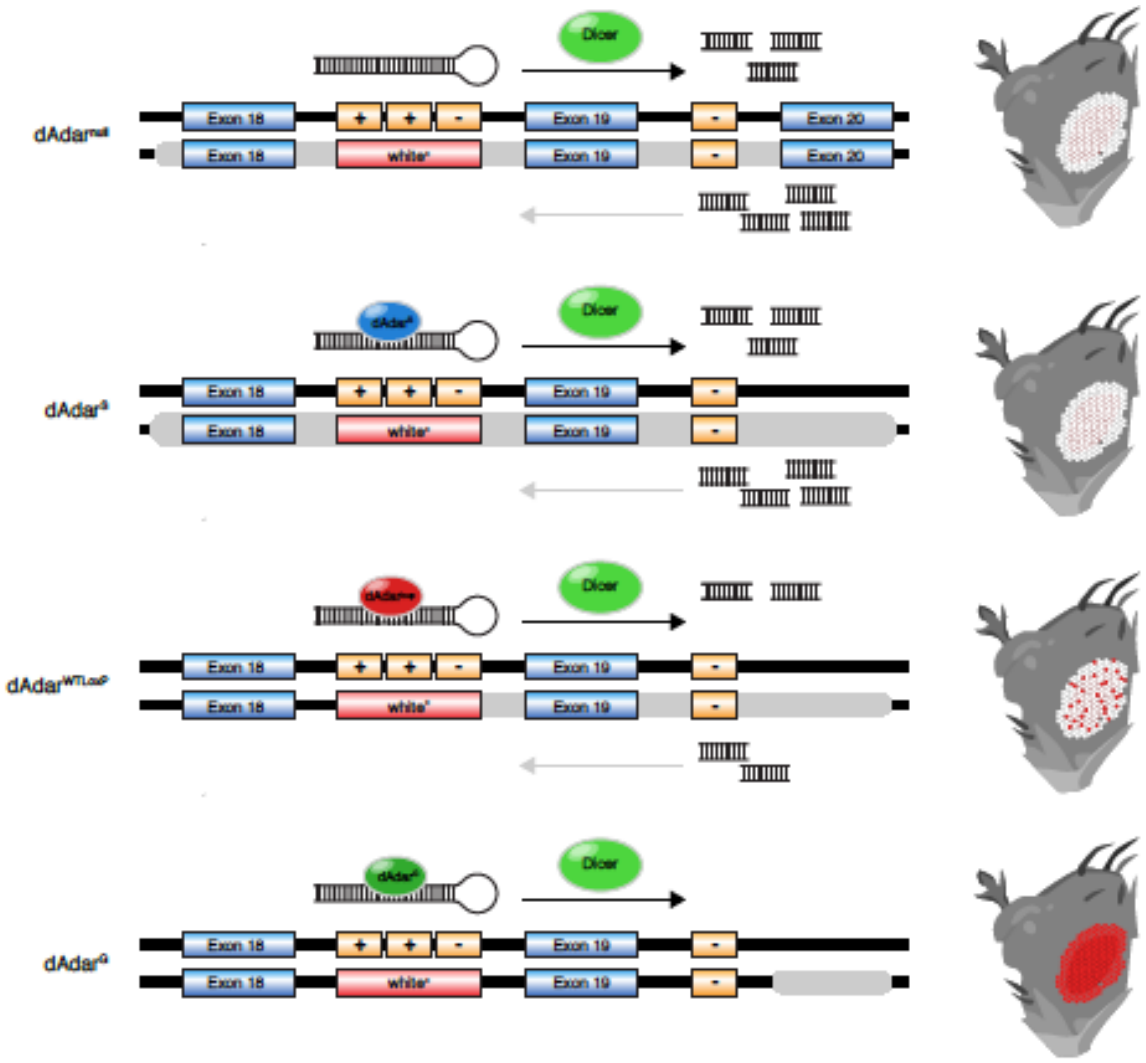

FIGURE 5.14. A mechanistic model for cell-autonomous tuning of gene silencing via dADAR regulated heterochromatin formation. The *dAdar*^{G} allele acts as a Su(var) while the *dAdar*^{S} allele acts as an E(var). Hypothetically, *d*ADAR may intersect with gene silencing pathways very early in the process (at the site of generation of dsRNA molecules destined to enter the RNAi pathway), and could thus regulate the concentration of siRNAs. Neuronal cells expressing dADAR at low levels, or only dADAR(S) would experience no diminution of the silencing effect of expressed long dsRNAs, thus acting as enhancers of variegation. Furthermore, cells expressing varying amounts of dADAR(G) and dADAR(S), as in the case of dADAR^{loxP} allele, would lead to moderate antagonistic effects on dsRNAs and the balance of chromatin states is determined between the strength of activities that promote either heterochromatin or euchromatin formation. Finally, intervention at this key point by the dADAR(G) protein, acting in a manner similar to viral proteins which mask dsRNA from dicer activity, could result in reduced siRNA levels that leads to loss of silencing. Grey arrows and lines indicate the spreading of heterochromatin.

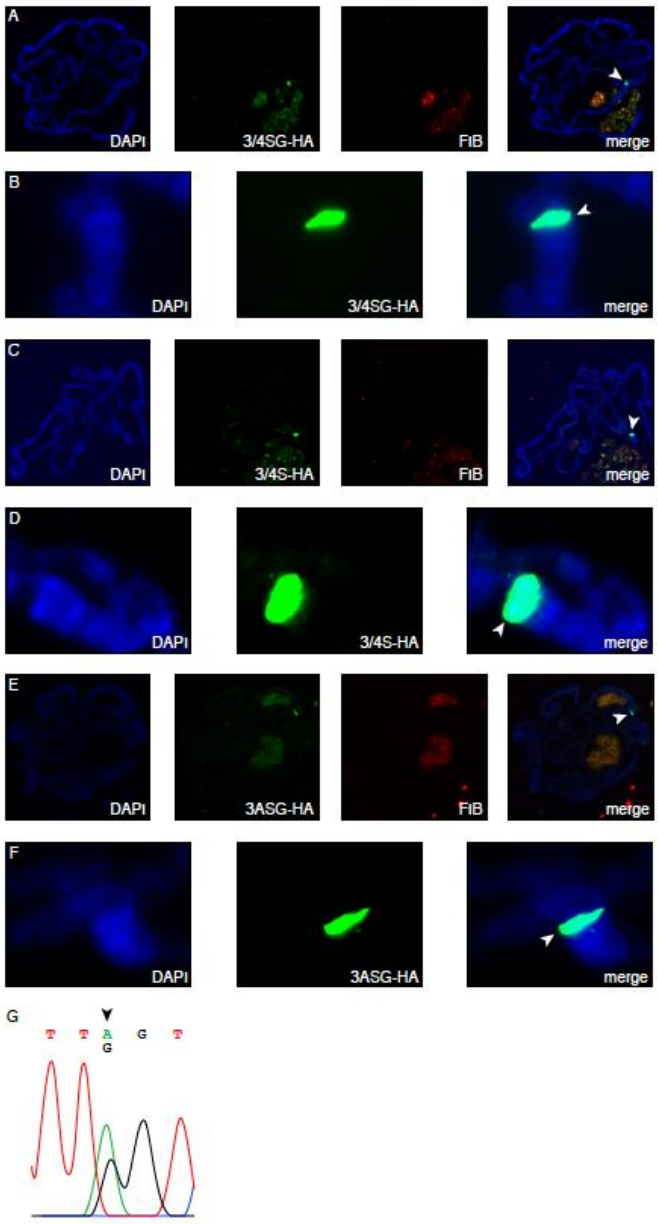

FIGURE S5.1. Localization of dADAR to the fourth chromosome is independent of auto-editing and alternative splicing. Three separate dADAR transgenes were expressed in larval salivary glands using the *c155*-Gal4 driver. (A-B) Localization of a transgene representing the predominant adult-stage isoform dADAR, which lacks the alternative spliced 3a exon (termed 3/4). At the auto-editing site, the serine codon is wild-type (S/G) and is capable of being edited by the dADAR transgene (G). This transgene is localized to the fourth chromosome (arrows). (C-D) Localization of a 3/4 dADAR transgene that is incapable of auto-editing, due to the serine codon being mutated to an un-editable synonymous TCT codon (S). The un-editable dADAR transgene localizes to the fourth chromosome (arrows) in similar fashion to the editable one. (E-F) Localization of a transgene to the fourth chromosome (arrows) representing the 3a alternatively spliced dADAR isoform. (G) Example electropherogram depicting the auto-editing state of 3/4 S/G transgene in salivary glands.

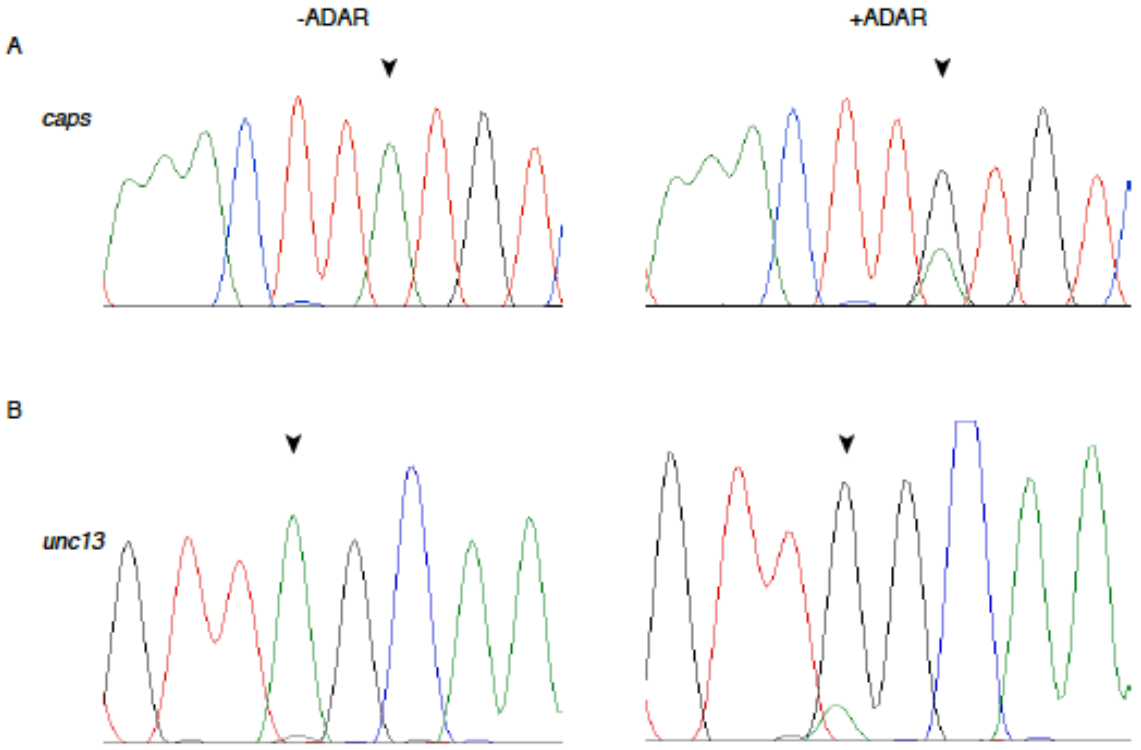

FIGURE S5.2. Editing status of *caps* and *unc13* in salivary glands after dADAR expression. Example electropherograms depicting the editing state of *caps* (A) and *unc13* (B) in salivary glands in the absence or presence of dADAR. Both targets are highly edited after a dADAR transgene was expressed in salivary glands using the *c155*-Gal4 driver. Black arrows point out the editing sites.

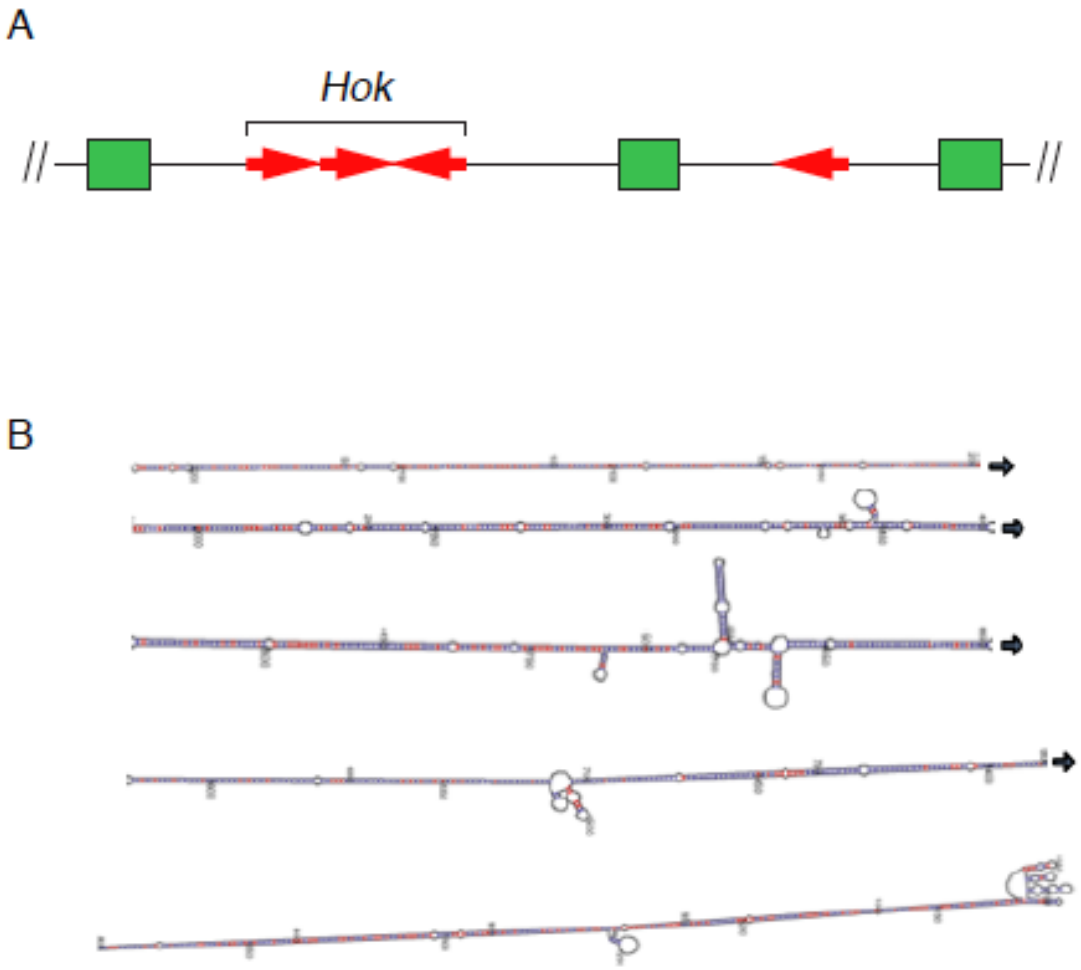

FIGURE S5.3. *Hoppel* elements are capable of forming an extensive nearly perfect dsRNA foldback. (A) Schematic of the *caps* locus illustrating the arrangement of the *Hoppel* elements. There are four copies of the transposable element *Hoppel* within the *caps* locus, three of which are tandemly repeated. Red arrows point out the orientation of each element. (B) The Mfold web server dsRNA program predicted that the *Hoppel* elements are capable of forming ~1kb nearly perfect dsRNA structure.

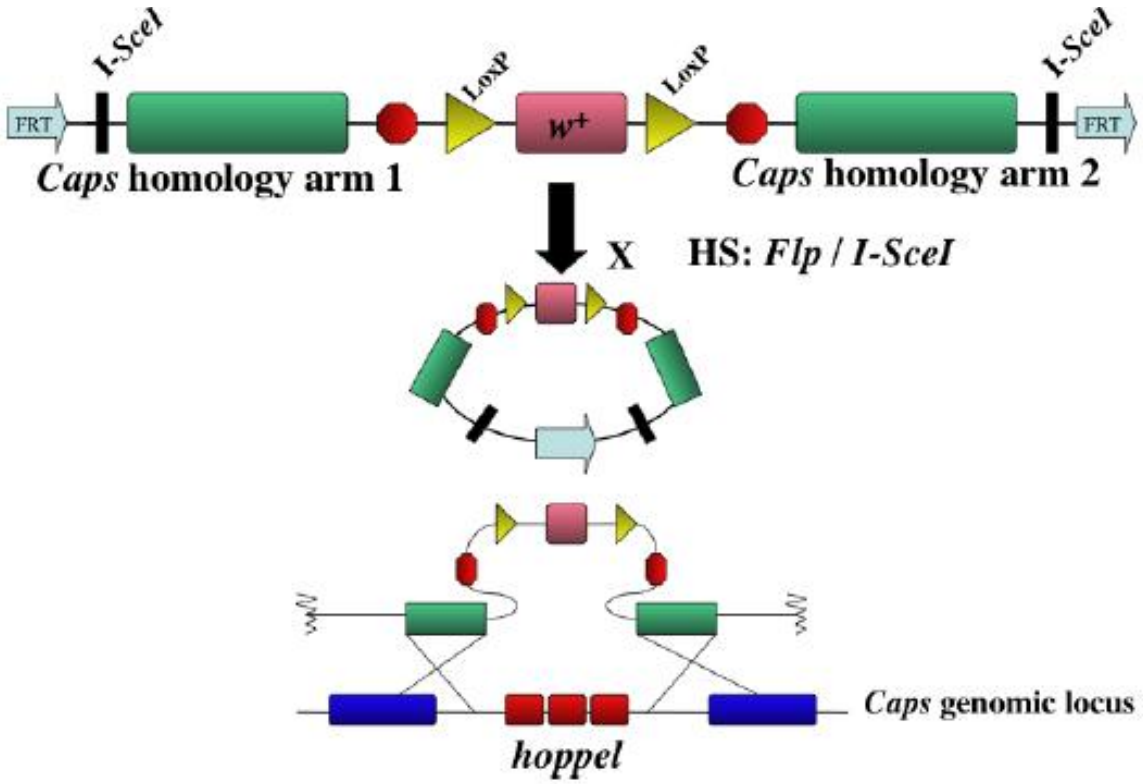

FIGURE S5.4. Schematic illustrating the homologous recombination process used for the deletion of the *Hoppel* elements. Two arms that have perfect homology to the sequences flanking the *Hoppel* elements within the *caps* locus are integrated into a targeting vector. After standard *P*-element transformation the vector is inserted randomly into the *Drosophila* genome. Homologous recombination is initiated by the action of FLP recombinase and *I-sceI* enzymes. After remobilization and linearization the donor DNA is integrated into the *caps* locus along with the *white*$^{+}$ gene that replaced the three tandem *Hoppel* elements. Finally, expression of Cre recombinase removes the *white*$^{+}$ gene from the *caps* locus. The end product is a genetically engineered *caps* locus with a single LoxP site with no *Hoppel* elements present.

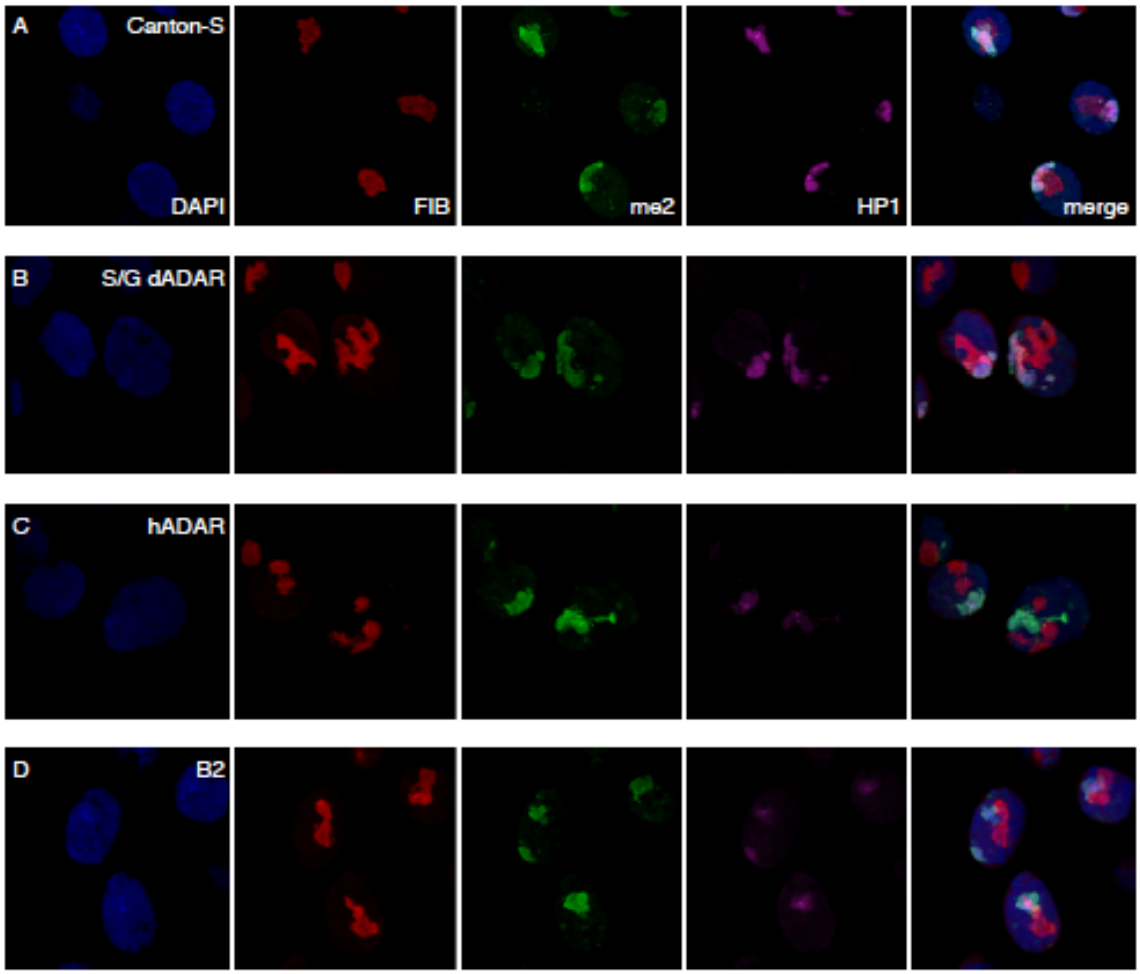

FIGURE S5.5. Expression of dADAR, hADAR, and B2 transgenes in salivary gland nuclei results in a disorganized nucleolus phenotype. Salivary glands were stained with anti-FIB, anti-H3K9me2, and anti-HP1 after expression of dADAR(S/G), hADAR, and B2 transgenes using the *c155*-Gal4 driver. (A) WT salivary gland cells have one nucleolus. (B-D) Salivary gland cells that express dADAR(S/G), hADAR, and B2 transgenes display multiple disorganized nucleoli. In addition, HP1 expression is reduced when compared to wild-type cells.

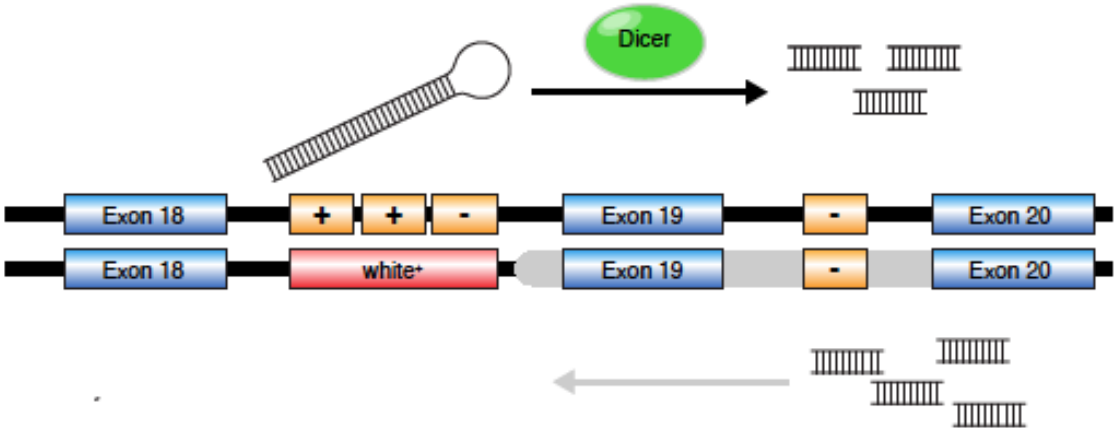

FIGURE S5.6. The proposed mechanism for the PEV observed in $Hok^{del.w+}/Hok^{+}$ animals. Dicer processing of *Hok* dsRNA generates siRNAs that direct an RNA silencing complex to the fourth *Hoppel* element within the *caps* locus. Hypothetically, this recruits heterochromatic marks, such as HP1 to initiate the spresding of heterochromatin that silences the $white^{+}$ gene found in close proximity (~7kb).

CHAPTER 6:

Discussion and Conclusions

A-to-I RNA editing modifications are functionally important within the nervous system of organisms as diverse as nematodes, insects and mammals (Higuchi et al., 2000; Palladino et al., 2000a; Tonkin et al., 2002). Diversification of the neuronal proteome via RNA editing is required for neuronal function, behavior and physiology (Nishikura, 2010). RNA editing enzymes are functionally pleiotropic through their ability to bind to both short imperfect and long perfectly base-paired dsRNA molecules (Bass, 2002; Nishikura). In short imperfect dsRNA templates, ADARs modify specific adenosines to inosines that usually leads to genomic recoding, since inosine is interpreted as guanosine by the translational machinery (Basillo et al., 1962). ADAR-mediated ion-channel diversification results in subtle modifications of protein function (Ingleby et al., 2009; Jones et al., 2009), suggesting that RNA editing acts as a "fine-tuning" mechanism to regulate enzymatic activity (Bass, 2002). Furthermore, ADARs recognize and modify perfectly long dsRNA templates that are required for the initiation of RNAi (Nishikura, 2006). ADAR-mediated modification of these dsRNA templates is promiscuous resulting in the deamination of up to 50% of the adenosines. Promiscuous editing activity of RNAi dsRNA precursors affects both siRNA biogenesis and activity (Nishikura, 2006).

Although much progress has been made in ADAR biology over the last two decades, the biological consequences of specific and promiscuous A-to-I RNA editing are not well understood, especially in an *in vivo* setting. In order to better understand the

contributions of RNA editing in both behavior and organismal fitness via specific and promiscuous ADAR catalytic activities, we precisely genetically engineered the *Drosophila* genome to create a series of mutant *adar* loci. This *in vivo* setting allowed us to investigate thoroughly the molecular mechanism of dADAR regulation of neuronal mRNA recoding and behavior. In addition, my work has focused on ADAR interactions with dsRNA templates that enter the RNAi pathway and demonstrated a novel role of RNA editing enzymes in the regulation of heterochromatin formation. My work here highlights a more global role for RNA editing enzymes regarding the regulation of neuronal transcriptomes and emphasizes their pivotal roles in organismal fitness.

Generation of a Hypomorphic *dAdar* Allele Implicates A-to-I RNA Editing in Serving a Modulatory Role in Complex Behavior

The extreme neurological phenotypes resulting from deletions of *adar* loci (Palladino et al., 2000a), have precluded investigations of how mRNA recoding regulates complex behaviors. Using a novel hypomorphic allele of *dAdar* generated via ends-out homologous recombination, we have demonstrated that RNA editing modulates multiple adaptive behaviors in *Drosophila*. More specifically, reduction in ADAR activity (>80%) leads to substantial alterations in circadian motor patterns and abnormal male courtship behavior (Fig. 2.5, 2.6). Our molecular analysis of the inosinome in *dAdar* hypomorhs revealed an unexpected dichotomous response of ADAR target transcripts. Interestingly, editing of certain adenosines is severely decreased or eliminated, whereas editing of others is minimally affected (Fig. 2.3). Based upon the nonuniform reduction in specific

editing of ADAR targets, we classified RNA editing sites into two groups, which we termed “high and low efficiency” (HE and LE) sites. According to this differential sensitivity of RNA editing sites to dADAR levels, we provided an explanatory basis for the developmental regulation of a select population of adenosines (Fig. 2.4). Furthermore, we used a novel reporter to map RNA editing activity across the fly nervous system. We demonstrated that editing activity varies widely between neuronal subpopulations, suggesting a cell-specific variation in dADAR expression (Fig.2.2). Together, our data suggest that variation of dADAR expression across the nervous system may allow spatial control of LE sites while simultaneously maintaining robust network-wide editing of HE sites, thus providing means to fine-tune neuronal physiology via the diversification of a select population of proteins (Fig. 2.8). This fine-tuning mechanism is required for appropriate adult stage behaviors since $dAdar^{hyp}$ males often exhibit abnormal waveform patterns (Fig. 2.7). This suggests that alterations in RNA editing could impinge organismal fitness. Within the *Drosophila* lineage, species-specific changes in the magnitude of editing at ortholous adenosines have been previously observed (Grauso et al., 2002; Jin et al., 2007; Reenan, 2005). Thus, our data open the possibility that RNA editing may contribute to species-specific song waveforms, a key mechanism in the process of speciation. It will be intriguing to see whether species-specific editing sites contribute to the generation of adult-stage species-specific behavioral patterns.

dADAR is Localized to the Neuronal Nucleus in the *Drosophila* Brain

dAdar transcripts are detected predominately in the brain of both *Drosophila* embryos and adults (Ma et al., 2002; Palladino et al., 2000b). However, the complete dADAR expression and cellular distribution pattern in the adult nervous system is still unknown. The lack of a commercially available antibody has hindered our understanding on this subject. To remedy this, we used ends-out homologous recombination to generate recombinant lines with HA epitope-tagged sequences at the 3' end of the *dAdar* locus (Fig. 2.1). Confocal microscopy revealed broad expression of dADAR in the brain and thoracic ganglion (Fig. S2.1). Specifically, co-immunostaining for HA and the nuclear envelope protein Lamin showed that dADAR expression was prominent only within nuclei (Fig. 2.1).

dADAR auto-editing as a Master Regulator of mRNA Re-coding and Behavior

Intriguingly, both mammalian and *Drosophila* ADARs have evolved distinct auto-regulatory feedback loops as a mechanism to tune enzymatic function, based on the deamination of adenosines within their own transcripts (Palladino et al., 2000b; Rueter et al., 1999). Rat ADAR2 auto-editing acts as a negative feedback mechanism by generating a novel AI splicing acceptor site, leading to an N-terminal frame-shift and translation of a truncated ADAR2 isoform at reduced levels (Rueter et al., 1999). Correspondingly, abolition of ADAR2 auto-editing *in vivo* increases ADAR2 expression and editing at several target adenosines (Feng et al., 2006). In contrast, dADAR auto-editing results in a

serine to glycine coding change in the C-terminal catalytic domain (Palladino et al., 2000b). *In vitro* experiments using two dADAR substrates indicate that auto-editing acts to reduce dADAR activity, suggesting an evolutionary convergence in function of dADAR and ADAR2 auto-regulation (Keegan et al., 2005). However, it is unknown whether dADAR auto-editing acts generically to reduce editing at all target adenosines *in vivo* or, rather to modify particular sites in a substrate-specific manner.

We used ends-out homologous recombination to bi-directionally interfere with dADAR auto-editing (Fig. 3.1) and defined the *in vivo* role of this auto-regulation at both the molecular and behavioral levels. We demonstrated that dADAR auto-editing dramatically remodels the landscape of the *Drosophila* inosinome in a site-specific matter (Fig. 3.1). Furthermore, we showed that alterations in re-coding events correlate with altered localization of dADAR within the neuronal nuclear compartment (Fig. 3.3). Finally, we demonstrated that modifying dADAR auto-editing affects adaptive complex behaviors (Fig. 3.4). Our results greatly expand on the previous *in vitro* methods used to investigate dADAR auto-editing and yielded distinct paradigms in relation to the functional consequences of this auto-regulation in an *in vivo* setting. Specifically, our data suggest that auto-editing effectively acts to generate a weak hypomorphic *dAdar* allele through ADAR sequestration to a nuclear sub-compartment, thus lowering the active concentration of dADAR at active sites of transcription. It will be interesting to see if this mysterious sub-nuclear compartment corresponds to paraspeckle-associated complexes since in mammalian cells, transcripts with high inosine content are often retained within these nuclear compartments. It will also be interesting to determine the

mechanistic basis of how a single amino acid change can result in such a profound effect in protein localization.

dADAR Auto-editing Generates a Natural Regulator of Heterochromatic Gene Silencing

In somatic tissues, nuclear pools of endogenous small interfering RNAs (esiRNAs) ranking from 20-22nt in length guide RNA induced silencing complexes (RISCs) to discrete regulatory targets for initiation of a sequence-specific silence mechanism known as RNAi (Chapman and Carrington, 2007; Peters and Meister, 2007). The biogenesis of esiRNAs proceeds through the action of Dicer on dsRNAs transcribed from distinct genomic sources (Ghildiyal and Zamore, 2009). In *Drosophila*, the majority of esiRNAs derive from read-though transcription of transposable elements (TE) that are widely distributed throughout the fly genome (Kawamura et al., 2008). Mutations in Dicer-2, the ribonuclease involved in the biogenesis of esiRNAs, result in elevated TE transcript levels, suggesting that this RNAi pathway operates to inhibit transposon activation in somatic cells (Chung et al., 2008; Czech et al., 2008; Ghildiyal et al., 2008; Kawamura et al., 2008). Additionally, Mutations in components of the esiRNAi pathway lead to suppression of heterochromatic silencing (Fagegaltier et al., 2009), suggesting that nuclear pools of esiRNAs initiate heterochromatin formation in somatic tissues in *Drosophila*. Intriguingly, sequence analysis of esiRNAs from *Drosophila* S2 cultured cells revealed that a large number of these small RNAs contain adenosine to guanosine single mismatches relative to the genomic sequence, indicating that dsRNA structures

that enter this RNAi pathway serve as ADAR substrates (Kawamura et al., 2008). However, it is unknown whether dADAR regulates heterochromatin formation.

Over-expression studies of tagged dADAR-HA transgenes in salivary glands revealed that dADAR localizes on the fourth chromosome in *Drosophila* (Fig. 5.1). Using FISH we identified a unique sequence feature, which could account for the abundant localization of dADAR within the *caps* locus (Fig. 5.4, S5.3). By using homologous recombination, we demonstrated that dADAR binds to long dsRNA mediated by the *Hoppel* transposable elements *in vivo* (Fig. 5.6). Furthermore, we showed that *Hoppel* deletions via homologous recombination dramatically alter the chromatin architecture of the fourth chromosome (Fig. 5.10). We also determined that the *Hoppel* mediated dsRNA template regulates PEV (Fig. 5.8, 5.9). More importantly, we demonstrated that dADAR can act as an enhancer or suppressor of variegation and this action can be bi-directionally modulated by auto-regulatory RNA editing (Fig. 5.12). Together, our findings support a versatile mechanism for bestowing cell-autonomous tuning of gene silencing through ADAR regulation of heterochromatin formation (Fig. 5.14).

A-to-I RNA Editing Could Mediate Inter-neuronal Variation

Using a novel reverse-engineered fluorescent reporter of dADAR activity, we inferred cell-specific control of auto-editing levels within the Drosophila nervous system (Fig 4.2). Intriguingly, we observed differential auto-editing levels between neurons projecting to the mushroom bodies, antennal lobes, and even within sub-populations of

Kenyon cells. *dAdar* auto-editing levels may thus be set on a neuron-to-neuron basis, and contribute to optimizing cell-specific electrophysiological and synaptic release properties. The mechanistic basis for such variable regulation of auto-editing is unclear. Hypothetically, the degree of auto-editing may be controlled by trans-acting factors whose expression varies between neurons. These results suggest that distinct neuronal subtypes exist within a nervous system regarding dADAR auto-editing states; a neuron in which *dAdar* auto-editing is lacking (S), a neuron in which edited and unedited states of *dAdar* are present in a 1:1 ratio, and a neuron in which *dAdar* auto-editing is at maximum (G). The collective observations that dADAR auto-editing regulates both mRNA re-coding and heterochromatin formation provide tantalizing clues about a complex molecular mechanism that leads to inter-neuronal variation regarding transcriptomic potentials and chromatin architectures (Fig. 6.1). In neurons in which *dAdar* auto-editing is lacking, mRNA re-coding is at maximum. In addition, these neurons exhibit a potent RNAi response that leads to heterochromatin gene silencing. Conversely, in neurons in which *dAdar* auto-editing is at maximum, mRNA re-coding is at minimum. In these neurons RNAi is inefficient, resulting in a loss of silencing. If correct, this hypothesis predicts neuronal position effect variegation mediated through A-to-I RNA editing.

ADAR-mediated neuronal somatic mosaicism?

In rodents, recent studies have shown that neuronal genomes are not static because of active LINE-1 (L1) retrotransposition that results in the generation of somatic mosaicism (Muotri et al., 2005). L1 “jumping” can lead to transcriptional disruption,

which suggests that novel insertion sites can influence gene expression (Han et al., 2004). The observation that edited esiRNAs are occupying active RISC complexes (Kawamura et al., 2008) suggests that ADARs may potentially affect transposon silencing since the esiRNA pathway acts to repress trasposon activation in somatic tissues (Chung et al., 2008; Czech et al., 2008; Kawamura et al., 2008). Specifically, in neurons in which *dAdar* auto-editing is at maximum (G), inhibition of esiRNA biogenesis could lead to somatic activation of trasposons and result in stochastic trasposition. Therefore, ADARs may create quantitative genetic variation within neuronal populations that "fine-tunes" gene expression. The observation that substantial variability exists in dADAR activity between individual male *Drosophila* (Fig. 4.3), insinuates that RNA editing could represent a credible molecular mechanism for generating individual-to-individual variation in neuronal plasticity and behavior. Thus, A-to-I RNA editing in the nervous systems of higher metazoans could represent a molecular force towards individuality.

REFERENCES

Basillo, C., Wahba, A., Lengyel, P., Speyer, J., and Ochoa, S. (1962). Synthetic polynucleotides and the amino acid code. V. Proceedings of the National Academy of Sciences of the United States of America *48*, 613-616.

Bass, B.L. (2002). RNA editing by adenosine deaminases that act on RNA. Annual review of biochemistry *71*, 817-846.

Chapman, E.J., and Carrington, J.C. (2007). Specialization and evolution of endogenous small RNA pathways. Nat Rev Genet *8*, 884-896.

Chung, W.J., Okamura, K., Martin, R., and Lai, E.C. (2008). Endogenous RNA interference provides a somatic defense against Drosophila transposons. Curr Biol *18*, 795-802.

Czech, B., Malone, C.D., Zhou, R., Stark, A., Schlingeheyde, C., Dus, M., Perrimon, N., Kellis, M., Wohlschlegel, J.A., Sachidanandam, R.*, et al.* (2008). An endogenous small interfering RNA pathway in Drosophila. Nature *453*, 798-802.

Fagegaltier, D., Bouge, A.L., Berry, B., Poisot, E., Sismeiro, O., Coppee, J.Y., Theodore, L., Voinnet, O., and Antoniewski, C. (2009). The endogenous siRNA pathway is involved in heterochromatin formation in Drosophila. Proceedings of the National Academy of Sciences of the United States of America *106*, 21258-21263.

Feng, Y., Sansam, C.L., Singh, M., and Emeson, R.B. (2006). Altered RNA editing in mice lacking ADAR2 autoregulation. Molecular and cellular biology *26*, 480-488.

Ghildiyal, M., Seitz, H., Horwich, M.D., Li, C., Du, T., Lee, S., Xu, J., Kittler, E.L., Zapp, M.L., Weng, Z.*, et al.* (2008). Endogenous siRNAs derived from transposons and mRNAs in Drosophila somatic cells. Science (New York, NY *320*, 1077-1081.

Ghildiyal, M., and Zamore, P.D. (2009). Small silencing RNAs: an expanding universe. Nat Rev Genet *10*, 94-108.

Grauso, M., Reenan, R.A., Culetto, E., and Sattelle, D.B. (2002). Novel putative nicotinic acetylcholine receptor subunit genes, Dalpha5, Dalpha6 and Dalpha7, in Drosophila melanogaster identify a new and highly conserved target of adenosine deaminase acting on RNA-mediated A-to-I pre-mRNA editing. Genetics *160*, 1519-1533.

Han, J.S., Szak, S.T., and Boeke, J.D. (2004). Transcriptional disruption by the L1 retrotransposon and implications for mammalian transcriptomes. Nature *429*, 268-274.

Higuchi, M., Maas, S., Single, F.N., Hartner, J., Rozov, A., Burnashev, N., Feldmeyer, D., Sprengel, R., and Seeburg, P.H. (2000). Point mutation in an AMPA receptor gene

rescues lethality in mice deficient in the RNA-editing enzyme ADAR2. Nature *406*, 78-81.

Ingleby, L., Maloney, R., Jepson, J., Horn, R., and Reenan, R. (2009). Regulated RNA editing and functional epistasis in Shaker potassium channels. The Journal of general physiology *133*, 17-27.

Jin, Y., Tian, N., Cao, J., Liang, J., Yang, Z., and Lv, J. (2007). RNA editing and alternative splicing of the insect nAChR subunit alpha6 transcript: evolutionary conservation, divergence and regulation. BMC evolutionary biology *7*, 98.

Jones, A.K., Buckingham, S.D., Papadaki, M., Yokota, M., Sattelle, B.M., Matsuda, K., and Sattelle, D.B. (2009). Splice-Variant- and Stage-Specific RNA Editing of the Drosophila GABA Receptor Modulates Agonist Potency. J Neurosci *29*, 4287-4292.

Kawamura, Y., Saito, K., Kin, T., Ono, Y., Asai, K., Sunohara, T., Okada, T.N., Siomi, M.C., and Siomi, H. (2008). Drosophila endogenous small RNAs bind to Argonaute 2 in somatic cells. Nature *453*, 793-797.

Keegan, L.P., Brindle, J., Gallo, A., Leroy, A., Reenan, R.A., and O'Connell, M.A. (2005). Tuning of RNA editing by ADAR is required in Drosophila. The EMBO journal *24*, 2183-2193.

Ma, E., Tucker, M.C., Chen, Q., and Haddad, G.G. (2002). Developmental expression and enzymatic activity of pre-mRNA deaminase in Drosophila melanogaster. Brain research *102*, 100-104.

Muotri, A.R., Chu, V.T., Marchetto, M.C., Deng, W., Moran, J.V., and Gage, F.H. (2005). Somatic mosaicism in neuronal precursor cells mediated by L1 retrotransposition. Nature *435*, 903-910.

Nishikura, K. (2010) Functions and regulation of RNA editing by ADAR deaminases. Annual review of biochemistry *79*, 321-349.

Nishikura, K. (2006). Editor meets silencer: crosstalk between RNA editing and RNA interference. Nature reviews *7*, 919-931.

Palladino, M.J., Keegan, L.P., O'Connell, M.A., and Reenan, R.A. (2000a). A-to-I pre-mRNA editing in Drosophila is primarily involved in adult nervous system function and integrity. Cell *102*, 437-449.

Palladino, M.J., Keegan, L.P., O'Connell, M.A., and Reenan, R.A. (2000b). dADAR, a Drosophila double-stranded RNA-specific adenosine deaminase is highly developmentally regulated and is itself a target for RNA editing. RNA (New York, NY *6*, 1004-1018.

Peters, L., and Meister, G. (2007). Argonaute proteins: mediators of RNA silencing. Molecular cell *26*, 611-623.

Reenan, R.A. (2005). Molecular determinants and guided evolution of species-specific RNA editing. Nature *434*, 409-413.

Rueter, S.M., Dawson, T.R., and Emeson, R.B. (1999). Regulation of alternative splicing by RNA editing. Nature *399*, 75-80.

Tonkin, L.A., Saccomanno, L., Morse, D.P., Brodigan, T., Krause, M., and Bass, B.L. (2002). RNA editing by ADARs is important for normal behavior in Caenorhabditis elegans. The EMBO journal *21*, 6025-6035.

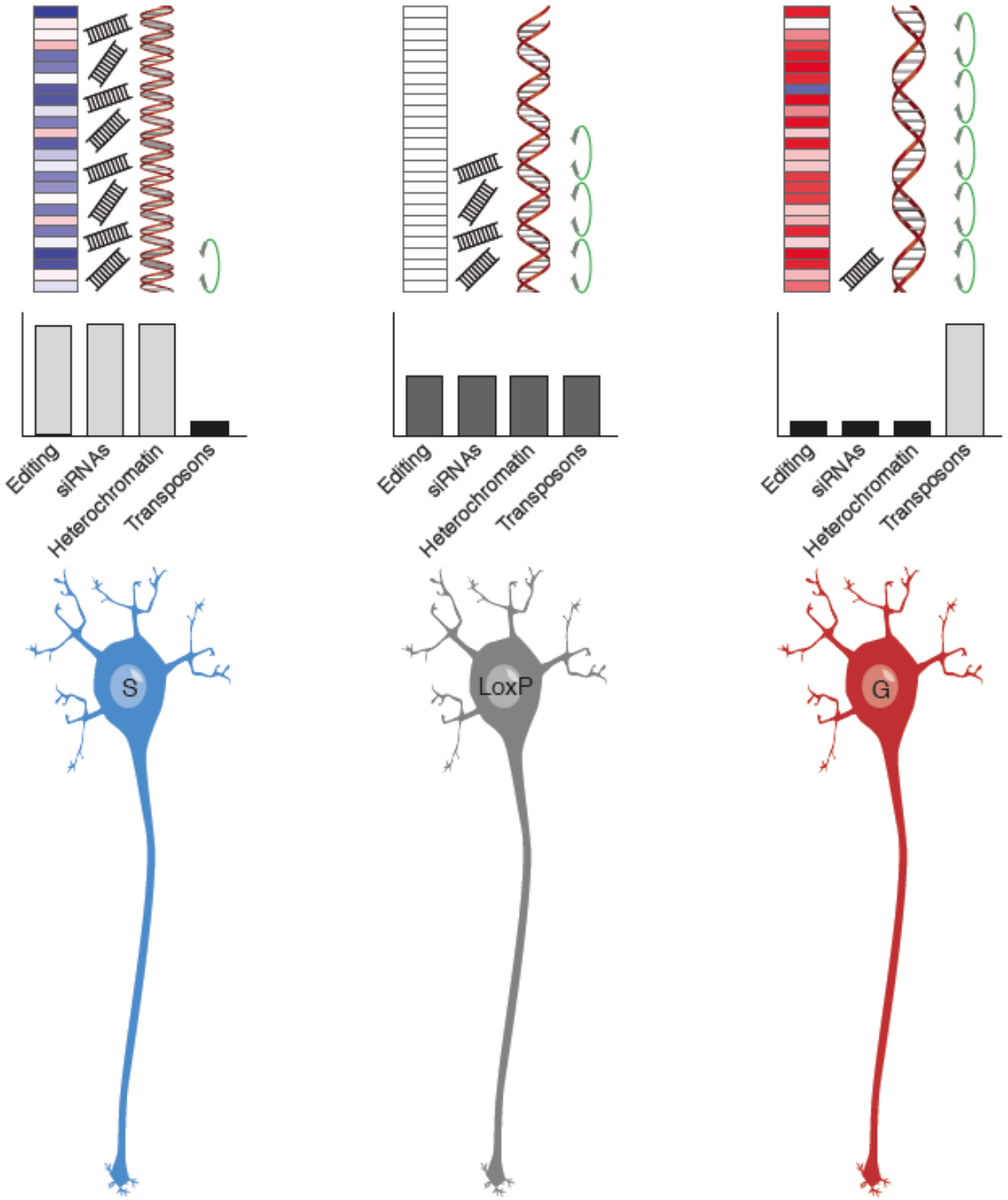

FIGURE 6.1. Inter-neuronal variability via dADAR auto-editing. A diagrammatic representation of three distinct neuronal subtypes that represent differential dADAR auto-editing states. In neurons in which *dAdar* auto-editing is lacking (S), mRNA re-coding is at maximum. In addition, these neurons exhibit a potent RNAi response that leads to heterochromatin gene silencing and transposon silencing. Conversely, in neurons in which *dAdar* auto-editing is at maximum (G), mRNA re-coding is at minimum. In these neurons RNAi is inefficient, resulting in a loss of silencing and activation of transposons. Neurons in which dADAR auto-editing is in a 1:1 ratio exhibit intermediate molecular phenotypes.